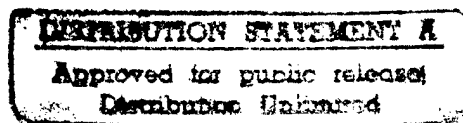


VOLUME II
FLYING QUALITIES PHASE

CHAPTER 15
DYNAMIC
PARAMETER ANALYSIS



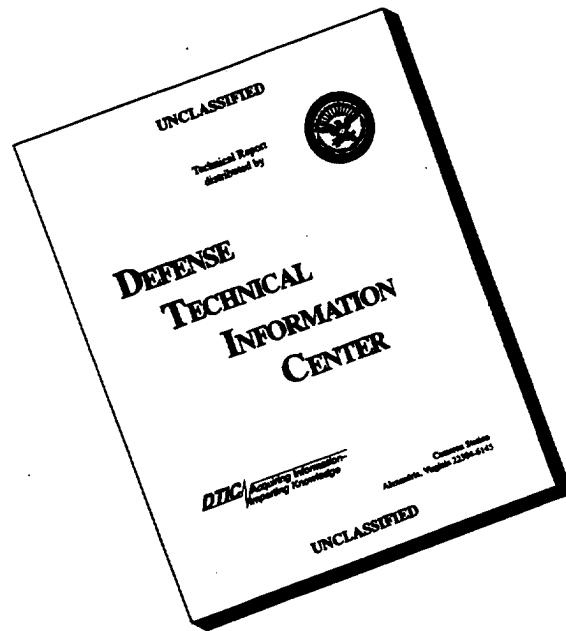
DECEMBER 1981

USAF TEST PILOT SCHOOL
EDWARDS AFB CA

19970122 001

UNCLASSIFIED

DISCLAIMER NOTICE



**THIS DOCUMENT IS BEST
QUALITY AVAILABLE. THE
COPY FURNISHED TO DTIC
CONTAINED A SIGNIFICANT
NUMBER OF PAGES WHICH DO
NOT REPRODUCE LEGIBLY.**

TABLE OF CONTENTS

<u>SECTION</u>	<u>TITLE</u>	<u>PAGE</u>
1	Foundations of Dynamic Parameter Analysis	1
2	Systems Identification and Parameter Estimation	21
3	Stability Parameters and Derivatives	77
4	Individual Stability Derivatives	111
5	Stability Derivative Accuracy	225
6	Parameter Analysis	285
7	Other Uses of Systems Identification	287
8	The MLE Program	287
	References	288

FOREWORD

This text was written to be "self contained" for use in a course titled Dynamic Parameter Analysis at the USAF Test Pilot School. Extensive use of references is made since the material tends to be quite technical in nature and most current information is available only in engineering or flight test reports. The course is not currently being taught.

Comments, corrections, and suggestions from students and other readers of this material are solicited.



RAYMOND L. JONES
Curriculum Advisor
USAF Test Pilot School
TEN, Stop 209
Edwards AFB CA 93523
AUTOVON 350-2803 or (805) 277-2803

SECTION 1

FOUNDATIONS OF DYNAMIC PARAMETER ANALYSIS

INTRODUCTION

The term "dynamic parameter analysis" is used in this course to mean a discussion of (1) the general systems identification problem, (2) parameter estimation techniques, and (3) parameter analysis methods. Systems identification is the determination of the characteristics of a physical system from experimental test data. Parameter estimation techniques are methods used in systems identification problems, and parameter analysis is putting the results of these experiments to good use.

The application of systems identification and parameter estimation techniques to aircraft flight testing is simply the process of obtaining quantitative measures of various aircraft characteristics. More specifically, it is often the determination, or extraction of stability and control derivatives from flight test data. This process is also called parameter identification in some current literature and at the AFFTC.^{106, 141}

The need for determining aircraft parameters from flight test measurements has existed since before the Wright brothers first flight. In 1894 Chanute concluded that whoever solved the problem of powered flight would have to go into the air to determine under what circumstances equilibrium could be maintained.^{104,105} Wilbur and Orville Wright did this in 1903 after becoming first engineers, then scientists, and finally test pilots.¹⁰⁵ By 1929 even the general public believed that a new design would fly, but quantitative measures of "good" and "bad" about designs was necessary so that future designs could be improved.¹ Flight test has always been important in advancing aircraft technology. Unfortunately, most of the aircraft characteristics of interest, such as the aerodynamic and propulsive forces and moments, cannot be directly measured in flight. For

evaluation it has been necessary to develop computational techniques that use measureable quantities, such as the motion resulting from a change in a force or moment.

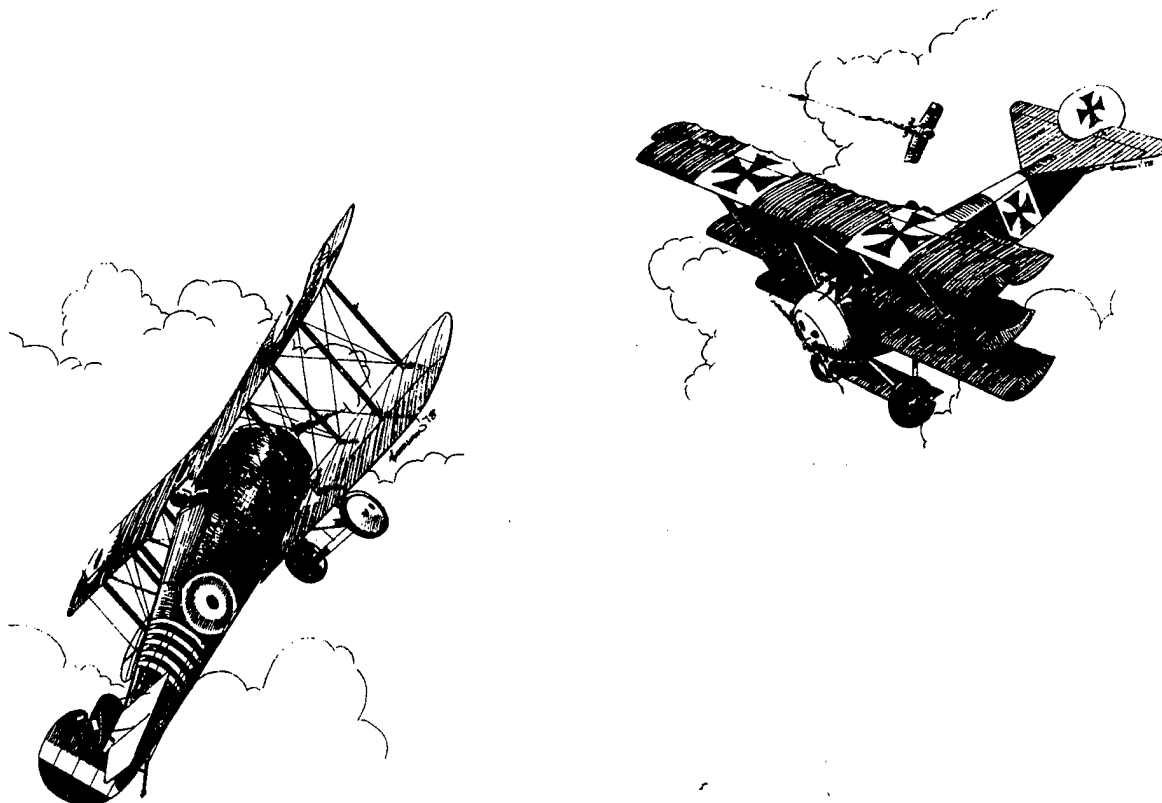
The advantage and benefits of developing a complete mathematical description of an aircraft's stability and control characteristics have been recognized by the flight test community for a long time. This technology makes it possible to (1) develop and verify flying quality criteria, (2) extrapolate flight characteristics dependably, (3) optimize aircraft performance efficiently, (4) give engineering and operational simulators more accuracy and higher fidelity, (5) reduce flight test time required to assess aircraft flight characteristics, and (6) provide a data base for improving analytical and wind tunnel estimates.^{106,107}

Flight test determined stability and control data are also used at the AFFTC for aircraft comparison, and verification of contractor compliance with guarantees and requirements such as the Military Flying Quality Specification, MIL-F-8785C.¹⁵¹

Variations in stability and control characteristics also relate to pilot opinions of flying qualities. The term "flying qualities" in this text is used to encompass the subjects of "stability and control" and "handling qualities." This distinction is discussed in detail in Reference 2.

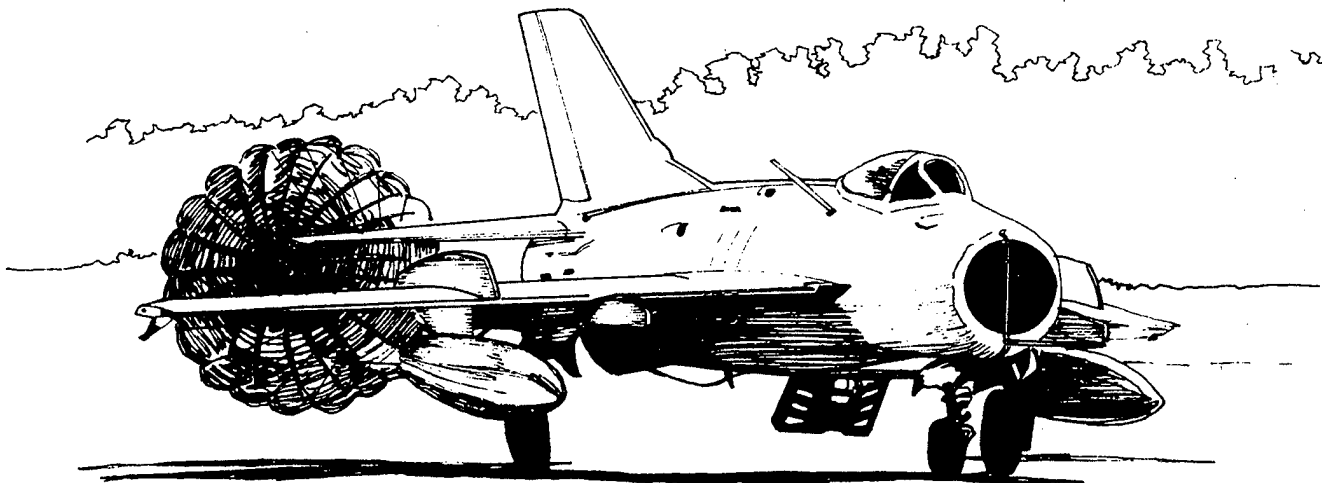
There are many possible approaches to the problem of obtaining flying quality data and the search for more accurate and efficient methods continues. The evolution of techniques has been motivated primarily by the changing nature of the dominant aircraft dynamics as higher performance was attained, and also by the desire to have more effective techniques in terms of improved accuracy, improved efficiency, and reduced costs. Recently, the availability of highly automated data acquisition systems

has enabled the development of techniques to extract useable flying-quality information efficiently. Most flight test organizations now have experience with one or more parameter estimation techniques to determine aircraft stability and control derivatives, inflight characteristics of the control system, or the overall system transfer function.



BACKGROUND

This section traces the key developments primarily in the United States in the technology of determining dynamic aircraft parameters from flight test. Specifically, the discussion will be oriented toward development of the techniques used for the extraction of stability derivatives and the development of flying quality requirements.



In December 1907, the United States Army Signal Corps issued Signal Corps Specification 486 for procurement of a heavier-than-air flying machine. The specification stated, "During this trial flight of one hour it must be steered in all directions without difficulty and all times be under perfect control and equilibrium." This was clearly a flight demonstration requirement.³⁹ The Air Force Lightweight Fighter Request for Proposal in 1972 in addressing stability and control specified only that the aircraft should have not handling qualities deficiencies which would degrade the accomplishment of its air superiority mission.^{92, 108} In response, the contractor predicted that the handling qualities of the prototype would, "... permit the pilot to maneuver with complete abandon."^{92, 109} The requirements placed on the Wright Flyer and the Lightweight Fighter contractor's flying quality predictions were remarkably similar. From these examples, one might assume that the art, or science of specifying flying quality requirements has not progressed since 1907. However, such simplistic approaches to flying quality specification can lead to undesirable results. The F-16 developed for the Lightweight Fighter proposal has been used as a "Lessons Learned" example of how not to optimize and flight test aircraft with highly augmented control systems.¹⁶⁰

The whole problem of aircraft dynamics was put on a rigorous mathematical basis in 1911. British mathematician Bryan introduced the concept of stability derivatives and uncovered the nature of airplane natural frequencies. Bryan's work was the real foundation for subsequent mathematical approaches to the problem of aircraft dynamics.^{4, 6}

In 1912, Baristow and Jones brought the aircraft equations of motion into the usual dimensional form seen today.⁵ They also showed that there were independent longitudinal and lateral-directional solutions. Since then many researchers have nondimensionalized these equations in many ways.⁶

BACKGROUND

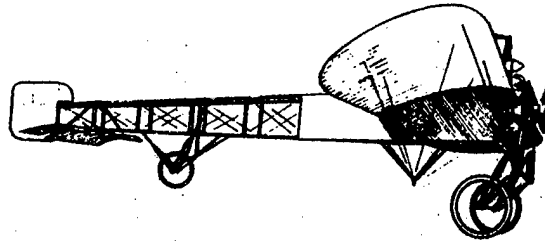
This section traces the key developments primarily in the United States in the technology of determining dynamic aircraft parameters from flight test. Specifically, the discussion will be oriented toward development of the techniques used for the extraction of stability derivatives and the development of flying quality requirements.

In December 1907 the United States Army Signal Corps issued Signal Corps Specification 486 for procurement of a heavier-than-air flying machine. The specification stated, "During this trial flight of one hour it must be steered in all directions without difficulty and at all times be under perfect control and equilibrium." This was clearly a flight demonstration requirement.³⁹ The Air Force Lightweight Fighter Request for Proposal in 1972 in addressing stability and control specified only that the aircraft should have no handling qualities deficiencies which would degrade the accomplishment of its air superiority mission.^{92, 108} In response, the contractor predicted that the handling qualities of the prototype would, " ... permit the pilot to maneuver with complete abandon."^{92, 109} The requirements placed on the Wright Flyer and the Lightweight Fighter contractor's flying quality predictions were remarkably similar. From these examples, one might assume that the art, or science of specifying flying quality requirements has not progressed since 1907.

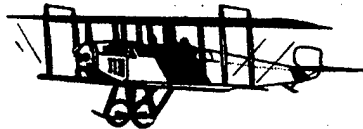
The whole problem of aircraft dynamics was put on a rigorous mathematical basis in 1911. British mathematician Bryan introduced the concept of stability derivatives and uncovered the nature of airplane natural frequencies. Bryan's work was the real foundation for subsequent mathematical approaches to the problem of aircraft dynamics.^{4, 6}

In 1912 Baristow and Jones brought the aircraft equations of motion into the usual dimensional form seen today.⁵ They also showed that there were independent longitudinal and lateral-directional solutions. Since then many researchers have nondimensionalized these equations in many ways.⁶

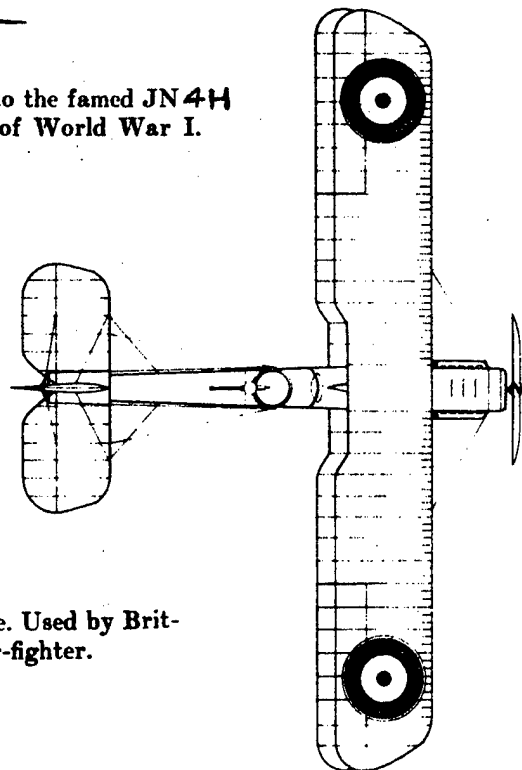
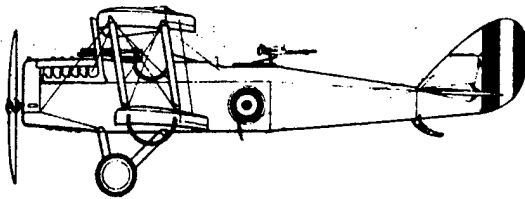
The early days of manned flight are discussed very well in Reference 6. Aircraft of the 1910-1912 time period had inadequate stability, moreover proper levels of stability were not understood.



BLÉRIOT The famed cross-channel model on which Louis Blériot flew the English Channel in 1909 was powered with a 20-25-h.p. Anzani radial engine.



CURTISS The Curtiss JN-2 was predecessor to the famed JN-4H "Jenny." Most famous U.S. training plane of World War I.



DE HAVILLAND D.H.4 400-h.p. Liberty engine. Used by British and U.S. air arms as a long-range bomber-fighter.

Figure 1: Early Aircraft Tested^{90,91}

Early wind tunnel tests during the period 1912-1916 determined that the Curtiss JN-2 and Bleriot Monoplane (See Figure 1) were directionally stable and that they had positive dihedral effect; however, no effort was made to relate control power with basic stability.^{5,7} It was apparent that the investigators had generated considerable data but were unsure how to interpret it. Their principal measures of stability dealt with phugoid damping and spiral convergence. Their conclusion was that an aircraft should have a little stability, but not much. They also stated that the levels of stability required could not be decided upon until there had been correlation with pilot's experience.^{5,6}

One of the first flight tests for stability and control was an NACA program performed in 1919 by Warner and Norton.⁸ These tests were performed on a Curtiss JN4H and on a DeHavilland DH-4. The researchers hoped to correlate the results obtained from flight tests with those obtained earlier from wind tunnel tests on the Curtiss JN-2. It is interesting that the authors again came to the point where, although they recognized that the JN4H was longitudinally unstable and the DH-4 stable, they were not sure of the significance.⁶ The flight test technique used was to determine elevator angle and stick force variations with airspeed change from trim, and to relate these curves to stick-fixed and stick-free longitudinal static stability. This method remains today as the primary test technique for determining compliance with the longitudinal static stability requirements of MIL-F-8785C.^{16,151}

In 1922 Norton and Brown determined the roll control and damping coefficients of a biplane by analyzing the initial and steady-state portions of a rolling maneuver.⁹ Norton estimated the longitudinal static stability and damping coefficients by analyzing data from a combination of static maneuvers and phugoid oscillations in 1923.¹⁰ Soule' and Wheatley appear to be the first to have determined all the major longitudinal stability and control derivatives of an aircraft from flight test

data and compared the results with theoretical predictions.¹¹ The analysis in each of these last two studies used simplified equations representing one-degree-of-freedom motion and solved for one parameter at a time, assuming values for other parameters based on wind tunnel tests or other flight tests.¹² This basic approach was used with only minor changes up to the mid-1940s. In the late 1930s flying quality requirements appeared in a single but all encompassing statement appearing in the Army Air Corps designers handbook: "The stability and control characteristics should be satisfactory."³⁹

In 1940 the NACA concentrated on a sophisticated program to correlate aircraft stability and control characteristics with pilots' opinions on the aircraft's flying qualities. They determined parameters that could be measured inflight which could be used to quantitatively define the flying qualities of airplanes.⁶ At this time, the most important aerodynamic characteristics could be measured inflight with acceptable accuracy by analyzing steady-state conditions.¹² The NACA also started accumulating data on the flying qualities of existing aircraft to use in developing design requirements.

Probably the first effort to set down an actual specification for flying qualities was performed by Warner for the Douglas DC-4 development.⁶ During World War II both research branches of the Army Air Corps and Navy became involved in flying quality development and started to build their own capabilities in this area. An important study headed by Gilruth published in 1943 was the culmination of all of this work up to that time.¹³ This study was supplemented by additional stability and control tests conducted at Wright Field under the auspices of Perkins.¹⁴ Shortly thereafter the first set of Air Corps requirements were issued as a result of joint effort between the Army Air Corps, the Navy, and NACA. At the same time the Navy issued a similar specification. These specifications were superseded and revised in 1945.^{15,39} Perkins also published a manual which

presented methods for conducting flight tests and reducing data to demonstrate compliance with the stability and control specification.¹⁴ This manual published in 1945 is remarkably similar to the flying quality handbook currently in use at the USAF Test Pilot School.¹⁶

As higher performance aircraft were being developed during the 1940s the nature of aircraft dynamics affecting longitudinal flying qualities was changing. A comparison of the discussions of Soule¹² in 1940 and Phillips in 1949 shows that the dominant characteristic shifted from the phugoid mode in 1940 to the short period mode in 1949.^{12,17,18} In fact, in 1945 Perkins concluded that the damping of the phugoid had no correlation with the pilots' judgement and emphatically stated that flight tests of this mode were not required; however, the short period was troublesome. Stick-fixed short period oscillations were normally heavily damped, but the damping of stick-free oscillations was often reduced to a point where it could be objectionable to the pilot. It was termed "porpoising" or "elevator snake" by pilots during those days and unfortunately was sometimes accompanied by a very rapid oscillation of the elevator about its hinge.¹⁴ This was an early encounter with what is presently defined as control system oscillations. About this time it was also discovered that current techniques were inadequate for determining stability derivatives from short period data for heavily damped oscillations. Milliken pointed out in 1947 that the increasing use of automatic control systems required more accurate modeling of the aircraft dynamic characteristics.¹⁹ In 1948, the accumulated experience of the war and early post-war years was used to update the military flying quality requirements.^{20,39}

The motivation to improve the accuracy of flight test results stimulated the development of techniques for determining stability and control characteristics from flight data. In the late 1940s through the mid-1950s, servomechanism theory was expanded rapidly, and the frequency-domain

techniques of Nyquist and Bode became popular. It was a natural extension to use frequency-response techniques for determining the dynamic characteristics of an aircraft from flight test data. The first approach was to obtain a frequency response inflight by oscillating the aircraft, using the autopilot, at discrete frequencies and measuring the steady-state amplitude ratio and phase angle between the control surface and pitch rate.^{12,19} This was further investigated in 1966 on test programs at the AFFTC and in 1967 at the USAF Test Pilot School.⁵⁵ At the School, data were taken by pilots oscillating an F-104A aircraft manually in-phase with a timed tone broadcast from the ground. A disadvantage of this approach was the considerable flight time required to sweep through all the frequencies of interest at each flight condition. Seamans used a method for determining the aircraft frequency response from a single transient response maneuver by Fourier analysis, and Greenberg discussed several frequency-response methods in Reference 22.^{21,83} If the aircraft frequency response or transfer function is the final result desired from flight test, these methods are appropriate; however, if stability derivatives are needed, another step must be taken to obtain them from the measured frequency response.^{12, 19, 23,96,97,98}

Because the problem of determining stability and control derivatives was based on a linearized, small-perturbation model of the aircraft dynamics, it was natural to consider using a linear least-squares fit of flight data to the linearized equations of motion as Greenberg did in 1951.²² In 1954 Shinbrot developed a generalized least-squares method which encompassed the earlier least-squares methods and had a greater potential.²⁴ A real drawback to these methods at that time was that they involved extensive calculations which had to be done by hand, because digital computers were not yet available. Furthermore, it was desirable to "fit" the equations at many time points in order to obtain good accuracy; this meant that a large volume of data had to be processed manually from photopanel film or oscillograph recordings. A fundamental problem with linear least-squares methods is that noisy measurements result in biased estimates of the

stability derivatives. However, the general lack of acceptance of the methods was attributed more to the difficulty of applying them than to concern over biased estimates.¹²

A rather simple technique was often used in the 1950s for determining the longitudinal short-period parameters. This technique is still adequate for many situations. When the short-period mode frequency is much greater than the phugoid frequency and the damping ratio is low (less than 0.3), the primary short-period mode stability derivatives can be estimated directly from measurements of the frequency, damping, and amplitude ratio of normal acceleration to angle of attack.^{12,25,26} Similar approximate methods were not satisfactory for the highly coupled lateral-directional dynamics, but an effective graphical technique developed by Doetsch was used extensively. These techniques were straight-forward and not difficult to apply but required ideal, free-oscillation maneuvers.^{12,27,28}

Reference 29 summarizes four different methods used at the AFFTC for obtaining damping ratio and natural frequency from aircraft oscillations. These are: logarithmic decrement, time ratio, maximum slope, and curve matching using film. The logarithmic decrement (subsidence ratio method) can be used to analyze the response of lightly damped (damping ratio less than 0.5 preferably less than 0.35) oscillations. The time ratio method is based on calculations by Trimmer and is used for heavily damped systems (damping ratio greater than 0.6).^{29,30} These two methods are in current use at the USAF Test Pilot School.¹⁶ Obviously there is a gap from a damping ratio of 0.35 to 0.60 which cannot be analyzed accurately by either method. In fact, in practice with typical flight test instrumentation, neither of the above methods is particularly accurate at any damping ratio. This fact will be attested to by most USAF Test Pilot School students who have attempted to reduce dynamics data. The maximum slope method was found in Reference 29 to be useful only for heavily damped systems and accurate only around natural frequencies of one radian/second.^{29,31} The remaining

method which was developed in Reference 29 was a curve matching method using photographed time histories of flight data on a film reader. By matching the computer response recorded on film with the aircraft response, the damping ratio and frequency could be obtained. Of the four methods discussed, the film curve matching was found to be the best.²⁹ This method appears to be the natural predecessor to a technique called analog matching.

As aircraft performance reached progressively higher Mach numbers, the damping decreased to such low values that at times it was too risky to obtain test data without the damper systems turned on. Attempts were made to correct for the effect of the damper system, but the empirical approach used left considerable uncertainty in the results. Basically, these simple techniques were applicable only if there were no pilot or automatic control system inputs during the free oscillation.³²

An analog matching technique was used to overcome the problem of poorly conditioned (those with unplanned extraneous inputs) maneuvers.^{32,53} It is a manual curve-fitting technique in which an analog computer is used to compute the response of a model. This response is then matched to the flight measured response by adjusting the stability and control derivatives of the model. This approach was not a spontaneous development for determining derivatives but was, rather, an outgrowth of the use of analog computers as flight simulators. Analog matching was used as early as 1951 to check aircraft parameters determined by other methods. Even though the technique of analog matching has been greatly improved, the accuracy of the results is highly dependent on the skill of the individual operator. Furthermore, it can take an excessive number of man-hours to obtain an acceptable solution if several parameters are to be determined.^{12,33,34}

The best techniques available for stability derivative extraction up to 1966 are reviewed by Wolowicz in Reference 35. Progress in the development of military flying quality specifications is well documented in

References 36 and 39. Work on the current MIL-F-8785C was started in 1966, with publication in August 1969 as MIL-F-8785B (ASG). The specification was revised in 1974 and again in November 1980 with the title change to MIL-F-8785C.^{3,151} Reference 36 is a document written to explain the concept and arguments upon which the current requirements were based. Data reduction techniques recommended to determine military specification compliance are essentially those already described and presently in use at the USAF Test Pilot School. The School was actively involved in the development of MIL-F-8785B (ASG), and its first use was by students evaluating their data group aircraft (T-33A, T-38A, and B-57) against specification requirements. The first use of MIL-F-8785C was by students of Class 81A evaluating the T-38A, F-4C, A-7, and KC-135.

The School also participated in the effort to develop MIL-F-83300 which places flying quality requirements on piloted V/STOL aircraft.³⁷ Reference 38 is a companion background document for this specification. No effort was made to evaluate the School's H-13 helicopters against specification requirements.⁶⁸

Two factors caused a revolution in parameter estimation techniques starting in the mid-1960s: (1) Highly automated data acquisition systems were becoming standard in flight testing, and (2) large-capacity, high-speed digital computers were available to solve complicated algorithms efficiently. The ability to transfer the flight data directly to the computer with no manual operations on the data and the availability of high-speed computation permitted techniques to be considered that were previously impractical.¹² Though seldom mentioned in recent literature, in 1951 Shinbrot developed the concept that is fundamental to many contemporary techniques.⁴⁰ At that time, however, it was not practical to use his concept, which involved manually computing the numerical minimization of a nonlinear functional. An application to the simplest flight-test problem of determining only four longitudinal parameters took up to 24 hours.¹²

Interest in parameter estimation was renewed in 1968. Larson applied the method of quasi-linearization at Cornell Aeronautical Laboratory, and Taylor and Iliff applied basically the same method, but referred to as the modified Newton-Raphson technique.^{41,42,43} The latter technique was based on the theoretical works of Balakrishnan.^{44,45,46} There have been numerous parallel developments since then in universities, private research companies, and major aircraft companies, as well as at Air Force, Navy, and NASA installations (References 47 to 52).¹²

In 1973, at the AFFTC, two techniques were available for the extraction of stability derivatives from short duration dynamic maneuvers (normally control system doublets). These techniques were known as hybrid matching and Newton-Raphson. Both techniques using their associated computer programs could analyze maneuvers with stability augmentation system either ON or OFF. Hoey discussed various factors which influenced the aerodynamic stability derivatives and the methods which could be used for isolating these factors by proper test planning in Reference 54. With a judicious selection of flight test conditions a great deal of knowledge of the stability derivatives and military specification compliance can be gained in a relatively small amount of test time.

The stability derivative extraction program presently used at the AFFTC is known as the Modified Maximum Likelihood Estimator (MMLE) program and is based on the work of Iliff, Maine, and Taylor of the NASA Dryden Flight Research Center.^{43,56,57} This method which has been used by the Dryden Center since 1966 has become the primary technique for extracting stability derivatives from flight test data. NASA Dryden has performed nearly 3,000 derivative extraction flight maneuvers in 30 aircraft types. Recent NASA studies have been made on maneuvers performed with the Beech 99, Minisniffer, B-1, F-15, F-17, oblique wing aircraft, and shuttle carrier Boeing 747 aircraft with and without the shuttle vehicle.^{58,59}

The interfacing necessary to use this NASA program at the AFFTC was performed by Nagy. In addition, he has written a report which provides a handbook for operating the digital programs required for analysis and for understanding the results. Setup, operation and output is discussed for both the stability derivative extraction program and a characteristic analysis program. The essential information required to conduct a successful stability and control test program using this approach is included in Nagy's report, Reference 60.

Over the past several years the MMLE program has been used on most major AFFTC test programs. Some of these are the X-24B, YF-16, YF-17, A-9, A-10, YC-14, YC-15, F-16, and B-1. The uniqueness of MMLE application at the AFFTC has been in its use as a production analysis tool. By 1978, the AFFTC had processed more than 1,500 flight maneuvers using the MMLE program. This parameter identification experience was summarized by Maunder in Reference 106. One of the most recent applications of the MMLE program was analysis of the Space Shuttle Orbiter during the first orbital flight where stability and control derivatives were obtained at Mach numbers as high as 24.4.¹⁵⁸

Probably the most concentrated effort to date to correlate stability and control derivatives determined by analysis, from wind tunnel testing, and from flight testing was made during the Transonic Aircraft Technology (TACT) F-111A supercritical wing program. This correlation task was conducted jointly by NASA and the USAF. NASA Dryden conducted the flight test program and extracted stability and control derivatives from flight test data using the MMLE program. Both NASA Dryden and the Air Force Flight Dynamics Laboratory (AFFDL) analyzed wind tunnel data and ran computer programs for determining derivatives analytically. The AFFDL also analyzed flight test data for MIL-F-8785B (ASG) compliance and determined flying qualities characteristics such as short period and Dutch roll natural frequency and damping ratios. Comprehensive analysis of this large experimental data base has not yet been published; however, the AFFDL has already concluded that flying quality parameters obtained from MMLE determined derivatives can be considered interchangeable with measured values.¹¹⁰

THE FLYING QUALITY SPECIFICATION DILEMMA

Formal discussions of aircraft flying qualities almost always revolve about the military document MIL-F-8785C.¹⁵¹ This flying quality specification focuses almost entirely on open-loop vehicle characteristics in attempting to ensure that piloted flight tasks can be performed with sufficient ease and precision; that is, the aircraft has satisfactory handling qualities. This approach is quite different from that used in specifying the acceptability of automatic flight control systems, where desired closed-loop performance and reliability are specified. This occurs despite the fact that most flying quality deficiencies appear only when the pilot is in the loop acting as a high-gain feedback element.¹⁵⁴

Since the introduction of MIL-F-8785C, there has been an increased emphasis on the analytical aspect of flying quality analysis.¹⁵¹ This current military specification is the first version to address higher-order control systems by placing requirements on allowable aircraft response time delay following a pilot input, and allowing the use of an equivalent system for aircraft response analysis.

Determination of stability and control derivatives from flight test data provides an accurate basis for airframe analysis. On the other hand, the importance of precision tracking to the development and evaluation of flying qualities suggests that the specification could be rewritten in terms of performance standards during prescribed tracking tasks. This approach raises a long-standing controversy. Should the specification be oriented more toward providing design guidance by placing requirements on design parameters, or should it be oriented toward requiring flight test demonstrations? Currently the specification contains elements of both philosophies, and perhaps a clear dichotomy can never be made.⁸⁹ In the current period of rapid technological change, it is impossible for a specification to anticipate future flying quality requirements so long as it remains rooted in the empirical practices of the past. An additional handicap is that a physically realistic theory for handling qualities is lacking.¹⁵²

The existence of handling qualities as an entity stems from the human pilot's unique abilities as both an adaptive and a verbal control system element; that is, he can effectively comment on the relative ease and precision with which a task can be performed in a reasonably unambiguous manner.¹⁵⁴ This task-related nature of handling qualities is now popularly recognized. However, for modern flight control systems concepts, it is not clear just what the critical pilot tasks will be; therefore, how can sufficient data be collected to develop design criteria for such fly-by-wire or higher-order control systems? A complicating factor is the changing nature of air warfare tactics as a result of the changing threat, improving avionic capability, and the increasing functional integration of hardware and aircraft subsystems.¹⁵²

The search for an alternative approach to the specification of aircraft flying qualities has been going on for some time. The difficulty is in developing a physically sound approach which is acceptable to the military services and to those contractors who must design to stated requirements.¹⁵² The current attempt to define an approach is an Air Force Flight Dynamics Laboratory funded effort by Systems Technology Incorporated to develop a military standard for flying qualities to replace the present MIL-F-8785C. Reference 160 is a preliminary copy of this standard and its associated handbook.

Airframe-flight control control system dynamics which look "good" with respect to the classic measures of systems response are useless if the pilot cannot accomplish intended tasks with acceptable performance, or if flight safety is compromised by pilot-vehicle dynamic mismatches. This is happening with increasing frequency as control systems become more complex. Design mistakes happen too often with reasonably conventional control systems; however, the opportunity for errors in both concept and execution is vastly increased with digital flight control systems. A further complication is that digital technologists generally belong to one of two clubs: the software club or the hardware club. Stories are legion about the problems of systems design and operation due to poor or nonexistent communications between these two groups and the design interface problems that can result from one group's failure to adequately address the needs of the other.¹⁵²

Historically, an attempt has been made to avoid specifying requirements on the pilot-vehicle combination because of the reliance of such requirements on pilot skill, experience, and background. These variables can and have led to inconsistencies in evaluating the degree of compliance with such requirements. It is further felt by the AFFDL that specifying flight test objectives or demonstrations would leave unanswered the question of how to design a flight control system capable of meeting those objectives. The approach taken in developing MIL-F-8785C was based on the obvious premise that if aircraft flying qualities are going to be judged in closed-loop tracking, then the specification should provide guidance and requirements oriented toward developing an aircraft which will exhibit good flying qualities during tracking.^{89,151}

The greatest single deficiency in many test programs conducted on aircraft with advanced flight control systems is the lack of consideration given to the overall systems integration of specific hardware approaches to control system design. The problems of prototype hardware design, man-rating, and the difficulties and expense of flight test, appear to have almost completely overridden considerations of experiments designed for the collection of handling qualities data. In part, this has resulted from the lack of any unifying plan for research for this purpose. It is comparatively easy to build and test equipment; handling qualities problems, in contrast, are depressingly elusive to classify or quantify and expensive to evaluate. No one has ever successfully quantified the benefits to weapons systems effectiveness or flight safety of good handling qualities. The quarrelsome handling qualities "community" can never--except for extreme cases--agree about what constitutes good or poor handling qualities. Since major research and development test programs, whatever their original objectives, inevitably become cost and schedule driven, it is not difficult to understand why so much testing is done with so little impact on the handling qualities state-of-the-art. However, it is difficult to understand how reasonable and timely advice to flight test managers about handling quality test requirements can be ignored. This has

happened in the recent past to the detriment of present hardware design, test capabilities, and weapons system effectiveness.¹⁵²

It does appear that the potential for interaction among weapons employed, display, and flight control is now widely recognized. The notion that clever display design can remedy deficiencies in airframe-flight control system dynamics is no longer as radical as it once seemed. More important, it now seems to be fashionable to consider that handling qualities can be affected as much by display design as by the airframe or the flight control system.¹⁵² Students here at the School have found this to be the case during A-7 DIGITAC evaluations.¹⁵⁷

The field of pilot-vehicle system analysis includes pilot mathematical modeling and prediction of system dynamics and performance. Literature in this field has concluded that although they are closely related, neither the pilot-vehicle system dynamic response nor system performance necessarily completely defines handling qualities. Analysis methods which predict dynamics and performance of a pilot-airframe-flight control system combination do not lead automatically to the prediction or assessment of handling qualities.^{152,153} As a result, an adequate physical theory for predicting pilot rating does not exist. This is mainly due to the fact that the attribute which makes the pilot such a valuable asset in the aircraft, that is, his adaptive capability, tends to frustrate attempts to provide a mathematical pilot model with sufficient accuracy and broad enough applicability to be useful to the control system designer. This is particularly true in cases which require a multivariable system representation.¹⁵⁴

A useful physical theory for predicting pilot rating requires an adequate mathematical model for pilot dynamic response. Some of the earliest efforts at including pilot models in handling qualities research were made by Westbrook, McRuer, and Ashkenas.^{155,156} Attempts at developing such a mathematical model are documented in Reference 154. A recently developed handling qualities theory by Smith has as its basis a nonlinear pilot mathematical model. Although this model is inadequate in many respects, it has been used to generate useful criteria for the prediction of Pilot Induced Oscillations (PIO).^{153,154}

Several empirical methods for handling qualities prediction do exist. The better known of these are: C*, TRP, CAP, Neal-Smith Criterion, McPilot, Paper Pilot, and Equivalent Systems by Mayhew. The first three are time response methods; they relate handling qualities to parameters of aircraft time response. The others are frequency response methods; they use a model for pilot dynamics, perform a loop closure and use the results for handling qualities prediction. These methods are discussed in Reference 152; however, it is worth repeating that the capability for predicting or measuring aircraft or system dynamics does not imply that accurate estimates of handling qualities will necessarily follow.¹⁵²

The current MIL-F-8785C uses an equivalent systems approach for higher-order control systems based on recommendations by Mayhew; however, this approach has been attacked as creating as many problems as it solves. It is not clear that if an aircraft's "equivalent system" meets MIL-F-8785C requirements, adequate handling qualities will result.¹⁵²

Analysis methods based on the Neal-Smith criterion and C* are in routine use at various companies to develop aircraft flight control systems. There is a clear and pressing need for methods of this character. The simplicity of the time response methods, in particular, has a tremendous appeal for use in design studies; however, the specification of aircraft control system design requirements is an altogether different problem from that of designing an aircraft to have acceptable handling qualities. This is not a popular viewpoint, but the prevailing alternative viewpoint is responsible for much of the current specification dilemma for advanced flight control systems.¹⁵²

The flying quality specification is a design guide of sorts, but to view it only in those terms is to ignore the reasons why such specifications exist. The intent of MIL-F-8785C was to insure the desired performance of the pilot-vehicle system. This, however, is not easily done in any quantitative sense without prior identification of a physical, measurable description of handling qualities. There is, as yet, no satisfactory measure for handling qualities other than pilot opinion rating; but for reasons previously mentioned, it has not been an acceptable metric for use in a design specification.¹⁵²

The philosophy of MIL-F-8785C rests upon the implicit use of pilot opinion rating to "map" airframe dynamic parameters into regions of acceptable or unacceptable handling qualities. This approach has never been entirely successful; exceptional cases, at both extremes, which violated MIL-F-8785C and its predecessors have always existed. The relationships between handling qualities and modal response parameters of the classic aircraft (ζ_{sp} , ω_{sp} , etc.) have been empirically derived with some general guidance from the technology of pilot-vehicle systems analysis. The problem, in essence, is that a reliable method for the prediction of pilot opinion rating has not existed.^{152,153}

It is generally true that the development of engineering specifications for something so elusive as handling qualities has been an art form; however, there is no basis for believing that Cooper-Harper ratings--properly obtained-- are not adequate measures of handling qualities. Pilot opinion rating is the only acceptable, available method for handling qualities quantification.¹⁵²

In fact, in current literature, pilot opinion rating is considered to be synonymous with handling qualities.¹⁵⁴ The Cooper-Harper scale has its deficiencies; they are not restrictive so long as the evaluation pilot is well indoctrinated in the use of the scale and an adequate experimental design is provided. Pilot ratings then, are the important dynamic parameters in the determination of handling quality adequacy.

Military flying quality specifications have been failures as "requirements." That is, they have not recently (at least since 1970) been used as procurement compliance documents. They have served as historical records since their authors have honored "successful" aircraft designs by modifying the specification after the fact to permit any noncompliance the aircraft exhibited. They have also been found useful for test pilot and flight test engineer training since the somewhat less than modern stable of aircraft in the test pilot school inventories is part of the specification's data base.

CURRENT DYNAMIC CLOSED-LOOP FLIGHT TEST METHODS

The AFFTC has attempted to optimize aircraft flight control systems to operational requirements for fighter and ground attack aircraft by using tracking test techniques commonly referred to as Handling Qualities During Tracking (HQDT).

HQDT is a technique developed at the AFFTC in 1971 for obtaining pilot ratings and qualitative comments from precision tracking maneuvers.¹¹¹

Another technique, System Identification From Tracking (SIFT) offers one potential solution to the problems of identifying the inflight characteristics of the control system and the bare airframe characteristics while the stability augmentation system is operating. The most important characteristics of the SIFT test techniques are that they are pilot-in-the-loop, mission oriented techniques, and that they provide quantitative as well as qualitative results. The SIFT maneuvers are precision air-to-air tracking, formation flying, and air refueling. Data from these maneuvers are analyzed in the frequency domain to provide multiple frequency response transfer functions, Laplace domain transfer functions, spectral characteristics, and coherence functions. The flight control system, bare airframe, and overall system transfer functions can be identified with a high level of confidence. These quantitative results can be correlated with pilot ratings and qualitative comments. While the SIFT technique is still in its infancy, sufficient experience has been gained to confirm its value.¹⁰³

The USAF Test Pilot School has been emphasizing the importance of air-to-air and air-to-ground tracking tasks for operational flying quality evaluations for several years. Currently, HQDT, and SIFT techniques are used in the School's Systems Test phase for evaluations performed in the Calspan variable stability NT-33A and in the A-7D DIGITAC multimode digital flight control system aircraft. Hopefully, the training and experience gained by test pilot students evaluating these aircraft will enable them to provide consistent pilot opinions in their future test programs. The "processing" and analysis of pilot opinion data is also emphasized to both pilots and engineers during flying quality courses at the School.

FLYING QUALITIES TODAY

The current MIL-F-8785C represents an attempt to address the realities of present and probable near-term future aircraft design approaches. Aircraft are not designed entirely on paper prior to their manufacture; the engineering flight

simulator has become an important tool for system design, test and evaluation. Analytical predictions of aircraft flying qualities and pilot-vehicle closed-loop system dynamics should play a vital role in the earliest stages of aircraft conceptual and preliminary design; however, they are preliminary in the sense that the impact they have on design is primarily qualitative. The quantification of an aircraft or flight control system design ultimately requires pilot-in-the-loop test and evaluation. The specification is based on the premise that both analysis and simulation will be used in a coordinated, sequential, and probably iterative fashion to predict and experimentally assess the implications to flying qualities of airframe and control system design trade-offs.^{89,151}

As discussed, there is still a general misconception about the use of pilot-vehicle systems analysis for the identification of suitable flying quality parameters, and the use of analytical prediction methods for the derivation of criteria for aircraft control system design. Methods developed which allow the prediction of flying qualities have had very little impact on either handling qualities prediction or on the flying qualities specification. The basic reason for this failure appears to be due to the belief by proponents that analysis methods can replace pilot opinion and flying quality specifications. They can do neither. "Paper pilot" and other analysis methods will never replace pilot opinions as long as control system technology keeps becoming more complex. The specification is a buyer's guide while pilot-vehicle analysis methods should be used for the development of design methods and for developing detailed control system design specifications.

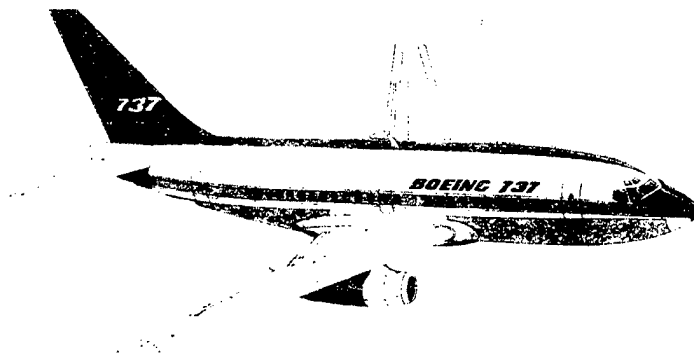
At a recent flying qualities symposium sponsored by the AFFDL, anxiety was expressed over some of the new requirements in MIL-F-8785C for which flight testing to demonstrate compliance would be extremely difficult or time-consuming. Requirements related to atmospheric disturbances were of particular concern. However, flight testing has always been a pragmatic occupation. That certainly holds with flying qualities testing.¹⁴⁹ As was true when MIL-F-8785B (ASG) was introduced, probably the best "laboratory" for developing new flight test techniques and modifying old techniques to check new specification requirements is the USAF Test Pilot School. This process is under way at the School thru student evaluation of data group aircraft against the requirements of MIL-F-8785C.

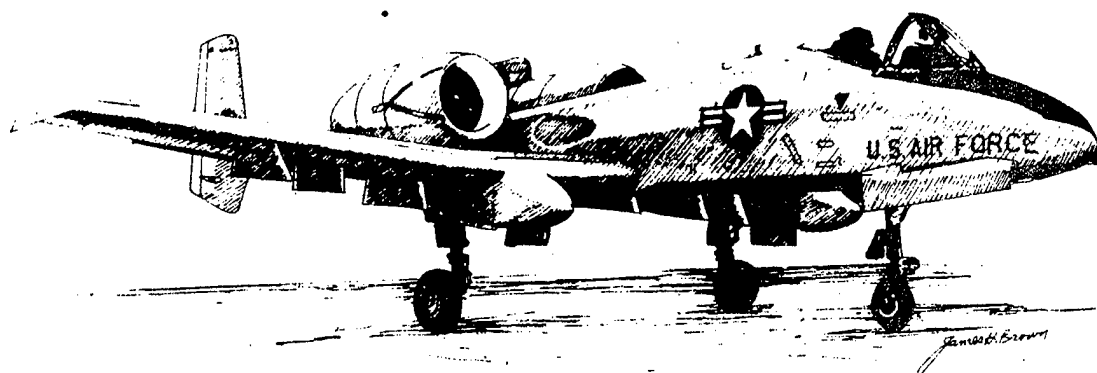
Since the first Army Air Forces flying quality specification in 1943, and in all the years since, no flight test program has ever thoroughly checked all the basic flying qualities of any test aircraft. A list of significant problems which impact on the extent of flying quality testing would include: sensor and data recording availability and capability; data reduction support availability; engineering manpower limitations; flight safety consideration; funds availability; test aircraft availability; configuration or subsystem changes during the test program; urgent development problems with other parts of the aircraft; emphasis on operational aspects of flight test--the list seems endless. The complexity of a contemporary flight control system itself may preclude flight test evaluation of all "probable" failure modes.¹⁴⁹ However, the approach taken recently at the AFFTC where failure state testing of a higher-order control system was totally ignored is not the answer. The statement in the F-16 flying qualities final report that, "Failure state testing was not investigated during this evaluation" will be little consolation to the operational pilot who becomes an instant "test pilot" when some mode of his flight control system fails.¹⁵⁹

Another aspect of fly-by-wire or high authority flight control systems that has scarcely been considered is the effect of control system saturation on handling qualities, flight safety, or any restrictions to the flight envelope. Control saturation, particularly with an aerodynamically unstable airframe, could easily lead to loss of control or PIO. It appears that the requirement exists to develop design specifications to avoid control saturation or loss of control if it does occur.¹⁵²

Currently, flight test costs are up, flying hours are down, and emphasis has shifted from engineering evaluation to investigation of conditions approximating operational use. In this climate, optimized flight test techniques are required to extract the greatest quantity of most-needed flying qualities data in the available flight test time. There is no hope of a flying qualities evaluation of the type and scope of AFFTC's Phase IV evaluations of earlier years.¹⁴⁹

While parameter estimation techniques will never replace pilot ratings or flight test time history records of aircraft response for some analysis purposes, they are seeing more widespread acceptance and application.¹⁴⁹ Even the AFFDL has concluded that MMLE and SIFT flight test techniques used at the AFFTC and described by Maunder and Twisdale result in accurate well-documented results which can be used to correct the aircraft designer's stability and control predictions to obtain a valid analytical model.^{106,149,150}





SECTION 2

SYSTEMS IDENTIFICATION AND PARAMETER ESTIMATION

INTRODUCTION

Parameter estimation techniques are methods used in systems identification problems. The general problem of systems identification (Figure 2) is to determine certain characteristics of the physical system from experimental test data. Measurements are made of external inputs and resulting output responses that depend in some way on the system characteristics to be determined. There may also be external disturbances that cannot be measured directly. Systems identification is the process of estimating the characteristics from the input/output measurements. Usually something is known beforehand about the system, such as the set of equations that describes its dynamic responses and approximate values of the forces and moments on the system. However, systems identification theory also includes the situation in which nothing is known except the input/output measurements.¹²

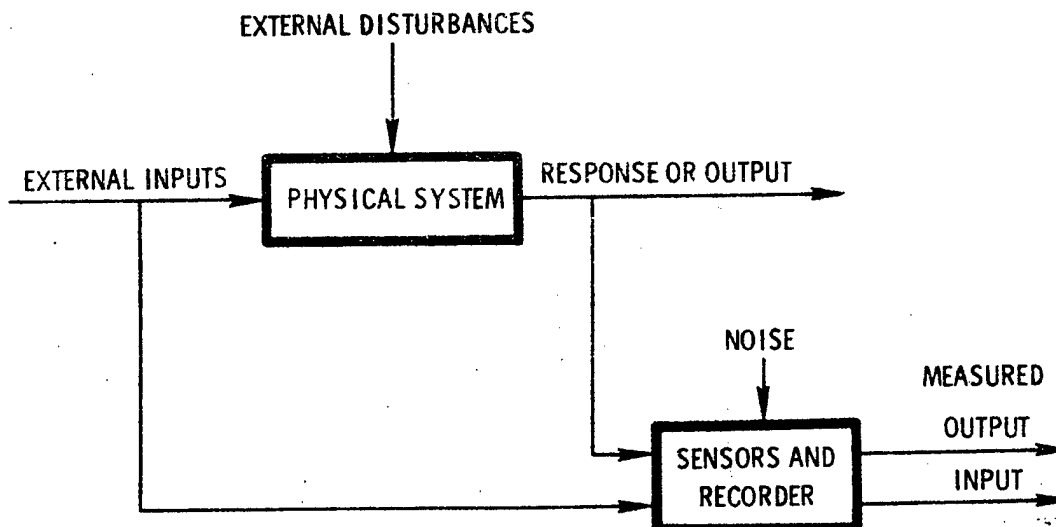


Figure 2: General Systems Identification Problem
(From Reference 12)

Stated in this way, it does not take much sophistication to realize that the problem has no solution, or too many solutions depending on the point of view. The outcome of any identification exercise is a bunch of numbers which can never really be verified. This is contradictory to the way in which most engineering practice proceeds. Fortunately, engineering problems involve obtaining operational, or useful answers whose validity is ultimately decided by their successful use in actual practice.¹⁴³

SYSTEMS IDENTIFICATION

Systems Identification is a very wide notion and different authors use it in slightly different ways. For practical purposes, systems identification can be described as the determination of the mathematical model of a process which is to be controlled.¹⁴⁴

From the mathematical point of view, experimental systems identification can almost always be considered as a problem of finding extrema of functionals. The form of the functional, the extremum of which is to be found, is given by the criterion accepted for the systems identification problem and by the mathematical model of the system. The accepted criterion for identification and the mathematical model of the system are the most significant features of every systems identification method.¹⁴⁴

In the 1960s there were attempts to describe all systems in terms of their input/output pairs alone. To be able to do this the concept of "state" was introduced. The notion of state had to be independent of any dynamic,

thermodynamic, or other principle. Although the introduction of a "state space" concept failed to live up to initial expectations, it did effect conceptual understanding. In particular, it emphasized the "time-domain" approach which was in turn helped by the fact that digital computation needs such a description.¹⁴³

At the basic level of starting from scratch to build a system, modern theories offer little. At present it is not known how to describe systems solely in terms of input/output data except for trivial cases. This is due largely to the fact that in general, the same input gives rise to many outputs.¹⁴³ Put another way, this means that many systems can be generated from a set of input/output pairs.

In practical systems identification problems the equations of a system may often be postulated on the basis of a priori knowledge of the structure and physics of the system.^{112, 143} Practical uses for systems identification techniques today are for finding better answers to already "solved" problems and for solving a restricted class of unsolved problems. The problem that has received the most attention is one in which the form of the system dynamics is known, input and noisy output data are available, and only the values of unknown model parameters are sought.¹¹³ The toughest problems are those where the system dynamics are unknown.

Practical aeronautical problems for which solutions are still needed are sometimes called systems with high levels of internal fluctuations. These systems typically have two types of behavior. The particular type

which exists is determined by the magnitude of a controlling parameter which influences stability. For a finite range of parameter values the system is stable and its structure may be described by a deterministic set of differential equations. If not subjected to external disturbances the system will achieve a state of equilibrium; however, at some "critical" value of the parameter the system becomes unstable and beyond this boundary the system no longer achieves a state of equilibrium but may exist, as a result of nonlinearities, in a steady state typified by continuous fluctuations. This state may be either limit-cycle type of oscillations or essentially random in nature.¹¹⁴

The following items which are areas of interest to the AFFDL are examples of systems identification problems where the system has high levels of internal fluctuations:

1. Stability and control parameter estimation for rigid and elastic aircraft.
2. Extension to stall/spin aerodynamics of rigid aircraft using a non-linear model.
3. Application to human pilot model identification.
4. Correlation of analysis with wind tunnel, drop model, and flight test data.¹¹⁵

Item 4 should more properly be called a parameter analysis problem rather than a systems identification problem.

The literature on systems identification is quite extensive. Reference

144 lists basic papers written prior to 1969 during the systems identification technical paper "explosion" of the early 1960s.

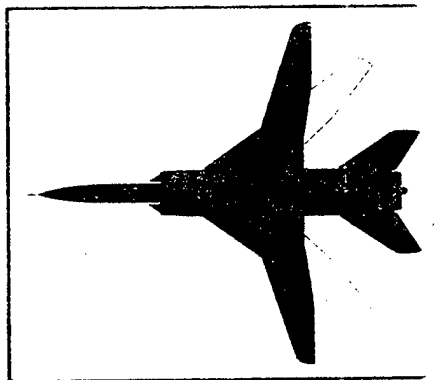
Sometimes in reading the literature, one gets the impression that the discipline of systems identification is an attempt to more-or-less formalize existing analytical and research techniques which have been historically known as the "scientific method." As an analysis technique, systems identification has the potential for wide use; however, it can easily be oversold.¹⁴³

Several theorems will be offered in this text to try to illustrate some of the key points of systems identification and parameter estimation theory. They are most likely not mathematically correct. The first three follow:

THEOREM I: If the input/output of a linear, time-invariant system is observed with a "sufficiently exciting" input then the system transfer function can be determined.

THEOREM II: The transfer function found in THEOREM I is unique.

THEOREM XX: It is easier to write an abstract technical paper than to do anything concrete.¹⁴⁵



LEADING DATA

Powerplants 2 x Kuznetsov NK-144 turbofans; 28,500lb thrust (127kN) dry, 45,000lb thrust (200kN) reheat

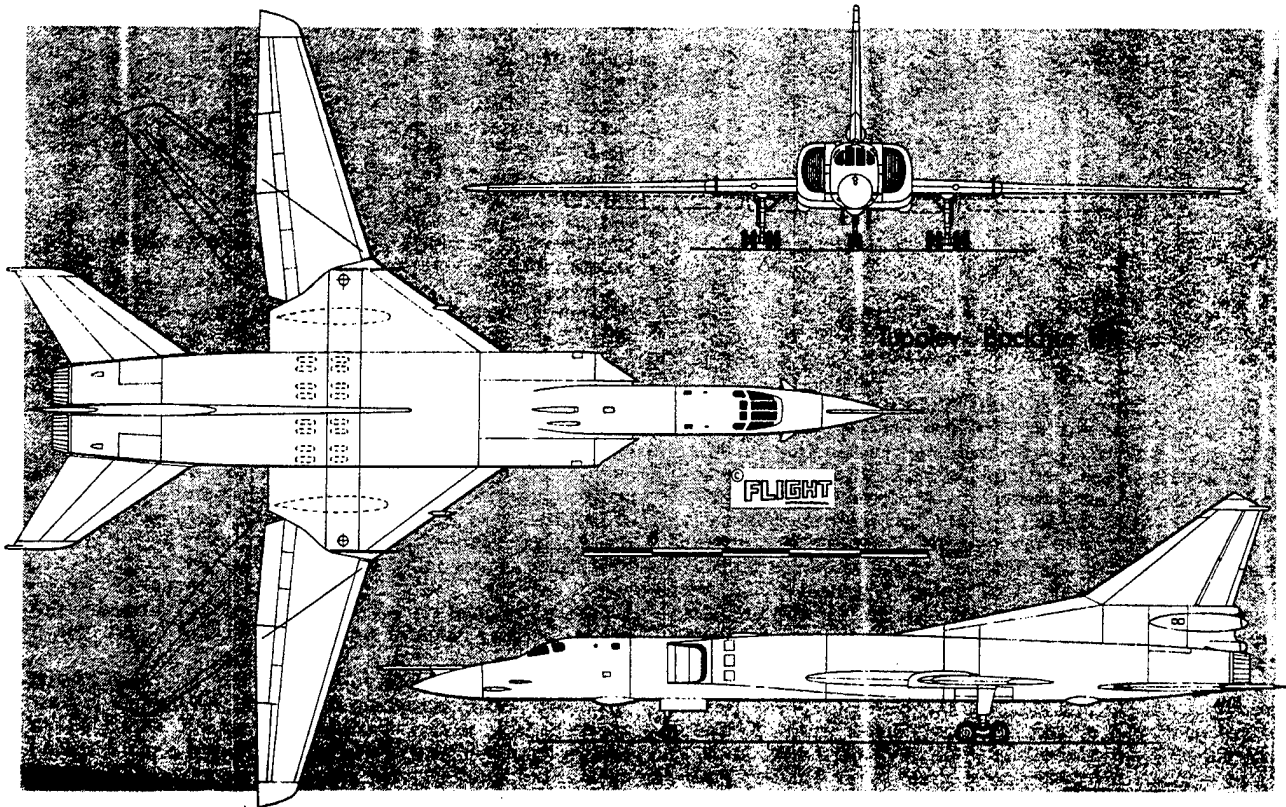
Dimensions Span 113ft/86ft (34.5m/26.2m) Length 132ft (40.2m) Height overall 30ft (9.1m) Gross wing area 1,785ft² (166m²)

Weights Operating empty weight 110,000lb (50,000kg)

Basic internal fuel capacity 105,000lb (47,500kg)

Maximum take-off weight 245,000lb (110,000kg)

Performance Maximum speed at 50,000ft (15,000m) Mach 1.8-2.0 clean, Mach 1.5 with two AS-6 Kingfish ASMs Cruising speed at 35,000ft (10,500m) Mach 0.8 Cruising speed at sea level Mach 0.65



PARAMETER ESTIMATION

Parameter estimation techniques can be applied to numerous aircraft flight testing problems. Traditionally they have been used for the determination of stability and control derivatives. There are current efforts being made at the AFFTC in the DyMoTech program to apply parameter estimation techniques to the dynamic determination of aircraft performance data.

There are several approaches to solving systems identification problems, and all are strongly influenced by the amount and type of a priori knowledge available. Parameter estimation techniques are the most common approaches. The general concept is illustrated in Figure 3 for a flight-test situation.¹²

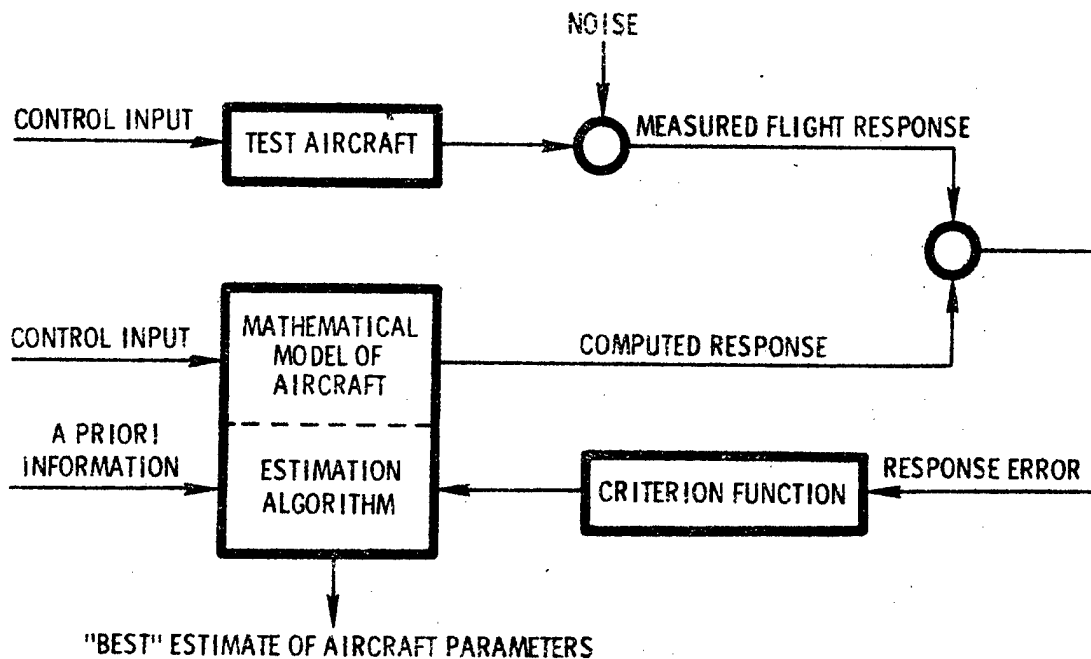
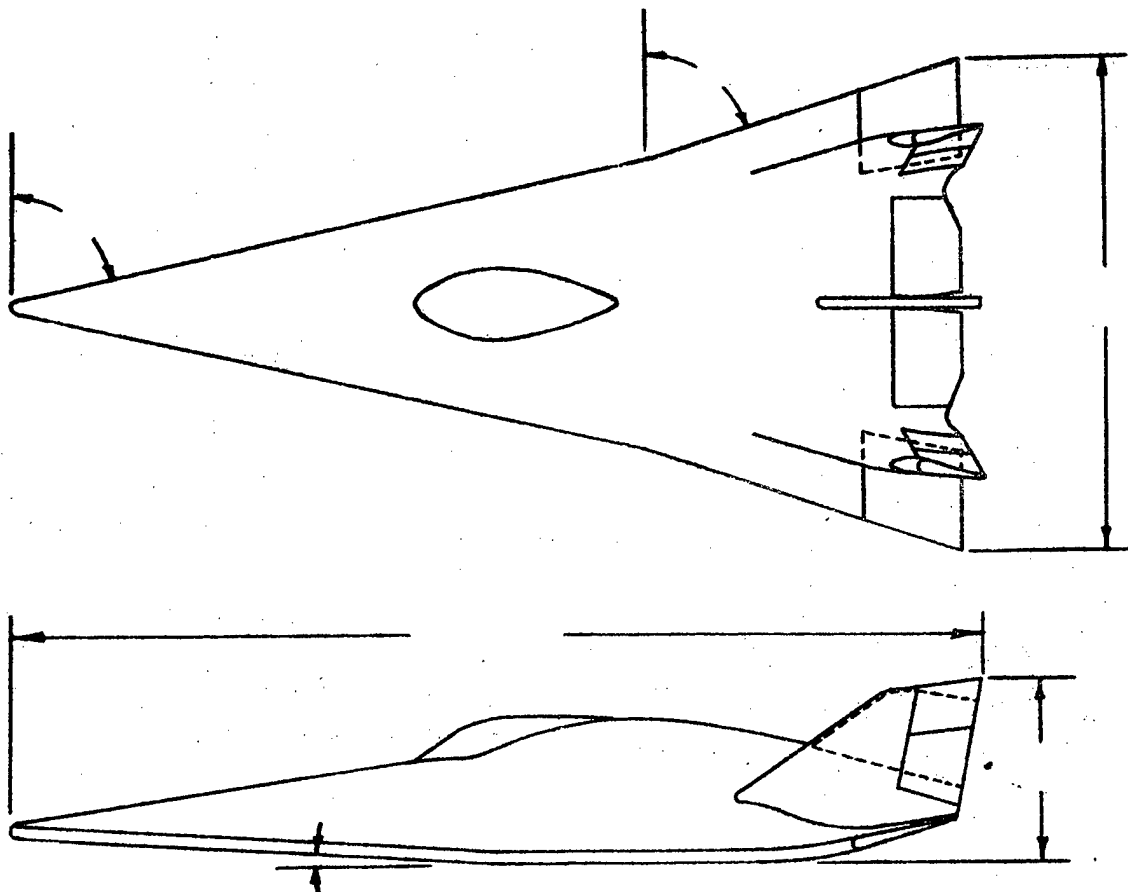


Figure 3: Basic Concept of Contemporary Parameter Estimation Techniques (From Reference 12)

As a specific example of this concept, consider the problem of determining the stability and control characteristics for small perturbations

about a trim flight condition. The types of data used are shown in Figure 4, which is from a flight test of a lifting-body vehicle.⁶¹ The control inputs are small-amplitude aileron and rudder pulses, and the measured responses are roll rate, yaw rate, sideslip angle, bank angle, and lateral acceleration. External random disturbances (turbulence) were negligible. These data were recorded as pulse code modulation signals on magnetic tape, then formatted, scaled, and restored on tape for reading into a digital computer. The recorded inputs were used as inputs to the mathematical model, and the recorded response was compared with the computed response. The model in this case was the set of linearized differential equations for lateral-directional motion, and the parameters to be estimated were the linear coefficients, which are stability and control derivatives.¹²



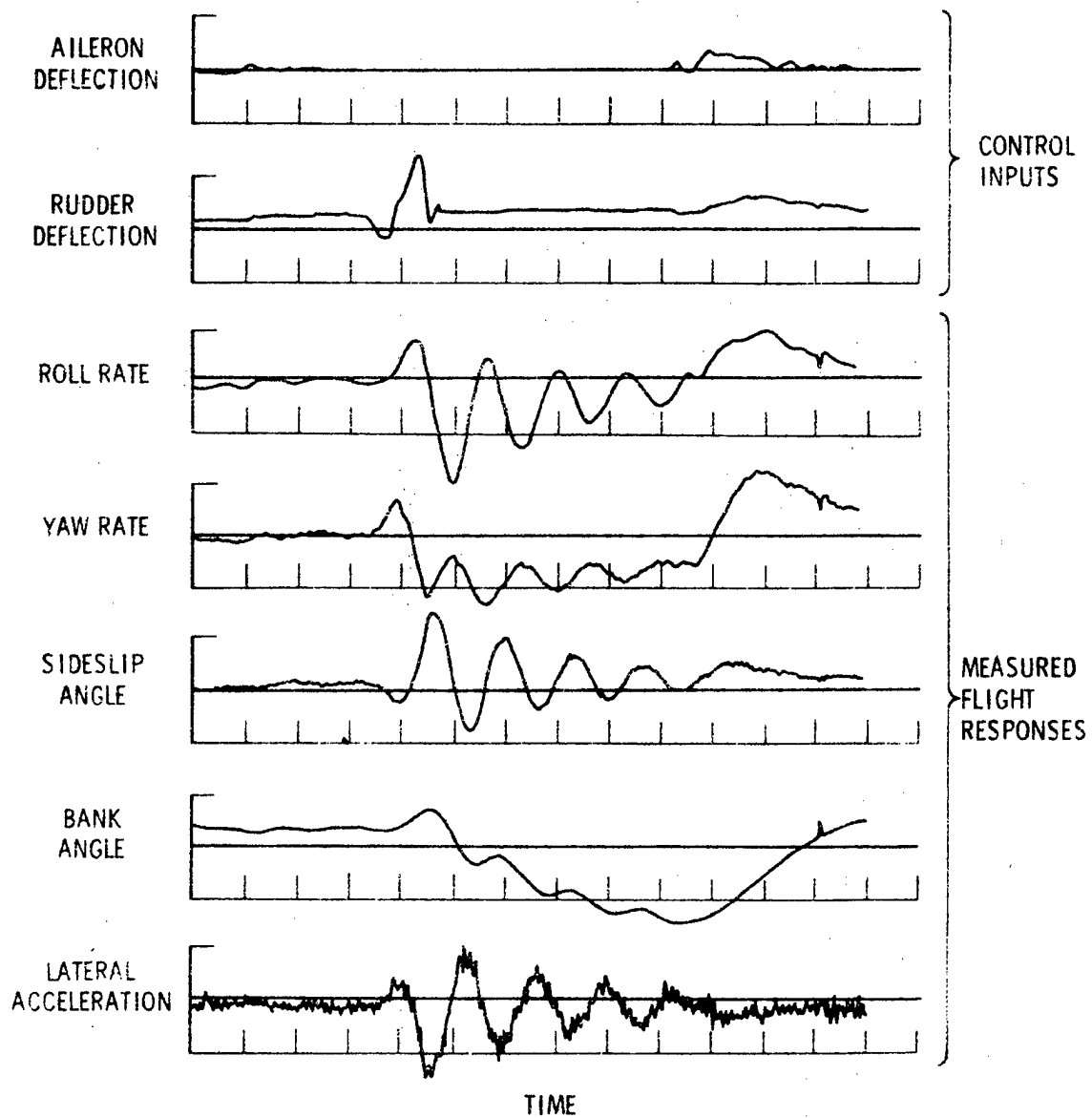


Figure 4: Typical Lifting-Body Flight Test Data for Parameter Estimation (From Reference 43)

Typically the techniques start with some a priori estimate of the derivatives, such as wind tunnel data. Usually the wind-tunnel data do not provide a good match, as shown in Figure 5. In applying parameter estimation techniques, some algorithm is devised to adjust the stability and control derivatives in the model until a set is obtained that minimizes the error between the computed and measured time histories. A typical match is shown in Figure 6.¹²

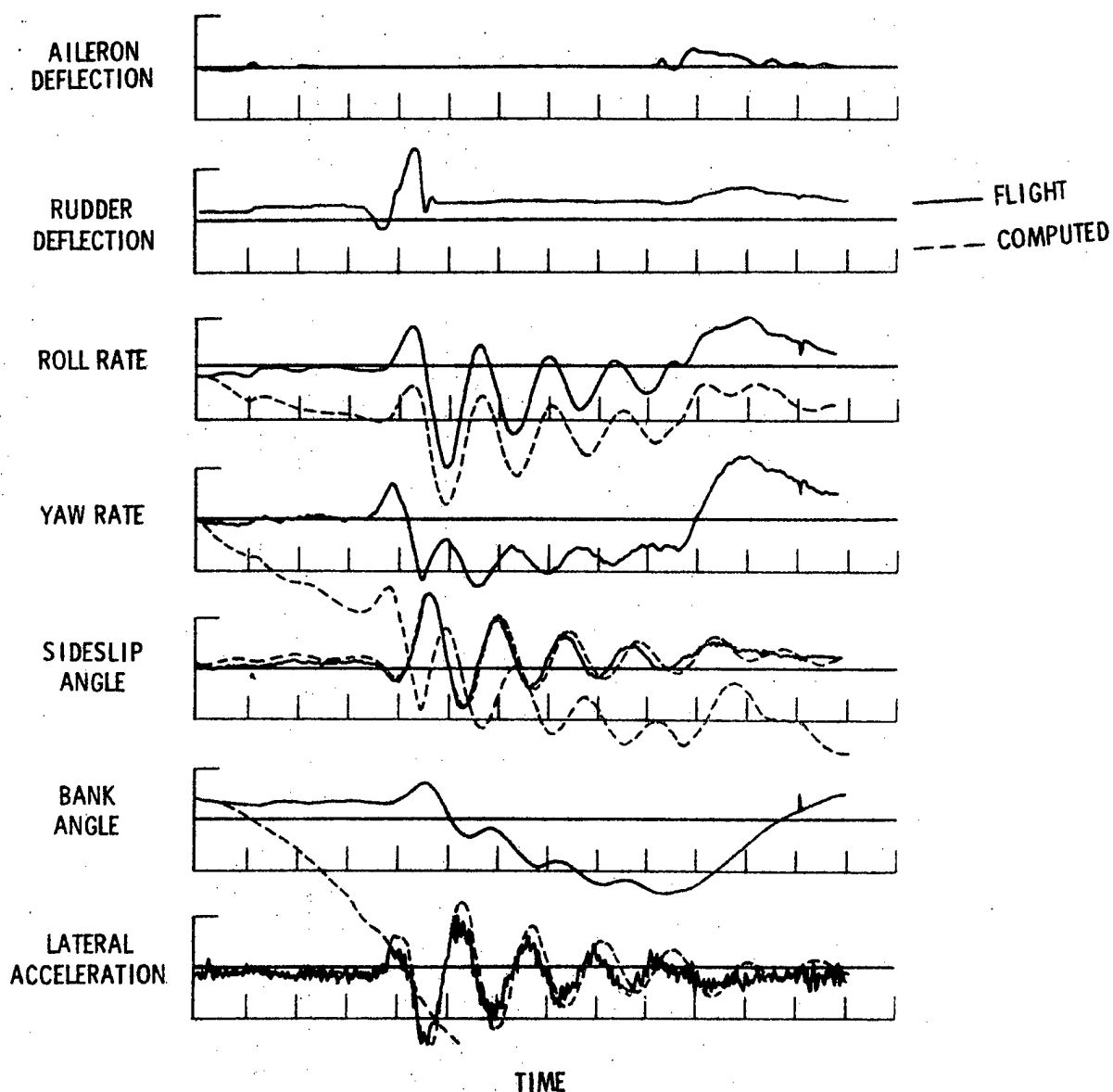


Figure 5: Comparison of Computed Response Using Wind Tunnel Parameter Values with the Flight Test Measured Response (From Reference 43)

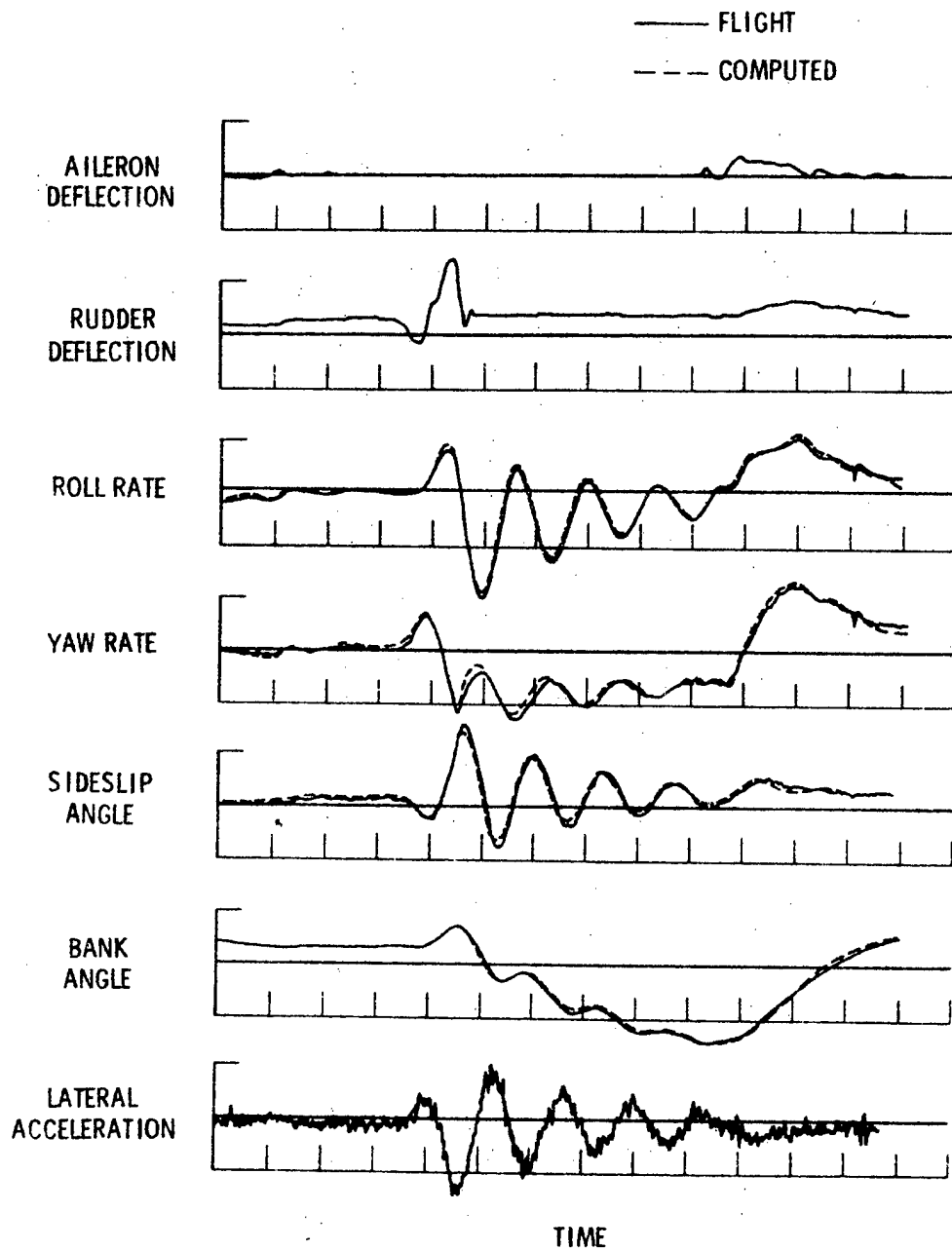


Figure 6: Typical Match of Computed Response Using Estimated Parameter Values with the Flight Test Measured Response (From Reference 43)

Current work by Balakrishnan and Tung in parameter estimation is involved with determining aircraft stability and control derivatives from flight test data taken in turbulence (random wind gusts). In this case the gust intensity can also be determined. Figure 6A shows Jetstar data taken at NASA Dryden in turbulence. The data shown have been matched by Tung for four elevator singlet inputs.¹⁴³

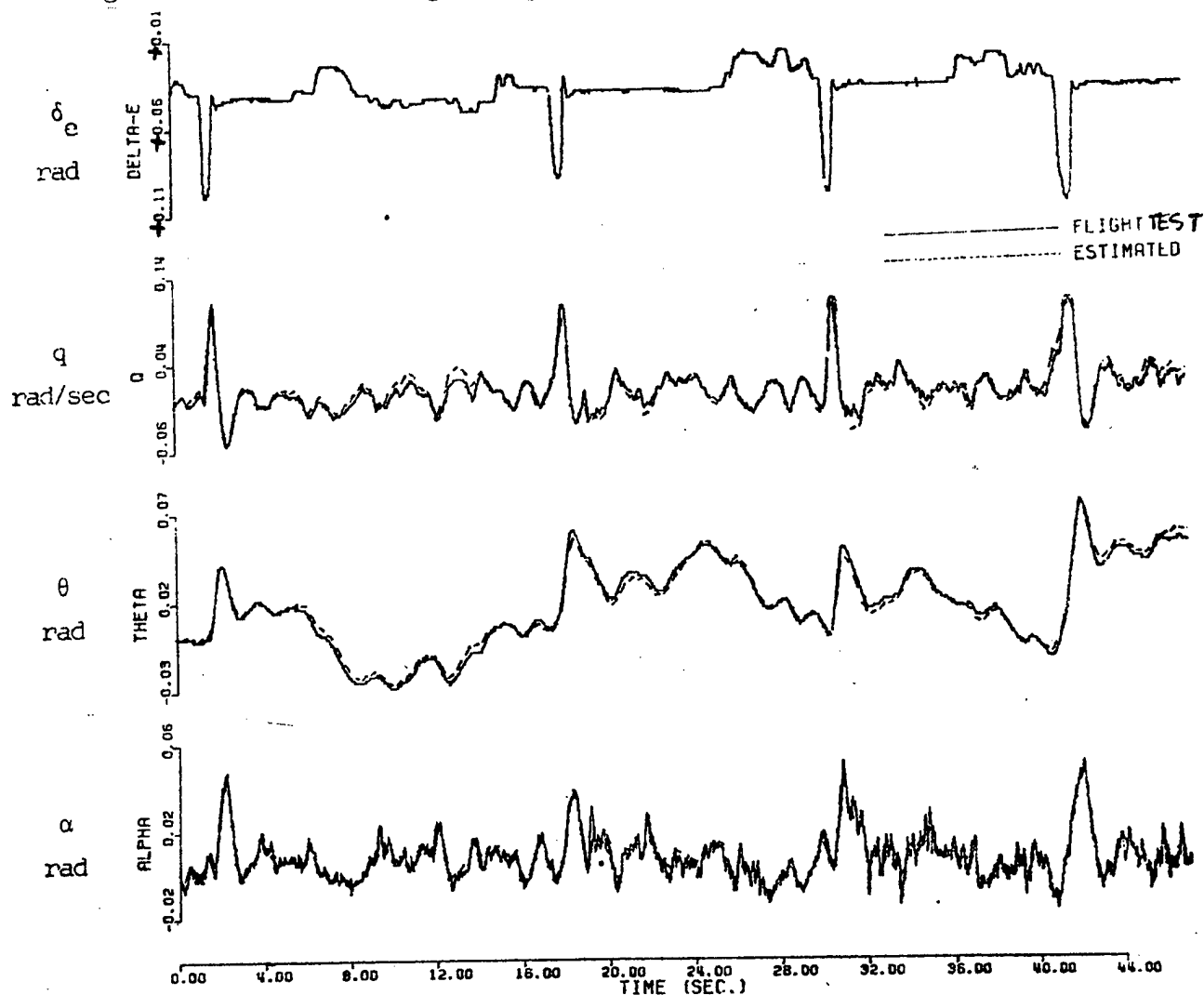


Figure 6A. NASA Dryden Jetstar Response in Turbulence Compared to Computed Response Using Estimated Parameter Values.¹⁴³

Figure 6B presents the power spectral density of the turbulence which was encountered while the Jetstar data were recorded. It is probably worth pointing out that in order to analyze this wind gust case practically all of the ideas in systems theory and stochastic control developed in the last ten or so years have to be employed.¹⁴³ The AFFTC does not presently have the capability to extract stability derivatives in turbulence.

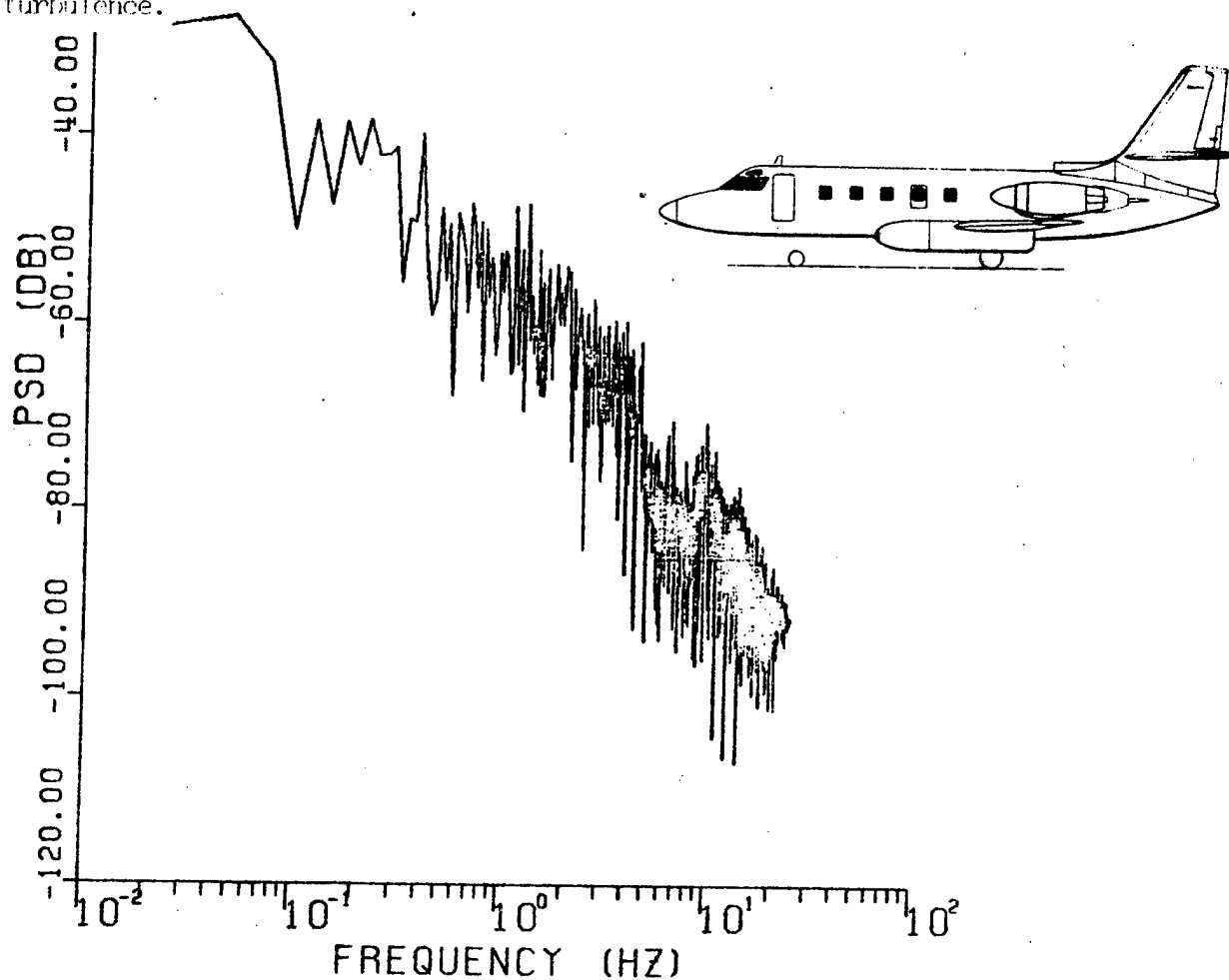


Figure 6B. Estimated Turbulence Encountered in NASA Dryden Jetstar During Response Measurements.¹⁴³

Most of the results published in the literature look as good as those shown in Figure 6. An obvious question is: What degree of accuracy do these results represent? The term accuracy implies an absolute measure of the error between some estimated parameter and the true parameter value. This error is impossible to compute since the true value of the parameter is unknown. Accuracy would be best evaluated by determining how well the model predicts system response using the flight test estimated parameters.¹¹³ More often it is evaluated by determining how well the model fits the measured response using the flight test estimated parameters. It should do this well since the parameter estimates were chosen by fitting the flight test measured response.

There are three other indicators which have been used at the AFFTC to try to lend confidence and credibility to the results of stability and control derivative estimation from flight test data. These are (1) repeatability, (2) correlation, and (3) statistical error analysis.¹⁰⁶ The repeatability indicator is also a measure of predictability. If fitting different sets of flight test measured data results in the same parameter estimates, then system response can be accurately predicted, at least over some range or class of inputs. The following theorems seem appropriate:

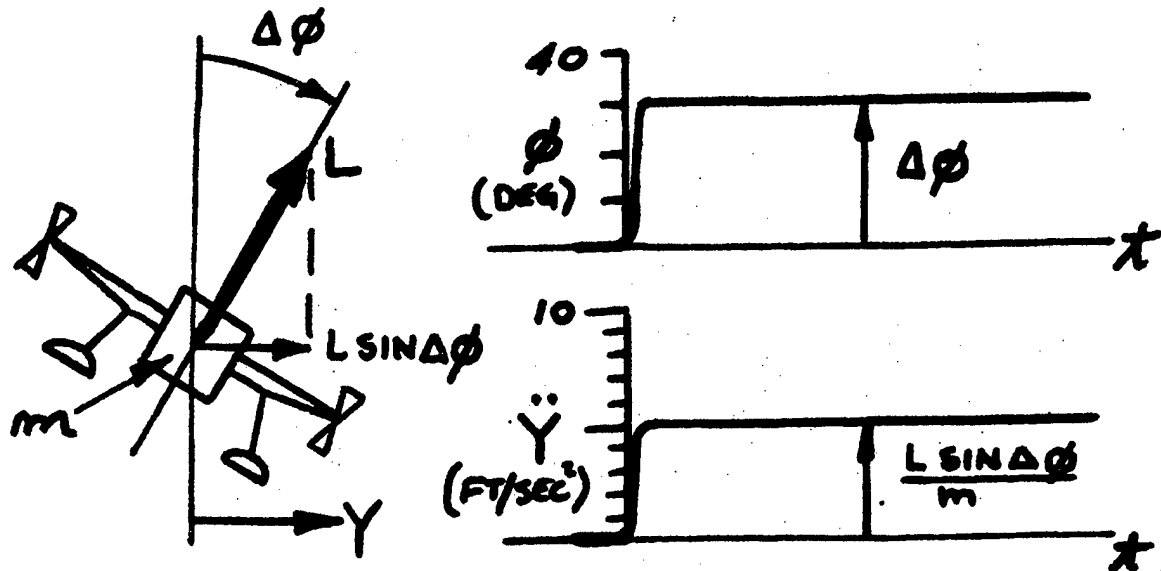
THEOREM III: Parameters which have no effect on the data cannot be identified.

THEOREM IV: A priori values are usually random numbers.

THEOREM V: Determined parameters are never more accurate than the data.



Another specific example which is rather trivial may help to point out the key aspects of parameter estimation. Consider a lunar lander vehicle under lateral translation in the Y direction due to a step input in bank angle, $\Delta \phi$:



PROBLEM: From a measured input (bank angle) and flight measured response (lateral acceleration) estimate the value of the parameter (force) L , or in other words, extract the value of L from flight test data.

The governing translational equation of motion is:

$$\bar{F} = m \bar{a}$$

or,

$$L \sin \Delta \phi = m \ddot{Y}$$

Solving for translational acceleration, \ddot{Y} :

$$\ddot{Y} = \frac{L \sin \Delta \phi}{m}$$

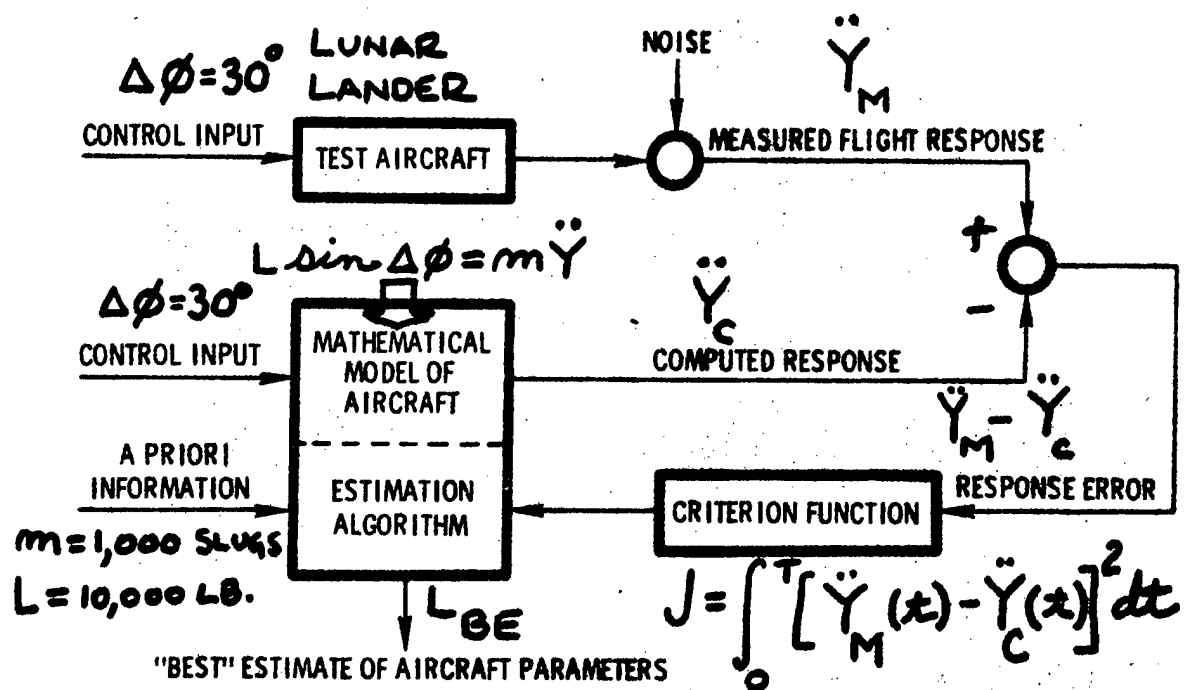


Figure 3A: Lunar Lander Example of Parameter Estimation Techniques.

As shown in Figure 3A, the lunar lander control or test input is a step bank angle change, $\Delta\phi$, of 30 degrees. The measured flight test response is given the symbol \ddot{Y}_M . The mathematical model of the lander is simply the equation of motion:

$$L \sin \Delta\phi = m\ddot{Y}$$

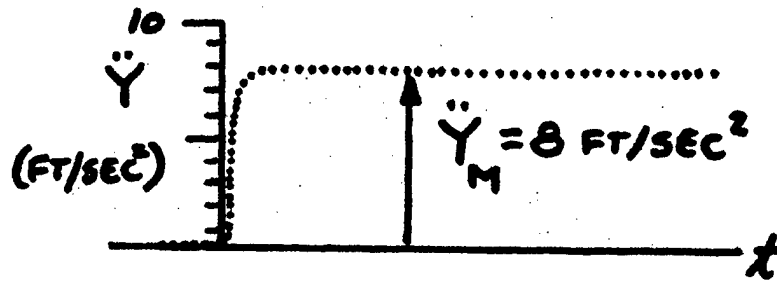
The computed response which is given the symbol \ddot{Y}_C is computed using the mathematical model, the control input, and the a priori information. In this example the a priori information given is a known mass, m , of 1,000 slugs, and an initially estimated value of L of 10,000 lb. The initial estimate for L might have been obtained by assuming that L was equal to the weight of the lunar lander. The best estimate of L is the parameter to be determined or extracted from the flight test measured data. This best estimate is given the symbol L_{BE} . The response error is defined as the difference between the computed and measured response, or $(\ddot{Y}_M - \ddot{Y}_C)$.

The best estimate, L_{BE} , is determined by the estimation or computational algorithm selecting a value for L which minimizes the given estimation criterion or cost function:

$$J = \int_0^T \left[\ddot{Y}_M(t) - \ddot{Y}_C(t) \right]^2 dt$$

This cost function, J , is in the form of a least squares data fit.

To illustrate the fitting process, assume that for the given inflight step control input of 30 degrees, the response was measured to be a mean value of 8 ft/sec².



The estimation algorithm would be a computer program to perform the following calculations:

$$L \sin \Delta\phi = m\ddot{Y}$$

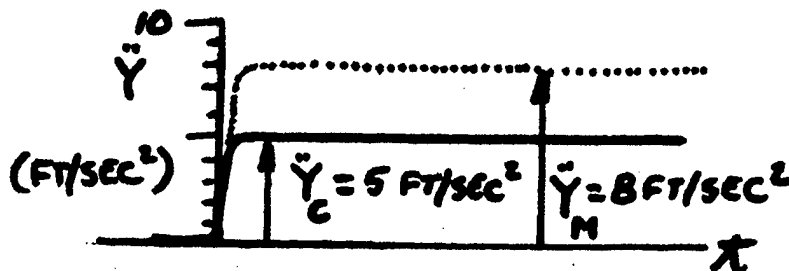
$$(10,000) (\sin 30^\circ) = 1,000 \ddot{Y}_C$$

$$\ddot{Y}_C = \frac{(10,000) (0.5)}{1,000}$$

$$\ddot{Y}_C = 5 \text{ ft/sec}^2$$

The response error then is:

$$\ddot{Y}_M - \ddot{Y}_C = 8 - 5 = 3 \text{ ft/sec}^2$$



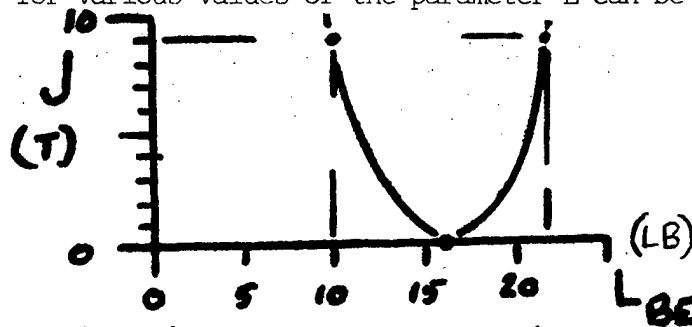
The problem now is to minimize the criterion function, J , by picking a value for L_{BE} . In this example, \ddot{Y}_M and \ddot{Y}_C are not functions of time, t , but are step output constants; therefore, the minimum value of J will be zero if L_{BE} is chosen so that \ddot{Y}_C is equal to \ddot{Y}_M . The equation of motion can be used to solve for L_{BE} :

$$L \sin \Delta\phi = m\ddot{Y}$$

$$L_{BE} (\sin 30^\circ) = (1,000) (8)$$

$$L_{BE} = \frac{(1,000) (8)}{(0.5)} = 16,000 \text{ lb.}$$

A plot of J for various values of the parameter L can be shown as:



In summary, for this example, the best estimate, L_{BE} , of the lunar lander parameter L was 16,000 lb. which was selected by the computational algorithm fitting the measured flight response by minimizing the criterion function.

Two pertinent questions still remain:

1. Using the mathematical model, L_{BE} , and m will the computational algorithm predict accurate values of lateral acceleration for other size step inputs, e.g., $\Delta\phi = 10, 20$, or 60 degrees?
2. Will it predict accurate values of lateral acceleration for an arbitrary input, e.g., $\Delta\phi$ being some arbitrary function of time instead of a step input?

The conceptual diagram in Figure 3 and the previous examples point out five key aspects of parameter estimation techniques: (1) the mathematical model, (2) the estimation criterion, (3) the computational algorithm, (4) the total data acquisition system, and (5) the test input. These key aspects will be discussed individually.¹²

MATHEMATICAL MODEL

The choice of the mathematical model, or more precisely, the form of the input/output relationship adopted, obviously plays a major role in the parameter estimation procedure. Balakrishnan has pointed out that the most suitable form of the model depends on many factors among which the most important are:

1. The purpose for which the systems identification is undertaken,
2. The physical nature of the process,
3. The a priori knowledge available about the system being studied.¹⁴⁴

The model format or governing equations of any physical system are always unknown in an absolute sense because it is impossible to obtain complete system isolation. A number of candidate system models must be compared to see which best achieves the desired result which is usually predicting the response of the system. Taylor has shown that for modeling aircraft lateral-directional motion a math model (set of equations) with sixteen unknown parameters (stability derivatives to be determined) fit his experimental data best, but a model with ten unknowns predicted system response best.¹¹² Work is still being done on developing criteria for

evaluating candidate models. There is no method currently available for detecting errors in modeling.¹⁴³

THEOREM XXI: Engineering judgment must be used in defining models.¹⁴⁵

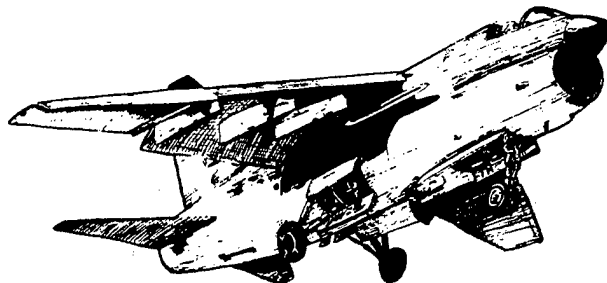
THEOREM VI: If a model is selected solely on the basis of minimizing fit errors to a given set of data, the model will probably be less accurate in predicting system response than a simpler one.¹¹³

THEOREM VIA: Defining things too much reduces the probability of obtaining good results.¹⁴⁵

THEOREM XXII: Too complicated models as well as too simple models are equally useless.¹⁴³

THEOREM VII: No model is any good unless it originates with the user.¹¹⁷

This discussion suggests that several mathematical models should be examined. Candidate models can be tested by having them predict the response for test data which was not used in model parameter determination.¹¹⁶ This is not a popular approach since it requires obtaining additional test data or reserving part of the original data for model testing.

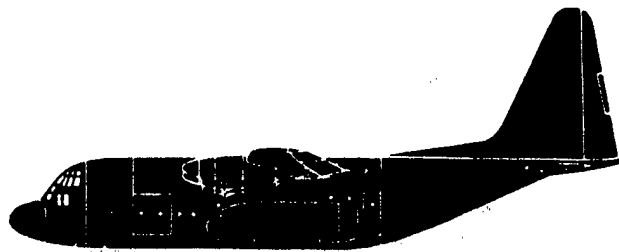


For extracting stability and control derivatives from flight test data, a model must be selected that adequately represents the aircraft characteristics to be measured. The aerodynamic forces and moments on an aircraft are nonlinear functions of several variables, such as Mach number, angle of attack, control surface deflection, and sideslip angle. There may be significant structural modes, aeroelastic effects, nonstationary aerodynamic effects, and flow separation. Yet in many instances it is adequate to use a stationary, linearized, rigid-body model. In other instances a more complicated model is necessary, such as at very high angles of attack for which a nonlinear model may be required. An inappropriate model, however, can degrade the accuracy of the parameter estimate and even prevent convergence of the computation algorithm.¹²

Linear Equations of Motion

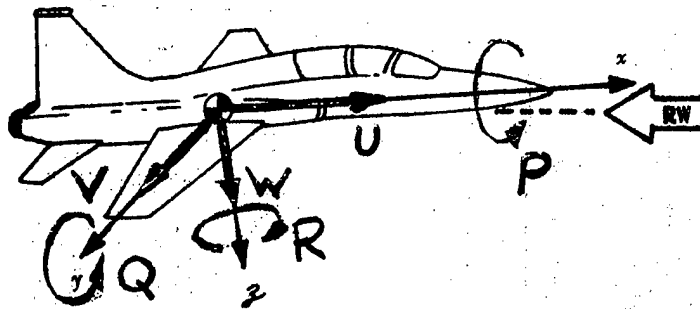
Before introducing nonlinear aircraft equations of motion, the set of linear equations derived in the Equations of Motion course at the USAF Test Pilot School will be reviewed.⁶⁴

An aircraft has six degrees of freedom. In order to solve for the three unknown velocity components (U , V , W) and three unknown rotations (P , Q , R), six equations are required which can be solved simultaneously. Starting with Newton's second law, which is valid only with respect to inertial space, the following equations can be derived:⁶⁴



$$\begin{aligned}
 & F_x = m (\dot{U} + QW - RV) & (1) \\
 \text{Longitudinal } & F_z = m (\dot{W} + PV - QU) & (2) \\
 & G_y = \dot{Q} I_y - PR (I_z - I_x) + (P^2 - R^2) I_{xz} & (3) \\
 \hline
 & F_y = m (\dot{V} + RU - PW) & (4) \\
 \text{Lateral-} & G_x = \dot{P} I_x + QR (I_z - I_y) - (R + PQ) I_{xz} & (5) \\
 \text{Directional} & G_z = \dot{R} I_z + PQ (I_y - I_x) + (QR - P) I_{xz} & (6)
 \end{aligned}$$

The left-hand side of the equations represents the forces and moments on the aircraft while the right-hand side represents the aircraft's response to these forces and moments. The sign convention is shown in Figure 7:



Positive control deflections, δ_e , δ_r , and δ_a are defined as those causing positive Q, R, and P.

Figure 7: Body Axis System

There are four major assumptions made in the derivation of Equations 1 through 6. These are:

1. Rigid Body. The aircraft is considered rigid; therefore, aeroelastic effects are not considered.
2. Fixed Earth and Atmosphere. This allows use of a moving earth axis system as an inertial reference so that Newton's law can be applied.

3. Constant Mass. Stability and control maneuvers take place in a short time so fuel burned can be neglected and weight, center of gravity location, and moments of inertia are considered constant.
4. The x-z plane is a Plane of Symmetry. This causes two products of inertia, I_{xy} and I_{yz} , to be zero.

The applied forces and moments can be broken up according to the sources shown in Figure 8:

		Source					
		Aero-dynamic	Direct Thrust	Gravity	Gyro-scopic	Other	
LONGITUDINAL	F_x	X	X_T	X_g	0	X_{oth}	$= m\dot{U} + - - -$
	F_z	Z	Z_T	Z_g	0	Z_{oth}	$= m\dot{W} + - - -$
	G_y	M	M_T	0	M_{gyro}	M_{oth}	$= \dot{Q}I_y + - - -$
LATERAL-DIRECTIONAL	F_y	Y	Y_T	Y_g	0	Y_{oth}	$= m\dot{V} + - - -$
	G_x	L	L_T	0	L_{gyro}	L_{oth}	$= \dot{P}I_x + - - -$
	G_z	N	N_T	0	N_{gyro}	N_{oth}	$= \dot{R}I_z + - - -$

Figure 8: Sources of Left-hand Side Forces and Moments

By far, the most important terms on the left-hand side are the aerodynamic terms. Unfortunately, they are also the most complex. If small angles are assumed then the aerodynamic forces X and Z in Figure 8 become the negative of lift and drag, -D and -L.

Stability and control analysis is concerned with the question of how the aircraft responds to certain perturbations or inputs. Unfortunately, the equations we have discussed so far are nonlinear. Small perturbation

theory is used to linearize the equations by using a Taylor series expansion and excluding higher order terms. When operating under small perturbation theory, aircraft motion can usually be thought of as two independent motions each of which is a function only of the variables shown in Equations 7 and 8:

Longitudinal Motion

$$(D, L, M) = f(U, \alpha, \dot{\alpha}, Q, \delta_e) \quad (7)$$

Lateral-Directional Motion

$$(Y, Z, N) = g(\beta, \dot{\beta}, P, R, \delta_a, \delta_r) \quad (8)$$

If it is assumed that the aircraft motion consists of small perturbations from initial conditions of steady straight flight, the problem can be simplified and each of the forces and moments expressed in a Taylor series expansion as a function of its variables as aerodynamics lift is in Equation 9:

$$L = \begin{bmatrix} L_0 + \frac{\partial L}{\partial U} \Delta U + \frac{1}{2} \frac{\partial^2 L}{\partial U^2} \Delta U^2 + \dots \\ + \frac{\partial L}{\partial \alpha} \Delta \alpha + \frac{1}{2} \frac{\partial^2 L}{\partial \alpha^2} \Delta \alpha^2 + \dots \\ + \frac{\partial L}{\partial \dot{\alpha}} \Delta \dot{\alpha} + \dots \\ + \frac{\partial L}{\partial Q} \Delta Q + \dots \\ + \frac{\partial L}{\partial \delta_e} \Delta \delta_e + \dots \end{bmatrix} \quad (9)$$

Dropping higher order terms involving u^2 , q^2 , etc., Equation 9 now becomes

$$L = L_0 + \frac{\partial L}{\partial u} u + \frac{\partial L}{\partial \alpha} \alpha + \frac{\partial L}{\partial \dot{\alpha}} \dot{\alpha} + \frac{\partial L}{\partial q} q + \frac{\partial L}{\partial \delta_e} \delta_e \quad (10)$$

The lateral-directional motion can be handled in a similar manner. For example, the aerodynamic terms for rolling moment become:

$$\begin{aligned} \mathcal{L} = \mathcal{L}_0 + \frac{\partial \mathcal{L}}{\partial \beta} \beta + \frac{\partial \mathcal{L}}{\partial \dot{\beta}} \dot{\beta} + \frac{\partial \mathcal{L}}{\partial p} p + \frac{\partial \mathcal{L}}{\partial r} r + \frac{\partial \mathcal{L}}{\partial \delta_a} \delta_a + \dots \\ \dots + \frac{\partial \mathcal{L}}{\partial \delta_r} \delta_r \end{aligned}$$

This development can be applied to all of the aerodynamic forces and moments. The equations are linear and account for all variables that have a significant effect on the aerodynamic forces and moments on an aircraft.

The small perturbation technique can also be applied to the weight (gravity) and thrust terms in Figure 8. Assuming disturbances are from a steady state condition, and engine thrust does not change with velocity, an order of magnitude analysis shows that the only significant contribution of weight or thrust is drag due to pitch Euler angle change and the effect of weight on side force. For most analysis, gyroscopic effects are insignificant. They begin to become important as angular rates increase. For static and dynamic stability analyses these are often not considered large. In the area of spins and maximum roll rate maneuvers, they are large and definitely affect the motion of the aircraft. Therefore, for spin and roll coupling analyses gyroscopic effects should be considered; however, at those high angles of attack the small angle assumption is also invalid and the equations of motion are nonlinear.

The linearized equations of motion are put into a more useable form by "normalizing." In order to do this, each equation is multiplied through by a "normalizing factor." This factor is different for each equation and is picked to simplify the first term on the right-hand side. Normalizing factors are shown in Figure 9.

Equation	Normalizing Factor	First Term is Now Pure Accel or $\dot{\alpha}$	Units
"DRAG"	$\frac{1}{m}$	$-\frac{D}{m} + \frac{X_T}{m} + \dots = \dot{u}$	$[\frac{ft}{sec^2}]$
"LIFT"	$\frac{1}{mU_o}$	$-\frac{L}{mU_o} + \frac{Z_T}{mU_o} + \dots = \dot{w}_o$	$[\frac{rad}{sec}]$
"PITCH"	$\frac{1}{I_y}$	$\frac{M}{I_y} + \frac{M_T}{I_y} + \dots = \dot{q}$	$[\frac{rad}{sec^2}]$
"SIDE"	$\frac{1}{mU_o}$	$\frac{Y}{mU_o} + \frac{Y_T}{mU_o} + \dots = \dot{v}_o$	$[\frac{rad}{sec}]$
"ROLL"	$\frac{1}{I_x}$	$\frac{L}{I_x} + \frac{L_T}{I_x} + \dots = \dot{p}$	$[\frac{rad}{sec^2}]$
"YAW"	$\frac{1}{I_z}$	$\frac{N}{I_z} + \frac{N_T}{I_z} + \dots = \dot{r}$	$[\frac{rad}{sec^2}]$

Figure 9: Normalizing Factors

Stability parameters are simply the partial coefficients of each term multiplied by its respective normalizing factor. For example Equation 10 becomes:

$$\frac{L}{mU_0} = \frac{L_0}{mU_0} + \underbrace{\frac{1}{mU_0} \frac{\partial L}{\partial u}}_{L_u} u + \underbrace{\frac{1}{mU_0} \frac{\partial L}{\partial \alpha}}_{L_\alpha} \alpha + \underbrace{\frac{1}{mU_0} \frac{\partial L}{\partial \dot{\alpha}}}_{L_{\dot{\alpha}}} \dot{\alpha} + \underbrace{\frac{1}{mU_0} \frac{\partial L}{\partial q}}_{L_q} q + \underbrace{\frac{1}{mU_0} \frac{\partial L}{\partial \delta_e}}_{L_{\delta_e}} \delta_e \quad (11)$$

The indicated quantities in Equation 11 are defined as stability parameters and the equation can be written:

$$\frac{L}{mU_0} = \frac{L_0}{mU_0} + L_u u + L_\alpha \alpha + L_{\dot{\alpha}} \dot{\alpha} + L_q q + L_{\delta_e} \delta_e \left[\frac{\text{rad}}{\text{sec}} \right] \quad (12)$$

Stability parameters have various dimensions depending on whether they are multiplied by a linear velocity, an angle, or an angular rate. For this reason, they are sometimes called dimensional derivatives.



The complete set of aerodynamic terms is written out in Equations 13 through 18.

$$\begin{array}{l} \text{L} \\ \text{O} \\ \text{N} \\ \text{G} \\ \text{I} \\ \text{T} \\ \text{U} \\ \text{D} \\ \text{I} \\ \text{N} \\ \text{A} \\ \text{L} \end{array} \quad \frac{D}{m} = \frac{D_o}{m} + D_u u + D_\alpha \alpha + D_{\dot{\alpha}} \dot{\alpha} + D_q q + D_{\delta_e} \delta_e \quad (13)$$

$$\frac{L}{mU_o} = \frac{L_o}{mU_o} + L_u u + L_\alpha \alpha + L_{\dot{\alpha}} \dot{\alpha} + L_q q + L_{\delta_e} \delta_e \quad (14)$$

$$\frac{m}{I_y} = \frac{m_o}{I_y} + m_u u + m_\alpha \alpha + m_{\dot{\alpha}} \dot{\alpha} + m_q q + m_{\delta_e} \delta_e \quad (15)$$

$$\begin{array}{l} \text{L} \\ \text{A} \\ \text{T} \end{array} \quad \frac{Y}{mU_o} = \frac{Y_o}{mU_o} + Y_\beta \beta + Y_{\dot{\beta}} \dot{\beta} + Y_p p + Y_r r + Y_{\delta_a} \delta_a + Y_{\delta_r} \delta_r \quad (16)$$

$$\begin{array}{l} \text{D} \\ \text{I} \\ \text{R} \end{array} \quad \frac{\mathcal{L}}{I_x} = \frac{\mathcal{L}_o}{I_x} + \mathcal{L}_\beta \beta + \mathcal{L}_{\dot{\beta}} \dot{\beta} + \mathcal{L}_p p + \mathcal{L}_r r + \mathcal{L}_{\delta_a} \delta_a + \mathcal{L}_{\delta_r} \delta_r \quad (17)$$

$$\frac{n}{I_z} = \frac{n_o}{I_z} + n_\beta \beta + n_{\dot{\beta}} \dot{\beta} + n_p p + n_r r + n_{\delta_a} \delta_a + n_{\delta_r} \delta_r \quad (18)$$

The resulting two sets of equations (longitudinal and lateral-directional) can be simplified and set equal to the right-hand side Equations 1 through 6. Simplifying assumptions for the longitudinal equations are:

1. Initial Steady State (Trim $\beta = 0$)
2. No thrust effects.
3. Weight only affects the drag equation.
4. No lateral-directional motion, which means longitudinal motion is analyzed independent of lateral-directional motion. As a result: $pr = rv = pv = 0$.
5. From an order of magnitude analysis: $qw = 0$.
6. $D_{\dot{\alpha}}$, D_q , and D_{δ_e} are small and can be neglected.

After some algebraic substitutions, Equations 19, 20, and 21 result:

$$-\left(D_u u + D_{\alpha} \alpha + D_{\theta}\right) = \dot{u} \quad (19)$$

$$-\left(L_u u + L_{\alpha} \alpha + L_{\dot{\alpha}} \dot{\alpha} + L_q q + L_{\delta_e} \delta_e\right) = \dot{\alpha} - q \quad (20)$$

$$m_u u + m_{\alpha} \alpha + m_{\dot{\alpha}} \dot{\alpha} + m_q q + m_{\delta_e} \delta_e = \dot{q} \quad (21)$$

These three equations can be rewritten in conventional form substituting $\dot{\theta}$ for q and rearranging:

$$\begin{array}{c|c|c|c|c} & (\theta) & (u) & (\alpha) & \\ \hline \text{DRAG} & D_{\dot{\theta}} \dot{\theta} & + \dot{u} + D_u u & + D_{\alpha} \alpha & = 0 \end{array} \quad (22)$$

$$\begin{array}{c|c|c|c|c} \text{LIFT} & (1-L_q) \dot{\theta} & - L_u u & - (1+L_{\alpha}) \dot{\alpha} - L_{\alpha} \alpha & = L_{\delta_e} \delta_e \end{array} \quad (23)$$

$$\begin{array}{c|c|c|c|c} \text{PITCH} & \ddot{\theta} - m_q \dot{\theta} & - m_u u & - m_{\dot{\alpha}} \dot{\alpha} - m_{\alpha} \alpha & = m_{\delta_e} \delta_e \end{array} \quad (24)$$

There are now three independent equations with three variables. The terms on the right-hand side are control inputs or forcing functions. Therefore, for any elevator input, δ_e , the equations can be solved for θ , u , and α .

Simplifying assumptions for the lateral-directional equations are:

1. Initial wings-level steady state (Trim $\beta = 0$).
2. No thrust effects.
3. Weight only affects the side force equation.
4. No longitudinal pitching motion, which means lateral-directional motion is analyzed independent of longitudinal motion. As a result: $\dot{q} = 0$.
5. Pitch Euler angle, θ , is about zero; therefore, $p = \dot{\phi}$ and $\dot{p} = \ddot{\phi}$.
6. $Y_{\dot{\beta}}$, $N_{\dot{\beta}}$, $L_{\dot{\beta}}$, and Y_{δ_a} are assumed small and neglected.

The lateral-directional equations can be written in conventional form after some algebraic substitutions and rearranging as Equations 25, 26, and 27:

$$\begin{array}{c|c|c|c}
 & (\beta) & (\phi) & (r) \\
 \hline
 \text{SIDE FORCE} & \dot{\beta} - Y_{\beta} \beta & - Y_p \dot{\phi} - Y_{\phi} \phi & + (1 - Y_r) r \\
 \hline
 & & & = Y_{\delta_r} \delta_r
 \end{array} \quad (25)$$

$$\begin{array}{c|c|c|c}
 & (\beta) & (\phi) & (r) \\
 \hline
 \text{ROLLING MOMENT} & - L_{\beta} \beta & + \ddot{\phi} - L_p \dot{\phi} & - \frac{I_{xz}}{I_x} \dot{r} - L_r r \\
 \hline
 & & & = L_{\delta_a} \delta_a + L_{\delta_r} \delta_r
 \end{array} \quad (26)$$

$$\begin{array}{c|c|c|c}
 & (\beta) & (\phi) & (r) \\
 \hline
 \text{YAWING MOMENT} & - N_{\beta} \beta & - \frac{I_{xz}}{I_z} \ddot{\phi} - N_p \dot{\phi} & + \dot{r} - N_r r \\
 \hline
 & & & = N_{\delta_a} \delta_a + N_{\delta_r} \delta_r
 \end{array} \quad (27)$$

Again, there are three independent equations with three variables. For any control input, δ_a or δ_r , the equations can be solved for β , ϕ , and r .

Equations 22 through 27 derived in terms of stability parameters give all the information necessary to describe aircraft motion. The problem is that the stability parameters are functions of dynamic pressure and aircraft size. Deriving a set of non-dimensional equations eliminates this problem and allows (1) direct comparison between wind tunnel and flight test data, and (2) direct comparison of the stability and control characteristics of different types of aircraft.

The steps in non-dimensionalizing the equations of motion are straight-forward conceptually, but rather complicated algebraically. This process is detailed in Reference 64, and involves introducing certain compensating factors to form dimensionless stability derivatives. This can be illustrated using a pitching moment equation term:

$$m_{q^1} = \frac{\rho U_o^2 S c}{2I_y} C_{m_q} \hat{q}$$

m_{q^1} → Stability Parameter
 $\frac{\rho U_o^2 S c}{2I_y}$ → Constants
 C_{m_q} → Dimensionless Stability Derivative
 \hat{q} → Dimensionless Variable $\equiv \frac{cq}{2U_o}$

Since pitch rate, q , appears in the pitching moment equation as $\dot{\theta}$, the following substitution must also be made:

$$\hat{q} \equiv \frac{cq}{2U_o} = \frac{c}{2U_o} \dot{\theta}$$

After operating on each term in the equations of motion in a similar fashion, the equations can be written in conventional form using stability derivative notation as follows:



NON-DIMENSIONAL LONGITUDINAL EQUATIONS

	(θ)	(\hat{u})	(α)	
Drag	$C_{L_o} \theta$	$+(2\mu v + C_{D_u} + 2C_{D_0}) \hat{u}$	$+ C_{D_\alpha} \alpha$	$= 0 \quad (28)$
Lift	$(2\mu v - C_{L_q} v) \theta$	$-(C_{L_u} + 2C_{L_o}) \hat{u}$	$-(2\mu v + C_{L_\alpha} v + C_{L_\alpha} \alpha)$	$= C_{L_{\delta_e}} \delta_e \quad (29)$
Pitching Moment	$(i_y v^2 - C_{m_q} v) \theta$	$- C_{m_u} \hat{u}$	$-(C_{m_\alpha} v + C_{m_\alpha} \alpha)$	$= C_{m_{\delta_e}} \delta_e \quad (30)$

$$i_y = \frac{8I_y}{\rho S c^3}$$

$$\mu = \frac{2m}{\rho S c}$$

$$v = \frac{c}{2U_0} \frac{d(\)}{dt}$$

$$\hat{u} = \frac{u}{U_0}$$

NON-DIMENSIONAL LATERAL-DIRECTIONAL EQUATIONS

	(β)	(ϕ)	(\hat{r})	
Side Force	$(2\mu v - C_{Y_\beta}) \beta$	$-(C_{Y_P} v + C_{L_o} \phi)$	$+(2\mu - C_{Y_r}) \hat{r}$	$= C_{Y_{\delta_r}} \delta_r \quad (31)$
Rolling Moment	$- C_{l_\beta} \beta$	$+(i_x v^2 - C_{l_P} v) \phi$	$-(i_{xz} v + C_{l_r}) \hat{r}$	$= C_{l_{\delta_a}} \delta_a + C_{l_{\delta_r}} \delta_r \quad (32)$
Yawing Moment	$- C_{n_\beta} \beta$	$-(i_{xz} v^2 + C_{n_P} v) \phi$	$+(i_z v - C_{n_r}) \hat{r}$	$= C_{n_{\delta_a}} \delta_a + C_{n_{\delta_r}} \delta_r \quad (33)$

$$i_x = \frac{8I_x}{\rho S b^3}$$

$$v = \frac{b}{2U_0} \frac{d(\)}{dt}$$

$$i_{xz} = \frac{8I_{xz}}{\rho S b^3}$$

$$\mu = \frac{2m}{\rho S b}$$

$$i_z = \frac{8I_z}{\rho S b^3}$$

$$\hat{r} = \frac{rb}{2U_0}$$

These non-dimensional equations can be used to compare geometrically similar aircraft. Within the assumptions made, they describe the complete motion of an aircraft. They can be programmed directly into a computer and connected to a flight simulator. They are also used for design analysis. Due to their simplicity, they are especially useful as an analytical tool to investigate aircraft flying qualities and determine the effect of changes in aircraft design.

The equations of motion (Equations 28 through 33) were referred to the stability axis system and are the standard form of the linear six-degree-of-freedom equations of motion derived at the USAF Test Pilot School.⁶⁴ Reference 65 presents a much more rigorous derivation, and discusses the consequences of each assumption in great detail. The five-degree-of-freedom equations which are in general use for engineering problems at the AFFTC are derived in Reference 60. This reference also shows how the equations evolve into the body axis linear matrix equations used in the Modified Maximum Likelihood Estimator (MMLE) digital program.

There are some differences between Equations 28 thru 33 and those used in the MMLE program. In deriving the MMLE equations the assumption that pitch Euler angle is about zero was not required; however, bank angle excursions must remain small (about $\pm 20^\circ$) about trim. Non-zero trim bank angle is accounted for by the MMLE program, but $\sin \phi$ is assumed equal to ϕ in radians. The MMLE determined flight test derivatives combine the effects of $\dot{\alpha}$ and $\dot{\beta}$ into pitch rate and yaw rate respectively. The results of trying to separate the lag and rate derivatives from flight test have been poor.⁶⁰ The derivative $C_{Y_{\delta a}}$ is not assumed small in the

MMLE equations and it can become significant, particularly for aircraft with rolling tails or for control configured vehicles.

Sometimes it is more convenient to use a body axis system aligned with the wing chord line or fuselage reference line. Often in flight test

this is the case since flight test data are generally measured by instruments fixed with respect to the aircraft. When the body axis system is used, force coefficients are defined as normal force coefficient, C_N , and chordwise force coefficient, C_C . Wind tunnel and stabilized flight test results are usually measured in terms of lift and drag forces which are measured perpendicular and parallel to the relative wind and which are logically referred to stability axes. Stability derivatives calculated from subsonic flow theory are also calculated with reference to stability axes. The important point is that stability derivatives are referred to either the body or stability axes, according to the method of derivation, and that the equations of motion can easily be altered to apply to either axis system.^{65,66,99}

Nonlinear Equations of Motion

The aerodynamic model for the linear equations of motion was obtained by a Taylor series expansion of the aerodynamic forces. The structure of this model is unknown in the high angle of attack flight regime and for V/STOL aircraft operating at very low speeds or in the hover flight regime.

Modeling problems result when the assumptions made in deriving the linear equations of motion are violated. Derivation of the linear equations assumed that all motion occurs in either the longitudinal or lateral-directional mode. The linear model is usually valid for level flight, steep spiral descents, or maneuvering flight.⁵⁷ However, when aircraft motion does not fit this description, modeling problems arise.

As an example, Figure 9A shows how the dynamics of an aircraft can change with changes in trim angle of attack, α_0 , and trim sideslip angle, β_0 . In the case shown, phugoid stability is a strong function of trim sideslip angle and Dutch roll is a strong function of trim angle of attack.

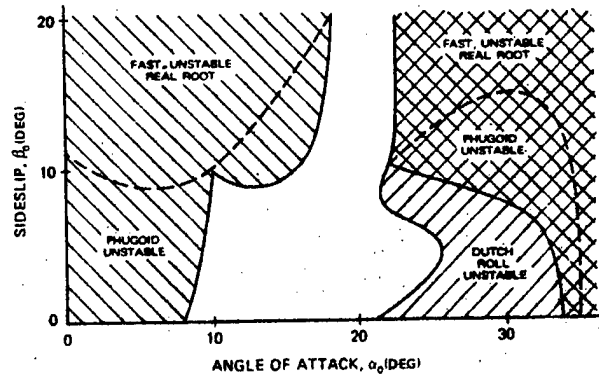


Figure 9A: Effect of Trim Angle of Attack and Sideslip on Aircraft Stability.¹⁰¹

Sometimes when the linear model no longer adequately approximates aircraft motion a nonlinear model is known. Problems more difficult to solve arise when the aircraft is subjected to unknown external inputs or when no model is known for a phenomenon affecting the aircraft.⁵⁷ Problems of each type will be discussed:

Known Nonlinear Model. The nonlinear problem that is easiest to solve occurs when the model, reflecting actual aircraft nonlinearities, is nonlinear but can be made linear. As an example, the longitudinal equations were found to be highly coupled with the lateral-directional mode:

$$\begin{array}{ll}
 \text{Longitudinal} & \begin{array}{l} F_x = m (\dot{u} + q w - r v) \\ F_z = m (\dot{w} + p v - q u) \\ G_y = \dot{q} I_y - pr (I_z - I_x) + (p^2 - r^2) I_{xz} \end{array} \\
 & \left. \begin{array}{l} (1A) \\ (2A) \\ (3A) \end{array} \right\} \begin{array}{l} \text{Equations (1),} \\ \text{(2), and (3)} \\ \text{in terms of} \\ \text{perturbed} \\ \text{variables.} \end{array}
 \end{array}$$

In Equation 1A observe that the terms qw and rv are second degree terms, where degree means the number of variables in any product. Although there have been inroads into the solution of some nonlinear equations, i.e., equations of degree greater than one, this is a branch of calculus that

is still under development and its complexity is such to preclude its use in most engineering applications. The fact that $q\dot{w}$ and $r\dot{u}$ are the culprits in whose absence Equation 1A would be a linear equation certainly suggests a way to obtain a solution regardless of its validity. The next step is to establish the conditions under which $q\dot{w}$ and $r\dot{u}$ may be discarded. The term $q\dot{w}$ is a centrifugal acceleration term and can be shown to be small normally.⁹⁴ The term $r\dot{v}$ will be zero if mode coupling does not occur.

THEOREM VIII: The easiest way to linearize nonlinear equations is to throw away the nonlinear terms.

Unfortunately, mode coupling between the longitudinal and lateral-directional modes does occur during stability and control maneuvers when the aircraft cannot be completely stabilized. This lack of ability to stabilize occurs frequently during steady turns or high angle of attack maneuvering. If it is assumed that the measurements of the motion in the modes not being analyzed are accurate, these motions can be treated as known. Therefore, the coupling terms appear as known external inputs or extra control inputs to the mode under investigation. The model is then made linear. Reference 57 presents an example of a longitudinal maneuver during which lateral-directional motion was significant at a high angle of attack. In this case, good agreement was obtained with derivatives obtained from maneuvers performed at the same flight condition but with little lateral-directional motion by determining \dot{u} , \dot{w} , and \dot{q} as functions of α , β , ϕ , p , r , and aircraft moments of inertia.

As an example consider the pitching moment equation:

$$G_y = \dot{q}I_y - pr \left(I_z - I_x \right) + \left(p^2 - r^2 \right) I_{xz} \quad (3A)$$

Neglecting thrust and gyroscopic effects and assuming initial moments are zero, from Equation 15 the left hand side of Equation 3A can be written:

$$G_y = \mathcal{M} = I_y \left(\mathcal{M}_u^u + \mathcal{M}_\alpha^\alpha + \mathcal{M}_{\dot{\alpha}}^{\dot{\alpha}} + \mathcal{M}_q^q + \mathcal{M}_{\delta_e}^{\delta_e} \right) \quad (33A)$$

If the p^2 and r^2 nonlinear terms can be considered negligible Equations 3A and 33A can be equated and rearranged:

$$\begin{aligned} \mathcal{M}_u^u + \mathcal{M}_\alpha^\alpha + \mathcal{M}_{\dot{\alpha}}^{\dot{\alpha}} + \mathcal{M}_q^q + \mathcal{M}_{\delta_e}^{\delta_e} + \dots \\ \dots + \left(\frac{I_z - I_x}{I_y} \right) pr = \dot{q} \end{aligned} \quad (33B)$$

Equation 33B can now be solved if p and r are considered as knowns or are treated as inputs. For example, they might be measured values from lateral-directional motion.

Sometimes the linear model of the aircraft becomes inadequate and the nonlinear model is known, but cannot be put into linear form. An example of this type of problem is the need to include the drag polar in the model.⁵⁷ The drag polar can be expressed as:

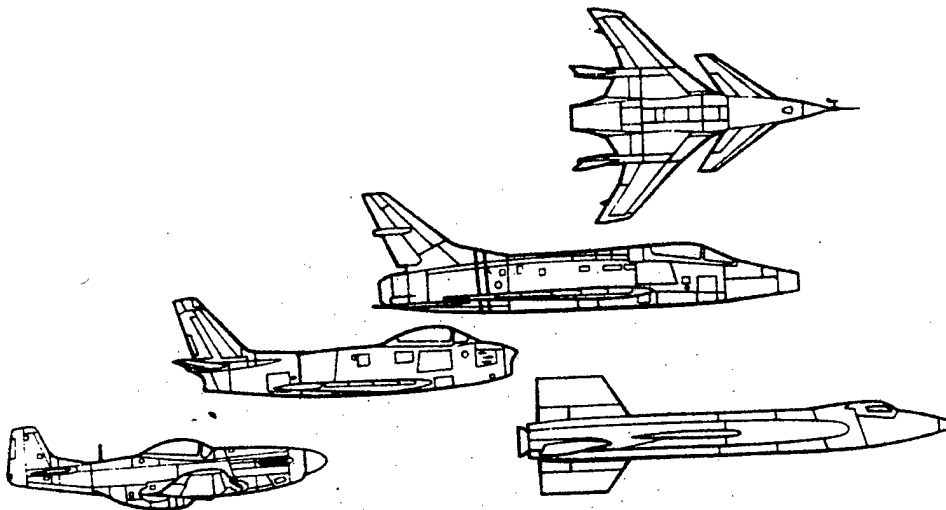
$$C_D = C_{D_P} + C_{D_{C_L^2}} C_L^2 \quad (34)$$

The lift coefficient can be expressed as a first-order Taylor series expansion of angle of attack and elevator deflection:

$$C_L = C_{L_0} + C_{L_\alpha} \alpha + C_{L_{\delta_e}} \delta_e \quad (35)$$

The substitution of Equation 35 into Equation 34 results in the following equation:

$$C_D = C_{D_p} + C_{D_{C_L^2}} \left(C_{L_0} + C_{L_\alpha} \alpha + C_{L_{\delta_e}} \delta_e \right)^2 \quad (36)$$



Upon expansion and redefinition of terms, Reference 67 shows that Equation 36 can be written as:

$$C_D = C_{D_0} + C_{D_\alpha} \alpha + C_{D_{\delta_e}} \delta_e + C_{D_{\alpha^2}} \alpha^2 + C_{D_{\alpha\delta_e}} \alpha \delta_e + C_{D_{\delta_e^2}} \delta_e^2 \quad (37)$$

The differential equations of motion can be written to include the power series expansion in Equation 37. The nonlinear effects defined by Equation 37 are expected to be functions of both angle of attack and elevator deflection. Keeping the number of nonlinear terms as small as possible increases the probability of obtaining meaningful estimates. A set of nonlinear equations derived demonstrating this approach is given in Reference 67. The nonlinear pitch equation is shown below as an example, and the previously derived linear pitch equation is shown for comparison:

NONLINEAR $\ddot{\theta} - \mathcal{M}_q \dot{\theta} - \mathcal{M}_u - \mathcal{M}_{\dot{\alpha}} - \mathcal{M}_{\alpha} - \dots$
 PITCH

$$\dots - \mathcal{M}_{\alpha^2} \alpha^2 = \mathcal{M}_{\delta_e} \delta_e + \mathcal{M}_{\delta_e^2} \delta_e^2 + \mathcal{M}_{\alpha\delta_e} \alpha \delta_e \quad (38)$$

LINEAR $\ddot{\theta} - \mathcal{M}_q \dot{\theta} - \mathcal{M}_u - \mathcal{M}_{\dot{\alpha}} - \mathcal{M}_{\alpha} = \mathcal{M}_{\delta_e} \delta_e \quad (24)$
 PITCH

VSTOL aircraft present another example where nonlinear models are sometimes required. Again, using the pitch equation as an example, from Equation 7 considering small perturbations:

$$\mathcal{M} = f(u, \alpha, \dot{\alpha}, q, \delta_e) \quad (39)$$

Equation 39 was used in deriving the linear equations of motion to expand the pitching moment in a Taylor series expansion. In the hover, most VSTOL aircraft display neutral stability or worse because relative wind, u , and α are undefined and contribute little to static stability. In addition, the propulsive force arrangement usually provides no restoring moment. Ground effect may provide either positive, neutral, or negative stability contributions. As the aircraft transitions to conventional flight, the velocities appear and bring with them the conventional aircraft stabilities.⁶⁸ The variables which affect the pitching moment equation in the hover mode are considered to be:⁶⁹

$$M = f(u, w, \dot{w}, q, \delta_{\text{Control}}) \quad (40)$$

Using a Taylor series expansion, Equation 40 could be written in terms of linear stability parameters; however, the nonlinear variable relationship shown in Equation 41 has also been used to express the hover pitching moment equation:

$$M = f(u, u^2, w, uw, q, uq, \delta_{\text{Control}}, u\delta_{\text{Control}}). \quad (41)$$

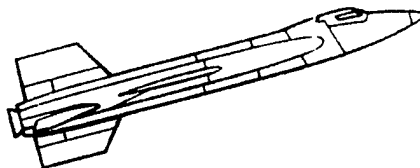
Unknown External Disturbances. Modeling problems caused by unknown external disturbances are encountered when an aircraft flies in atmospheric turbulence or in the vortex of another aircraft. A method has been devised to apply to data obtained in atmospheric turbulence using the Dryden model of turbulence. The method estimates the turbulence as a function of time. Reference 57 and 143 demonstrate good results with the use of this approach. Data from Reference 143 was presented in Section 2, Figures 6A and 6B.

Unknown Model. The third type of modeling problem, the case in which no known model exists, usually cannot be handled. Many nonlinear

models can be approximated easily by a power series expansion like Equation 38 was, but the results of this type of analysis are often meaningless in that the coefficients extracted have little physical significance. An example of a modeling problem for which even a power series expansion does not approximate the nonlinearity occurs during flow separation. Although there are many causes of flow separation, the time at which the separation occurs and the frequency with which it occurs are random. Thus, little can be done to extract meaningful stability and control derivatives unless the separation is mild enough to permit a known model to approximate the resulting motion adequately.

THEOREM IX: Extracting coefficients with little physical significance is a waste of time.

Another time when no proven model exists is when maneuvers are performed at high angles of attack. One way to treat this problem when perturbations about the nominal are small is to assume that a system is still described by the linear equations of motion. For example, pitching moment coefficient, C_m , as a function of angle of attack is nonlinear over a large range of angle of attack; however, if the change in angle of attack can be kept small enough for a given flight condition, the derivative C_{m_α} can be estimated as piecewise linear and plotted as a function of angle of attack. Reference 57 shows an example where linearizing for small excursions from the nominal allows use of a linear approximated model where there is no known nonlinear model.



One recent high angle of attack analytical study used a "model-determination" algorithm to try to estimate which nonlinear parameters significantly effect aircraft response. Polynomials were chosen for the model. Wind tunnel results and aircraft dynamics were analyzed to define possible polynomial functions for aerodynamic forces and moments. Then, actual response data were used to specify which of these functions was most probable by a subset regression method. The goal was to identify only those polynomial coefficients which were required in the model to reproduce the actual force and moment characteristics. Subset regression is a sequential least squares method which adds and deletes variables to a particular model in an iterative manner, isolating a significant subset of the possible polynomial coefficients using a statistical hypothesis testing technique. While identifying the most significant model parameters, this technique also finds least squares estimates of the parameters which are used as a priori starting values for the MMLE program.¹⁴⁰

As an example of this technique, one (obviously carefully selected) high angle of attack rolling departure maneuver performed by an F-4E aircraft was used for model identification and extraction of longitudinal and lateral-directional stability derivatives. The resulting aerodynamic force and moment equations are listed as Equations 41A thru 41F:^{139, 140}

$$C_X = C_{X_0} + C_{X_{\alpha^2}} \alpha^2 + C_{X_{\alpha^4}} \alpha^4 + C_{X_{\beta}} \beta + C_{X_q} q \quad (41A)$$

$$C_Z = C_{Z_0} + C_{Z_{\alpha}} \alpha + C_{Z_{\alpha^2}} \alpha^2 + C_{Z_{\beta^2}} \beta^2 + C_{Z_q} q + C_{Z_{\delta_e}} \delta_e + C_{Z_{\alpha \delta_e}} \alpha \delta_e \quad (41B)$$

$$C_m = C_{m_0} + C_{m_{\alpha}} \alpha + C_{m_{\alpha^2}} \alpha^2 + C_{m_{\alpha^3}} \alpha^3 + C_{m_{\beta}} \beta + C_{m_q} q + C_{m_{\delta_e}} \delta_e \quad (41C)$$

$$C_{\ell} = C_{\ell_o} + C_{\ell_{\beta}} \beta + C_{\ell_{\alpha^2 \beta}} \alpha^2 \beta + C_{\ell_r} r \quad (41D)$$

$$C_n = C_{n_o} + C_{n_{\alpha \beta}} \alpha \beta + C_{n_p} p \quad (41E)$$

$$C_Y = C_{Y_o} + C_{Y_{\beta^3}} \beta^3 + C_{Y_{\alpha \beta}} \alpha \beta + C_{Y_{\alpha \delta_r}} \alpha \delta_r + C_{Y_{\alpha p}} \alpha p \quad (41F)$$

There are several interesting things about these expansions. The order of expansion in terms of angle of attack is different for each coefficient. Also, in the expansion for C_X , the fourth-order expansion term is included, but the third-order expansion term is not. Apparently, during this maneuver there was significant coupling in the longitudinal motions from variation in sideslip angle. Note also that the expansion for the control coefficient is different for the three force and moment coefficients.

This analysis concludes that at high angles of attack the F-4E lateral-directional controls are almost ineffective.¹⁴⁰ In fact, conventional control power terms do not even appear in the lateral-directional equations of motion. Strangely enough, there is a sideforce coupled term due to rudder, but no roll or yaw due to rudder.

Reference 140 also concludes that F-4E high angle of attack lateral-directional motion can be adequately explained by an unstable system driven by coupling with the longitudinal motion. These results will come as a surprise to pilots who have flown the F-4E at high angle of attack. A certain amount of discretion has to be used in trying to derive general conclusions with any physical significance from one nonlinear departure maneuver.

Overly Complete Model. The three preceding sections suggest various alterations which have been made to the standard linear aircraft model for specific situations. Care must be taken, however, not to introduce unnecessary complications in the model. In some cases, such alterations significantly degrade the estimates. An example of this is an attempt to make a full six-degree-of-freedom match for a longitudinal maneuver. Since the lateral inputs are small, normally insignificant modeling errors can predominate in the analysis of lateral motion. This, in combination with the greater number of unknowns, can seriously affect the estimates of all the unknowns. If lateral motion has to be considered, the best approach known is to use the measured lateral data as mentioned before. A similar procedure could be used for longitudinal motion during a lateral-directional maneuver. Many problems similar to these can arise from overly complex models. Thus, the use of the simplest model found to produce acceptable results is recommended; alterations should be made to the model only when the basic model is obviously inadequate.⁵⁷

In summary, the only proven, or completely accepted nonlinear technique is local linearization. No efforts made to date toward general solutions of nonlinear equations have been successful. When nonlinearities can be defined, then the equations can be solved; however, there is little confidence in interpretation of the significance of the results.¹⁴⁵

Nevertheless, work on nonlinear equations is continuing. Bilinear systems which are sometimes called "variable structure" systems are special case nonlinear systems which have received a lot of attention from theoreticians in recent years. For example, Equation 41G is bilinear in u and x ; that is, it is linear in each variable separately.^{143, 145}

$$\dot{x} = Ax + (Bu)x + Cu \quad (41G)$$

As might be expected, results from analysis of this type of bilinear equation are nowhere near as useful as results from linear equation analysis. The practical utilization of bilinear equations is still in its infancy.¹⁴³

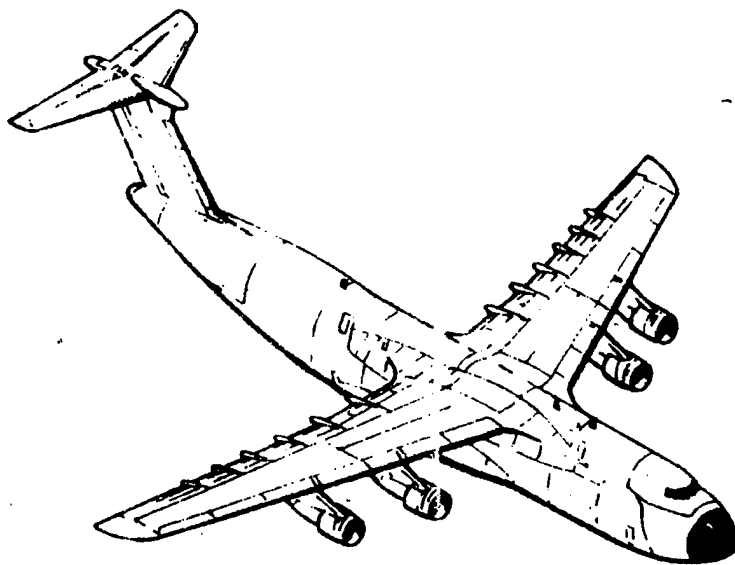
Considering the reluctance to use parameter estimation techniques for linear systems, the urgency found in the literature to apply them to nonlinear equations is surprising.¹⁴⁵ Some of the following nonlinear theorems apply:

THEOREM XXIII: Current analysis of nonlinear systems follows the basic engineering premise, "By twiddling the dials you can make it work."

THEOREM XXIV: Analysis of nonlinear systems yields any desired result.

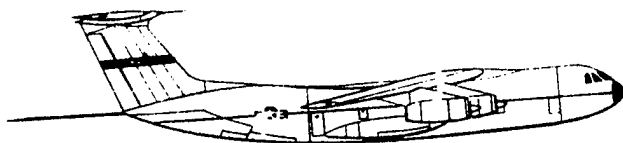
THEOREM XXV: Results from nonlinear analysis are insignificant.

THEOREM XXVI: The input/output relationship of a nonlinear system is not unique.



ESTIMATION CRITERION

There must be some means of assessing the fit of the computed response to the flight measured response.¹² The process of selecting the means of assessing the fit is known as identifying the cost functional or criterion function. When the process is implemented manually, as in analog matching, the cost functional is obscure in that what constitutes a good fit is primarily a function of the judgement of the operator.³⁴ The operator minimizes his subjective cost functional by adjusting potentiometers until, in his opinion, the fit is attained. The procedure can be time consuming, and the results vary greatly from operator to operator.^{34,43} Regression methods alleviate some of the problems of analog matching in that a cost functional is specified and is readily minimized because the formulation is linear.²⁴ Unfortunately, the resulting fit to the measured data is unsatisfactory.⁴³ In automated techniques a criterion function is used as shown in Figure 3. It is usually some form of an integral square of the error between the computed and measured response.¹² Ultimately, a mathematical model is desired with a computed response that best fits the measured data. It has been demonstrated that the fit obtained by analog matching is superior to that obtained with earlier methods. This suggests that the cost functional should reflect the difference between the computed response based upon the coefficient estimates and the measured response. Therefore, more satisfactory results would be expected if the problem were posed as one of minimizing a quadratic cost functional of this difference. Many other criteria could be proposed, but the quadratic



is the most thoroughly analyzed form and has the most desirable mathematical characteristics.⁴³ Under certain conditions the criterion function corresponds to the maximum likelihood criterion, which is intended to produce the most probable values of the parameters. The best estimate of the parameters is that set of parameters that minimizes the cost (criterion) function.^{12,44} Reference 60 presents a discussion of the cost function used in the data reduction program which will be used to determine stability derivatives from dynamic maneuvers performed here at the USAF Test Pilot School.

COMPUTATIONAL ALGORITHM

Once the mathematical model for the system and the cost functional to be minimized have been selected, an algorithm to minimize the cost functional must be specified to identify the system.⁴³ The cost function is nonlinear with respect to the parameters to be estimated; therefore, it has to be minimized by an iterative computational algorithm. Several algorithms that have been used are steepest descent, Newton-Raphson, modified Newton-Raphson (also referred to as quasi-linearization or differential correction), various conjugate gradient methods, various direct and random search techniques, stochastic approximation, and an iterative Kalman filter method.^{12,61,62,70} Probably the simplest minimization technique is the gradient technique, which changes the coefficients to be estimated by proceeding in the direction of the greatest decrease of the cost functional. Unfortunately, although the fit error is reduced considerably, the values of the unknown coefficients are not determined with sufficient accuracy, because the minimum is never reached. The Newton-Raphson technique is an iterative method for finding a zero of the gradient of the cost functional. This method is much more efficient than the gradient method because it attempts to predict where the local minimum point is and to step directly to it rather than merely stepping in the local downhill direction. However, it is much more complex because of the computation of a second gradient matrix. This complexity can be reduced significantly as shown by

Balakrishnan by an appropriate approximation to the second gradient matrix which results in a method termed either modified Newton-Raphson or quasi-linearization.⁴⁵ It is most clearly derived by the method of quasi-linearization. The modified Newton-Raphson method was found to be superior to the gradient method both in terms of the number of iterations and the computation time required for stability derivative extraction. To demonstrate that the method was generally applicable to a wide range of modern aircraft, it was applied to the X-15 research vehicle, a light general aviation aircraft, a large supersonic aircraft, and a lifting body vehicle. The method proved to be satisfactory for each of the maneuvers analyzed.⁴³ Although the mathematics behind this modified Newton-Raphson algorithm which will be used to determine stability derivatives from dynamic maneuvers here at the School is complex, Reference 60 shows that the basic idea is simple and can be neatly illustrated with a one-degree-of-freedom example. The nature of nonlinear minimization is such that no one algorithm can be classified as the best for all problems. Important factors in selecting the minimization algorithm are startup routines, convergence, computational efficiency, dimensionality, local minima, and whether the data processing will be on-line or batch.¹²

THEOREM X: The mathematical basis for extracting stability derivatives from flight test data is not elementary.

THEOREM XI: There is a major difficulty in solving two or three equations for ten or twelve unknowns.

THEOREM XII: There is no optimum algorithm.

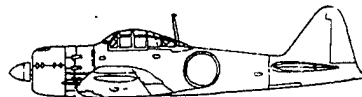


Messerschmitt ME-109

TOTAL DATA ACQUISITION SYSTEM

Parameter estimation is highly dependent on the quality of the flight-measured data. In Figure 3 the uncertainties in the measured flight response are represented by additive noise. In reality the "noise" comes from several sources, and it is necessary to consider the entire data acquisition process. Bias and random errors can arise from imprecise location or orientation of sensors, calibration of the measurement and recording system, and data drop out. Other errors can be introduced from electrical noise, engine vibration pickup, sensor dynamics, inappropriate signal filters, and quantization. A comprehensive discussion of flight-test instrumentation for aircraft parameter estimation is given in Reference 35. Any elimination of errors, noise, or uncertainties within the data acquisition process will improve the accuracy of the estimates. However, it is not always possible to optimize the instrumentation specifically for parameter estimation because of project schedule or manpower limitations. It is desirable to have techniques that are effective despite measurement noise and uncertainties.¹²

In any flying quality flight test program, difficulties with data are to be expected. Sometimes these problems, such as data spikes, are apparent from even a cursory look at the flight test results; however, other, less obvious problems should also be expected. One of the most common sources of major error is the improper specification within the model of the instrumentation and data acquisition system.⁵⁷



Mitsubishi A6M-5 'Zero'

The instruments on the aircraft should be positioned to prevent them from being affected by structural vibration or flow phenomena. Aircraft stability and control analyses must include the capability for making corrections for differences between the actual and assumed instrument locations. The accurate modeling of the angle of attack and angle of sideslip vane positions and accelerometer positions is particularly important, and corrections for these positions can be made. If the data are not corrected for vane location, the fit of the data is poor, particularly when angular rates are high. If the data are not corrected for accelerometer position, some of the estimated derivatives are affected. It usually becomes evident that the latter correction has not been made when the measured and computed data are compared.⁵⁷

The resolution and accuracy of the instrumentation must also be taken into account. If measurement noise is small, fairly low resolution can be tolerated in any noncontrol measurement, although the lower the resolution, the poorer the estimates. Low resolution in a control measurement can be intolerable, because most motions are derived from control movement. If the position of a control is not accurately defined in a sampled time history, the predicted motion will not be acceptable. If the predicted



North American P 51 Mustang

motion is incorrect, the estimates of the derivatives, particularly the control derivatives, will be severely degraded. When the resolution of a control measurement is extremely low, the movement of the control may be missed completely.⁵⁷

The sampling rate chosen for the data can also affect the quality of the estimated derivatives significantly. In most aircraft stability and control analyses, the determining factor is the accurate definition of control motion. Rapid excursions are caused by rapid control inputs, and these dictate the required sampling rate. With a low sampling rate, the initiation of control motion might be missed, causing the vehicle to appear to respond before the control is moved. The resulting control time history would result in unacceptable predictions of motion, degrading the estimated derivatives. To economize on computer utilization, each vehicle being tested should be studied to determine the lowest sampling rate that can be tolerated. After this lowest level has been established, the effect of sampling rate should be checked periodically to make sure that the estimation process yields sufficiently good estimates.⁵⁷

Time and phase shifts must also be considered. Time shifts occur when digitally acquired data are sampled sequentially. Particularly when the sample interval is large, the time shift between a measurement sampled at the beginning of the interval and a measurement sampled at the end of the interval is significant. The maximum likelihood estimation algorithm assumes that all measurements are sampled simultaneously, so this time shift causes errors in the estimated coefficients. This becomes particularly important when the control input is sampled at a significantly different time than one or more of the other measurements within the sample interval. If the instrumentation system cannot otherwise meet the requirements for a minimum time between the beginning and end of the sample interval, this effect can be compensated for in the data before the analysis begins by time shifting the appropriate signals.⁵⁷

A phase shift due to instrumentation filters can cause a similar problem. All filter rolloff frequencies should be kept much higher than the aerodynamic frequencies of interest. If a filter is unavoidable, all the measurements should be filtered with the same filter or phase shift corrections should be applied to the raw data for all the filtered measurements.

Reference 60 presents the data requirements for the two different stability derivative extraction programs in use at the AFFTC. Parameter range, resolution, and sampling rates are specified and filtering problems are discussed. Data acquisition system operational procedures and magnetic tape recorder formats for Test Pilot School aircraft are presented in Reference 71.

THEOREM XIII: Unmodeled instrumentation errors can cause inaccuracies in estimated parameters comparable to their nominal values.¹²³

TEST INPUT

As a minimum requirement, the test input must excite the principal response modes that depend on the parameters to be determined. In the previous example a combination of rudder and aileron pulses adequately excited the lateral-directional motion. Thus the question arises whether one type of control input might be better than another, in the sense that it provides better estimates. Several papers have considered that question and have shown that in theory a test input can be found that will tend to minimize the variance of the estimated parameters.⁶³ However, there is also the possibility that unsteady aerodynamic effects might account for observed parameter variances.¹⁴⁶ These concepts have not been fully explored in a flight test application and there are no examples of the successful application of optimum input design.^{12, 145} Unfortunately, in order to design an optimum input the unknown parameters have to be known.¹⁴⁵

Since the type and quality of flight maneuver used is the most important

factor in the success of the stability derivative extraction process, Reference 60 discusses possible maneuvers in some detail; however, rapid pitch, yaw, and roll control doublets are recommended.

THEOREM XIV: Difficulty will be encountered trying to obtain consistent parameter estimates using dissimilar inputs.

THEOREM XV: Difficulty may be encountered trying to obtain consistent parameter estimates using similar inputs.¹¹⁸

THEOREM XVI: No matter what input is used, output will be less than optimum.

THEOREM XVII: There is no optimum input.

THEOREM XXVII: If there is an optimum input using it will not improve the parameter estimates much.¹⁴⁵

SUMMARY

Although there are variations from the basic concept depicted in Figure 3, depending on the specific situation being considered or the mathematical approach used, the five key aspects of parameter estimation discussed are always included in some form. For example, if there are nonmeasured external disturbances, such as air turbulence, it is necessary to add a state estimator to these five aspects.¹²

It should be clear at this point that parameter estimation techniques are not restricted to determining linear stability and control derivatives. Virtually any flight test that can be modeled as an input/output dynamic system is amenable to this approach. Areas being considered for study include nonlinear aerodynamics, aircraft structural dynamics, estimates of external disturbances such as air turbulence and vortex wakes, and air-frame/propulsion system interaction effects.¹² It should be kept in mind, however that in spite of high powered massive memory computers and elegant nonlinear algorithms, parameter estimation still depends largely on the ingenuity of the engineer since the technique is still far from being

automatic.

THEOREM XVIII: Systems identification problems are a hunt for some unknown parameter during which some unverifiable answer is obtained.¹¹⁷

FUTURE POTENTIAL

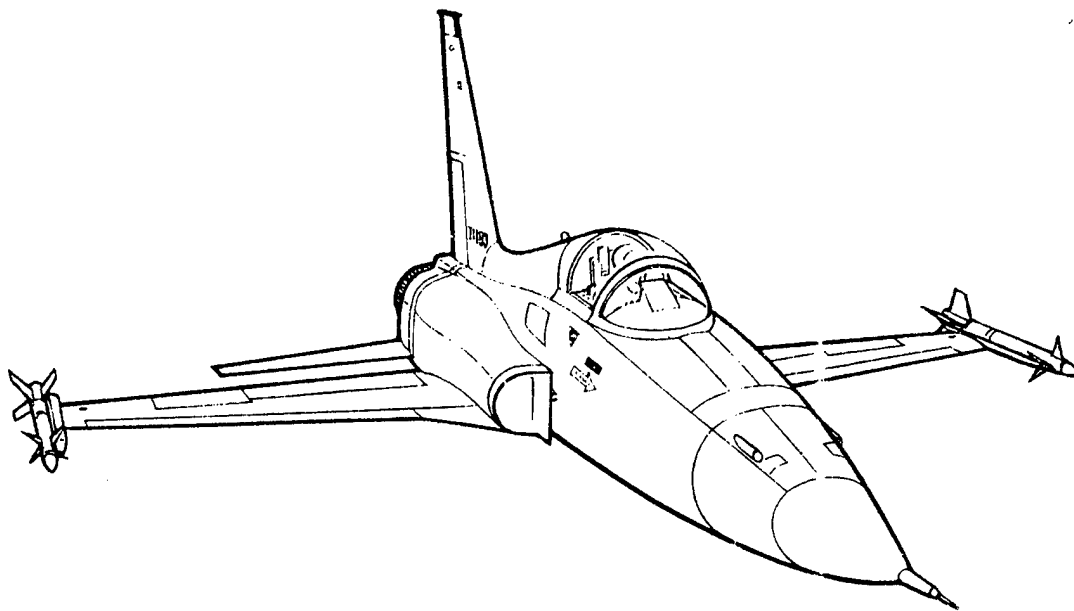
The future effect of applying parameter estimation techniques to aircraft flight testing is anticipated to be twofold: It should reduce the overall schedule of a flight test program and at the same time increase the amount of information extracted from the tests.¹²

The reduced schedule is expected to result from savings in analysis time, through more effective methods; flight time, through use of dynamic tests in place of the more time-consuming quasi-static tests, such as those used in measuring lift/drag polars; and the preparation time, by not requiring special instrumentation for each flight test task. These savings should result in lower overall program costs.¹²

Parameter estimation provides a trend toward increased information output. Data previously discarded because of turbulence contamination are now useable. It is now possible to use a single dynamic maneuver to obtain lift and drag coefficients as well as stability derivatives.⁶⁷ With further improvements and refinements, other combinations may be possible, such as determining structural modes, turbulence, performance, and stability and control characteristics simultaneously.¹² One of the most intriguing applications of parameter estimation to be found in the current literature is its use in a control system which tracks parameters and continuously updates the control system model.¹⁴⁵

In view of the capabilities and potentials of parameter estimation techniques, flight test engineers should reevaluate the test procedures and instrumentation that have been used for many years. The AFFTC is committed

to the continued use and development of these techniques and expects further improvements in flight testing with the development of nonlinear systems identification programs with broader application.¹⁰⁶ However, as has been shown in this section, development of nonlinear parameter estimation techniques which yield meaningful results is probably still far in the future.



SECTION 3

STABILITY PARAMETERS AND DERIVATIVES

INTRODUCTION

It is possible to evaluate the flying qualities of an aircraft without ever considering stability derivatives. Stability derivatives are not determined here at the School during the flying qualities phase. The main reason for this is that MIL-F-8785B (ASG) does not explicitly require that stability derivatives be determined from flight test. The specification is based to a considerable extent upon a large number of opinions expressed by pilots concerning desirable or undesirable flying qualities of military aircraft. Consequently, most of the flight testing for stability and control is carried out for the one purpose of demonstrating that the contractor's particular aircraft meets these specifications.⁶⁵

In order to accomplish this, flight test techniques have been devised to evaluate flying qualities using a combination of stabilized and dynamic maneuvers. Dynamic maneuvers are performed to determine the frequency and damping ratio of the phugoid, short-period, and dutch roll modes and ϕ/β parameters used in the dutch roll and roll-mode investigations. Roll rates are also measured and roll-mode time constants determined. The underlying philosophy of this type of testing is to determine if the aircraft meets the required level of flying qualities specified for each test point evaluated. The level of flying qualities required depends on whether the aircraft is in either the operational, service, or permissible flight envelopes and whether or not a defined failure state exists.

Hopefully, this course and its associated data gathering and analysis will show that flight testing for the purpose of obtaining stability derivatives is of much more than purely academic interest. Reference 60

discusses some of the deficiencies in conventional flying quality testing and presents arguments for extracting stability derivatives. Two points of that argument are worth expanding:

1. If conventional tests are performed on an aircraft with a high gain augmentation system, it is impossible to determine the characteristics of the basic or unaugmented aircraft; therefore, each flight control operational mode or defined failure state must be tested individually. If stability derivatives are determined some degree of extrapolation may be possible. Interpolation would certainly be possible.

2. A high gain augmentation system can prevent aircraft motions from being analyzed at all. Conventional techniques are based on a comparison of aircraft dynamics with a second-order response which does not occur when augmentation systems are used. This allows a high gain system to mask a serious flying qualities deficiency until it is saturated. For example, a longitudinally statically unstable aircraft with a high gain augmentation system may have excellent flying qualities on the linear part of the C_L and C_m versus α curves; however, at high angles of attack where nonlinearities occur and separation begins the control system may not be able to stabilize the aircraft. This loss of ability to stabilize can be due to (1) software confusion, (2) the need for more than maximum elevator deflection, (3) or the need for a faster elevator input (response) than the actuators can generate. A study of the basic aircraft stability derivatives might help predict dangerous trends.

These are some possible disadvantages to a complete dependence on stability derivative extraction methods for flying quality testing:

1. Derivatives determined from flight test are "local slope" derivatives. For example, C_{m_α} is a function of angle of attack at high angles of attack; therefore, the value of C_{m_α} determined will be an average

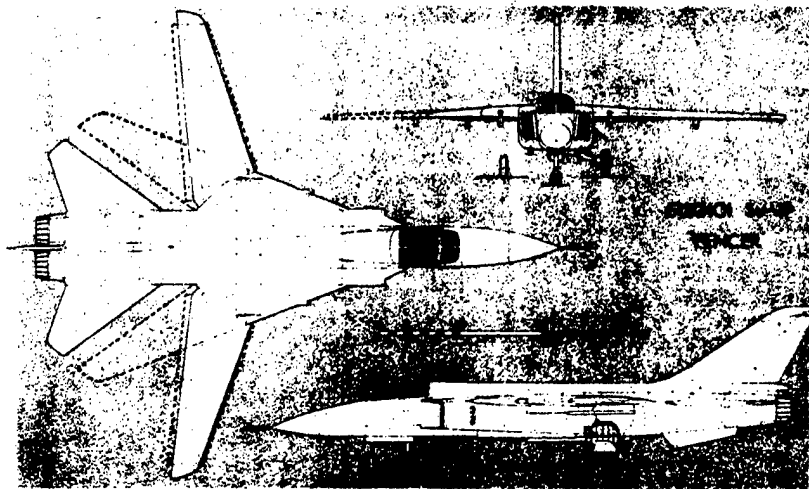
value of $C_{m\alpha}$ over the range of angle of attack covered during the test maneuver. Since stability derivative extraction maneuvers can be performed from any desired trim angle of attack this does not seem to be a problem; however, derivatives like $C_{n\beta}$ are also functions of sideslip angle at large values of sideslip. "Local Slope" values of $C_{n\beta}$ determined from a maneuver performed from a zero sideslip trim angle will not predict lateral-directional problems which might be encountered during large sideslips, e.g., during crosswind landings (slips), engine out flight, or rolling maneuvers performed at low speed - high angle of attack. The obvious solution is to perform test maneuvers from various trim sideslip angles. Unfortunately, the equations of motion are now nonlinear and do not uncouple. Current stability and control derivative extraction techniques will not handle this situation.

2. Flight test instrumentation costs could increase. For example, the School magnetic tape instrumentation systems do not have either the resolution or sample rates recommended by Reference 60. The additional cost at time of purchase to meet these requirements is unknown. It also remains to be seen if stability derivatives can be successfully extracted using School aircraft instrumentation systems.

3. It might be a problem proving contractual noncompliance with the military flying quality requirements when the specified parameters are not actually measured, but calculated from flight test determined derivatives. Most aircraft contractors do not have experience using parameter estimation to extract stability and control derivatives, and at least a few have some reservations about the technique. Reference 36 describes some of the classical flight test methods which are to be used to determine military specification compliance; however, parameters which the specification requires evaluated such as natural frequency and damping ratio can be calculated from flight test extracted derivatives if the procuring activity and contractor agree on this procedure.

4. In the case of modern highly augmented aircraft, the basic airframe (basic aircraft) characteristics may not correlate at all with flying quality measurements or pilot opinions of handling qualities. In fact, small changes in control laws may cause drastic changes in aircraft flying qualities. The more highly augmented the control system, the more this is true. In addition, for full authority systems there may not be a failure mode which permits the pilot to "fly" the basic aircraft on a direct more-or-less one-to-one basis with control force and/or deflection corresponding to control surface deflection. Having a flyable, basically stable bare airframe is of no consequence to the pilot if he cannot obtain direct control.

Stability parameters and derivatives are discussed in some detail in the remaining part of this Section. Methods of classifying and determining derivatives and examples of individual derivatives will also be presented.



DEFINITIONS

Before classifying stability parameters or derivatives it might be helpful to define them one more time. They both were defined mathematically in Section 2; however, judiciously following the example of most classical stability and control texts, word definitions were avoided. The definitions below are offered, but they are not particularly enlightening:

Stability Parameter: Normalized term expressing the change of a force or moment acting on an aircraft with respect to some variable, e.g.

$$m_q = \frac{1}{I_y} \frac{\partial m}{\partial q}$$

Stability Derivative: Nondimensional number expressing the change of a force or moment coefficient acting on an aircraft with respect to some non-dimensionalized variable, e.g.

$$C_{m_q} = \frac{\partial C_m}{\partial \hat{q}}$$

The pitching moment equation of motion in stability parameter form from Section 2 was:

$$\dot{q} = m_u u + m_\alpha \alpha + m_{\dot{\alpha}} \dot{\alpha} + m_q q + m_{\delta_e} \delta_e \quad (21)$$

where m_u , m_α , etc., are defined as stability parameters. The pitching moment equation can also be written in stability derivative form as:

$$\frac{2I_y}{\rho U_o^2 S c} \dot{q} = C_{m_u} \hat{u} + C_{m_\alpha} \alpha + C_{m_{\dot{\alpha}}} \hat{\dot{\alpha}} + C_{m_q} \hat{q} + C_{m_{\delta_e}} \delta_e \quad (42)$$

where C_{m_u} , C_{m_α} , etc., are defined as stability derivatives. It is readily

apparent that equations differ only by a constant multiplier at a given trim speed, or for example:

$$\left(\frac{2I_y}{\rho U_o^2 S c} \right) \mathcal{M}_{q1} = C_{m_q} \hat{q} \quad (43)$$

Rearranging:

$$\mathcal{M}_{q1} = \frac{\rho U_o^2 S c}{2I_y} C_{m_q} \hat{q} \quad (44)$$

which is the term discussed in Section 2 where C_{m_q} is a dimensionless number and \hat{q} is a dimensionless variable defined as $\frac{cq}{2U_o}$. Equation

44 can be written:

$$\mathcal{M}_{q1} = \frac{\rho U_o^2 S c}{2I_y} C_{m_q} \left(\frac{cq}{2U_o} \right) \quad (45)$$

or

$$\mathcal{M}_q = \frac{\rho U_o S c^2}{4I_y} C_{m_q} \quad (46)$$

Given a numerical value for C_{m_q} , \mathcal{M}_q can now be determined for any trim speed given the aircraft geometry.

Both stability parameters and derivatives are used in analysis. Given one, it's easy to get the other, so they can be talked about interchangeably. The use of stability parameters tends to simplify some of the approximate aircraft dynamic relationships. For example, in Reference 64 the following approximate relationship for short period natural frequency is derived:

$$\omega_n \approx U_o \sqrt{\frac{\rho S c}{2 I_y}} \sqrt{-C_{m_\alpha}} \quad (47)$$

It can be easily verified that this expression written in terms of stability parameters instead of stability derivatives is:

$$\omega_n \approx \sqrt{-m_\alpha} \quad (48)$$

However, stability parameters are a function of trim speed as well as aircraft geometry, while stability derivatives are nondimensional numbers and for a rigid aircraft may be constant at low Mach numbers.

CLASSIFICATION

For analysis problems where total aircraft motion can be thought of as two independent motions, stability parameters or derivatives can be thought of as either longitudinal or lateral-directional terms. From Equations 13 through 18:

Longitudinal Parameters:

$$D_u, D_\alpha, D_{\dot{\alpha}}, D_q, D_{\delta_e}$$

$$L_u, L_\alpha, L_{\dot{\alpha}}, L_q, L_{\delta_e}$$

$$m_u, m_\alpha, m_{\dot{\alpha}}, m_q, m_{\delta_e}$$

Longitudinal Derivatives:

$$C_{D_u}, C_{D_\alpha}, C_{D_{\dot{\alpha}}}, C_{D_q}, C_{D_{\delta_e}}$$

$$C_{L_u}, C_{L_\alpha}, C_{L_{\dot{\alpha}}}, C_{L_q}, C_{L_{\delta_e}}$$

$$C_{m_u}, C_{m_\alpha}, C_{m_{\dot{\alpha}}}, C_{m_q}, C_{m_{\delta_e}}$$

Lateral Directional Parameters:

$$Y_{\beta}, Y_{\dot{\beta}}, Y_p, Y_r, Y_{\delta_a}, Y_{\delta_r}$$

$$L_{\beta}, L_{\dot{\beta}}, L_p, L_r, L_{\delta_a}, L_{\delta_r}$$

$$N_{\beta}, N_{\dot{\beta}}, N_p, N_r, N_{\delta_a}, N_{\delta_r}$$

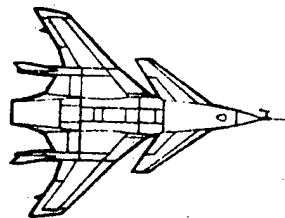
Lateral Directional Derivatives:

$$C_{Y_{\beta}}, C_{Y_{\dot{\beta}}}, C_{Y_p}, C_{Y_r}, C_{Y_{\delta_a}}, C_{Y_{\delta_r}}$$

$$C_{L_{\beta}}, C_{L_{\dot{\beta}}}, C_{L_p}, C_{L_r}, C_{L_{\delta_a}}, C_{L_{\delta_r}}$$

$$C_{N_{\beta}}, C_{N_{\dot{\beta}}}, C_{N_p}, C_{N_r}, C_{N_{\delta_a}}, C_{N_{\delta_r}}$$

Derivatives may also be divided into "stability"* derivatives which describe the natural tendency to return to trim when disturbed, force derivatives, control derivatives, damping derivatives, and lag or unsteady flow derivatives.



* Word used in a narrow sense.

Longitudinal "Stability" Derivatives:

$$C_{m_u}, C_{m_\alpha}$$

Lateral-Directional "Stability" Derivatives:

$$C_{\ell_\beta}, C_{n_\beta}$$

Longitudinal Force Derivatives:

$$C_{D_u}, C_{D_\alpha}, C_{L_u}, C_{L_\alpha}$$

Lateral-Directional Force Derivatives:

$$C_{Y_\beta}$$

Longitudinal Control Derivatives:

$$C_{D_{\delta_e}}, C_{L_{\delta_e}}, C_{m_{\delta_e}}$$

Lateral-Directional Control Derivatives:

$$C_{Y_{\delta_a}}, C_{Y_{\delta_r}}, C_{\ell_{\delta_a}}, C_{\ell_{\delta_r}}, C_{n_{\delta_a}}, C_{n_{\delta_r}}$$

Longitudinal Damping Derivatives:

$$C_{D_q}, C_{L_q}, C_{m_q}$$

Lateral Directional Damping Derivatives:

$$C_{Y_p}, C_{Y_r}, C_{\ell_p}, C_{\ell_r}, C_{n_p}, C_{n_r}$$

Longitudinal Lag or Unsteady Flow Derivatives:

$$C_{D\dot{\alpha}}, C_{L\dot{\alpha}}, C_{m\dot{\alpha}}$$

Lateral-Directional Lag or Unsteady Flow Derivatives:

$$C_{Y\dot{\beta}}, C_{l\dot{\beta}}, C_{n\dot{\beta}}$$

The lag or unsteady flow derivatives which are functions of $\dot{\alpha}$ and $\dot{\beta}$ cannot easily be distinguished from pitch rate and yaw rate respectively in either wind tunnel or flight testing. It is theoretically possible to separate the derivatives; however, it is not normally done in practice. The problems involved with separating them in wind tunnel testing will be discussed later in this section. Iliff at NASA Dryden has had some success with designing specific flight test maneuvers to allow separation of the lag and rate derivatives, but these techniques have not been adopted at the AEFTC.¹⁴⁵ In general, the damping derivatives determined from either wind tunnel or flight tests contain lag effects e.g.

$$C_{m_q} + C_{m\dot{\alpha}} \rightarrow C_{m_q}$$

It was pointed out in Section 2 that stability parameters or derivatives can be referred either to a body axis or stability axis system and conversion from one axis system to another can be easily accomplished.⁹⁹ For flight test it is useful to use the body axis system; therefore:

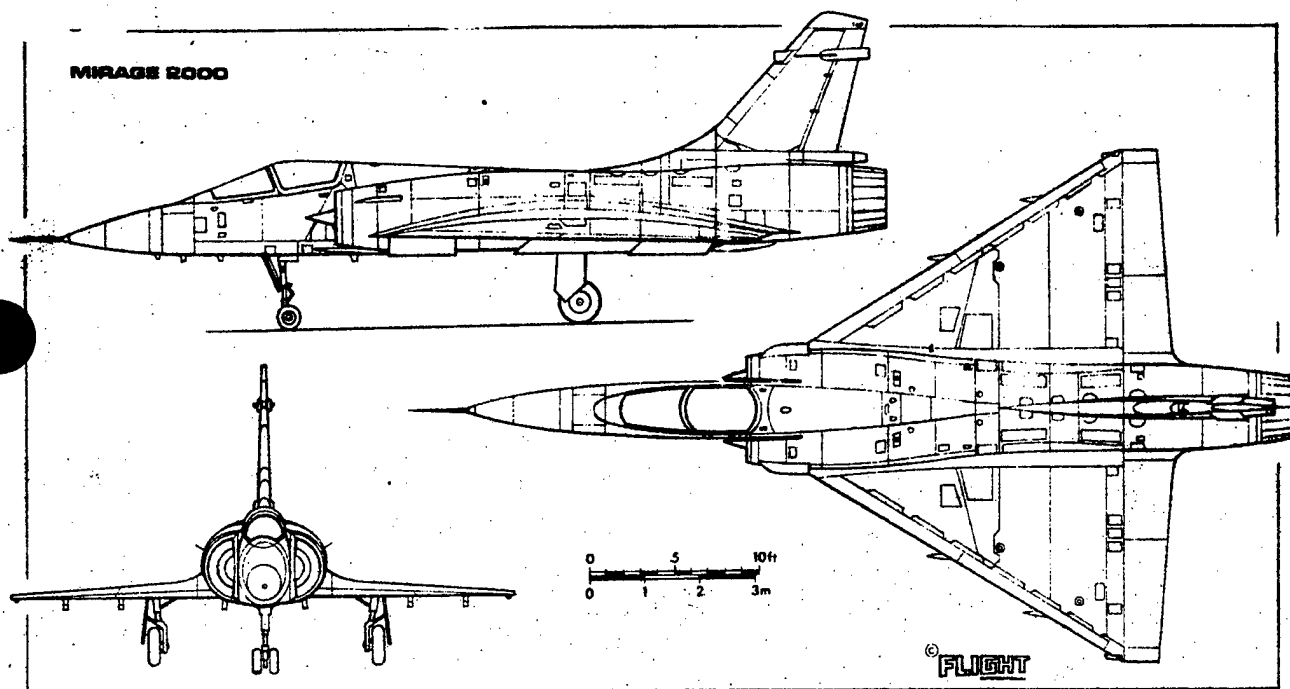
<u>Parameters</u>	<u>Derivatives</u>	
D → C or X	$C_D \rightarrow C_C$ or C_X	} Careful with signs!
L → N or Z	$C_L \rightarrow C_N$ or C_Z	

METHODS OF OBTAINING STABILITY DERIVATIVES

The purpose of this sub-section is to present a brief description of

the various methods and techniques in use today for the determination of the numerical values of stability derivatives and to discuss the relative accuracies of these methods.

Considerations relating to the accuracy with which aerodynamic data are known are of extreme importance in aircraft design. It is possible



that estimated stability derivatives for a given aircraft may be inaccurate due to insufficient or questionable basic information from which to compute the derivatives; this is particularly true in the transonic region. Aircraft designs must include sufficient tolerances to take into account potential derivative inaccuracies.

In general, there are three methods of obtaining stability derivatives which can be listed in the following order of increasing accuracy:

1. Estimating from theory and related empirical data.
2. Model testing.
3. Full-scale flight testing.

Each of these three methods will be considered.

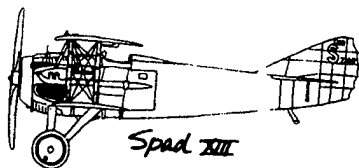
Estimating from Theory and Related Empirical Data

In general, the recommended procedure is to assume, first of all, a certain aircraft configuration or a strictly limited range of configurations. Reference 72, the Data Compendium (Datcom), presents a systematic summary of methods for estimating basic stability and control derivatives. The Datcom is organized in such a way that it is self-sufficient. For any given flight condition and configuration the complete set of derivatives can be determined without resort to outside information. The USAF has intended that the book be used for preliminary aircraft design. Its currency is maintained through periodic revisions (latest April 1978) and it is widely quoted and extracted from by current flying quality textbook authors.⁷⁴ Reference 73 is a USAF report prepared as a companion to the Datcom and presents methods for estimating flying qualities and insuring specification compliance. References 72 and 73 are all that are required to prepare an adequate aircraft preliminary design flying quality analysis.

Reference 119 is known as the Digital Datcom and is a computerized version of the Datcom manual. This Digital Datcom program can also be used in the preliminary design phase to obtain stability and control derivatives. These derivatives can then be converted to flying qualities parameters through the use of an additional digital computer solution of aircraft longitudinal and lateral-directional modes of motion as described in Reference 120. These two computer programs are still under development at the AFFDL and have only limited capability.¹²¹

Reference 65 includes a comprehensive list of references to NACA/NASA reports which can also be used for aircraft preliminary design and flying quality analysis.

Reference 74 presents a discussion of current analytical methods used to calculate stability derivatives of elastic aircraft based on work by the Boeing Company. Examples of analytical results obtained by Boeing will be discussed in Section 5 of this text.



In general, the subsonic values of stability derivatives for a rigid aircraft can be estimated quite accurately using the References discussed. For the transonic and low supersonic region, theoretical methods for determining stability and control derivatives for the complete aircraft are practically non-existent. As a result, the designer must resort to empirical data on similar aircraft. But because there is no theory which can be used as a guide, the trends indicated by empirical data are difficult to correlate, and this problem is further complicated by the fact that the data obtained by all the various techniques applicable to transonic investigations may be unreliable or inaccurate or both.⁶⁵ Reference 72 presents estimation methods which can be used in the transonic region.

For the supersonic region above a Mach number of about 1.5 limited theoretical methods are again available for estimating values of stability derivatives. In general, the higher the supersonic Mach number, the more reliable the theory.⁶⁵ Reference 72 presents methods and a list of bibliographies for estimating the supersonic derivatives of design configurations. Derivatives for the wing-alone can usually be determined very accurately, but usually empirical data is used to relate to complete airplane configurations.

Sometimes basic theory provides simplified relationships which give very accurate estimates of stability derivatives subsonically. The stability and control courses taught here at the School presented some of these simplified relationships.⁶⁴ These relationships will be reviewed as each stability derivative is discussed individually.

Model Testing

To increase the accuracy of the stability derivative estimates based upon theory and related empirical data, models duplicating the geometry of the contemplated full-scale airframe are usually built and tested. In fact, model testing has become such an important science that it is now considered indispensable to aircraft development.⁶⁵

Dimensional analysis shows that for measured force coefficients on a rigid scale model to be the same as those on a rigid aircraft in flight, the Mach number and Reynolds number of the model tests must be the same as those in flight.⁷⁷

If wind tunnel testing is restricted to low subsonic velocities, then Mach number effects can be neglected, but there still is an important scale effect which must be considered in applying the results of model testing to the full-scale aircraft. When the Reynolds numbers $\left(\frac{\rho V \ell}{\mu}\right)$ of two flows are equal, the flow characteristics are dynamically similar. Assuming a model and a full-scale aircraft operating at the same speed in the same atmospheric conditions, ρ , V , and μ are the same, but the Reynolds number of the model-flow combination is lower than the Reynolds number of the airplane-flow combination in direct proportion to the size of the model.⁶⁵

Full-scale aircraft operate in a Reynolds number range of 6,000,000 to 100,000,000, whereas model testing is normally done in a Reynolds number range of 500,000 to 10,000,000. Stability derivative data based on model tests performed at Reynolds numbers of 6,000,000 or more may be considered directly applicable to the full-scale airplane, but if the model tests are performed at Reynolds numbers of less than 6,000,000, it is likely that the stability derivative values will require modification before they can be applied to the full-scale airplane. One of the difficulties in using model test data is that the effects of Reynolds

number are in most cases quantitatively unpredictable, and the correct interpretation of the data is largely a matter of judgment based on experience.⁶⁵

There are two general types of model testing: wind tunnel testing and model flight testing. These types are considered in detail.

Wind Tunnel Testing. In general, the conventional wind tunnel consists of a tubular channel forming a closed circuit through which air is circulated at high velocities. During tests in this type of tunnel, the model remains stationary, and the various aerodynamic forces and moments acting on the model are measured by means of a balance system or by strain gages mounted on struts to which the model is attached.

● Static Derivative Wind Tunnel Testing.

Conventional wind tunnel testing is concerned with determining the derivatives which are not rates of change with time, the so-called "static" stability derivatives. The usual practice is to obtain six basic data; three forces, lift, drag, and side forces; and three moments, pitching, yawing, and rolling moments. In the longitudinal case, the coefficients C_L , C_D and C_m are functions of angle of attack α ; therefore, the static derivatives C_{L_α} , C_{D_α} , and $C_{m_{\delta_e}}$ are obtained from wind tunnel data. This process is illustrated in Figure 10.



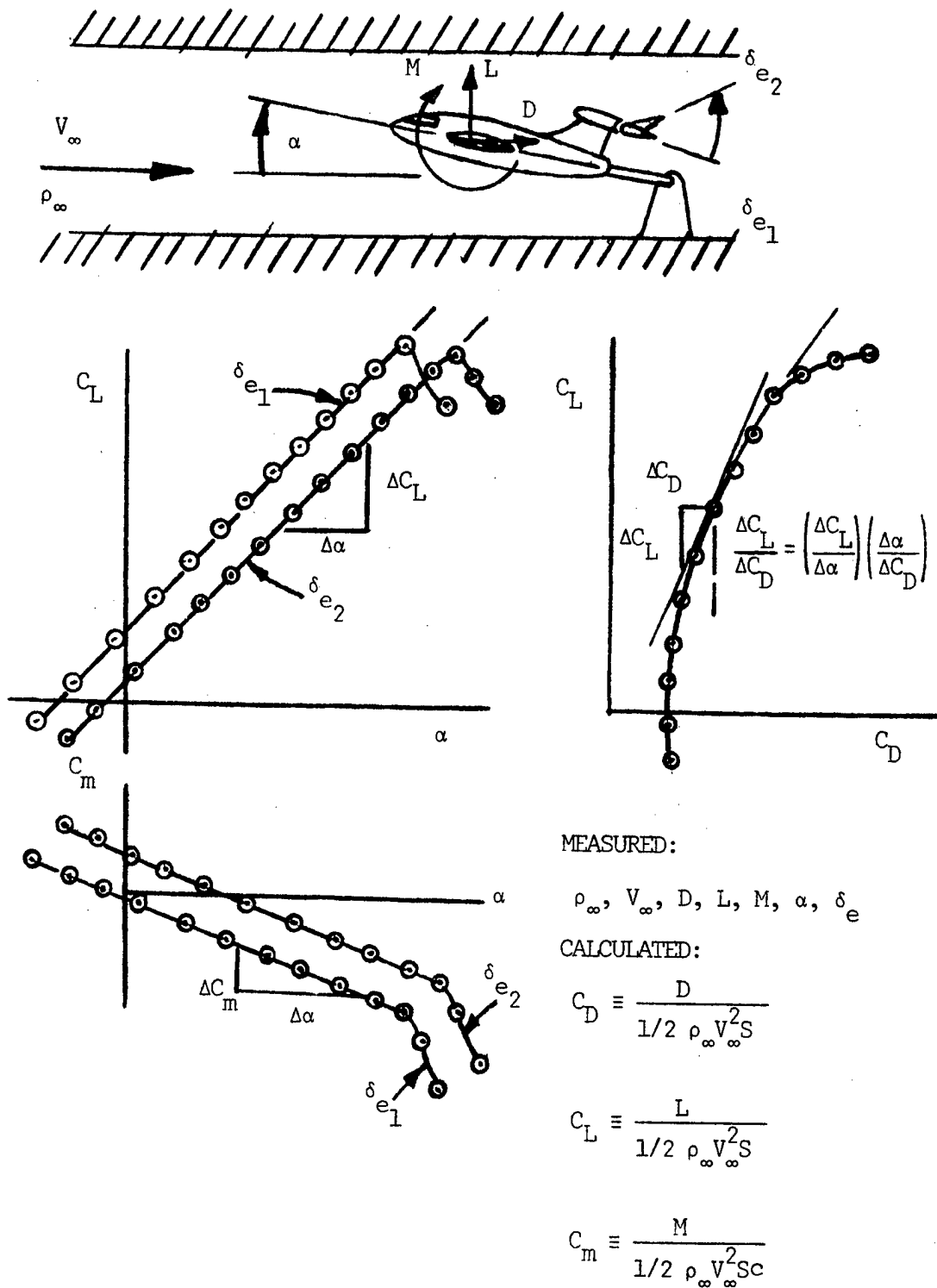


Figure 10: Longitudinal Wind Tunnel Testing

If the model shown in Figure 10 is tested at two different elevator angles (δ_{e1} and δ_{e2}) over a range of angle of attack the data shown in Figure 10 is generated. Stability derivatives are calculated directly:

$$C_{L_\alpha} = \frac{\Delta C_L}{\Delta \alpha}$$

$$C_{D_\alpha} = \frac{\Delta C_D}{\Delta \alpha}$$

$$C_{m_\alpha} = \frac{\Delta C_m}{\Delta \alpha}$$

$$C_{m_{\delta_e}} = \frac{\Delta C_m}{\delta_{e2} - \delta_{e1}} = \frac{\Delta C_m}{\Delta \delta_e}$$

Note that C_{D_α} is nonlinear, that is C_D is a function of C_L^2 and the local slope, C_{D_α} , is a function of α .

In the lateral case, the coefficients C_Y , C_n , and C_ℓ are functions of sideslip angle; therefore, the derivatives C_{Y_β} , C_{n_β} , C_{ℓ_β} , $C_{\ell_{\delta_a}}$, $C_{\ell_{\delta_r}}$, $C_{n_{\delta_r}}$, $C_{n_{\delta_a}}$, and $C_{Y_{\delta_r}}$ can all be directly calculated from wind tunnel tests performed at varying angles of sideslip. Longitudinal and lateral-directional control surface hinge moment parameters such as $C_{h_{\delta_e}}$, etc., can be similarly determined.

Wind tunnel data are not always as accurate as might be desired and the results must be interpreted by experienced personnel. For some stability derivatives, such as C_{L_α} , the experimental results provide satisfactorily accurate values; in cases such as C_{D_α} , C_{m_α} , $C_{m_{\delta_e}}$, $C_{\ell_{\delta_a}}$,

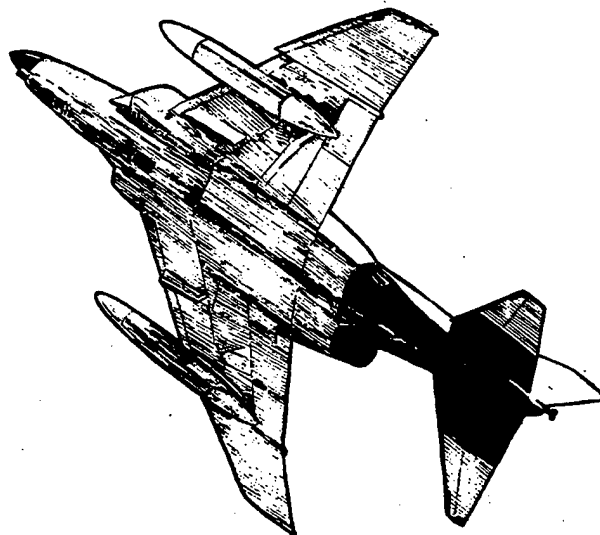
the wind tunnel data may not be directly applicable to the full-scale airframe because of Reynolds number and aeroelastic effects.⁶⁵

Some of the sources of error in conventional wind tunnel testing are:

1. Scale effects due to the low Reynolds number of the test continue to be the largest source of wind tunnel error.
2. The choking phenomena at high subsonic Mach numbers in subsonic wind tunnels was an early source of error; however, today this problem should be easily avoidable in practice.
3. Inaccurate corrections to the data, such as tare, alignment, and wall corrections can be a problem. Most modern wind tunnels try to keep corrections small to prevent serious errors.
4. Incorrect duplication (or no duplication) of power effects leads to inaccuracies. Recently great effort has been made to duplicate airflow thru model nozzles; however, this is still a source of error.
5. Inaccurate model representation of the aircraft by omission of protuberances, bomb racks, etc., has been a problem in the past; however, this can be avoided by making the accuracy of the model as accurate as necessary for the required data. This gets expensive.
6. Use of solid wood or solid metal models having different percentage structural deflections (different stiffness) under load than does the actual aircraft leads to errors in the data. Using "flexible" models to duplicate aircraft structural deformations gets really expensive.
7. Mechanical, instrumentation, and human errors occur in any type of testing or data reduction procedure.⁶⁵

An understanding of the sources, the importance, and the correction of errors is essential for interpreting the results of wind tunnel tests. Reynolds number effects appear to be prominent among these sources of error. For example, at low Reynolds numbers, there is a tendency for boundary layer separation to occur at a lower angle of attack on the model than on the full-scale aircraft, thereby causing earlier changes in such derivatives as

C_{m_α} , C_{L_α} , and C_{ℓ_β} , as functions of equilibrium angle of attack. Trips are generally used on the model to create turbulent flow, but there is some question as to the difference between naturally turbulent flow and artificially tripped flow. In spite of such limitations, wind tunnel testing is a powerful tool in the hands of the designer if he exercises great care in test procedures and in data interpretation.⁶⁵



● Damping Derivative Wind Tunnel Testing.

Very often in practice wind tunnel testing of a design stops with the procedure just described. Methods do exist for determining the damping derivatives (those due to rates such as C_{ℓ_p}), but facilities for this type testing are limited and their use for evaluations of aircraft designs is not widespread. Four methods of evaluating damping derivatives are in use.

The first method is use of a rolling flow tunnel. The basic purpose is to duplicate, as accurately as possible, the flow pattern conditions which exist around an aircraft when it executes a pure rolling motion in actual flight. One technique is use of a balance system which can be rotated. A second technique rotates the tunnel airstream by means of a rotor equipped with curved vanes. This technique has the advantage that it permits all forces and moments to be measured on the model mounted on a conventional balance system. But, this technique does not exactly simulate the conditions of an aircraft in steady roll or of a model in forced rotation, for there is a buildup of static pressure near the tunnel walls due to centrifugal force acting on the rotating air, which results in a pressure variation along any radius, a condition which does not exist when an airplane rotates. However, this pressure variation effect probably does not play an important part in most tests. Both these techniques appear to be attractive methods of obtaining rolling moment derivatives; data obtained from tests show them to be in consistent agreement, and in addition, such data check closely with calculated values of $C_{\ell_p}^{.65,75}$.

The second method is for measuring stability derivatives due to yawing velocity, r , and to pitching velocity, q , and is somewhat similar in principle to the rolling-flow technique. The air flow in the wind tunnel follows a curved path in the vicinity of the model and has a velocity variation normal to the circular arc streamlines in direct proportion to the local radius of curvature of the flow. Such a flow is

made possible by using a curved test section in combination with a variable-mesh screen designed to form a reduced velocity region on the inner side of the curved section. The model is fixed to a conventional balance system, and the forces and moments acting on the model are measured as functions of either yawing velocities or pitching velocities depending upon the orientation of the model with respect to the curved flow. By this means it is possible to determine the stability derivatives C_{Y_r} , C_{n_r} , C_{ℓ_r} , C_{L_q} and C_{m_q} . The curved flow technique does not exactly reproduce the conditions of an airplane flying in a curved path, since, for the model, there is a static pressure gradient created by the centrifugal forces on the air mass in rotation, which causes an apparent lateral buoyancy. Corrections for this effect can be calculated and applied. This static pressure gradient also produces a tendency for boundary layer air on the model to flow toward the center of rotation, a tendency opposite to that in actual flight. This effect cannot be evaluated accurately at present, but it is known to be of secondary importance. Turbulence is also a secondary complication not readily amenable to mathematical analysis.⁶⁵

Another method of attacking the problem of evaluating the damping derivatives is a model oscillation technique using either forced or free model oscillations. In either case, the model is mounted in a conventional wind tunnel on a single strut and is free to rotate essentially as a one-degree-of-freedom system in either pitch or yaw. In the free oscillation method, a torsion spring provides a restoring moment, so that a damped oscillation results from merely displacing and releasing the model. An oscillograph or high-speed motion picture camera records the resulting motion. The total damping is then evaluated from the decay of the amplitude of the oscillation. The forced oscillation method is somewhat more complex, for it requires a mechanism designed to maintain a steady oscillation by applying a sinusoidally varying yawing or pitching moment. This technique is similar to the frequency response method

of obtaining derivatives from flight test. Recorded time histories are analyzed for pitch or sideslip, angular acceleration, and applied moment. From these data, the moments acting on the model at zero acceleration can be determined, and from these moments, in turn, the damping derivatives can be obtained.⁶⁵

Reasonably good agreement has been reported among the curved-flow technique, the free oscillation technique, and the calculated results. In general, data obtained from the curved flow tunnel tests indicate satisfactory measurement of the rotary characteristics caused by yawing or pitching velocity, and the accuracy attained is considered superior to that of other techniques. Data derived by the forced oscillation procedures are not expected to be as accurate as those obtained by the free oscillation technique because of the difficulty in obtaining records free from random disturbances. On the other hand, forced oscillation enables one to determine results in the high lift coefficient range where difficulty is experienced with free oscillation.^{65,76}

If the values of C_{n_r} and C_{m_q} are determined for a particular model by means of the curved flow technique, it is theoretically possible to determine the derivatives $C_{n_{\dot{\beta}}}$ and $C_{m_{\dot{\alpha}}}$ by performing oscillation tests on the same model. This is not normally done in practice because of the inaccuracy of the data involved in the two types of testing.⁶⁵

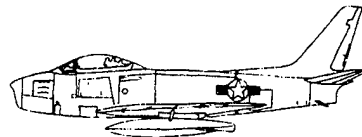
Comparisons of free oscillation and curved flow techniques indicate satisfactory agreement for moderate lift; however, at high lift coefficients, differing values of C_{n_r} are obtained by these two methods.^{65,78}

The latest method used for determining damping derivatives involved mounting the model on gas bearings and telemetering data outside the tunnel. This is a very expensive technique and has only been used on one test program to date.

● Transonic Wind Tunnel Testing.

Wind tunnel testing in the transonic range is extremely difficult and unreliable in subsonic tunnels because of choking phenomena between the model and the tunnel walls. One method of obtaining data in the transonic region is to modify existing high subsonic wind tunnel test sections with a suitably contoured bump on which small reflection plane (half-span) models can be mounted. Even though the tunnel is operating at subsonic speeds, the increase in flow velocity over the bump creates a localized area of transonic and supersonic Mach numbers. Because of the small size of the model used, tunnel choking phenomena are avoided. One disadvantage of this method is that the local increase in velocity over the bump is not uniform; there is a velocity gradient as a function of distance away from the surface of the bump. This means that the model is subjected to a Mach number gradient in the direction of the span. Another disadvantage of this method is that the data are obtained at low Reynolds numbers because the models of necessity must be very small—approximately six inches in half-span. Because half-span models are used, only static longitudinal stability derivatives can be determined. The Mach number gradient and the low Reynolds numbers of the tests are the inevitable penalties for the avoidance of choking, and they sometimes constitute sufficient reason for skeptical attitudes toward bump model test results.⁶⁵

Modern transonic wind tunnels are capable of stabilizing at any given Mach number in the transonic speed range. Reflected shock waves are kept off the model by using small models and porous walls in the tunnel test section.



North American F-86 Sabre

The primary USAF facilities for transonic wind tunnel testing are located at the Arnold Engineering and Development Center (AEDC), Tullahoma, Tennessee. The 16-ft transonic tunnel is a continuous-flow closed-circuit tunnel with a 16 ft by 16 ft test section capable of operating within a Mach number range of 0.2 to 1.6. The Reynolds number test range is from 100,000 to 7,500,000 per ft. This tunnel was designed primarily for testing the aerodynamic performance of full-scale engine installations on partial aircraft models, large aircraft models, or large and full-scale missiles. In general, test results should be satisfactory if a sting mounted model is no longer than 22 ft and if the wing span does not exceed 12 ft.¹⁰² Recently (August 78) tests were conducted in this tunnel as part of the Advanced Fighter Technology Integration (AFTI) program on small-scale models of the McDonnell Douglas AFTI-15 and the General Dynamics AFTI-16.¹²⁴

The AEDC also has a 4-ft transonic tunnel with a 4 ft by 4 ft test section capable of operating from Mach number 0.1 to 1.3 and 1.6 to 2.0. The Reynolds number range for this tunnel is 200,000 to 7,700,000 per ft. This 4-ft tunnel was designed primarily for store-separation testing but is also used extensively for stability and control testing.¹⁰²

The NASA Ames Research Center presently operates a transonic wind tunnel with an 11 ft by 11 ft test section. This tunnel was used recently for tests of a 1/6 scale half-span floor mounted F-111 TACT model.¹²²

The NASA Langley Research Center is about to start construction on a new transonic tunnel which will be part of a national test facility and available for use by all government agencies.

● Supersonic Wind Tunnel Testing.

At the present time, the design trend for supersonic tunnels is toward the conventional closed-circuit. Other arrangements have been or are being used, however. In the "blow down" type tunnel, for example, the air is pumped under pressure into a large reservoir before the test and is released during the test to atmospheric pressure through a model test section in which

supersonic velocities are attained on sting mounted models. Because of the large amounts of power required to drive the air at very high velocities in the conventional tunnel arrangement, the size of the tunnel is usually small, a restriction which in turn places severe limitations upon the size of the models to be tested. The resulting large difference in Reynolds number between the models and the full-scale aircraft makes the interpretation and application of most supersonic wind tunnel data on stability derivatives difficult.⁶⁵

The AEDC does have a big closed-circuit supersonic tunnel as well as several smaller ones. The big one has a 16 ft by 16 ft test section and when it runs all the lights between Cincinnati and Atlanta go dim. It usually runs about 2 AM. The AEDC supersonic wind tunnel capabilities are summarized in the following table:

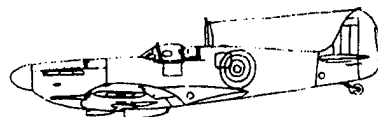
TABLE 1: AEDC Supersonic Wind Tunnels ¹⁰²		
Test Section Size	Speed (Mach No.)	Reynolds No. (per ft)
16' x 16'	1.50 - 4.75	100,000 - 2,500,000
40" x 40"	1.5 - 6.0	1,000,000 - 6,000,000

● Free-Flight Wind Tunnel Testing.

In the free-flight tunnel technique, the model is not attached to any sort of balance system, but is allowed to move freely within the test section of the tunnel. The model has movable control surfaces, and its motions can be controlled by a human "pilot" who flies the model as he would a full-scale aircraft. The free-flight tunnel is not used primarily to obtain specific numerical values of stability derivatives, but rather to study the general stability and control behavior with reference to desirable flying qualities from a pilot's viewpoint. However, it is possible to obtain quantitative stability derivative data by analyzing motion picture records of the response of the model to control inputs.^{65,79}

Recently maximum likelihood parameter estimation techniques were used on cable mounted models of the F-14 and Space Shuttle orbiter vehicle to extract stability derivatives. The conclusions were that the longitudinal and lateral-directional derivatives for each model generally appeared to be "reasonable" when compared with derivatives obtained from other sources and when used to predict other data points.¹⁰⁰

Some of the data from free-flight testing have been found to conflict with full-scale test data. The earlier boundary layer separation on the model due to the lower Reynolds number very likely accounts for the largest portion of the disagreement. Stall characteristics are not too clearly demonstrated by the free-flight model, and spiral stability is difficult to measure; but the test is useful for comparisons between different flight conditions and different configurations. Considerable scatter in observations is inevitable because steady conditions cannot be obtained before application of the controls.^{65,79} The characteristics of the B-1 at high angles of attack were investigated with a free-flight model. These tests predicted that the B-1 would have a pitch-up tendency. This tendency has not yet been conclusively shown by flight tests.



Supermarine Spitfire

Model Flight Testing. Early attempts at free-fall model testing were to attain transonic Mach numbers. The model was carried to high altitude then dropped, thus using gravity as a source of power. During its descent, the model was tracked by radar and optical tracking equipment to determine its "general" flight path. Models were equipped with radio-operated controls and instrumentation for determining the response of the model to control inputs. The response data was transmitted to ground stations. The method was used mainly to study lift and drag characteristics. The chief advantage of this method is that large models can be made to pass gradually through the transonic region under truly free-air conditions. The main disadvantage of early testing was that the model and its costly instrumentation package was destroyed upon ground impact.⁶⁵

Free-fall model tests were performed recently by NASA on a 3/8-scale model F-15. The model F-15 Remotely Piloted Research Vehicle (RPRV) and the F-15A aircraft were of the same configuration except that the F-15 RPRV is unpowered and the F-15A powered. Stability and Control maneuvers were performed on the F-15A airplane and the F-15 RPRV. The maneuvers on the F-15A airplane were performed at three engine mass flow rates to assess the effect of the propulsion system on the stability and control derivatives. A complete set of stability and control derivatives were obtained for both vehicles using the MMLE digital program.

These derivatives were obtained on both vehicles over an angle of attack range of approximately 15° to 20°. The propulsion system appeared to have little effect on the derivatives. In general, very good agreement was found between the estimates from the two vehicles. Agreement was good for C_{n_β} and C_{n_r} . The trend for $C_{n_{\delta_r}}$ was the same for both vehicles,

but the F-15A airplane had more rudder power. There was no trend in $C_{n_{\delta_r}}$ for the F-15A aircraft to indicate that an extrapolation of the mass

flow rates would account for this difference. Since C_{n_β} and C_{n_r} for both

vehicles were in good agreement, it is unlikely that an error in the moment of inertia in one of the vehicles would account for the difference. Therefore, the difference in $C_{n_{\delta r}}$ between these vehicles was attributed to scale effect.^{58,80,81}

Free-fall model testing has developed into free-flight model testing. The development of recovery procedures for the model has permitted an increase in the use of this technique. The concept of using Remotely Piloted Vehicles (RPVs) as test-beds has been under development at the NASA Dryden Flight Research Center. Since the experimental aircraft involved do not have to be man-rated, development can be speeded up and costs kept to a minimum. The next generation of free-flight models will be the Highly Maneuverable Aircraft Technology (HiMAT) aircraft which is an almost half-scale model of a 1990s fighter powered by a single General Electric J-85 engine.* Flight testing of this aircraft is scheduled to begin in June 1979.⁸²

There are other model flight test methods which have been used for flying quality testing, but are not widely used today. One technique used for transonic testing was to place a very small full-span or half-span model on the wing of an aircraft in the vicinity of maximum thickness. The test procedure consisted of diving the aircraft from high altitude and accelerating through the transonic range providing a continuous sequence of aircraft and model flight test data. Another technique launched or fired solid metal models carrying no instrumentation from a special gun. Aileron power and roll damping were determined from photographs of the ballistic trajectory. Rocket-powered models with and without instrumentation have also been used with varying degrees of success. These techniques are described in more detail in Reference 65.

*See page 13-106 for details

Highly Maneuverable Research Vehicle *

Wright-Patterson AFB, Ohio

The Air Force and NASA have unveiled a highly maneuverable aircraft technology (HiMAT) research vehicle at Rockwell International Corp.'s Los Angeles Division, El Segundo, Calif.

HiMAT—an unmanned, remotely piloted research vehicle—could be the basis for a fighter design of the 1990s. It is scheduled for flight testing in late November.

AFFDL Participates

AFSC's Air Force Flight Dynamics Laboratory (AFFDL) here is the Air Force organiza-

tion responsible for HiMAT, which is one-third the scale of most fighter aircraft.

HiMAT's missions will begin with air launch at about 45,000 feet from a B-52 bomber over NASA's Dryden Flight Research Center (DFRC), Edwards AFB, Calif. The unmanned vehicle will be flown for 20 to 30 missions by a ground pilot at the DFRC facility and land at AFFTC's Rogers Dry Lake bed on skids.

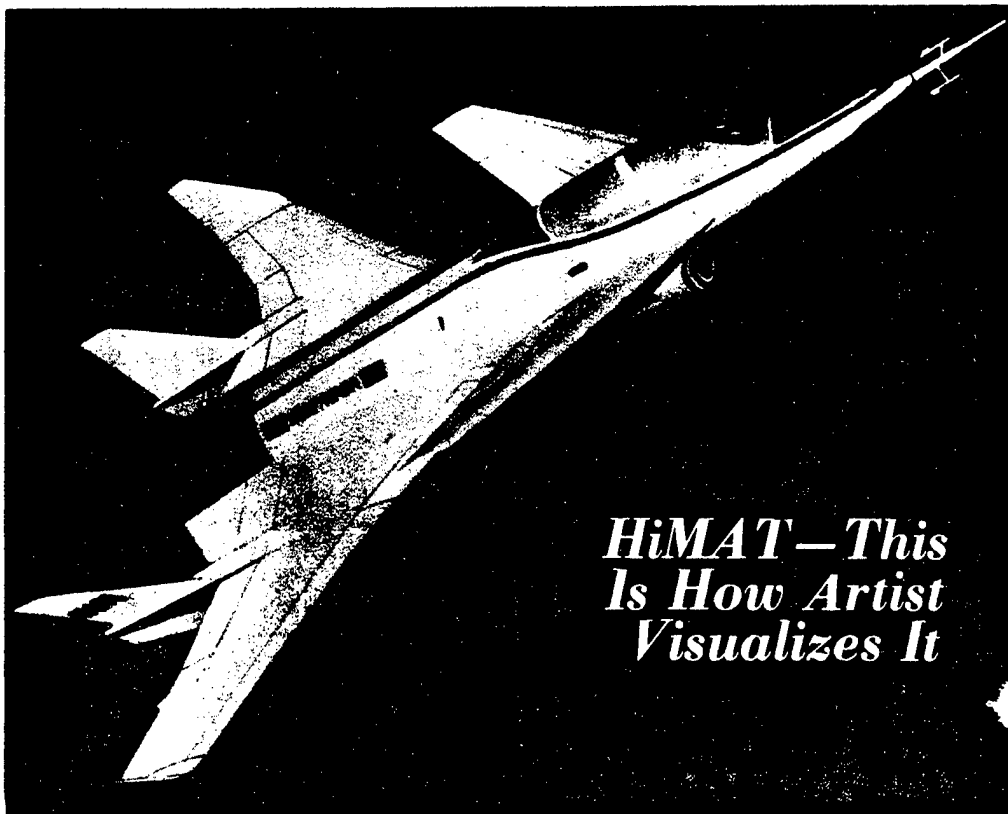
Primary purpose of the HiMAT program is to enhance the maneuverability of future U.S. fighter aircraft at transonic speeds (700 to 780 miles per hour) and during air-to-air combat.

The vehicle's flight test program especially

Composite Design

About 25 per cent of HiMAT's total weight involves graphite epoxy composite materials. In particular, those materials are designed into the wing and canard areas that are critical surfaces when the vehicle begins pulling high Gs.

During maneuvers HiMAT is expected to attain sustained 8G turns at mach .9 at 25,000 feet, and also sustained 6G turns at mach 1.2 at 30,000 feet.



HiMAT—This Is How Artist Visualizes It

THIS ARTIST's rendering shows what the HiMAT research aircraft will look like over NASA's Hugh L. Dryden Flight Research Center, Edwards AFB, Calif., where it will be flight-tested. The 3,400-pound unmanned vehicle is 22.5 feet long and 4.3 feet high with a 15.6-foot wingspan. (Rockwell International Illustration)

* From AFSC Newsreview, May 78, Vol. XXII, No. 5, Andrews AFB MD

will evaluate HiMAT's high-speed turns at 30,000 feet, plus diving and pullup maneuvers that simulate ground-strafting runs.

Such maneuvers would be possible largely because of aeroelastic tailoring (AT), a structural design concept conceived by AFFDL.

'First' Recorded

AFFDL consultants report that HiMAT is the first research vehicle anywhere to fly with an aeroelastically tailored composite lifting surface.

Other AFFDL-developed technologies to be flight-tested on HiMAT include a composite airframe and a digital flight-control system.

AFFDL engineers compare the directional properties of composites to wood veneer that is stiff in one direction but very pliable in another. When HiMAT begins "pulling Gs" (experiencing gravitational pull), the composite structure will deform enough to give the vehicle about 10 per cent additional maneuverability—including very tight turns.

These engineers describe AT as the ability to use the unique directional properties of composite materials to control bending and twisting under aerodynamic loading. That flexibility is achieved by stacking sheets of composite fibers in the direction that results in favorable wing-twisting as aerodynamic loading is increased.

Full-Scale Flight Testing

In general, the accuracy of the values of derivatives obtained from flight testing is considered better than that from any other method. The degree of accuracy obtained depends upon the flight test technique, the quality of the instrumentation, the data analysis technique, and, since some sort of averaging process must be applied, the total number of samples taken.⁶⁵

The history of the development of flight test techniques for determining stability derivatives was briefly traced in Section 1. In general, there are three flight test techniques from which stability derivatives can be obtained, (1) steady-state flight test techniques, (2) transient response techniques, and (3) sinusoidal oscillation techniques.⁶⁵

Steady-State Flight Test Techniques. Steady-straight techniques can be used to determine static derivatives. Steady-turning type maneuvers permit some rate derivatives to be determined e.g. C_{m_q} and C_{ℓ_p} .

By stabilizing the aircraft in straight and level flight at different airspeeds and at different center of gravity locations, and then measuring the elevator required for trim, it is possible to obtain numerical values of the derivatives C_{D_α} , C_{L_α} , C_{m_α} , $C_{L_{\delta_e}}$, and $C_{m_{\delta_e}}$. In many cases,

however, the explicit value of each derivative cannot be obtained separately unless the values of the other derivatives can be assumed or estimated from model tests or a different flight test technique.

If steady pull-up type maneuvers are performed at constant forward speed the value of C_{m_q} can be roughly evaluated, if $C_{m_{\delta_e}}$ is known, since the additional elevator deflection over that required for trim can be measured.

Steady sideslips yield data both on the static directional derivatives C_{Y_β} , C_{n_β} , and C_{ℓ_β} , and on the control derivatives $C_{Y_{\delta_r}}$, $C_{n_{\delta_r}}$, and $C_{\ell_{\delta_a}}$. Here again, however, as with the longitudinal case, none of the derivatives can be evaluated explicitly unless values of some of the others are assumed. This procedure is not as difficult as it may at first appear. Flight test values of C_{n_β} , can be easily obtained by measuring the period of the Dutch roll oscillation; and aileron effectiveness, $C_{\ell_{\delta_a}}$, can be estimated fairly accurately from model tests and rate of roll flight tests. If C_{n_β} , and $C_{\ell_{\delta_a}}$ are known, the remainder of the static directional derivatives can be evaluated from simple steady flight side force, yawing moment, and rolling moment equations.⁶⁵

All the maneuvers which are used in these steady flight techniques are prescribed as part of the contractor's demonstration that his airplane meets military flying quality requirements. These data will therefore be readily available for all prototype military aircraft. It may be seen, however, that these techniques yield little information on many of the dynamic derivatives; other techniques must be used to obtain such data.⁶⁵

Methods for reducing data to obtain derivatives from steady-state maneuvers will be described as each stability derivative is discussed individually.

Transient Response Techniques. The transient (dynamic) response technique appears to be the most practical flight test method for determining both the stability derivatives and the transfer functions of the airframe. In this technique, some measurable input is applied to the airframe, and stability derivatives and transfer functions are determined from the resulting transient response data.⁶⁵

The advantages of the transient technique over the sinusoidal flight testing technique are that much less actual flight time is required and that stability derivatives can be obtained directly from the transient data without performing a frequency response analysis. Further, the frequency response of an airframe can be derived mathematically from transient flight data.⁶⁵

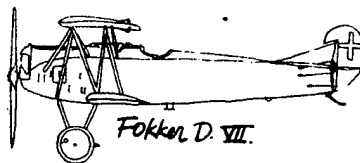
The input magnitude, duration, and form are important. Selection of input type is also strongly influenced by the method of data analysis. Step inputs are useful when the airframe is able to reach a steady-state value corresponding to the new trim flight conditions imposed by the input. When the airplane response cannot reach a steady-state value, but diverges, a pulse input is more practical and also has the advantage that the duration and shape of the pulse can be chosen to produce a response whose major contribution lies in the frequency range of interest. Simplified response approximations exist for step and impulse inputs. Various response curve-fitting methods such as analog matching, and mathematical techniques such as the Fourier transform method have been devised to obtain stability derivatives from step and impulse dynamic inputs. Some of these were described briefly in Section 1.^{34,65,83,96,97,98}

Simplified response approximations do not exist for more complex inputs, and insight can be lost in the complexity of the analysis.⁶⁵ Doublets are used for determining stability derivatives as well as for determining military flying quality specification compliance.¹⁶ The maneuver for extracting longitudinal derivatives using the MMLE program is a rapid elevator doublet. The lateral-directional maneuver is a rudder

doublet followed by three or four seconds of stick-free oscillation and terminated by an aileron doublet.⁶⁰

Arbitrary or random inputs can also be used, but analysis of the results then becomes more laborious. Three maneuvers have been investigated here at the AFFTC while developing SIFT techniques. These are: precision air-to-air tracking, precision formation flying, and air refueling. Precision air-to-air tracking has been the most successful. Investigation is continuing to tailor the SIFT precision tracking maneuver to permit good identification at frequencies below one to two radians per second, while minimizing the impact on short period identification. Tracking maneuvers should be designed to provide frequency content at both the high and low ends of the flying qualities spectrum (about one to ten radians per second) and the control system should be constrained to essentially linear operating conditions.¹⁰³ SIFT test techniques are discussed in detail here at the School in a course titled Closed Loop Handling Qualities taught during the Systems Test Phase.

Sinusoidal Oscillation Techniques. The sinusoidal oscillation technique can be used to determine the transfer function of the airplane. Although stability derivatives cannot be obtained directly by this method, it is possible to derive values of certain combinations of derivatives from plots of the transfer function. This test technique was described briefly in Section 1.^{12,55}



SECTION 4

INDIVIDUAL STABILITY DERIVATIVES

INTRODUCTION

The two primary factors which establish the basic non-dimensional stability derivatives for any aircraft are (1) the aircraft configuration, and (2) the flight conditions; in general, the first is the most important.⁶⁵

Aircraft Configuration

Of all the contributing factors that determine the basic non-dimensional stability derivatives, the most important is the basic aircraft geometry. A great deal of theoretical and experimental data are available on the effects of geometry. The value of stability derivatives at low Mach number can be evaluated to a fair degree of accuracy merely from an examination of a three-view drawing of the aircraft. Changes in weight distribution as an aircraft is operated throughout its flight regime also change the value of stability derivatives. The most important weight effect is the shift of the center of gravity either fore or aft which produces a very great change in the aircraft's longitudinal static stability.⁶⁵

Flight Conditions

Flight conditions which effect the value of stability derivatives are (1) Mach number, (2) angle of attack or lift coefficient, (3) dynamic pressure (aeroelasticity), (4) power or thrust, and (5) unsteady flow. These flight conditions are listed in decreasing order of importance and will be discussed individually.⁶⁵

Mach Number. The effect of Mach number on basic stability derivatives is second in importance only to the effect of aircraft geometry or configuration. Every derivative is changed to an appreciable extent as Mach number varies throughout the speed range of supersonic aircraft. If any one effect of Mach number is more important than the rest, it is the effect of increasing longitudinal static stability as the aerodynamic center shifts aft while accelerating into the supersonic regime. Another very important effect of Mach number is its great influence upon the primary control derivatives. Control power is usually increased an appreciable amount transonically, but at supersonic speeds approaches a value about one-half that at low subsonic Mach numbers.⁶⁵

Angle of Attack. The values of some basic non-dimensional stability derivatives depend on the angle of attack, or lift coefficient while others are relatively unaffected.⁶⁵ Most longitudinal derivatives are functions of angle of attack at high angles of attack where the lift curve becomes nonlinear. Of course, C_{D_α} is a function of angle of attack even on the linear part of the lift curve. Most lateral derivatives change with angle of attack, although a few remain fairly constant up to the stall. Even though stability derivatives are actually functions of angle of attack, they are usually evaluated at a given trim condition and are therefore assumed to remain constant during any angle of attack perturbation from equilibrium. This assumption must be made to maintain the linearity of the equations of motion. It is clear that the validity of this assumption depends, first, on how much the derivatives change with a small change in angle of attack; and second, on how much these changes in derivatives affect the aircraft dynamics.⁶⁵

Dynamic Pressure. Until a few years ago, the only aeroelastic effects on the dynamics of an aircraft considered important were the reduction in maximum roll rate due to a reduction in roll control power,

and the increase in maneuvering stability due to pitch rate. Since that time because of lighter structures and thinner wings, aeroelastic effects on other derivatives have become appreciable.

Aeroelastic effects are primarily functions of dynamic pressure. Since dynamic pressure can be expressed as $14816M^2$ it is clear that dynamic pressure increases as Mach number increases and as altitude decreases (pressure ratio increases). It can be concluded then that aeroelastic effects are largest flying at high Mach number at low altitudes.⁶⁵ For most stability and control investigations the change in altitude or Mach number during a test maneuver are small enough to be neglected.

Structural rigidity is very important in determining the magnitude of the aeroelastic effects on stability derivatives. The more rigid the structure, the more it can resist the air loads, and the less it is subject to aeroelastic deformations. The amount of rigidity possible is limited by considerations of weight and aerodynamics.⁶⁵

Power or Thrust. In general, power effects on the basic stability derivatives are small. It is not too difficult to calculate or estimate the major effects theoretically. Most dynamic analyses neglect jet power effects. Jet power effects considering longitudinal equilibrium or trim can be large due to the moment from a thrust line not passing through the center of gravity. Propeller-driven aircraft are subject to large power effects because the tail surfaces are usually immersed in the propeller slip-stream.⁶⁵

Unsteady Flow. Although the effect of unsteady flow on stability derivatives has been taken into consideration for many years in aerodynamic flutter, only recently has this effect become important in stability and control considerations mainly as a result of the higher operating speeds of today's aircraft.

Most unsteady flow effects arise from the fact that the final steady lift caused by an abrupt change in angle of attack of a lifting surface does not occur instantaneously. For an oscillating wing, where the angle of attack is varying sinusoidally, the lift will follow sinusoidally, but its magnitude will be smaller than that of the non-oscillating wing; in addition there will be a phase difference between lift and angle of attack. This unsteady flow effect is a function of the frequency of the oscillation and also of the Mach number at which the oscillation is occurring.

Before examining this, however, it is necessary to understand how unsteady flow effects are introduced into the equations of motion. In accordance with the practice of writing aerodynamic forces and moments in terms of conventional stability derivatives, the latter must be considered as functions of frequency because of unsteady flow effects. For example:

$$C_L = C_{L_\alpha} \alpha + C_{L_{\dot{\alpha}}} \dot{\alpha} + C_{L_{\ddot{\alpha}}} \ddot{\alpha} + C_{L_q} q + C_{L_{\dot{q}}} \dot{q} + C_{L_{\ddot{q}}} \ddot{q} + \dots$$

$$\dots + C_{L_{\delta_e}} \delta_e + C_{L_{\dot{\delta}_e}} \dot{\delta}_e + C_{L_{\ddot{\delta}_e}} \ddot{\delta}_e \quad (49)$$

where the stability derivatives are various functions of frequency and Mach number.

In general, all the aerodynamic derivatives of an aircraft behave in a similar manner. It is clear therefore that the effect of unsteady flow on conventional stability derivatives is to change them from real numbers to complex numbers, the real and imaginary parts of which are functions of the frequency of the oscillation and the Mach number at

which the oscillation is occurring.⁶⁵

Unsteady aerodynamic effects are generally neglected in most parameter estimation techniques. Several references have shown that aerodynamic parameters and their variances, as determined from flight test data, are influenced by the type of control input used to excite the aircraft motion.^{147, 148} These differences have generally been attributed to insufficient excitation of the aircraft states (poor inputs); however, the possibility exists that unsteady aerodynamic effects might account for the observed differences in variances. A recent study was made to develop simple concepts to permit modeling of unsteady aerodynamic effects into existing parameter estimation programs. Results from this study showed that a simplified theory duplicated more exact solutions in unsteady aerodynamics. A numerical example indicated that estimates of the parameters were degraded if unsteady effects were not included in the estimation algorithm. The most significant difference was found to be in C_{m_q} which was not unexpected since unsteadiness should have a pronounced effect on pitch rate response of an aircraft.¹⁴⁶

In spite of the great progress in unsteady flow research, it appears that no definite conclusions can be drawn at present concerning the conditions under which unsteady flow should or should not be considered in evaluating stability derivatives.^{65, 84}

Summary

Aircraft geometry is obviously the most important factor in determining the values of the basic non-dimensional stability and control derivatives. Modern day aircraft are strongly effected by Mach number changes and are subject to aeroelastic deformations. In addition, effects of changes in angle of attack on stability derivatives must be considered for flying quality investigations of low speed or high angle of attack maneuvering characteristics. The importance of unsteady flow effects is still a mystery.

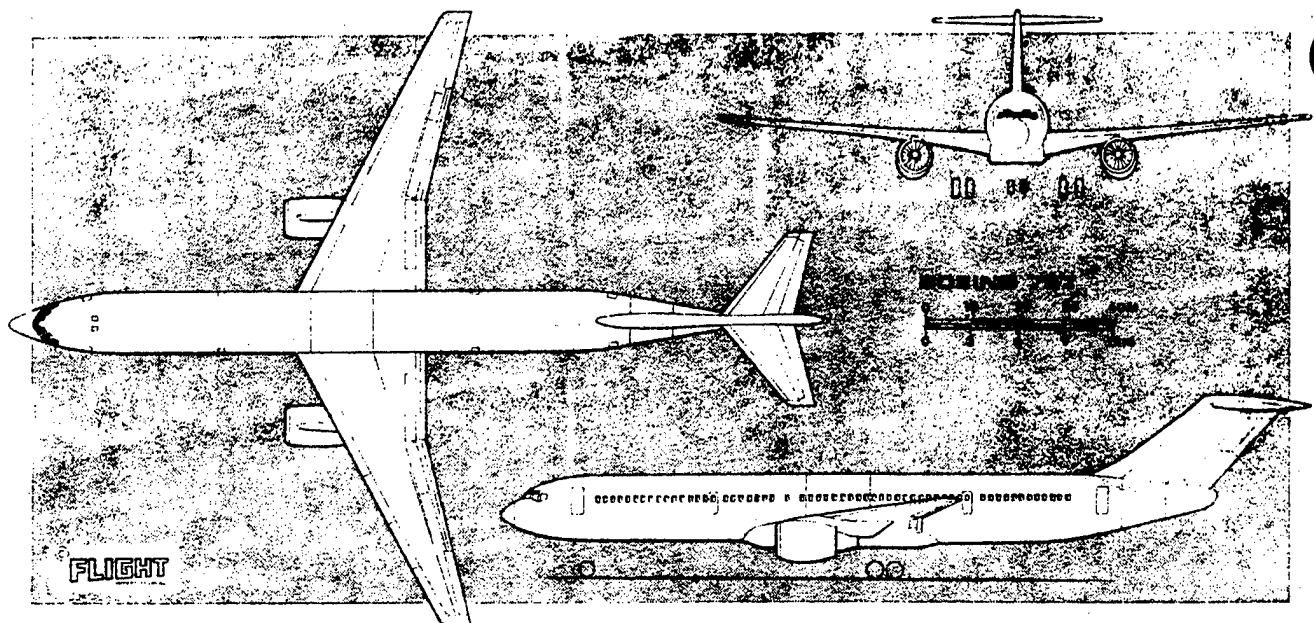
TYPICAL INDIVIDUAL DERIVATIVES

Reference 64 presents a discussion of some of the stability derivatives particularly pertinent in the study of the dynamic modes of aircraft motion; however, each stability derivative will now be examined individually. It should be remembered that stability derivatives are partial derivatives and when they are discussed individually other variables must be held constant. For example:

$$L = f(u, \alpha, \dot{\alpha}, q, \delta_e) \quad (50)$$

therefore when discussion C_{L_u} , all the other variables stay constant.

The basic plots used for presentation of the typical individual stability and control derivatives shown in Figures 11 thru 41 are from Reference 88 which was classified at time of initial publication in 1952. These numerical



derivative values should be considered estimates, based on trends shown by analysis, wind tunnel tests, and flight test. Original Reference 88 data can be identified by miniature aircraft planforms, and includes data for the D-558-II, XF-92, F-89D, F-86, X-1, F-80, XF-91, F7U, and X-4. Data from three other sources, References 74, 87, and 100, have been added to the basic plots from Reference 88.

Reference 87 contains a complete set of stability and control derivatives for the F-104A, C-5A, F-4C, X-15, Lockheed Jetstar, Boeing 747, North American XB-70A, and several other aircraft. In Reference 87, aeroelastic effects are shown by presenting data representative of different altitudes as shown by the example F-4C longitudinal static stability curve in Figure 10A.

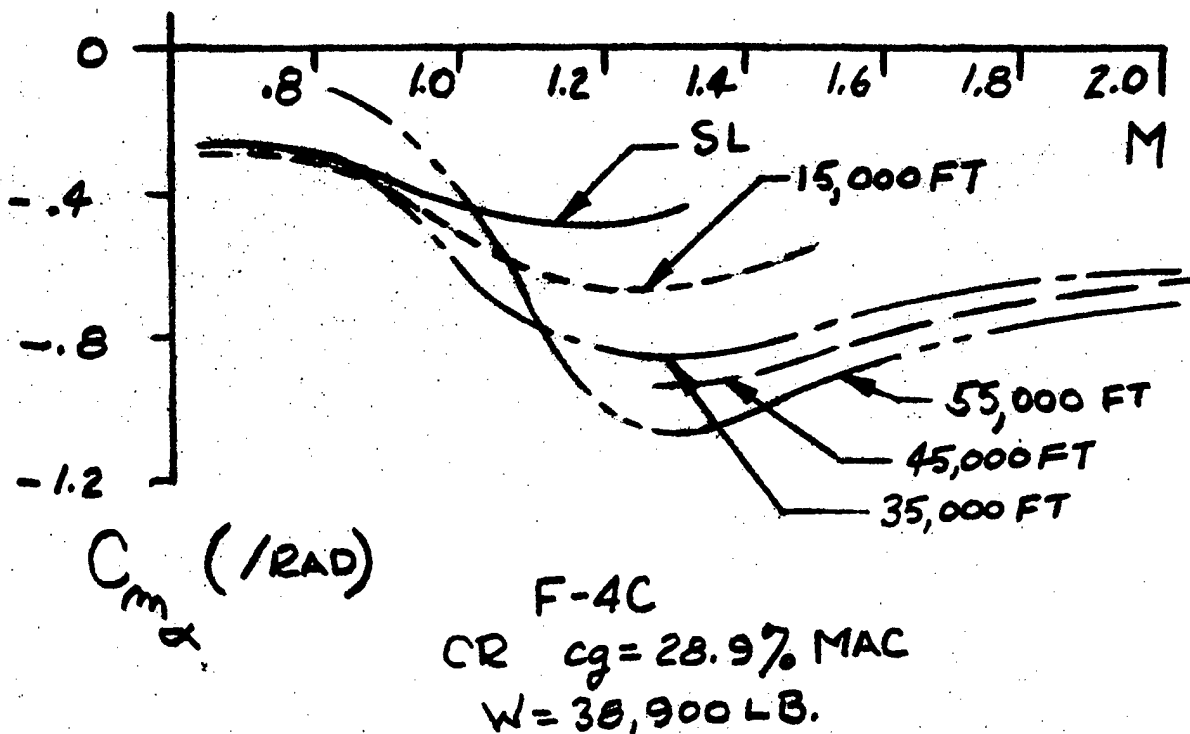


Figure 10A: Variation of C_{m_α} with Mach Number and Altitude for the F-4C Aircraft.⁸⁷

Aeroelastic effects were ignored and "average" derivative values were used in transcribing Reference 87 data to Figures 11 thru 41.

Some data from Reference 74 on the Boeing 727 and Gates Learjet Model 24B are also shown on Figures 11 thru 41. Aeroelastic variations were not considered, or at least not presented, in the original reference.

Reference 100 was the source for the Space Shuttle Orbiter vehicle and F-14 analysis and wind tunnel data shown on Figures 11 thru 41. These derivatives are point data, i.e., the F-14 derivatives are for a Mach number of 0.865 and a dynamic pressure of 81 lb/ft^2 , and the Orbiter derivatives are for a Mach number of 0.60 and a dynamic pressure of 100 lb/ft^2 . When wind tunnel and analysis agreed reasonably well, only one value is shown for the F-14 and Orbiter derivatives. When there was disagreement, derivatives are labeled either (analysis) or (wind tunnel), as appropriate. Reference 142 was the source for Space Shuttle Orbiter vehicle flight test derivatives which are labeled (MMLE). The F-14 and Orbiter derivatives combine q and $\dot{\alpha}$ effects into the q derivatives, and combine r and $\dot{\beta}$ effects into the r derivatives.

Where necessary, derivatives have been converted to the USAF Test Pilot School sign convention shown in Figure 7.

EQUILIBRIUM LIFT COEFFICIENT, C_L

Although not referred to as a stability derivative in the usual sense, equilibrium lift coefficient is one of the basic parameters used to specify the trim condition of an aircraft. In longitudinal dynamics, variations in C_L principally affect the phugoid mode, with both damping and period decreasing with an increase in C_L . In addition, because many lateral derivatives are functions of C_L , the lateral dynamics are also affected. The main effect is a decrease in Dutch roll damping with an increase in C_L .⁶⁵

For performance, a large range of equilibrium lift coefficients is desirable to allow trim at high and low airspeeds. These performance considerations obviously take precedence over the stability preference for low values of C_L .

The equilibrium lift coefficient for any trim point can be evaluated from flight test using the following relationships:⁸⁵

$$C_L = \frac{nW}{1/2 \rho_o V_e^2 S} \quad \text{or} \quad C_L = \frac{nW}{14816 M^2 S}$$

EQUILIBRIUM DRAG COEFFICIENT, C_D

Like C_L , equilibrium drag coefficient is not a stability derivative in the usual sense. For performance, C_D is one of the most important parameters and should be as small as possible. When dynamics are concerned, C_D is the main contributor to damping of the phugoid mode, and the larger the value of C_D , the better the damping. Clearly then, performance dictates low design values of C_D .

The equilibrium drag coefficient for any trim point can be evaluated from flight test using the following relationships which assume that inflight values of net thrust can be determined:⁸⁵

$$C_D = \frac{F_n}{1/2 \rho_o V_e^2 S} \quad \text{or} \quad C_D = \frac{F_n}{14816 M^2 S}$$

CHANGE IN LIFT COEFFICIENT WITH FORWARD VELOCITY, C_{L_u}

Variations in C_{L_u} arise from two sources, Mach number and aeroelastic effects. The magnitude of C_{L_u} can vary considerably and its sign can change, depending on airframe elastic properties and the flight Mach number and dynamic pressure. The magnitude of C_{L_u} is negligibly small for low speed and high supersonic Mach number, but it may reach large values near critical Mach number.^{77,86}

Since C_{L_u} is primarily caused by Mach number it is sometimes written as shown in Equation 53:

$$C_{L_u} = \frac{\partial C_L}{\partial \hat{u}} = \left(\frac{\partial C_L}{\partial M} \right) \left(\frac{\partial M}{\partial \hat{u}} \right) \quad (51)$$

$$= C_{L_M} \frac{\partial \left(\frac{u}{a} \right)}{\partial \left(\frac{u}{U_o} \right)} = C_{L_M} \frac{\partial u}{\partial u} \left(\frac{U_o}{a} \right) \quad (52)$$

$$= C_{L_M} M \quad (53)$$

Reference 74 gives the approximate transonic variation of C_{L_u} as from -0.2 to 0.6. This derivative is very sensitive to wing shape, high aspect ratio being most affected and highly-swept and delta wings being least affected.⁸⁶ Figure 11 shows typical variations of C_{L_u} with Mach

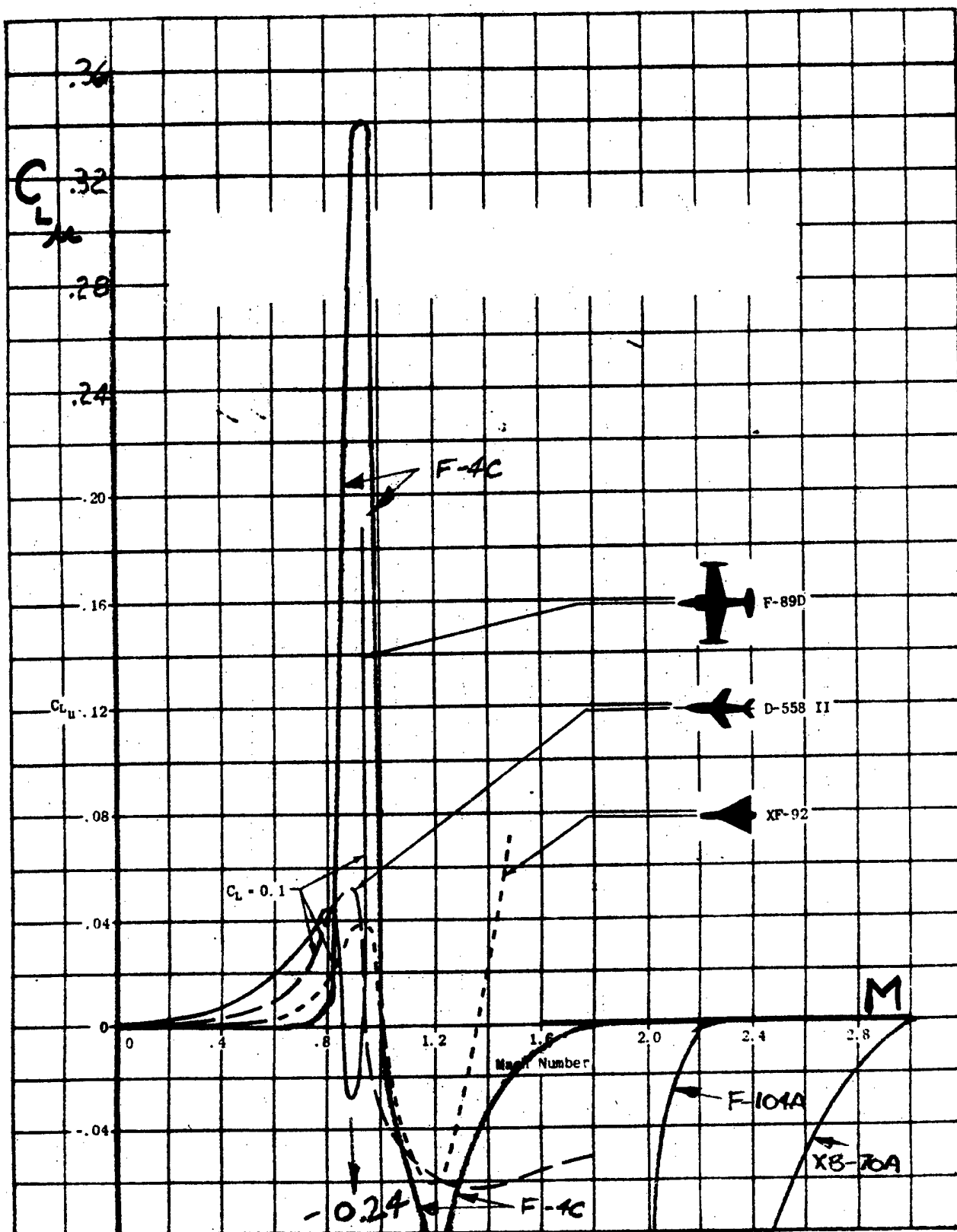


Figure 11: Variation of C_{L_u} with Mach Number for
Several Aircraft. 87,88

number. Note that the F-4C goes off-scale and varies from -0.24 to 0.34. The F-104A has a similar shape with variations from -0.28 to 0.57. Only part of the transonic variation is shown for the F-104A and XB-70 to avoid cluttering the figure.

Until recently, C_{L_u} was given little consideration in stability and control work. The effect of C_{L_u} on longitudinal stability is small and it mainly affects the phugoid mode such that increasing positive values of C_{L_u} decrease phugoid period.

SPEED-DAMPING DERIVATIVE, C_{D_u}

Aeroelastic effects can be neglected for this derivative. The magnitude of C_{D_u} is negligibly small for low speed and high supersonic Mach numbers. It assumes a positive value at critical Mach number and can reach high positive values transonically. It is generally small and negative for low supersonic Mach numbers.^{77,86,65}

Like C_{L_u} , C_{D_u} can be written in terms of Mach number as shown in Equation 54:

$$C_{D_u} = C_{D_M} M \quad (54)$$

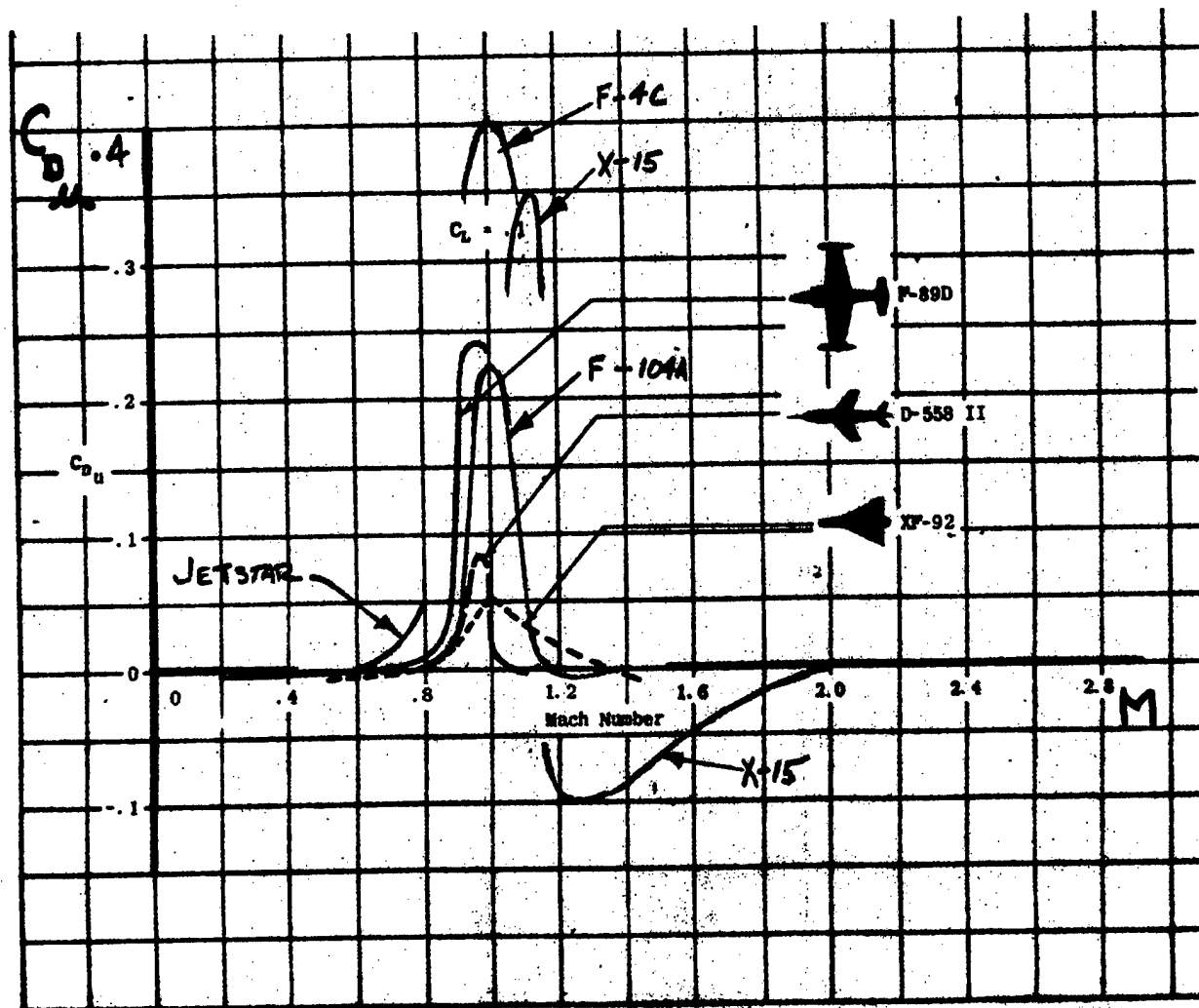


Figure 12: Variation of C_{Du} with Mach Number
for Several Aircraft. 87,88

Reference 74 gives the approximate transonic variation of C_{D_u} as -0.01 to 0.30. Figure 12 shows typical C_{D_u} variations with Mach number. The F-4C curve has the same basic shape as the F-104A curve, but only the peak is shown. Note that the X-15 exceeded the predicted range in the negative direction by a considerable amount.

The effect of a positive value of C_{D_u} on longitudinal dynamics is an increase in damping of the phugoid mode. From a performance viewpoint, the smallest possible value of C_{D_u} occurring at as high a Mach number as possible is desirable. This indicates a high drag-rise Mach number and a low transonic drag rise.

VELOCITY STABILITY, C_{m_u}

The magnitude of C_{m_u} can vary considerably and the sign can change depending on the magnitude of thrust or power, Mach number, and aeroelastic effects.⁶⁵ Early literature treated C_{m_u} only as a power effect arising from propwash; however, for modern jet aircraft thrust effects are small unless the thrust line is offset from the center of gravity. The magnitude of C_{m_u} is negligibly small for low speed and high supersonic Mach number, but it can reach high values near critical Mach number.^{77,86}

Like C_{L_u} , C_{m_u} can be written in terms of Mach number as shown in Equation 55:

$$C_{m_u} = C_{m_M} M \quad (55)$$

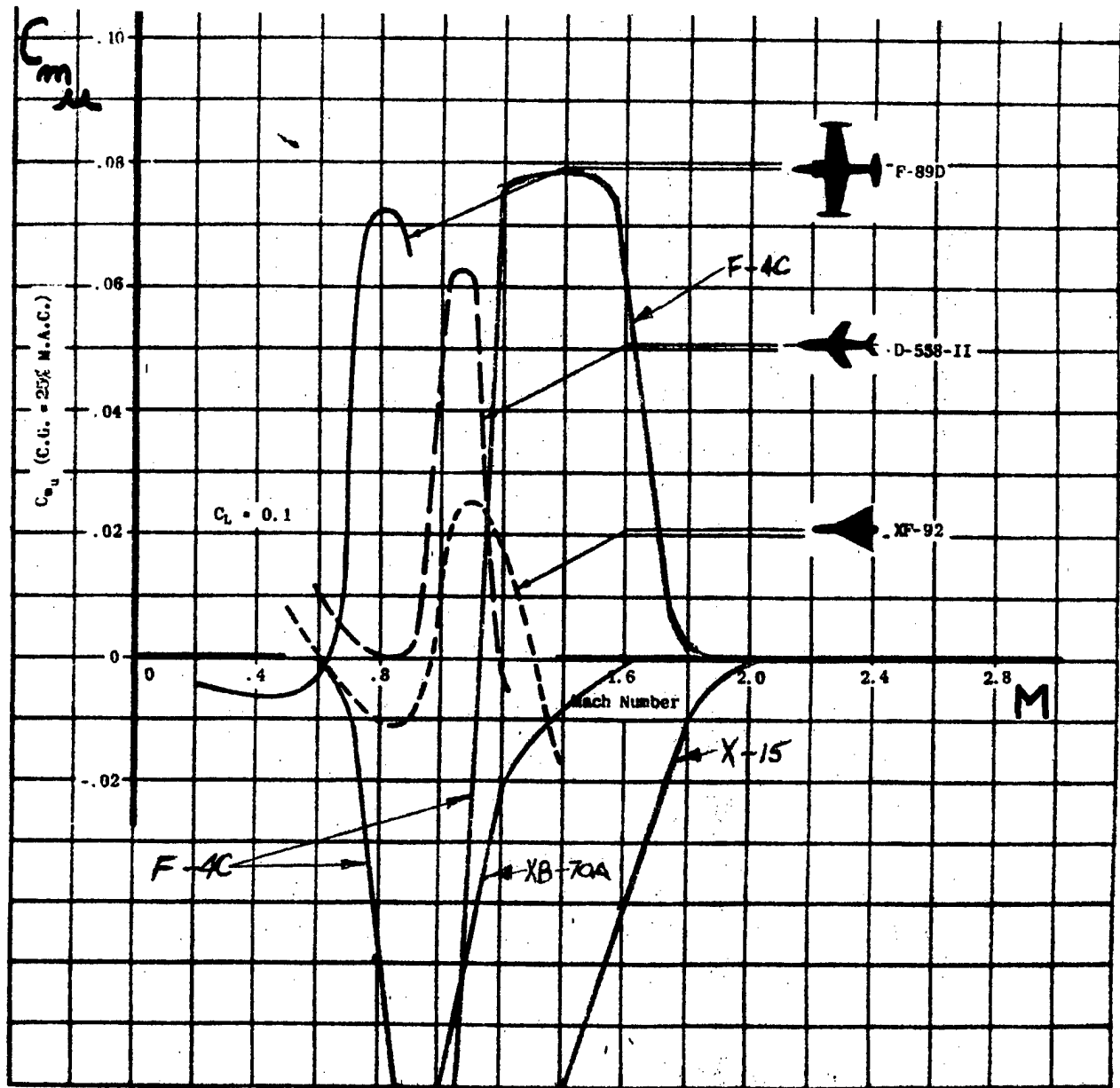


Figure 13: Variation of C_{μ} with Mach Number
for Several Aircraft^{87,88}

This derivative is very sensitive to wing shape and camber, high aspect ratio being most effected and highly-swept and delta being least affected. The main factor contributing to this derivative is the backward shift of the center of pressure which occurs in the transonic range.⁶⁵

Reference 88 gives the approximate transonic variation of C_{m_u} as -0.2 to 0.5. Figure 13 shows typical C_{m_u} variations with Mach number. The F-4C goes off-scale to about -0.3. Only the supersonic variation of the XB-70A and X-15 is shown to avoid cluttering the figure.

LIFT CURVE SLOPE, C_{L_α}

When the angle of attack of an aircraft is increased, the lift force will increase more or less linearly until stall. The derivative C_{L_α} is therefore always positive at angles of attack below stall. In fact, the most common definition of stall speed has it occurring at steady straight flight at the first C_{L_α} equals zero which occurs as C_L is increased from zero.³

In the equilibrium flight condition, a high value of C_{L_α} is desirable because, for a given angle of attack, the aircraft with the higher value of C_{L_α} will usually have a lower drag, and therefore better performance.

As far as dynamic stability is concerned, this derivative makes a contribution to the damping of the longitudinal short period for all aircraft and especially for tailless aircraft because in this case almost all of the damping comes from C_{L_α} .

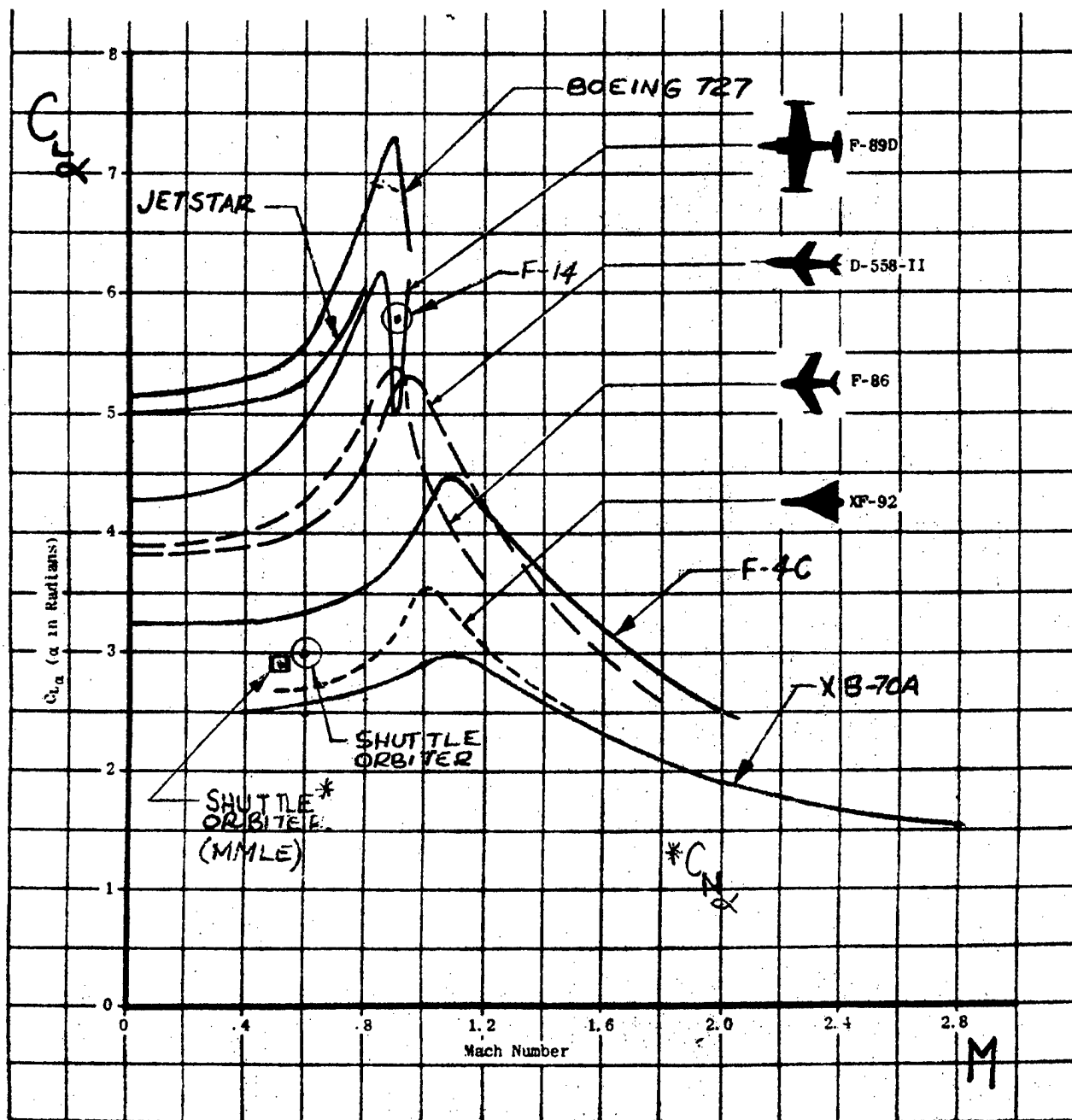
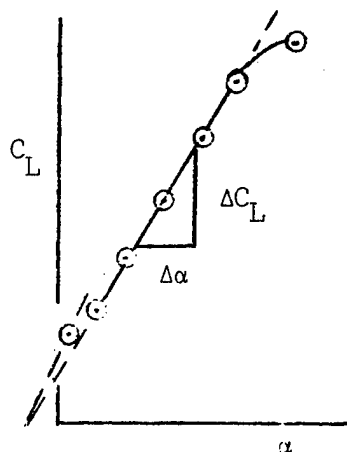


Figure 14: Variation of $C_{L\alpha}$ with Mach Number
for Several Aircraft^{74,87,88,100,142}

A high value of C_{L_α} would therefore always be desirable if it were not for the fact that high values of C_{L_α} result from designing aircraft with high aspect ratio unswept wings. This configuration does not represent current supersonic aircraft design trends for minimizing drag.

Reference 74 gives the approximate transonic variation of C_{L_α} as from 1.0 to 8.0. Figure 14 shows typical variations of C_{L_α} with Mach number.

The subsonic lift curve slope value can be determined easily from steady-state flight tests. If angle of attack had been measured here at the School on speed-power data missions, C_{L_α} could have been determined as shown in Figure 15:



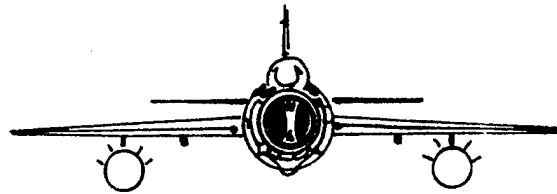
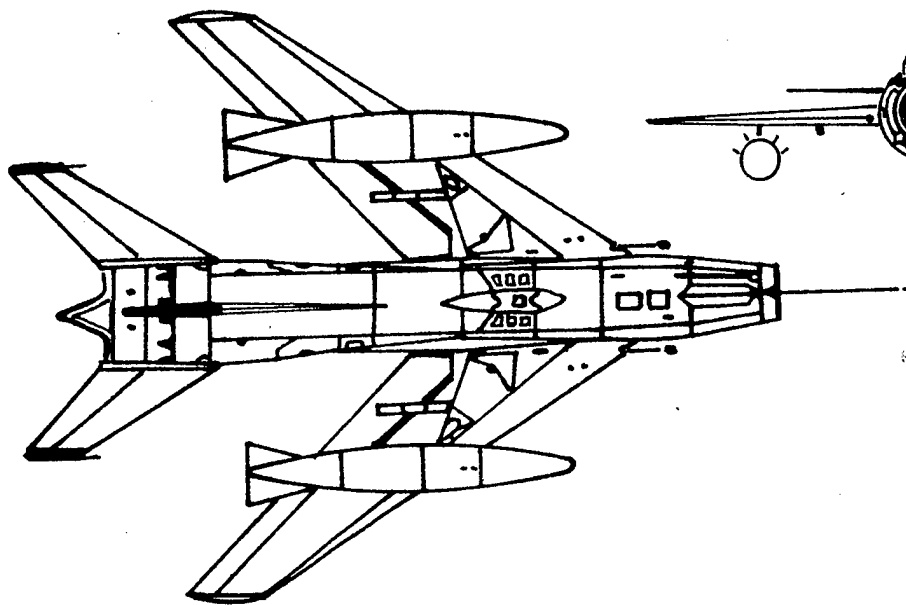
Measured: M , δ , W , and α stabilized in steady-state level flight over a range of M and δ .

Calculated:

$$C_L = \frac{nW}{1481\delta M^2 S}$$

$$C_{L_\alpha} = \frac{\Delta C_L}{\Delta \alpha}$$

Figure 15: Determination of C_{L_α} from Stabilized Level Flight Tests.



Designation: FARMER (Chinese: F-6)

Wing Span: 36'

Length: 44'

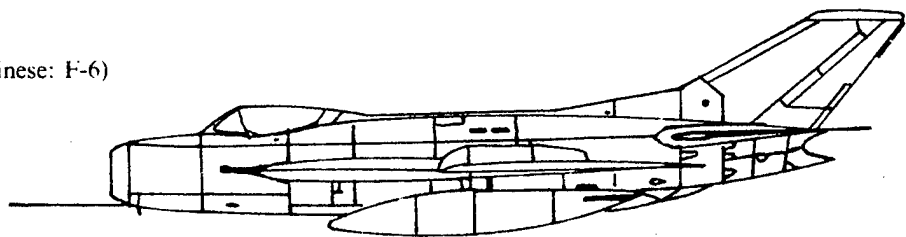
Speed: M 1.3 at 33,000 feet

Gross Wt.: 22,000 lbs.

Ceiling: 60,000 Ft.

Crew: 1

Armament: 30MM Guns, 2 X 500 lb.bombs, air-to-surface rockets, "Alkali" missiles

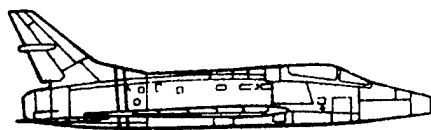


CHANGE IN DRAG COEFFICIENT WITH ANGLE OF ATTACK, C_{D_α}

When the angle of attack of an aircraft is increased, the drag coefficient will increase more or less parabolically (as a function of C_L^2) until stall. The derivative C_{D_α} is a function of angle of attack and is usually positive at angles of attack below stall; however, it can approach zero at high angles of attack on swept wing or low aspect ratio configurations where stall is not well defined.

This derivative is usually unimportant in airframe dynamics. It does affect the phugoid mode, where a decrease in C_{D_α} increases stability; however, this effect is small because changes in angle of attack are small during phugoid motion.

Reference 74 gives the transonic variation of C_{D_α} as from zero to 2.0. Figure 16 shows typical variations of C_{D_α} in the low subsonic region as a strong function of angle of attack (equilibrium lift coefficient).



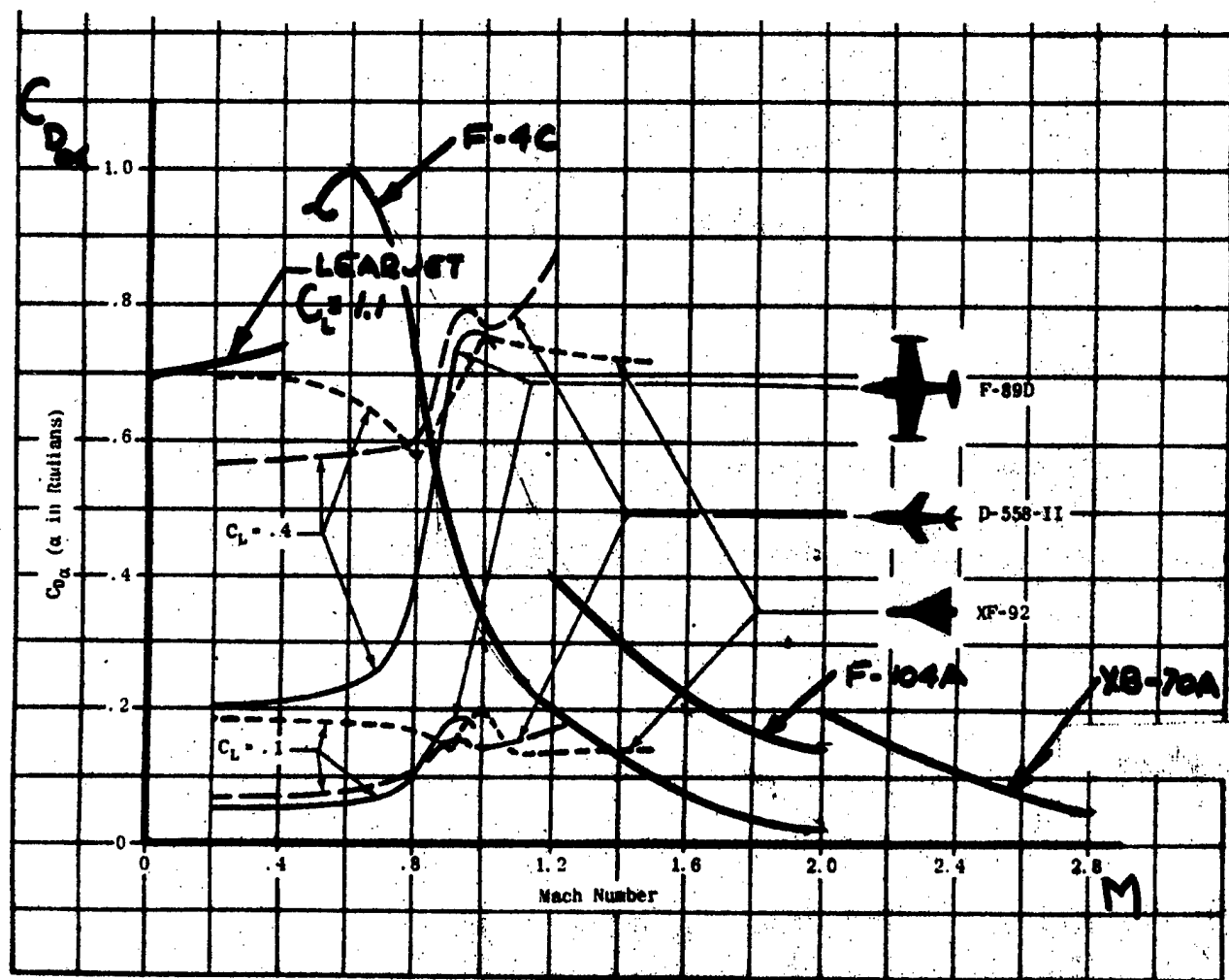


Figure 16: Variation of $C_{D\alpha}$ with Mach Number

For Several Aircraft 74,87,88

The subsonic drag polar slope can be determined easily from steady-state flight tests. If angle of attack had been measured here at the School on speed-power data missions, $C_{D\alpha}$ could have been determined as shown in Figure 17:

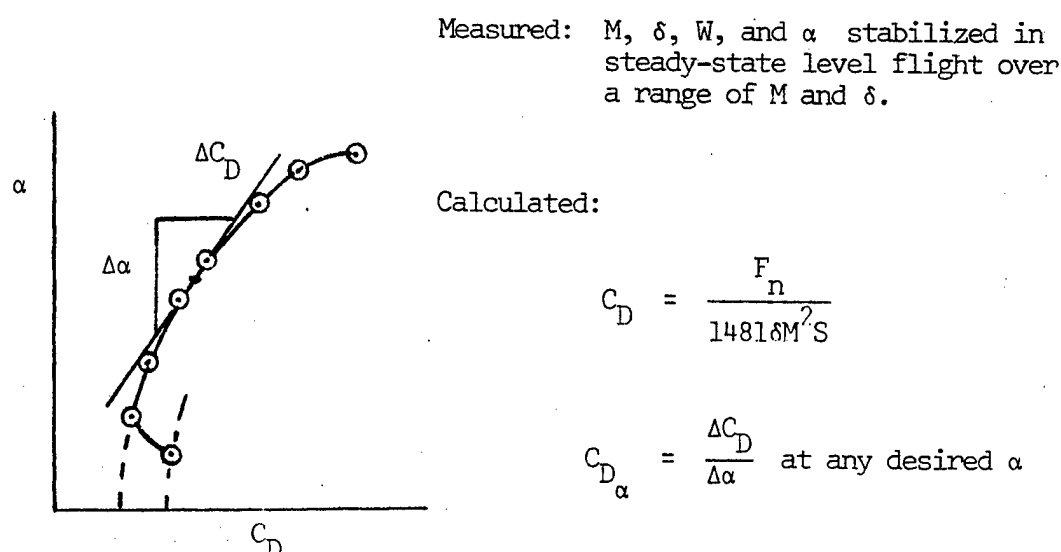


Figure 17: Determination of $C_{D\alpha}$ from Stabilized Level Flight Tests

LONGITUDINAL STATIC STABILITY, $C_{m\alpha}$

When the angle of attack of an aircraft is increased from equilibrium, the increased lift on the horizontal tail causes a negative pitching moment about the center of gravity. Simultaneously, the increased lift on the wing-fuselage combination causes a positive or negative pitching moment, depending on aircraft center of gravity location. The magnitude and sign of the total $C_{m\alpha}$ for a given configuration is a strong function of center of gravity position. $C_{m\alpha}$ is the most important longitudinal stability derivative.



C_{m_α} primarily establishes the natural frequency of the short period mode, and is a major factor in determining gust stability. In general, large negative values of C_{m_α} are desirable for stability and good flying qualities; however, if it is too large elevator power may be insufficient for satisfactory maneuverability.

Reference 74 gives the approximate transonic variation of C_{m_α} as from -3.0 to 1.0. Figure 18 shows typical variations of C_{m_α} with Mach number.

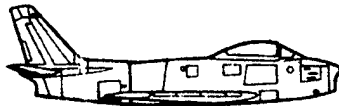
Reference 64 shows that C_{m_α} can be expressed as:

$$C_{m_\alpha} = C_{L_\alpha} (h - h_n)$$

stick-fixed, or

$$C_{m_\alpha} = C_{L_\alpha} (h - h'_n)$$

stick-free, where h is the aircraft's center of gravity position, h_n is the stick-fixed neutral point, h'_n is the stick-free neutral point, and C_{L_α} is the aircraft's lift curve slope. Methods for determining h_n and h'_n are discussed in detail in Reference 16; however, Figure 19 illustrates how stick-fixed C_{m_α} can be determined from the standard longitudinal static stability tests performed here at the School.



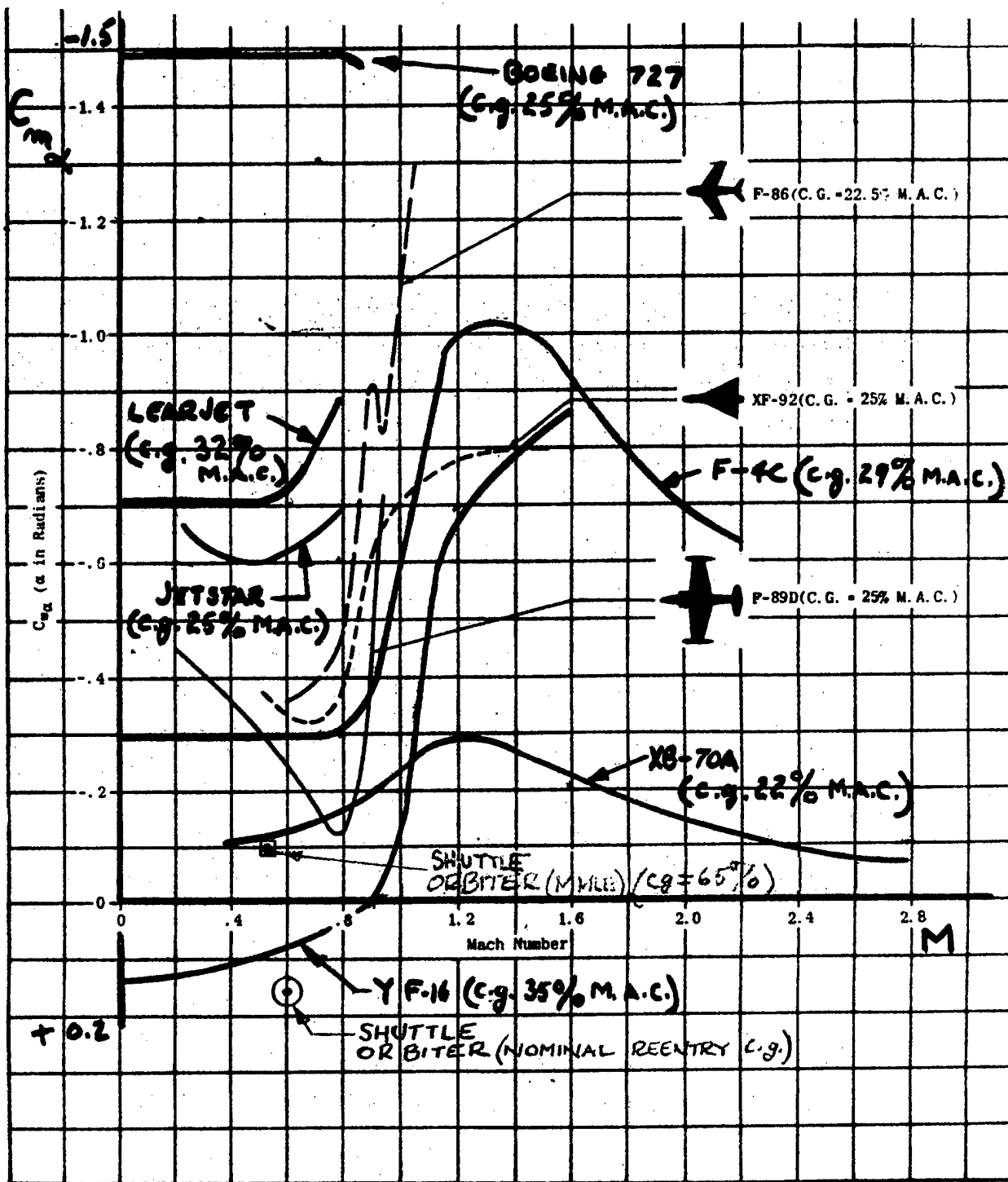
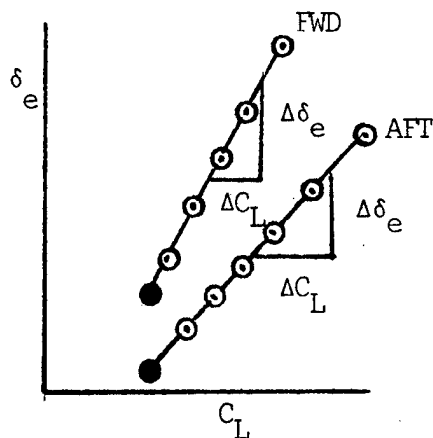


Figure 18: Variation of $C_{m\alpha}$ with Mach Number
for Several Aircraft^{74,87,88,92,100,142}



Measured: M , δ , W , and δ_e during longitudinal static stability testing at two h positions, one FWD and one AFT.

Calculated:

$$C_L = \frac{nW}{1481\delta M^2 S}$$

C_{L_α} As Described from stabilized level flight tests

$$C_{m_\alpha} = C_{L_\alpha} (h - h_n)$$

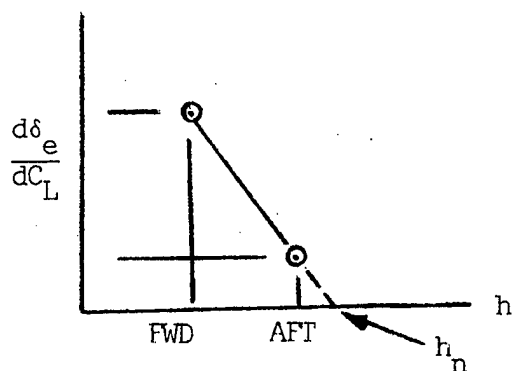


Figure 19: Determination of C_{m_α} from Longitudinal Static Stability Tests

For aircraft with truly irreversible control systems, stick-fixed and stick-free neutral points are the same point. For aircraft with reversible control systems, the stick-free neutral point is normally (depending on configuration and aerodynamic balancing) ahead of the stick-fixed neutral point. If there are no control system gadgets, such as downsprings or bobweights, the stick-free neutral point can be determined as shown in Figure 20. Since aircraft with reversible control systems are normally relatively low-speed, it may be more convenient to measure equivalent air-speed rather than Mach number during longitudinal static stability testing.

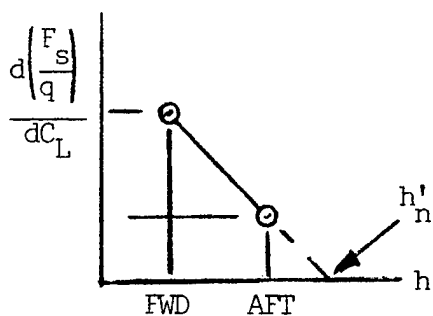
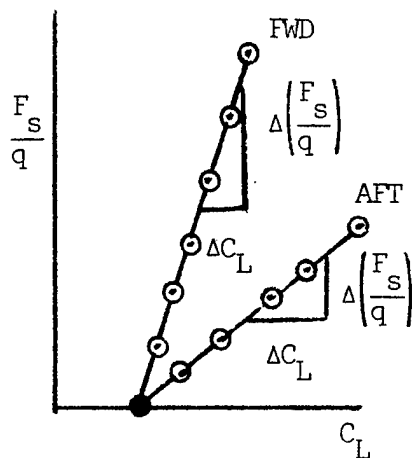
Measured: M (or V_e), δ , W , and F_s

Calculated:

$$C_L = \frac{nW}{1481\delta M^2 S} \quad \text{or} \quad \frac{nW}{1/2\rho_o V_e^2 S}$$

C_{L_α} as described from
stabilized level
flight tests

$$C_{m_\alpha} = C_{L_\alpha} (h - h'_n)$$



or, if elevator tab angle to trim, δ_T , instead of elevator force, F_s , is measured:

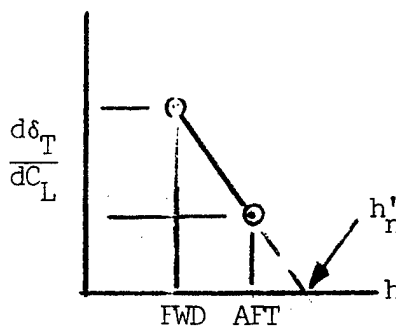
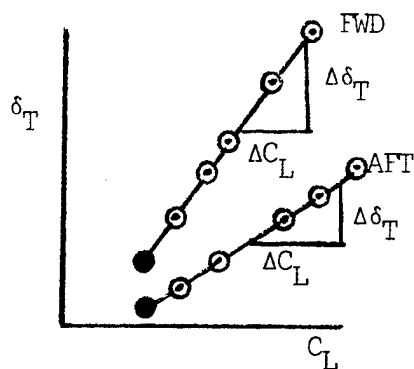


Figure 20: Determination of C_{m_α} from Longitudinal Static Stability Tests

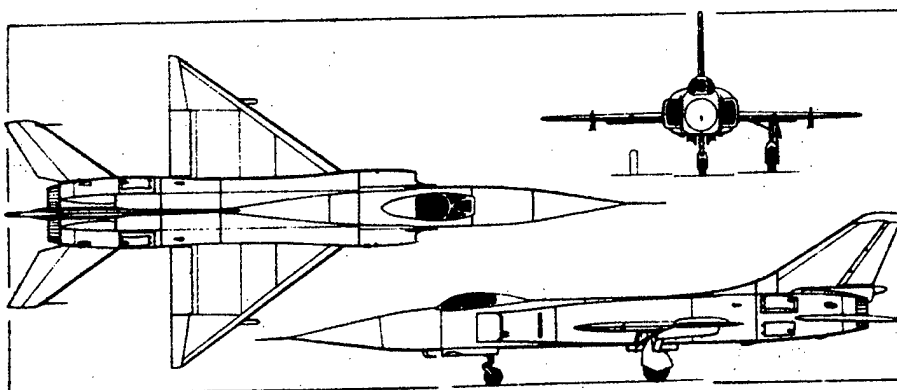
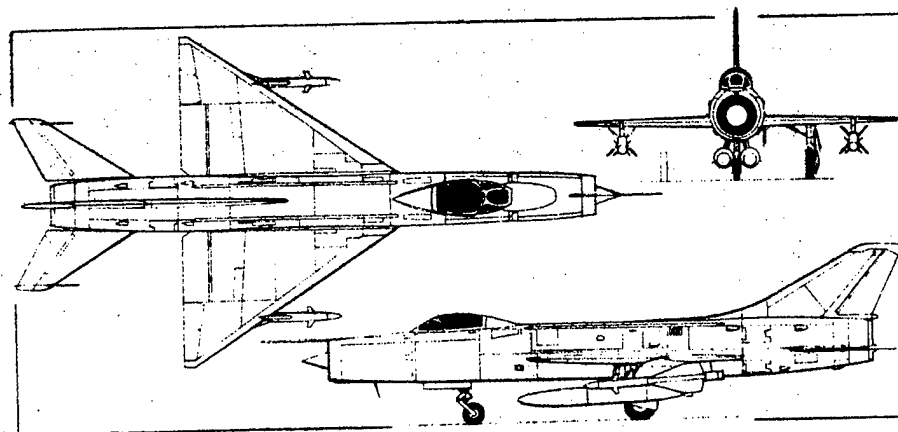
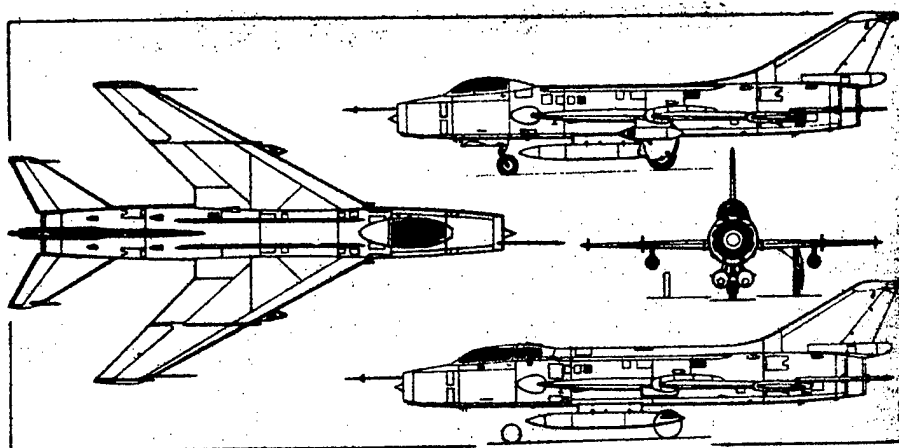
If the curves shown in Figure 20 of δ_e , F_s/q , or δ_T versus C_L are not linear then both stick-fixed and stick-free neutral points will be functions of lift coefficient. Therefore, C_{m_α} can also be a function of C_L . This occurs generally at high values of C_L .

LONGITUDINAL LAG DERIVATIVES, C_{L_α} , C_{D_α} , C_{m_α}

The $\dot{\alpha}$ derivatives are very different from those previously discussed which can be determined from steady-state flight tests. These $\dot{\alpha}$ derivatives partly owe their existence to the fact that the pressure distribution on a wing or tail does not adjust itself instantaneously to its equilibrium value when the angle of attack is suddenly changed. The calculation or measurement of this effect involves unsteady flow. These derivatives arise from a "plunging" type of motion along the z-axis resulting from a \dot{w} during which pitch angle remains constant. The horizontal tail of a conventional tail-to-the-rear aircraft is immersed in the downwash field of the wing and is mounted some distance aft of the wing. Whenever the wing undergoes a change in angle of attack, the downwash field is altered. Since it takes a finite length of time before this downwash alteration arrives at the tail, the resulting lift on the tail lags the motion of the aircraft. Since the type of motion under consideration is an acceleration, $\dot{\alpha}$ effects also can arise from aeroelastic or "dead weight" effects.⁶⁵

References 74 and 86 provide an analysis of the $\dot{\alpha}$ derivatives. Distinction between $\dot{\alpha}$ effects and pitch rate can be made analytically, and, as described in section 3, with some success in wind tunnel testing; however, attempts to separate the derivatives in flight testing have been unsuccessful.⁶⁰

C_{L_α} is the change in lift coefficient with variation in rate of change of angle of attack. Even for tailless aircraft C_{L_α} has a value since it



is primarily caused by the plunging motion of the wing. This effect is increased by the lag effect at the tail as explained in Reference 86. Aeroelastic effects such as wing twisting due to dead weight moment caused by nacelles projecting in front of the wing, and from fuselage bending caused by the dead weight of the aft fuselage and empennage can also cause $\dot{\alpha}$ effects. $C_{L\dot{\alpha}}$ is positive subsonically and can be either positive or negative supersonically.^{65,74,86}

The effect of $C_{L\dot{\alpha}}$ is essentially the same as if the aircraft's mass or inertia were changed in the equation relating the forces in the Z direction.⁶⁵

Reference 74 gives the approximate transonic variation of $C_{L\dot{\alpha}}$ as -5.0 to 15.0. Figure 21 shows typical $C_{L\dot{\alpha}}$ variations with Mach number. The $C_{L\dot{\alpha}}$ derivative is usually neglected in dynamic analysis and is considered to be unimportant.^{65,74}

$C_{D\dot{\alpha}}$ is the change in drag coefficient with variation in rate of change of angle of attack. This derivative is ignored in analytical work. Its effect would be even smaller than that of $C_{L\dot{\alpha}}$ or $C_{m\dot{\alpha}}$.^{65,74,86}

$C_{m\dot{\alpha}}$ is the change in pitching moment coefficient with variation in rate of change of angle of attack. Like $C_{L\dot{\alpha}}$, $C_{m\dot{\alpha}}$ is caused by both the plunging motion of the wing and by the lag effect at the tail. Apparently, the tail lag effect is the primary contributor to $C_{m\dot{\alpha}}$. Aeroelastic effects on $C_{m\dot{\alpha}}$ are the same as those on $C_{L\dot{\alpha}}$. The derivative $C_{m\dot{\alpha}}$ is negative subsonically and can be either positive or negative supersonically.^{65,74,86}

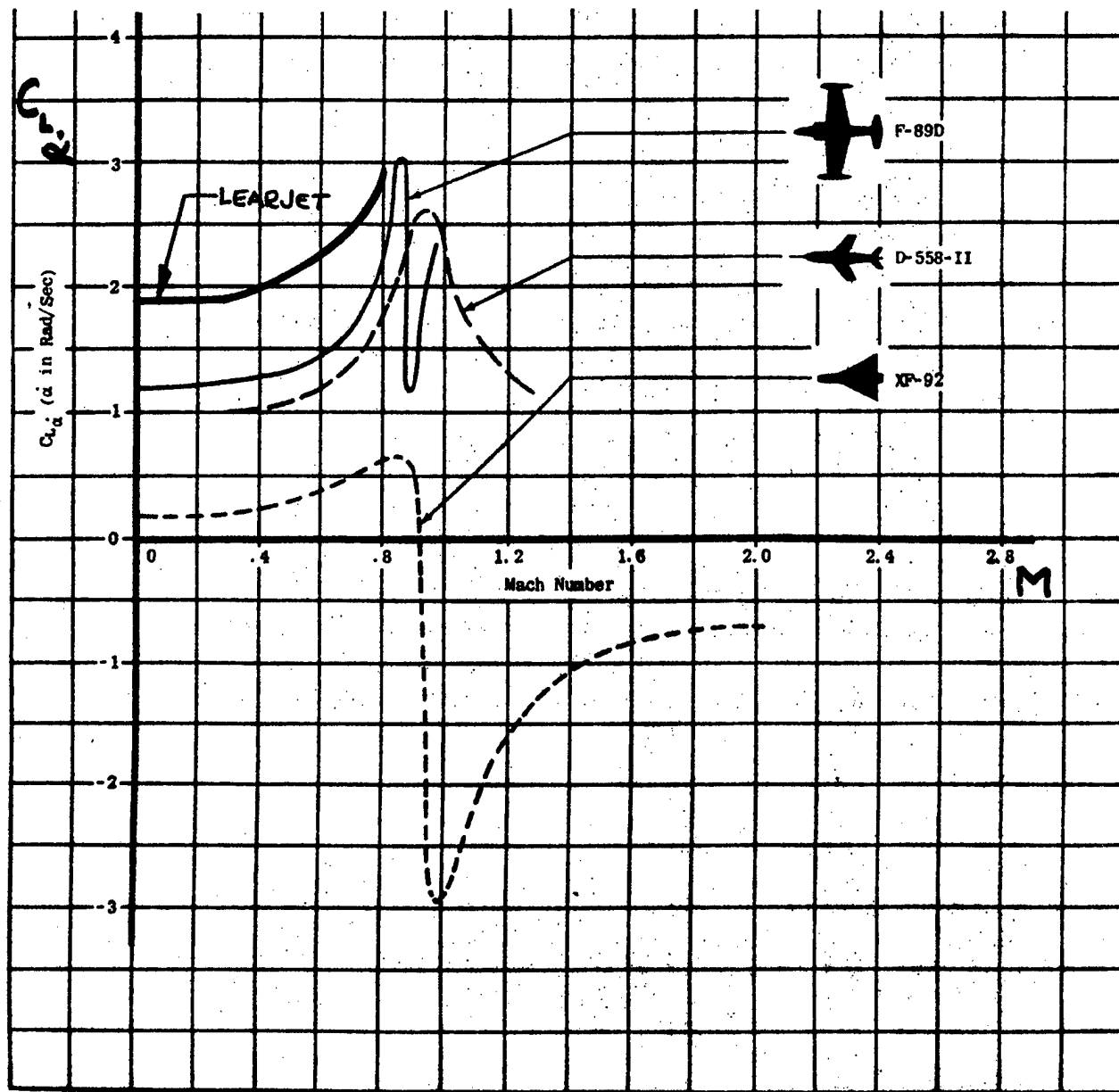
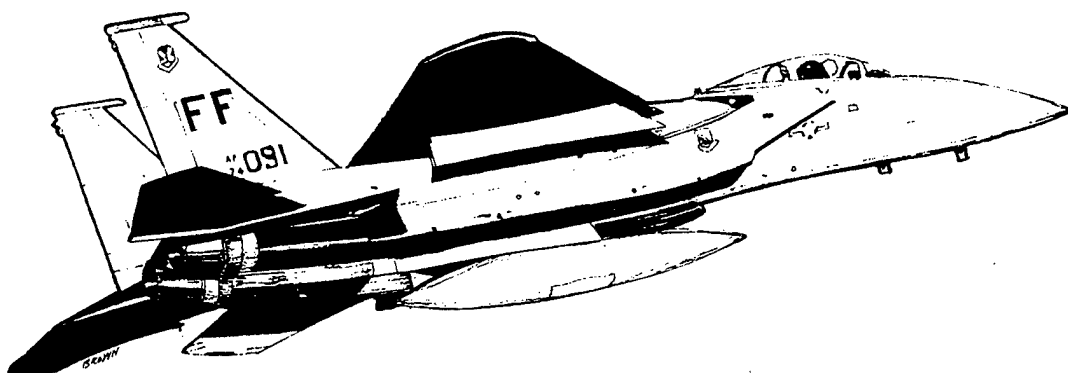
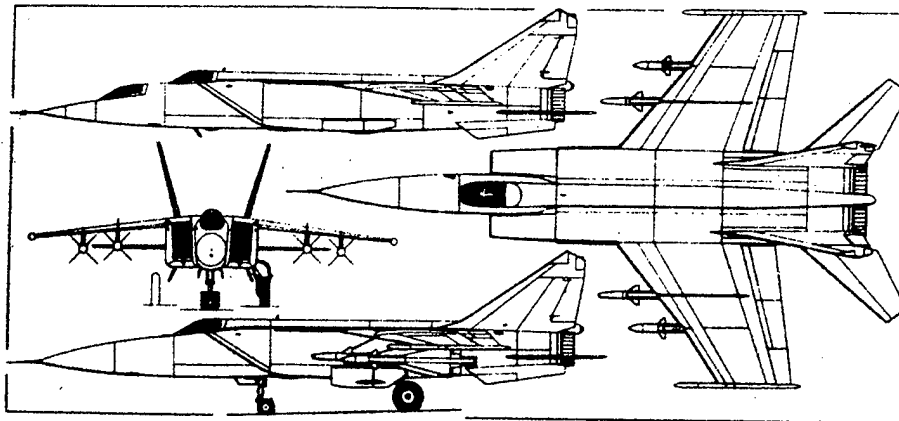
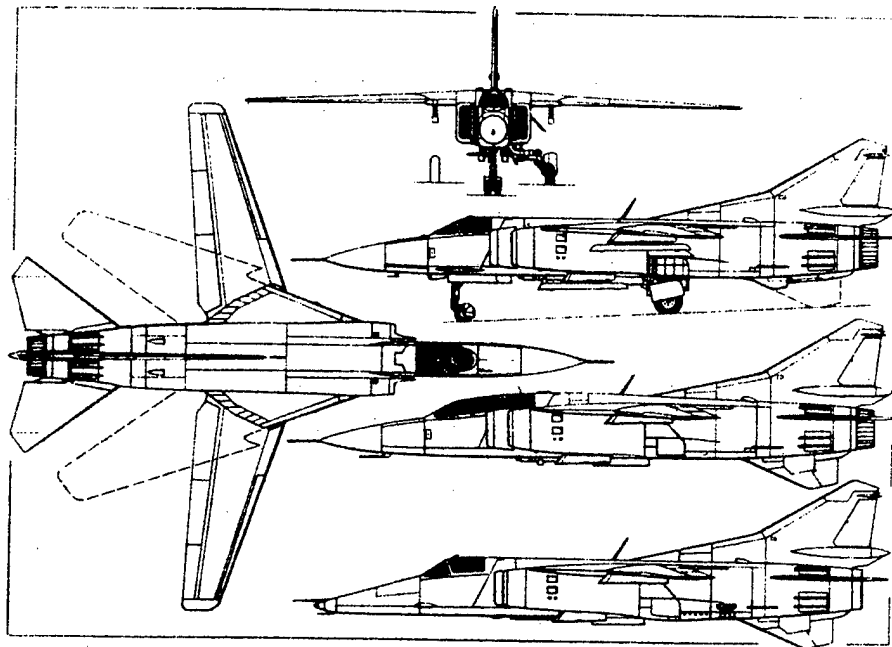
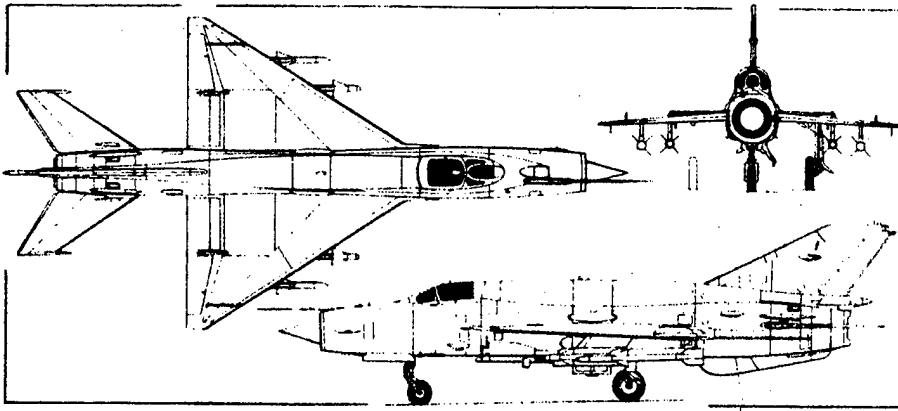


Figure 21: Variation of $C_{L_{\alpha}}$ with Mach Number
for Several Aircraft^{74,88}

Separation of $C_{m_{\dot{\alpha}}}$ and C_{m_q} can be made analytically if a wind tunnel value of downwash derivative is known. The ratio $C_{m_{\dot{\alpha}}}/C_{m_q}$ is precisely the downwash derivative, $d\epsilon/d\alpha$. Common practice is to take:^{97,86}

$$C_{m_{\dot{\alpha}}} = (d\epsilon/d\alpha) C_{m_q}$$





Reference 74 gives the approximate transonic variation of $C_{m_\alpha}^*$ as from zero to -10.0. Figure 22 shows typical $C_{m_\alpha}^*$ variations with Mach number. $C_{m_\alpha}^*$ is considered to be the most important of the longitudinal lag derivatives and its negative value increases the damping of the short period mode.^{65,74}

PITCH DAMPING, C_{m_q}

The stability derivative C_{m_q} is the change in pitching moment coefficient with varying pitch velocity. As the aircraft pitches about its center of gravity, the tail angle of attack changes, developing a lift force on the tail which produces a negative pitching moment contribution. There is also a contribution to C_{m_q} from various "dead weight" aeroelastic effects. Since the aircraft is moving in a curved path, the wing may twist as a result of the dead weight moment of overhanging nacelles, and the fuselage bends causing a change in tail angle of attack.⁶⁵

Reference 64 shows that C_{m_q} can be approximated by:

$$C_{m_q} = -2 a_T V_H \eta_T \frac{l_T}{c} \quad (56)$$

where a_T is the tail lift curve slope, V_H is the horizontal tail volume coefficient, η_T is the tail efficiency factor, and l_T/c is the distance from the aircraft center of gravity to the horizontal tail's aerodynamic center divided by wing chord. Equation 56 assumes that the entire value of C_{m_q} is from the tail contribution. If an additional ten percent is added as an empirical correction for fuselage and wing contribution, as shown in Equation 57, the subsonic value of C_{m_q} can be calculated quite accurately.^{86,93}

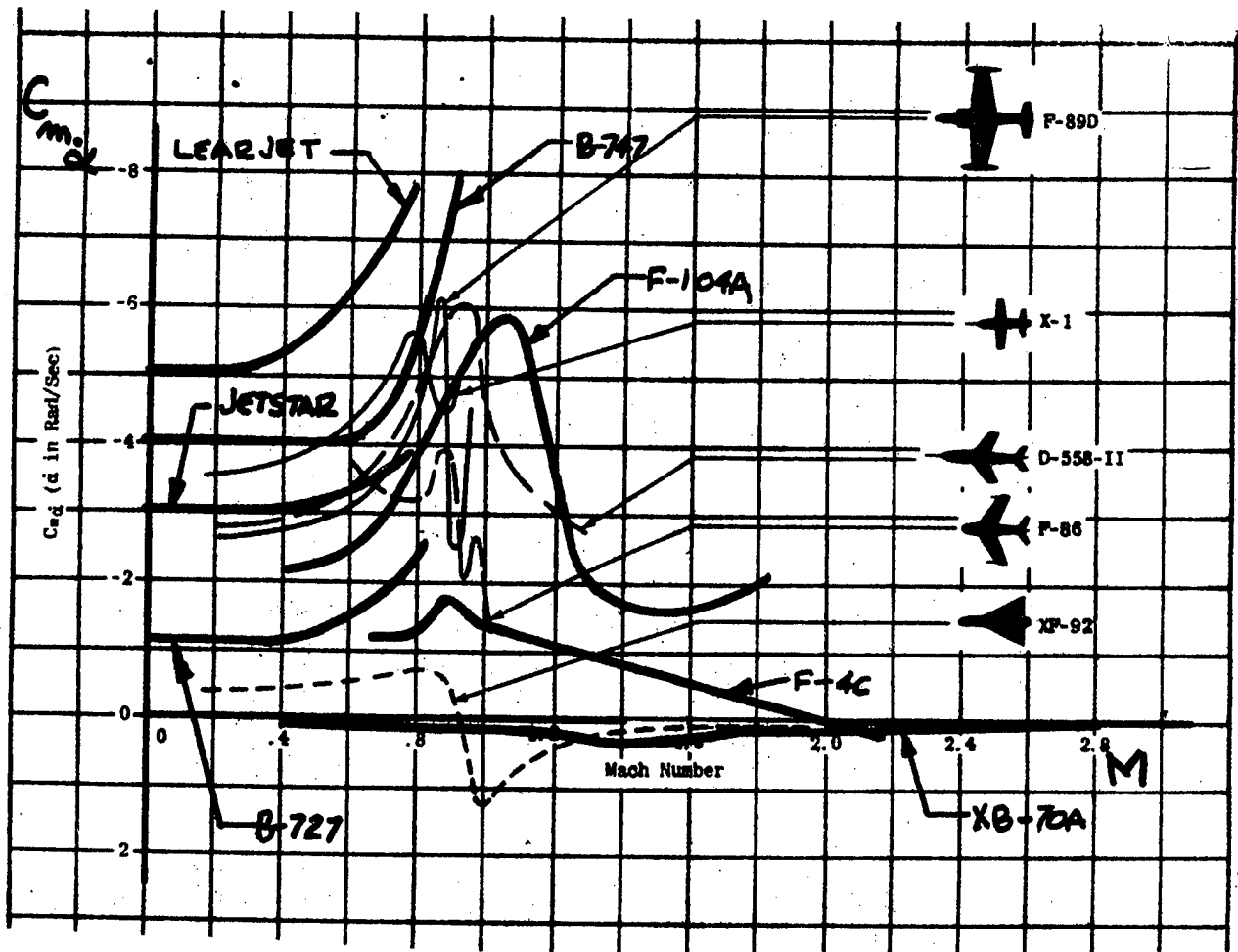


Figure 22: Variation of $C_{m\dot{\alpha}}$ with Mach Number for
Several Aircraft. 74, 86, 88

$$C_{m_q} = -2.2 a_T V_H n_T \frac{\ell_T}{c} \quad (57)$$

In low speed flight C_{m_q} is always negative. In high speed flight some references state that it may be either positive or negative depending on aeroelastic effects.⁶⁵

The derivative C_{m_q} is very important in longitudinal dynamics because it contributes a major portion of the damping of the short period mode for conventional aircraft. For tailless aircraft, C_{m_q} is consequently small and these configurations usually have poor damping. C_{m_q} is also involved with phugoid damping. In almost all cases, high negative values of C_{m_q} are desirable.⁶⁵

Reference 74 gives the approximate transonic variation of C_{m_q} as zero to -40.0. Figure 23 shows typical C_{m_q} variations with Mach number. Note that even at high supersonic speeds all of the C_{m_q} data shown remains negative.

The maneuver point and C_{m_q} are directly related. Methods for determining stick-fixed maneuver point, h_m , are discussed in detail in Reference 16; however, Figure 24 illustrates how C_{m_q} can be determined from maneuvering flight tests. Reference 64 shows that maneuver point and neutral point are related as shown in Equation 58.

$$h_m = h_n - \frac{\rho S c}{4m} C_{m_q} \quad (58)$$

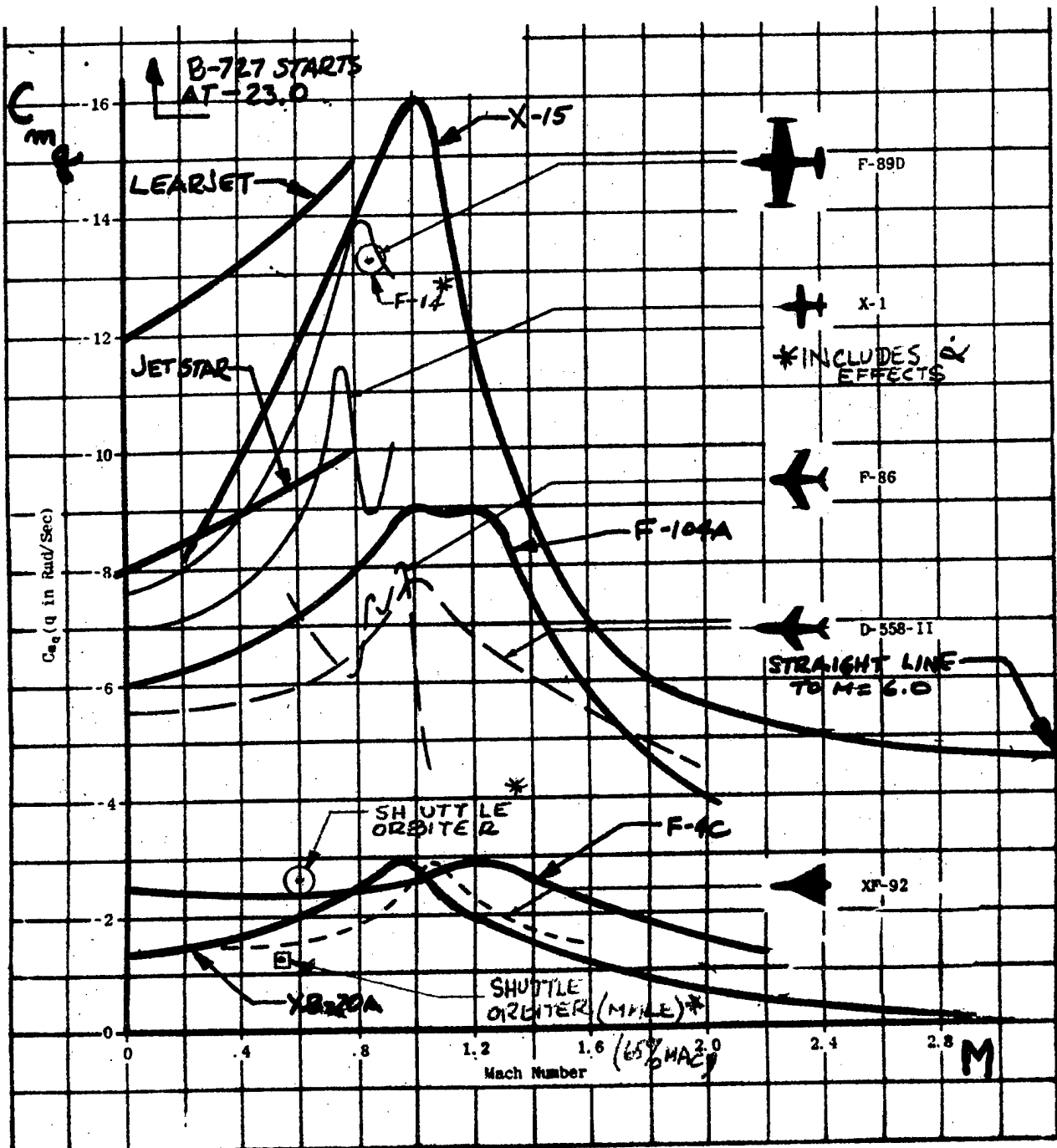


Figure 23: Variation of C_{mq} with Mach Number for
Several Aircraft^{74,87,88,100,142}

Solving Equation 58 for C_{m_q} gives:

$$C_{m_q} = - \frac{4m}{\rho S c} (h_m - h_n) \quad (59)$$

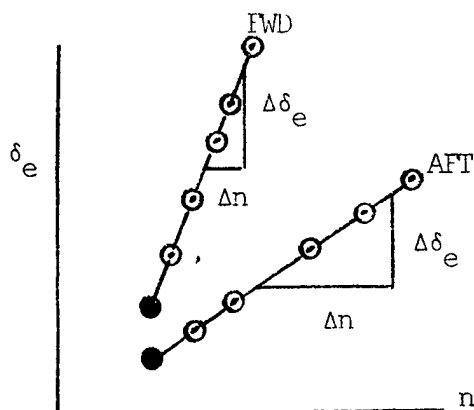
Therefore, if neutral point can be determined from linear data as shown in Figure 19, and if maneuver point can be determined from linear data as shown in Figure 24, then C_{m_q} can be determined.

CHANGE IN LIFT COEFFICIENT WITH PITCH RATE, C_{L_q}

Like C_{m_q} , C_{L_q} is caused by an increase in tail angle of attack which develops a lift force on the tail resulting in an increase in total aircraft lift coefficient. There is also a contribution to C_{L_q} from "dead weight" aeroelastic effects.⁶⁵

In low speed flight, C_{L_q} is always positive. In high speed flight some references state that it may be either positive or negative depending on aeroelastic effects.⁶⁵

Past experience shows that the effect of C_{L_q} on longitudinal stability has been small and it is usually neglected in aerodynamic analyses. . Because of the possibility of large aeroelastic effects at high Mach number it may have to be considered for high speed flight.⁶⁵

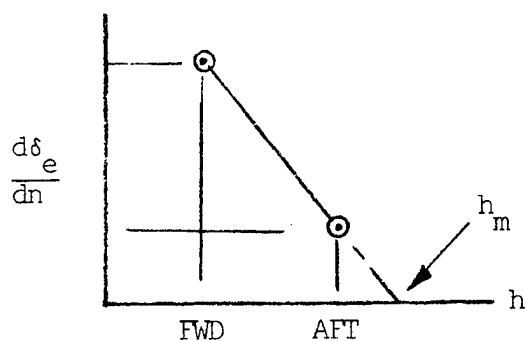


Measured: W , δ_e , and n during
maneuvering flight tests
at two h positions, one
FWD and one AFT, at a
given trim airspeed and
altitude, ρ

Calculated:

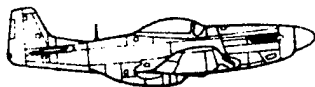
$$m = \frac{W}{g}$$

h_n as described in
Figure 19 from longi-
tudinal static
stability tests



$$C_{mq} = -\frac{4m}{\rho S c} (h_m - h_n)$$

Figure 24: Determination of C_{mq} from
Maneuvering Flight Tests



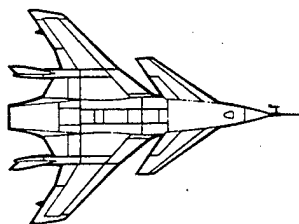
Reference 74 gives the approximate transonic variation of C_{L_q} as zero to 15.0. Figure 25 shows typical C_{L_q} variations with Mach number.

CHANGE IN DRAG COEFFICIENT WITH PITCH RATE, C_{D_q}

This derivative is ignored in analytical work. Its effect should be small.^{65,74,86}

CHANGE IN LIFT COEFFICIENT WITH ELEVATOR DEFLECTION, $C_{L_{\delta_e}}$

When the elevator is deflected upward a negative increment of lift is created on the horizontal tail; therefore, $C_{L_{\delta_e}}$ is negative in sign for a tail-to-the-rear aircraft. $C_{L_{\delta_e}}$ is positive for canard configurations, which gives the canard one of its major performance design advantages. On conventional tail-to-the-rear aircraft $C_{L_{\delta_e}}$ is usually very small and its effects neglected. On tailless aircraft, $C_{L_{\delta_e}}$ is comparatively large, and cannot be neglected.



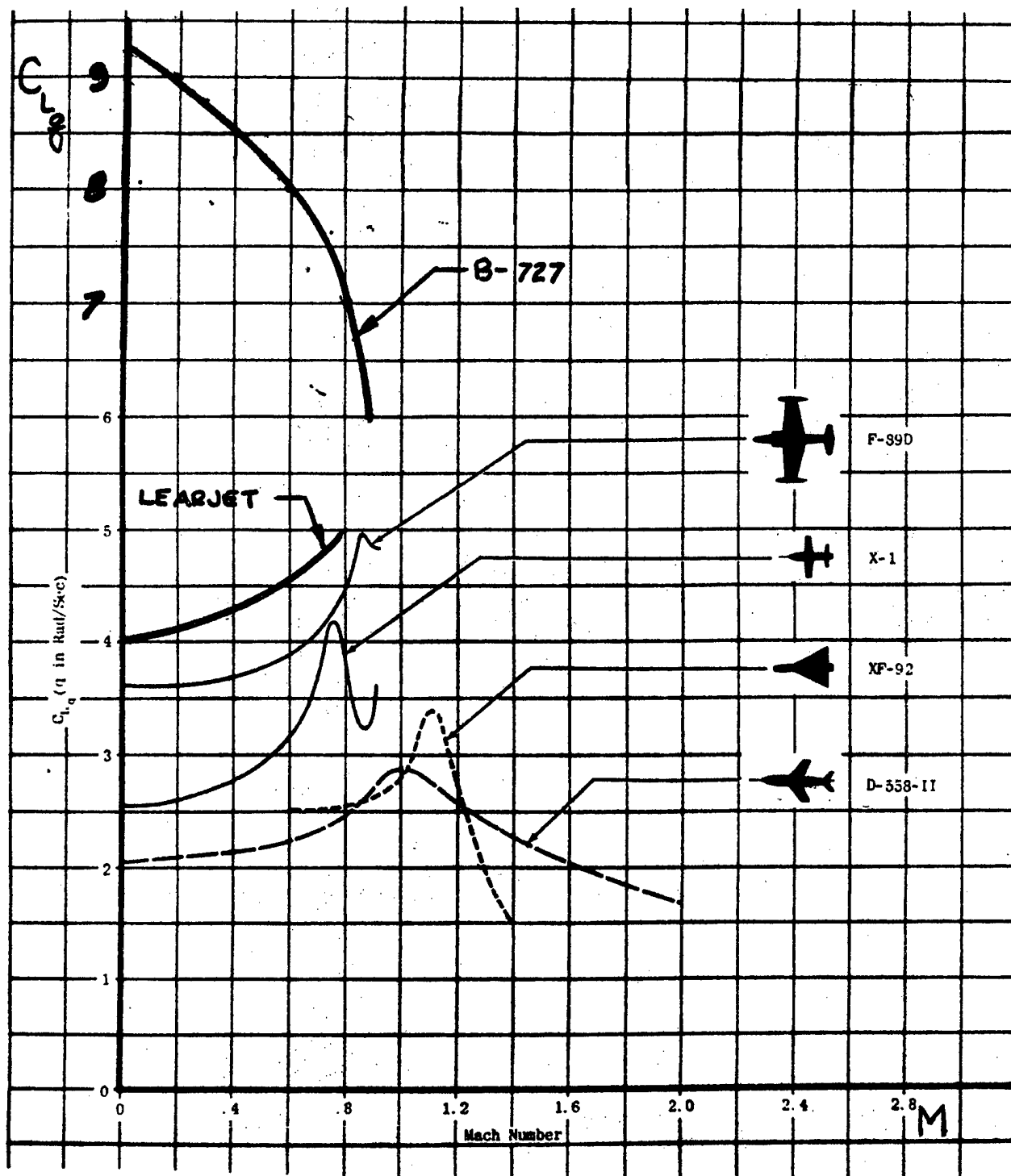


Figure 25: Variation of C_{L_q} with Mach Number
for Several Aircraft^{74,88}

The derivative $C_{L_{\delta_e}}$ can indirectly be determined from maneuvering flight tests if C_{L_α} is known. Reference 64 shows, that for tail-to-the-rear aircraft:

$$\Delta\alpha = \frac{1}{a} \left[C_L (n - n_0) - C_{L_{\delta_e}} \Delta\delta_e \right]$$

which can be written,

$$\Delta\alpha = \frac{1}{C_{L_\alpha}} \left[C_L \Delta n - C_{L_{\delta_e}} \Delta\delta_e \right]$$

or

$$C_{L_{\delta_e}} = \frac{\left(\frac{W}{qS} \right) \Delta n - C_{L_\alpha} \Delta\alpha}{\Delta\delta_e}$$

Therefore; if maneuvering flight data are linear, $C_{L_{\delta_e}}$ can be determined from two stabilized data points.

Alternatively, $C_{L_{\delta_e}}$ can be indirectly determined if $C_{m_{\delta_e}}$ is known by the following expression:⁹⁷

$$C_{L_{\delta_e}} = -C_{m_{\delta_e}} \left(\frac{c}{\ell_T} \right)$$

where c is the aircraft's mean aerodynamic chord and ℓ_T is the distance from the aircraft center of gravity to the horizontal tail aerodynamic center.

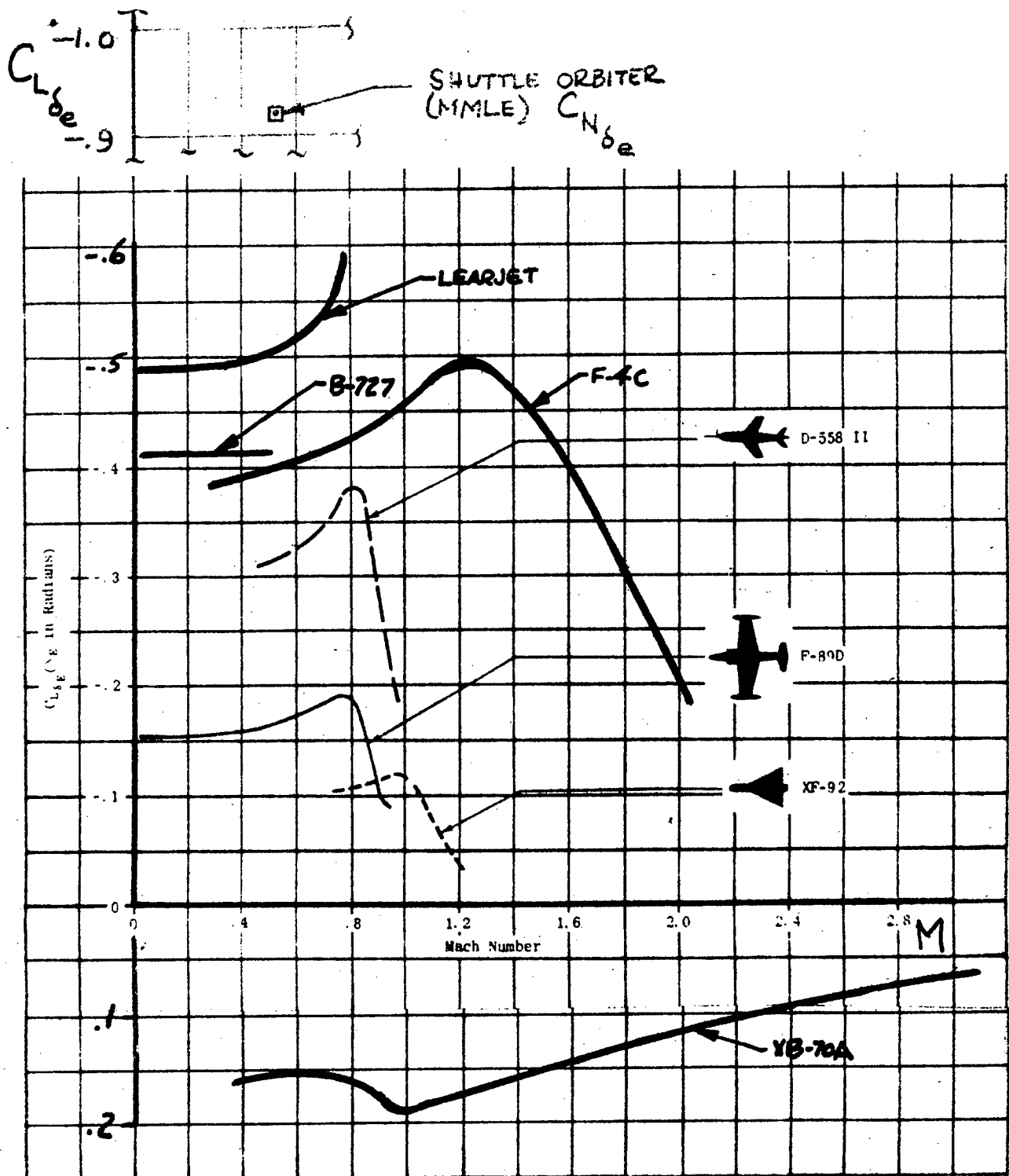
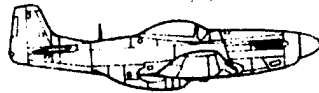


Figure 26: Variation of $C_{L_{\delta_e}}$ with Mach Number for
Several Aircraft. 74,88,87,142



CHANGE IN DRAG COEFFICIENT WITH ELEVATOR DEFLECTION, $C_{D_{\delta_e}}$

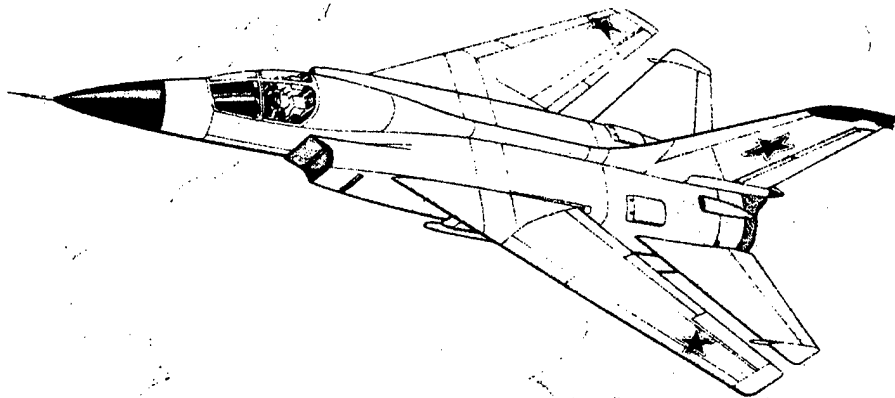
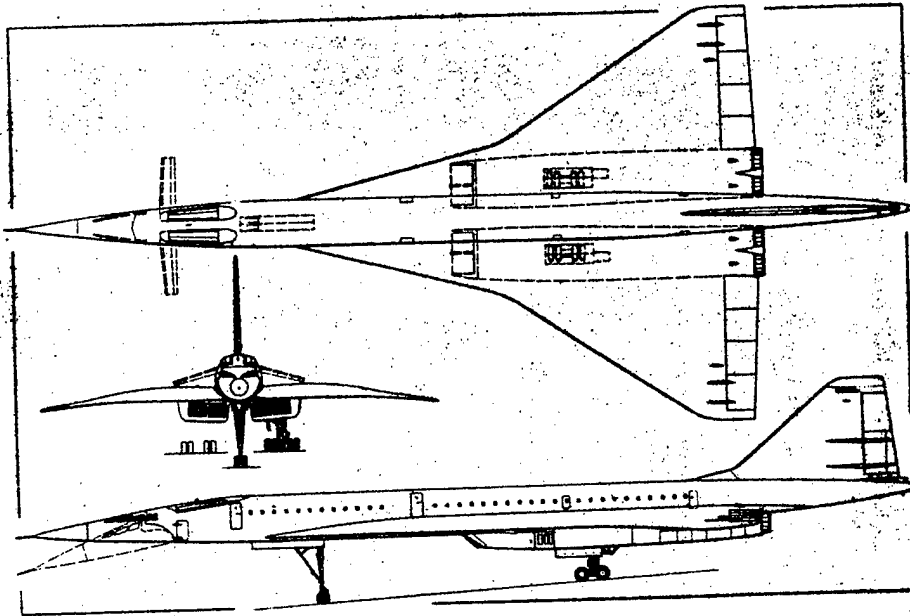
This derivative is ignored in flying quality analytical work; however, it has an effect on performance. It is associated with trim drag and is important when large values of elevator deflection are required to trim such as on tailless aircraft.^{65,74,86}

ELEVATOR POWER, $C_{m_{\delta_e}}$

This derivative is the change in pitching moment coefficient with elevator deflection. When the elevator of a tail-to-the-rear aircraft is deflected upward the resultant lift on the horizontal tail causes a positive pitching moment about the center of gravity. $C_{m_{\delta_e}}$ is therefore, positive by definition.

The primary function performed by the elevator of controlling the angle of attack both in equilibrium and maneuvering is considered the most important of all the control functions about the three axes. Elevator power is of great importance in aircraft design.⁶⁵

The design value of $C_{m_{\delta_e}}$ is essentially determined by the anticipated forward and aft positions of the center of gravity. The larger the center of gravity range, the larger the required value of $C_{m_{\delta_e}}$. Sometimes in design the maximum practical $C_{m_{\delta_e}}$ determines the allowable



center of gravity range, and in other cases the necessary center of gravity range determines design values of $C_{m_{\delta_e}}$.

It is difficult to give a desirable value for $C_{m_{\delta_e}}$ since each design, or configuration, must be analyzed separately. Reference 74 gives the approximate transonic variation of $C_{m_{\delta_e}}$ as from zero to 4.0. $C_{m_{\delta_e}}$ decreases significantly supersonically, especially for tailless aircraft. Figure 27 shows typical variations of $C_{m_{\delta_e}}$ with Mach number.

Reference 64 shows that Equation 60 can be used as a flight test relationship for determining $C_{m_{\delta_e}}$ from longitudinal static stability testing.

$$\frac{d\delta_e}{dC_L} = \frac{h_n - h}{C_{m_{\delta_e}}} \quad (60)$$

If plots of δ_e versus C_L are linear as shown in Figure 19 and neutral point, h_n , is determined as shown in Figure 19, then $C_{m_{\delta_e}}$ can be determined from the $d\delta_e/dC_L$ slope for either forward or aft center of gravity positions. Equation 61 can be used to determine $C_{m_{\delta_e}}$ from forward center of gravity data after the neutral point has been determined.

$$C_{m_{\delta_e}} = \frac{h_n - h_{FWD}}{\left(\frac{d\delta_e}{dC_L} \right)_{FWD}} \quad (61)$$

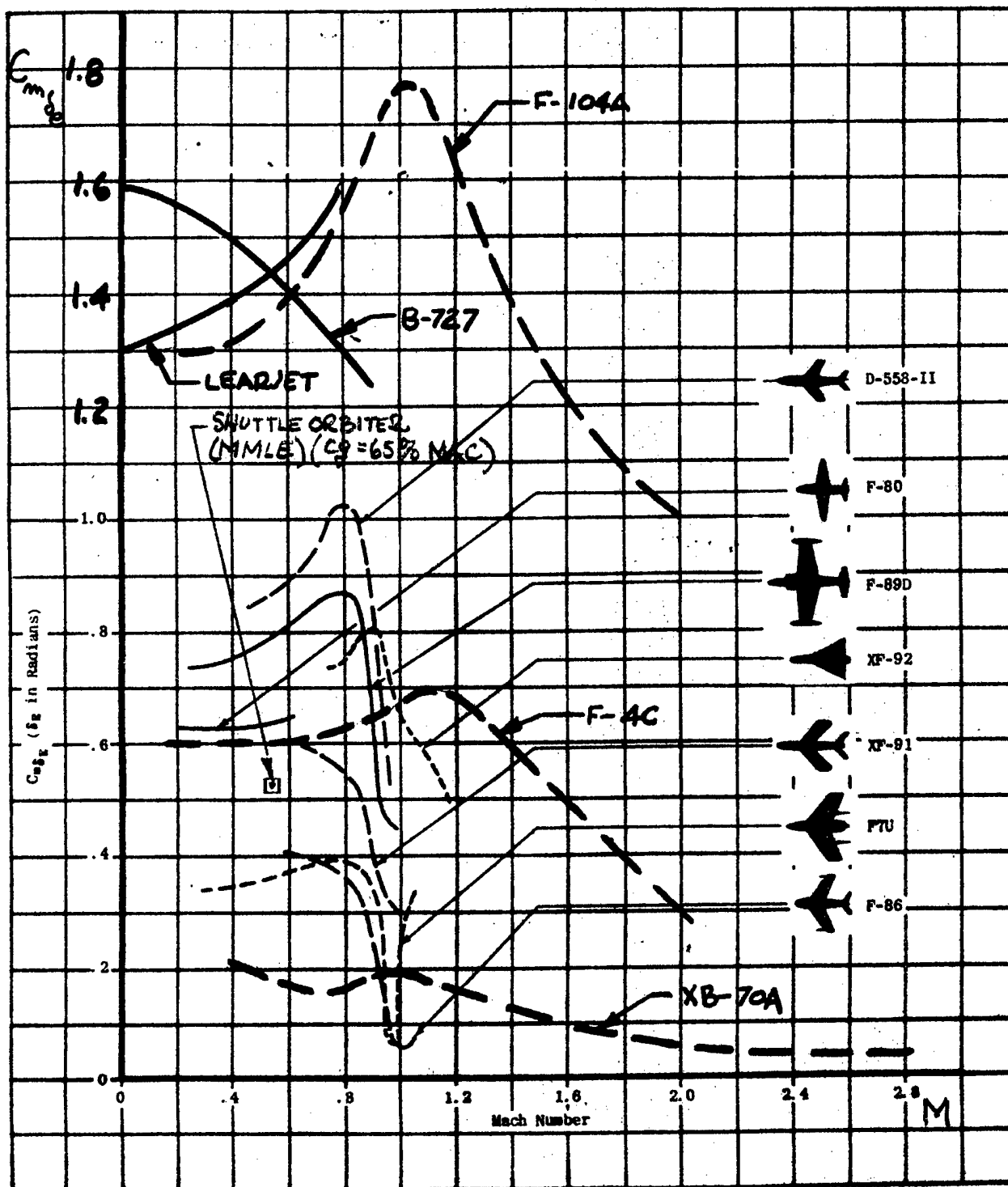


Figure 27: Variation of $C_{m\delta_e}$ with Mach Number
for Several Aircraft^{74, 87, 88, 142}

SIDE FORCE DAMPING, $C_{Y\beta}$

This derivative is the change in side force coefficient with changing sideslip angle. When an aircraft sideslips, the relative wind strikes it obliquely, creating a side force on the vertical tail, fuselage, and wing. The major contributor to $C_{Y\beta}$ is usually the vertical tail. It is negative in sign.⁶⁵

The derivative $C_{Y\beta}$ is fairly important in lateral dynamics, even though it dropped out of the simplified lateral-directional equations of motion derived here at the School. It contributes to damping of the Dutch roll mode. A large negative value of $C_{Y\beta}$ would appear desirable; however, a large negative value may create an undesirable lag effect in aircraft response when attempting to hold wings level in turbulence, or attempting to perform aileron maneuvers. $C_{Y\beta}$ is important in asymmetric power situations. Consideration of $C_{Y\beta}$ may be necessary for the design of some types of autopilots. $C_{Y\beta}$ is artificially generated by research aircraft which have side force generators, e.g. NT-33, and TIFS.

Reference 74 gives the approximate transonic variation of $C_{Y\beta}$ as from -0.10 to -2.0. Figure 28 shows typical $C_{Y\beta}$ variations with Mach number. In general, $C_{Y\beta}$ is a function of trim lift coefficient or angle of attack.

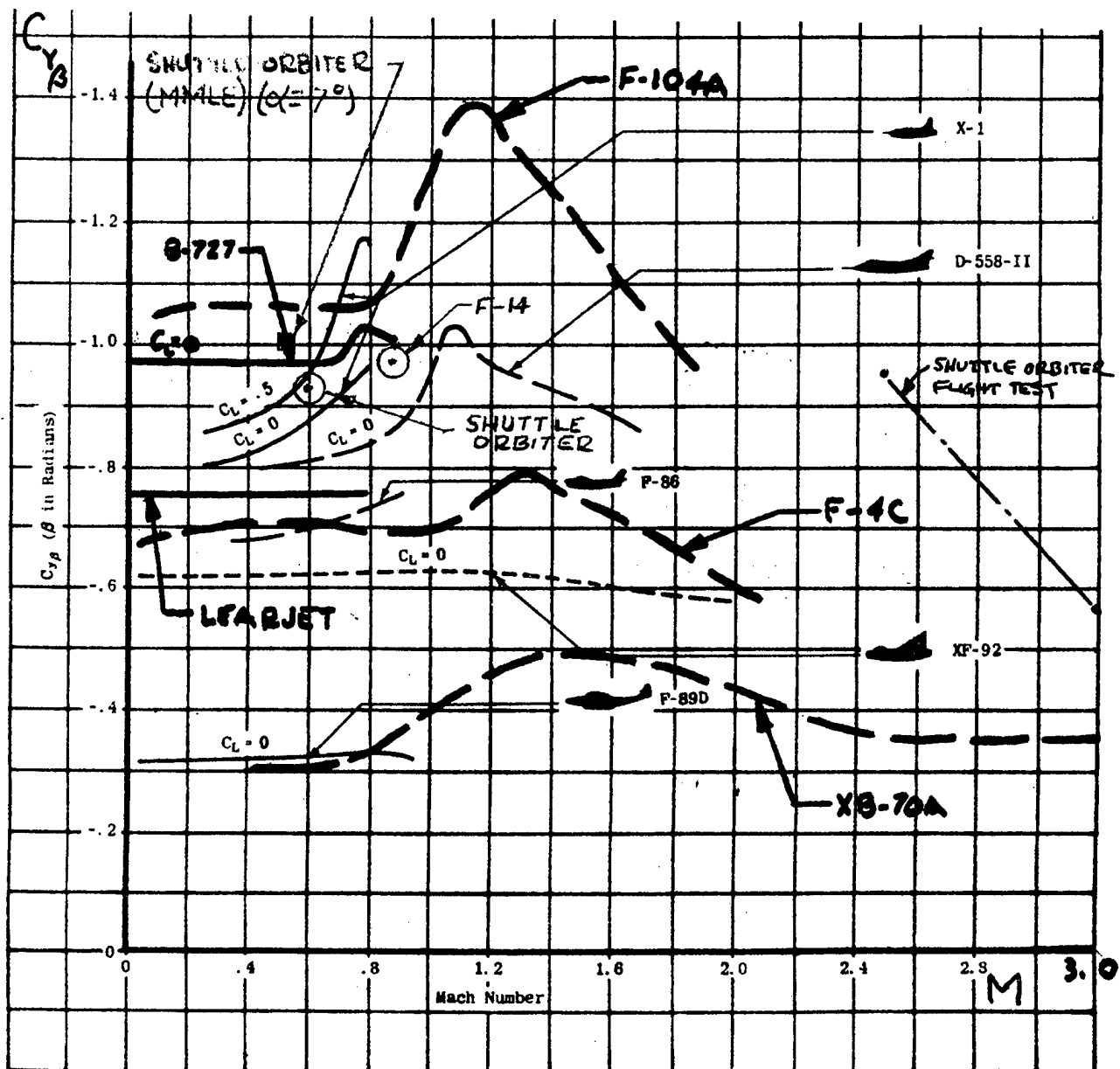


Figure 28: Variation of $C_{Y\beta}$ with Mach Number
for Several Aircraft^{74,87,88,100,142,158}

DIHEDRAL EFFECT, C_{ℓ_β}

This derivative is the change in rolling moment with variation in sideslip angle. When an aircraft sideslips a rolling moment is developed because of the geometric dihedral (or cathedral) of the wing and because of the usual high position of the vertical tail relative to the center of gravity. It is negative in sign for a stable aircraft.

The derivative C_{ℓ_β} is very important in lateral stability and control.

Although it does not appear in the simplified Dutch roll damping equation developed here at the School, it effects the damping of both the Dutch roll and spiral modes. It also affects the rudder alone maneuvering characteristics of an aircraft near stall. Small negative values of C_{ℓ_β} are desired for Dutch roll damping and for obtaining small ϕ/β ratios and large negative values for improving spiral stability; therefore, a compromise is necessary in design. Good flying qualities generally result when dihedral effect is negative but small.⁶⁵

Reference 74 gives the approximate transonic variation of C_{ℓ_β} as from 0.10 to -0.40; however, most of the typical variations shown on Figure 29 remain negative in value except for the XB-70A. In general, C_{ℓ_β} is a function of trim lift coefficient or angle of attack.



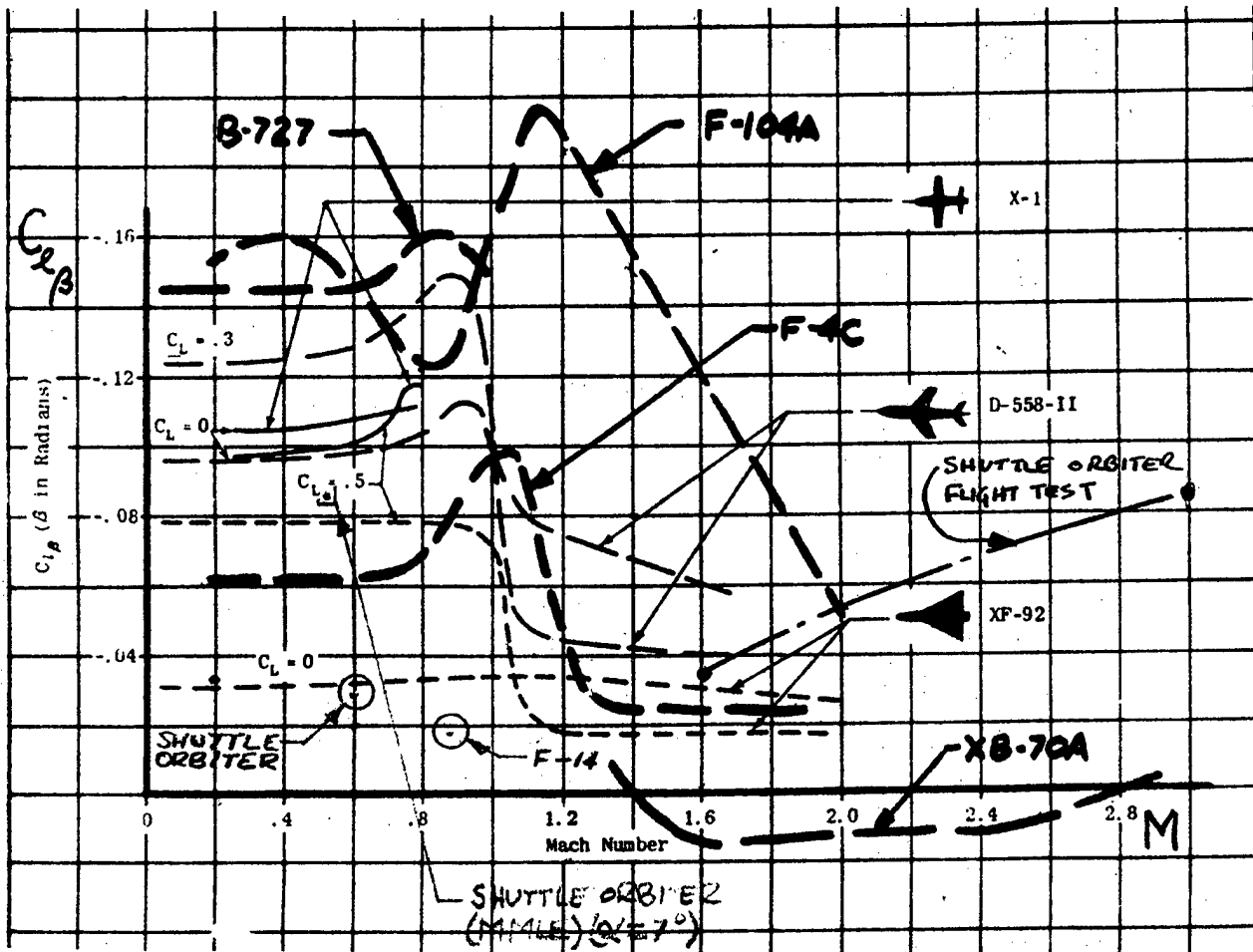
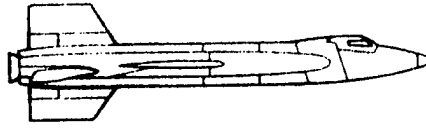


Figure 29: Variation of C_{l_β} with Mach Number
for Several Aircraft^{74,87,88,100,142,158}

DIRECTIONAL STABILITY, C_{n_β}

This stability derivative is the change in yawing moment with variation in sideslip angle. It is also called "weathercock stability" or "yaw stiffness." When an aircraft sideslips, the relative wind strikes it obliquely creating a yawing motion about the center of gravity. The major contribution to C_{n_β} is from the vertical tail which is located behind the aircraft center of gravity. C_{n_β} is positive in sign for a stable aircraft.

The derivative C_{n_β} is very important in determining static and dynamic lateral stability and control characteristics. In general, C_{n_β} should be as large as possible for good flying qualities. It aids in turn coordination and prevents excessive sideslip or yawing motion in rough air or while maneuvering. C_{n_β} primarily determines the natural frequency of the Dutch roll and is a factor in determining spiral stability.

Reference 74 gives the approximate transonic variation of C_{n_β} as zero to 0.40. Figure 30 shows typical C_{n_β} variations with Mach number. In general, C_{n_β} is a function of trim lift coefficient or angle of attack.

LATERAL-DIRECTIONAL LAG DERIVATIVES, C_{Y_β} , C_{ℓ_β} , C_{n_β}

The $\dot{\beta}$ derivatives are very different from those previously discussed which can be determined from steady state flight tests. They are similar to the $\dot{\alpha}$ derivatives and partly owe their existence to the fact that the pressure distribution on the fuselage and vertical tail does not adjust itself instantaneously to its equilibrium value when sideslip angle is suddenly changed by motion along the aircraft's y-axis. The result is a \dot{v} during which heading remains constant.

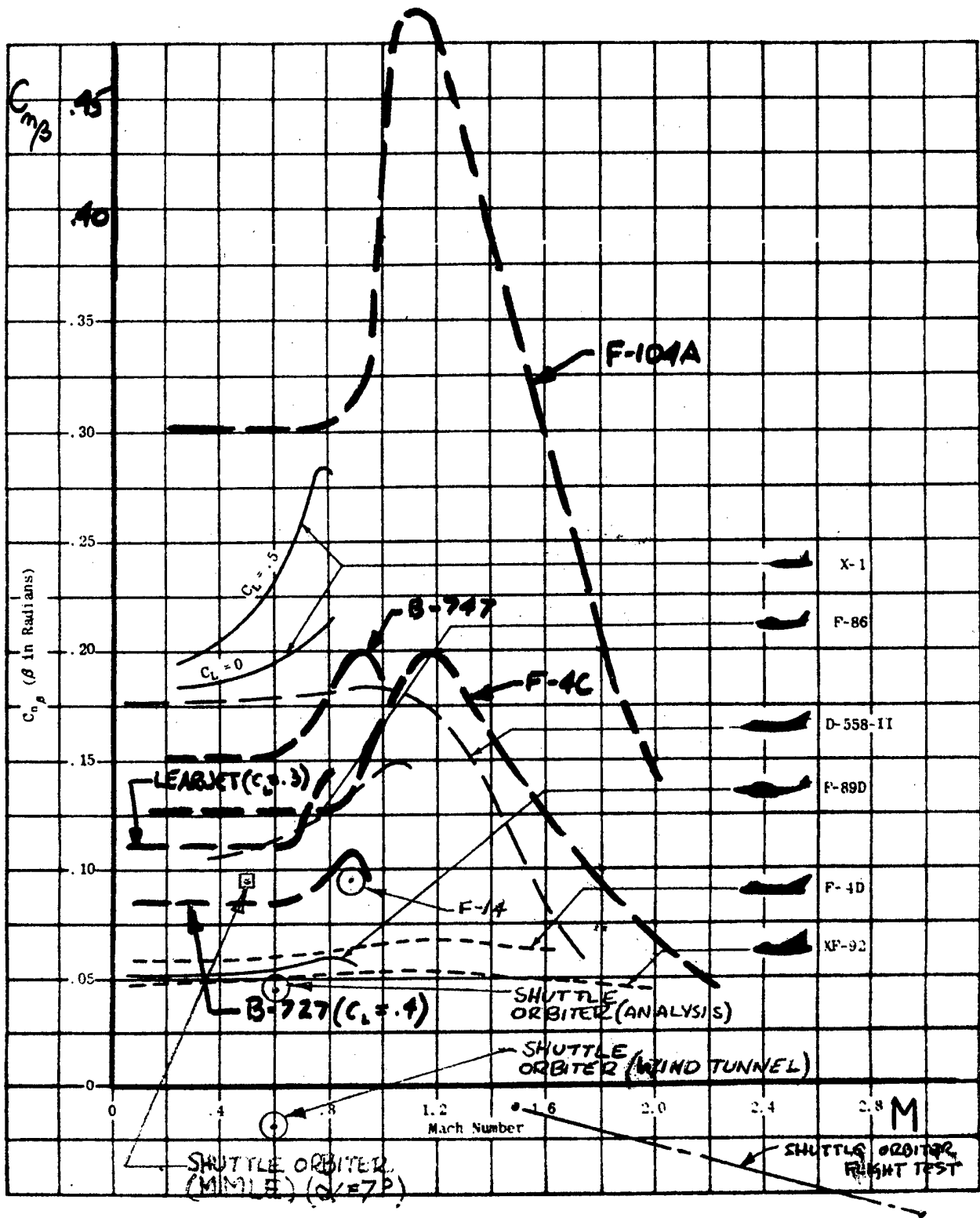


Figure 30: Variations of $C_{n\beta}$ with Mach

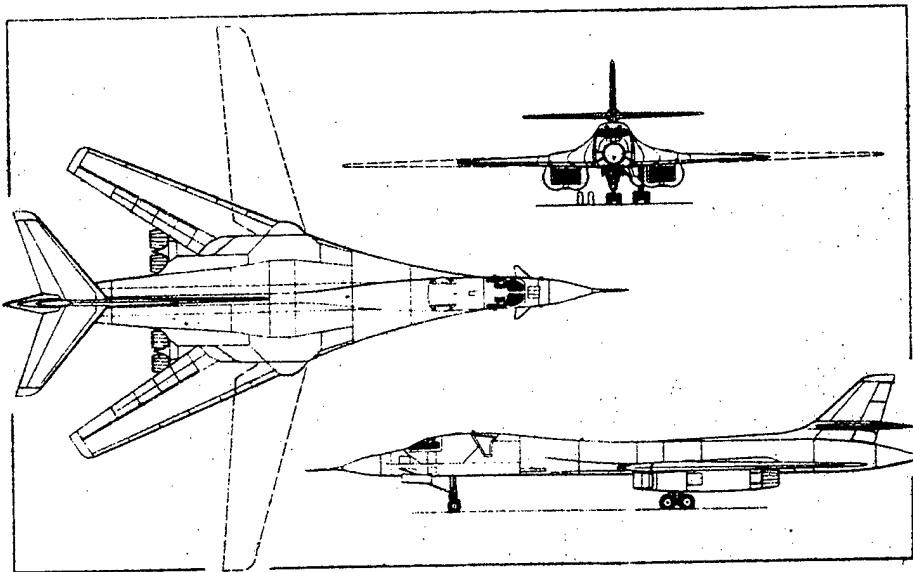
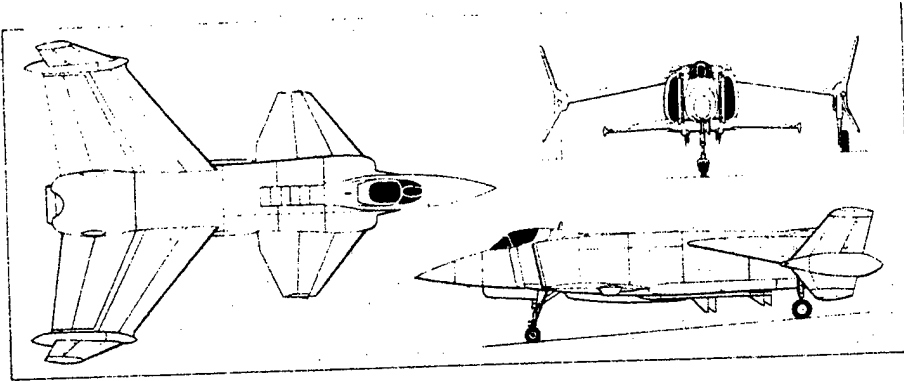
Number for Several Aircraft^{74,87,88,100,142,153}

The calculation of this effect involves unsteady flow. The sidewash at the tail has been shown to be affected by the wing. Since this is part of the vertical tail's angle of attack, the sidewash experienced by the tail is that which was shed earlier by the wing. Therefore, when the sideslip angle is changing, side force, rolling moment, and yawing moment have not caught up to their eventual steady state values and they are something less. This is often referred to as the lag of sidewash effect and it is analogous to the lag of downwash effect. Since the type of motion under consideration is an acceleration, $\dot{\beta}$ effects can also arise from aeroelastic or "dead weight" effects.⁶⁵ Reference 72 presents methods for calculating the $\dot{\beta}$ derivatives.

$C_{Y_{\dot{\beta}}}$ is the change in side force with variations in rate of change of sideslip angle. Lateral acceleration has essentially a negligible effect on side force.⁹⁴ This derivative is usually ignored in analytical work.^{65,94,74}

$C_{l_{\dot{\beta}}}$ is the change in rolling moment coefficient with variations in rate of change of sideslip angle. Changes in side force due to lateral acceleration have a negligible effect on rolling moment.⁹⁴ This derivative is usually ignored in analytical work.^{94,65,74}

$C_{n_{\dot{\beta}}}$ is the change in yawing moment coefficient with variations in rate of change of sideslip angle. Even though only a small side force change occurs due to lateral acceleration, it has a substantial moment arm precluding its neglect when considering yawing moments.⁹⁴ Although the derivative $C_{n_{\dot{\beta}}}$ is known to exist, very little can be stated about its magnitude or sign because of the wide variations in opinion and in interpretation of experimental data concerning it.⁶⁵ Some authors ignore its effect.⁷⁴ For most aircraft configurations it is apparently of rather small magnitude and probably can be neglected.⁶⁵ There are insufficient data to determine for which configurations it is important.⁶⁵



CHANGE IN SIDE FORCE WITH ROLLING VELOCITY, C_{Y_p}

This derivative is caused mainly by the vertical tail, although for some aircraft configurations there is also an appreciable contribution from the wing. A side force is created on the vertical tail when the aircraft rolls about its x-axis. C_{Y_p} would appear to be negative in sign for a vertical tail located above the aircraft x-axis; however, it can be either negative or positive depending on tail geometry and sidewash effects from the wing. It is also a strong function of trim lift coefficient or trim angle of attack.⁶⁵

Since C_{Y_p} is of very little importance in lateral-directional dynamics it is common practice to neglect it.^{65,74,86,94,95}

Reference 74 gives the approximate transonic variation of C_{Y_p} as from -0.3 to 0.8. Figure 31 shows typical C_{Y_p} variations with Mach number. The strong influence of trim lift coefficient is shown by these data.



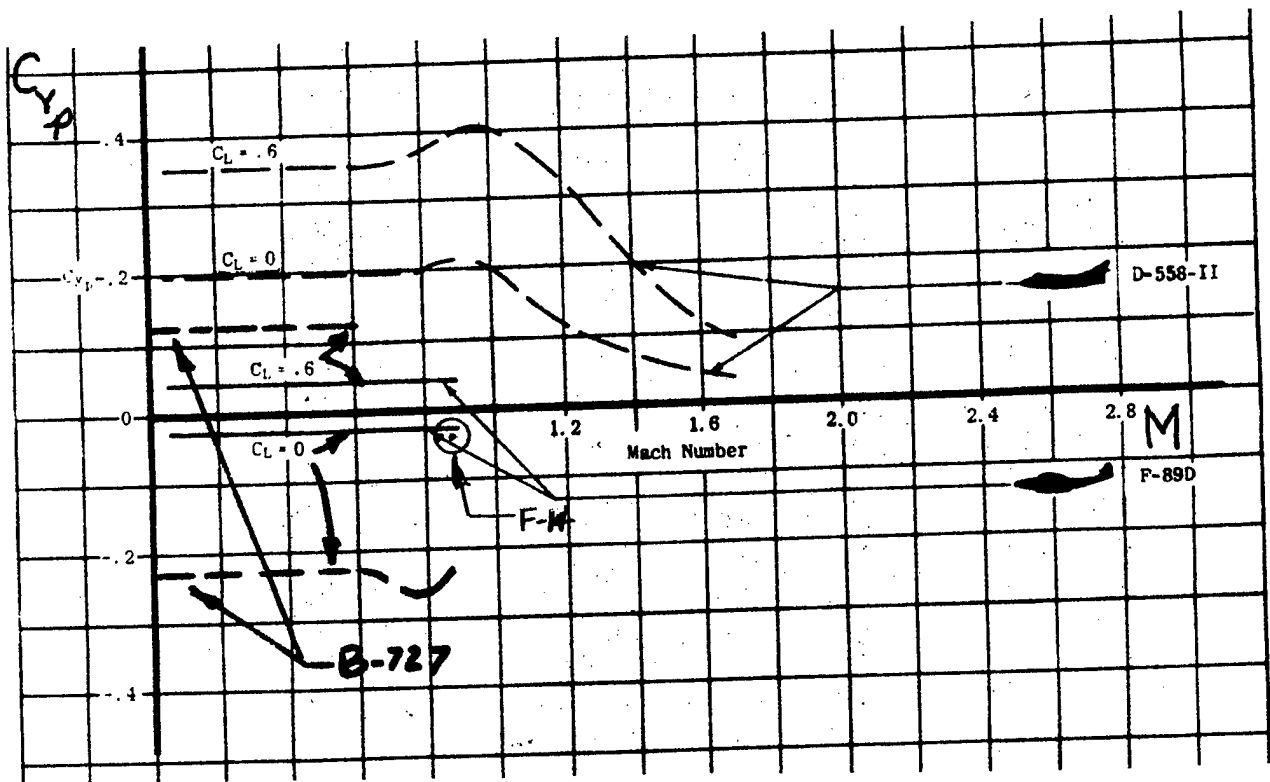
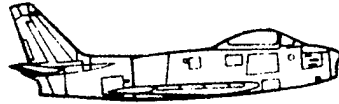


Figure 31: Variations of C_{Y_P} with Mach Number
for Several Aircraft^{74,88,100}

ROLL DAMPING, C_{ℓ_p}

This derivative is the change in rolling moment coefficient with change in rolling velocity. When an aircraft rolls with an angular velocity a rolling moment is produced which opposes the rotation. The wing is the major contributor to C_{ℓ_p} unless the horizontal and vertical tails are unusually large.⁶⁵

This derivative C_{ℓ_p} is quite important in lateral-directional dynamics since it alone determines the damping in the roll axis.⁶⁵ Decreasing C_{ℓ_p} increases spiral stability.⁶⁴ Normally, small negative values of C_{ℓ_p} are desirable because aileron response will be better and the aircraft will have less gust sensitivity.⁶⁵

C_{ℓ_p} will remain negative as long as the local angle of attack is below stall. If the downgoing wing angle of attack exceeds the stalling angle, the local lift curve slope may fall to zero or even reverse its sign. In this case C_{ℓ_p} may be zero or become positive. This is the situation when a wing autorotates, as in spinning.⁸⁶

Reference 74 gives the approximate transonic variation of C_{ℓ_p} as from -0.1 to -0.8. Figure 32 shows typical C_{ℓ_p} variations with Mach number.

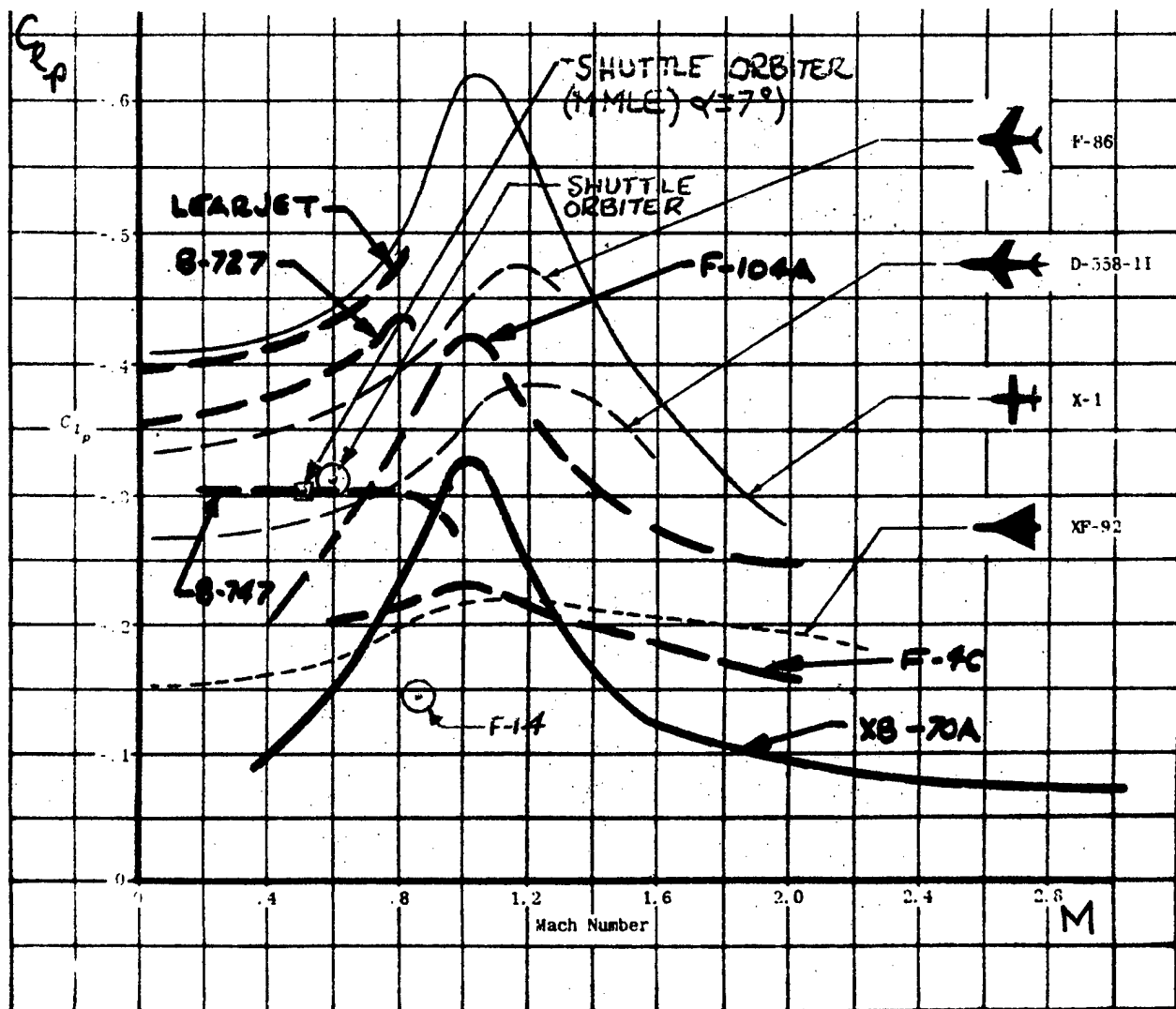


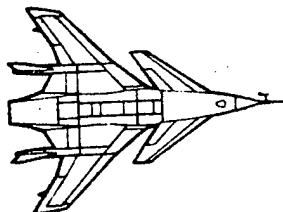
Figure 32: Variations of C_L with Mach Number
for Several Aircraft^{74,87,88,100,142}

CHANGE IN YAW MOMENT COEFFICIENT WITH ROLLING VELOCITY, C_{n_p}

This cross derivative arises from two sources: the wing and the vertical tail. A negative (adverse) yawing moment is developed on the aircraft because of the unsymmetrical lift distribution which causes a difference between the drag on the right and left wings when the aircraft is rolling. The vertical tail contribution can be either positive or negative depending on tail geometry, wing sidewash, and equilibrium lift coefficient or trim angle of attack.⁶⁵

The derivative C_{n_p} is fairly important in lateral-directional dynamics even though it dropped out of the simplified Dutch roll damping equation derived here at the School. It is usually negative in sign, and for most aircraft configurations, the larger its negative value, the greater the reduction in Dutch roll damping. Therefore, positive values of C_{n_p} are desired. For the aircraft alone, this derivative is not usually important; however, it has a strong influence on autopilot design.⁶⁵

Reference 74 gives the approximate transonic variation of C_{n_p} as from -0.5 to 0.1. Figure 33 shows typical C_{n_p} variations with Mach number. These data show the strong dependence of the value and sign of this derivative on trim lift coefficient or trim angle of attack.



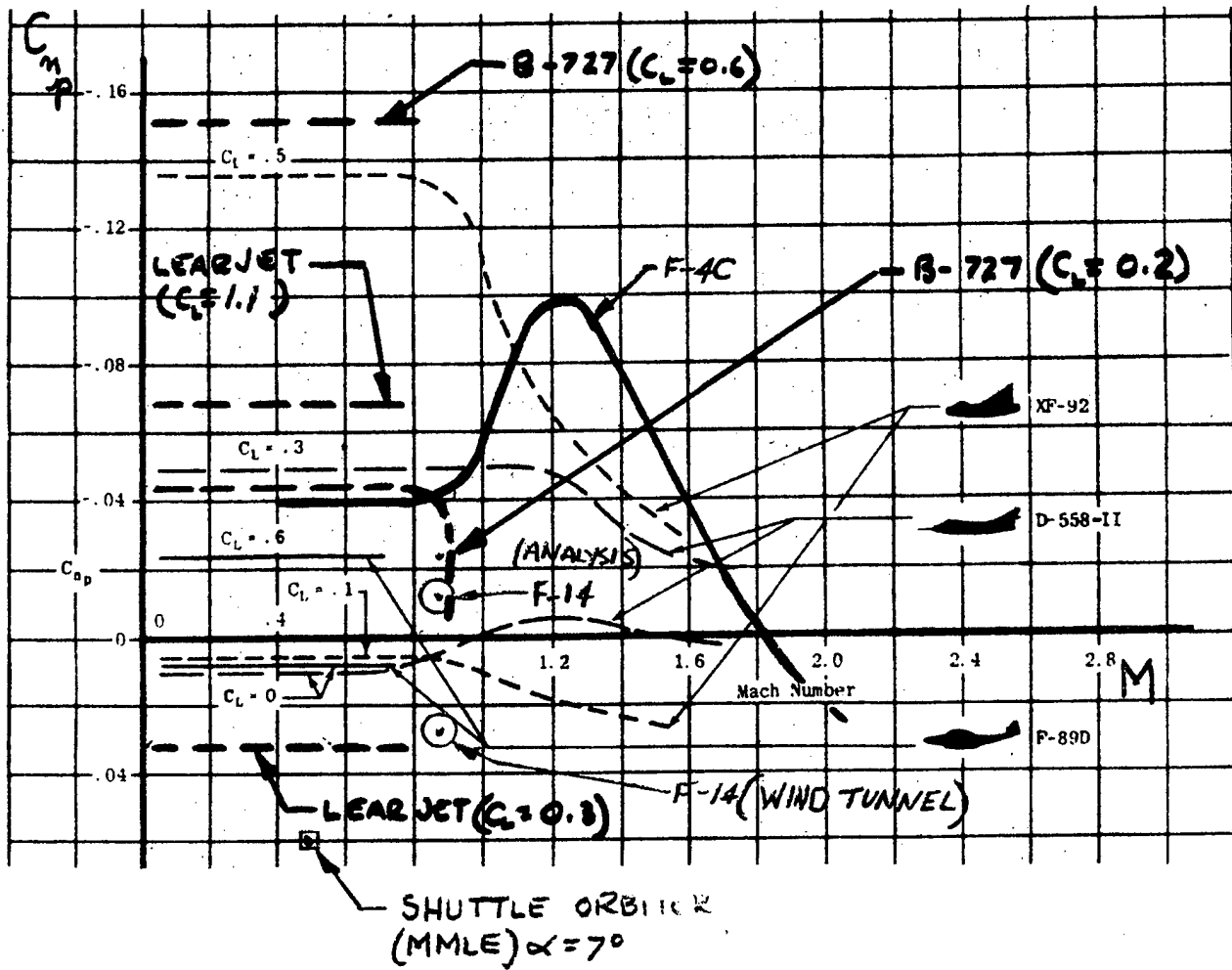
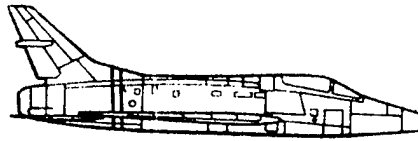


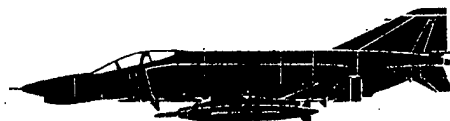
Figure 33: Variations of C_{np} with Mach Number
for Several Aircraft^{74,87,88,100,142}

CHANGE IN SIDE FORCE COEFFICIENT WITH YAW VELOCITY, C_{Y_r}

This derivative is caused mainly by the vertical tail which is mounted some distance behind the aircraft center of gravity. Whenever the aircraft is rotating at a yaw rate there is an effective side force developed on the tail. C_{Y_r} will be positive and quite small.⁶⁵

C_{Y_r} is of little importance in lateral-directional dynamics and it is common practice to neglect it.^{65,74,86,94,95}

Reference 74 gives the approximate transonic variation of C_{Y_r} as from zero to 1.2. Figure 34 shows typical C_{Y_r} variations with Mach number.



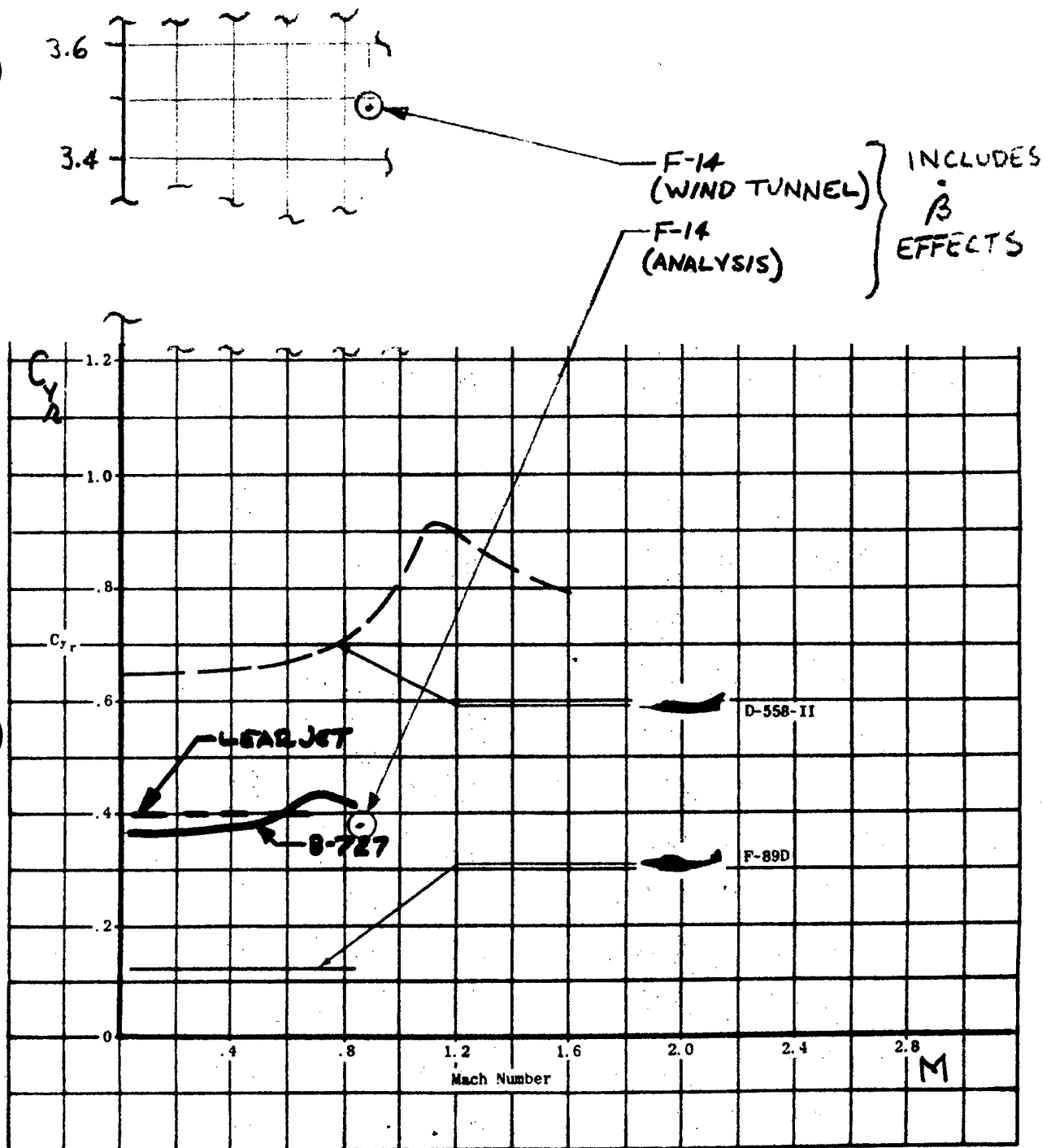


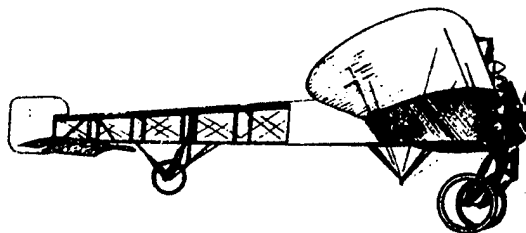
Figure 34: Variation of C_{Y_r} with Mach Number
for Several Aircraft. 74,88,100

CHANGE IN ROLLING MOMENT COEFFICIENT WITH YAW VELOCITY, C_{ℓ_r}

This cross derivative arises from a yaw rate about the vertical axis. For a positive yaw rate, the left wing moves faster than the right producing more lift on the left wing and consequently a positive rolling moment. In addition to the major wing contribution, the vertical tail will contribute to C_{ℓ_r} . The tail's contribution will be positive or negative depending on the vertical tail geometry and whether it is above or below the x-axis. C_{ℓ_r} is usually positive and it is a function of equilibrium lift coefficient or trim angle of attack.⁶⁵

The derivative C_{ℓ_r} is of secondary importance in lateral-directional dynamics.⁶⁵ It does effect the Dutch roll mode slightly even though it dropped out of the simplified Dutch roll damping equation derived here at the School.⁶⁵ Its effect is largest at low speed and it has considerable effect in the spiral mode. C_{ℓ_r} should be as positive and as small as possible for increasing spiral damping.⁶⁵

Reference 74 gives the approximate transonic variation of C_{ℓ_r} as from zero to 0.6. Figure 35 shows typical C_{ℓ_r} variations with Mach number. These data show the strong dependence of the value of this derivative on equilibrium lift coefficient or trim angle of attack.



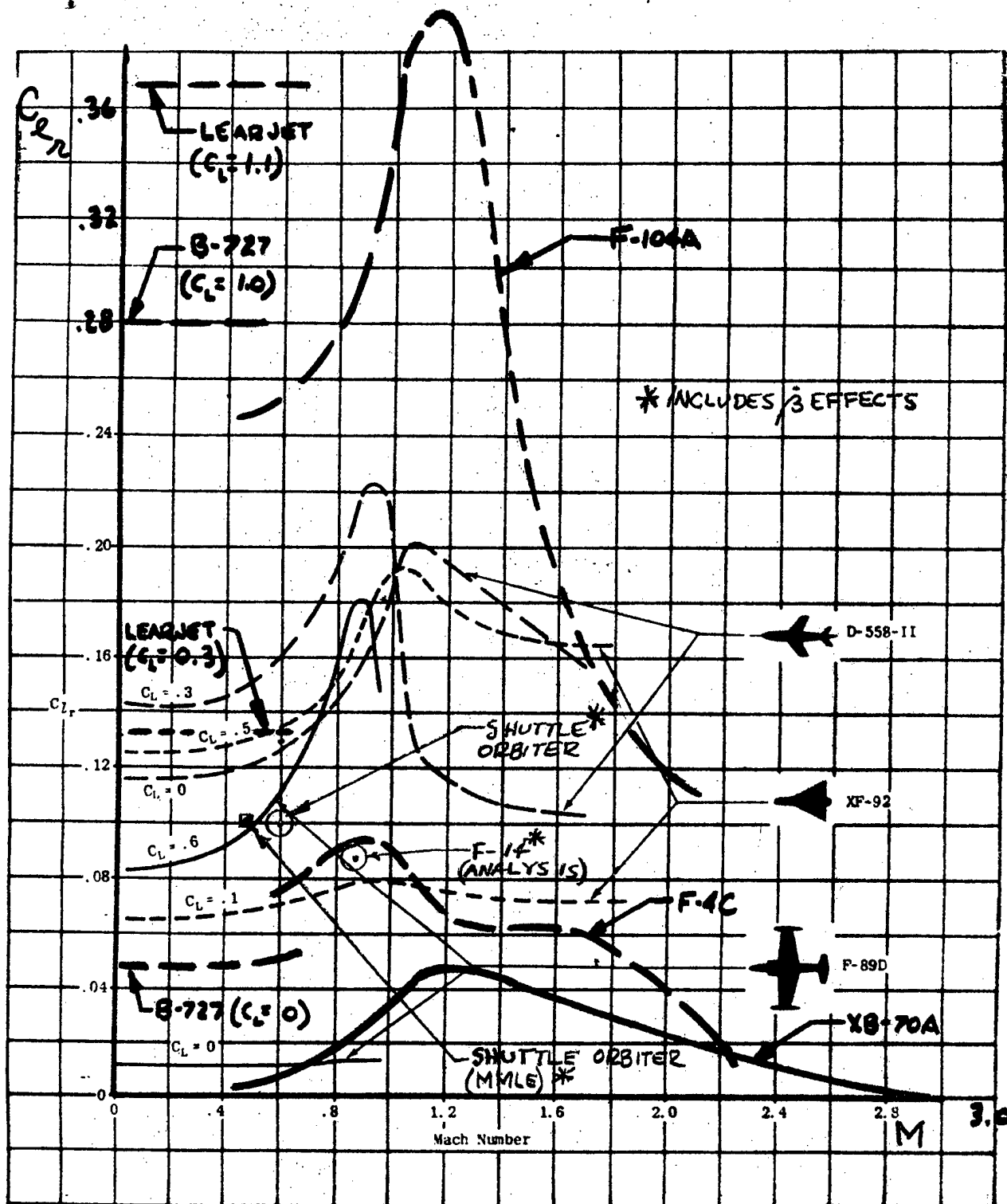


Figure 35: Variation of C_L with Mach Number

for Several Aircraft. 74, 37, 88, 100, 142

YAW DAMPING, C_{n_r}

This derivative is the change in yawing moment coefficient with yawing velocity. When an aircraft yaws, an aerodynamic moment is produced which opposes the rotation. C_{n_r} has contributions from the wing, fuselage, and vertical tail, all of which are negative in sign. The vertical tail is by far the largest contributor.⁶⁵

The derivative C_{n_r} is very important in lateral-directional dynamics because it is the main contributor to the damping of the Dutch roll mode. It is also important to the spiral mode. For each mode, large negative values of C_{n_r} are desired for good damping. This derivative is a function of equilibrium lift coefficient or trim angle of attack. In the past, a vertical tail which produced a reasonable value of C_{n_β} was almost certain to give adequate Dutch roll damping. For some current designs, with higher wing loadings and higher radii of gyration in yaw, during high altitude flight the vertical tail alone may not provide sufficient C_{n_r} for damping the Dutch roll. This problem has led to the extensive use of yaw dampers on modern aircraft.⁶⁵

Reference 74 gives the approximate transonic variation of C_{n_r} as from zero to -1.0. Figure 36 shows typical C_{n_r} variations with Mach number. Although the value of C_{n_r} is rather large for the D-558-II, this aircraft exhibits poor Dutch roll damping; this emphasizes the fact that Dutch roll damping cannot be predicted by examining this derivative alone.⁸⁸

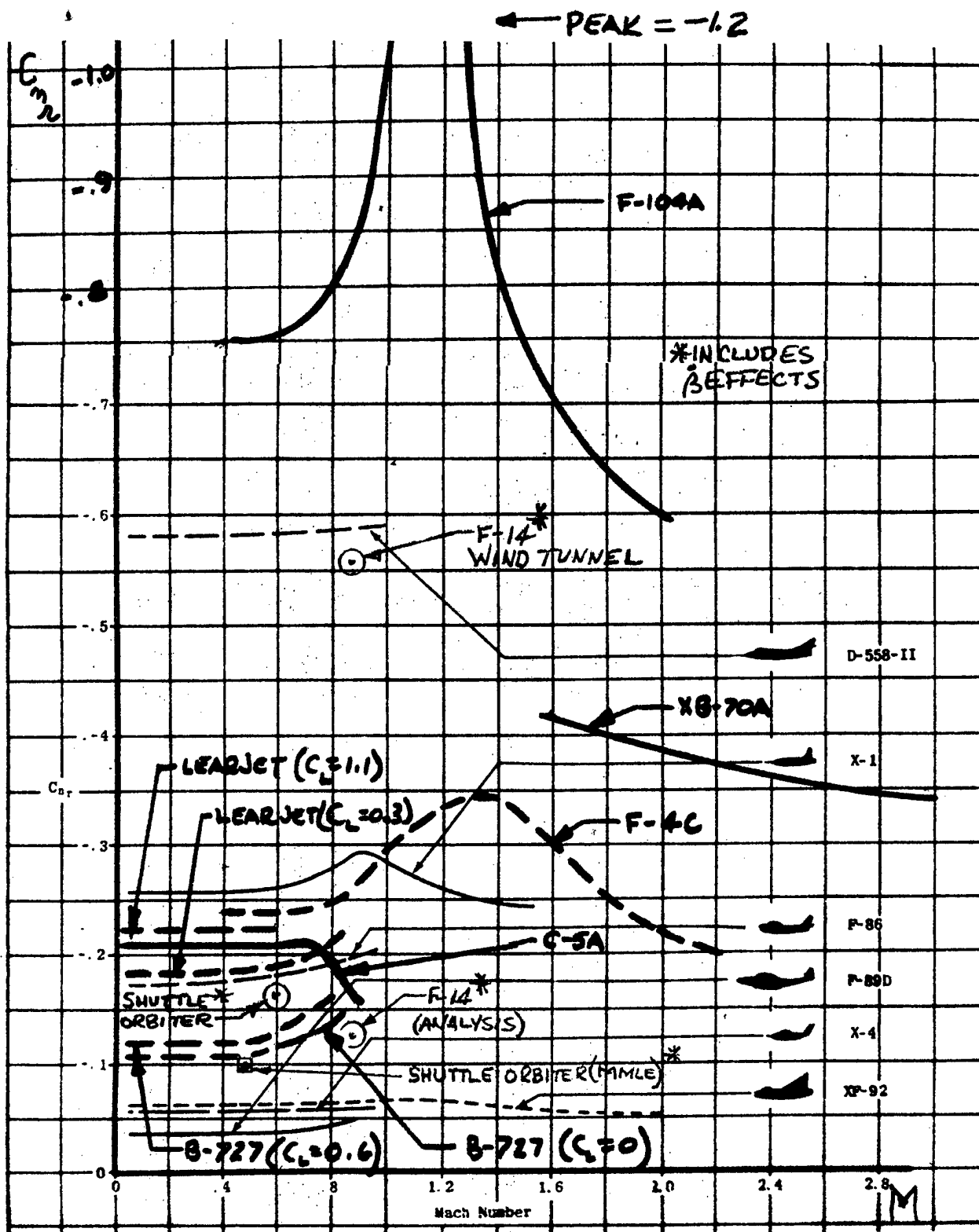


Figure 36: Variation of C_{n_r} with Mach Number
for Several Aircraft.^{74,87,88,100,142}

CHANGE IN SIDE FORCE COEFFICIENT WITH AILERON DEFLECTION, $C_{Y_{\delta a}}$

This control derivative is zero or negligibly small for most conventional aircraft configurations, but may have a value for highly swept wings of low aspect ratio.⁶⁵ When lateral control devices are located near vertical surfaces, this derivative may also have a value other than zero e.g. for a "rolling tail" such as the F-111.⁷⁴ The flight test value of $C_{Y_{\delta a}}$ for the shuttle orbiter was about -0.18 per radian at an angle of attack of about seven degrees and a Mach number of about 0.50.¹⁴²

ADVERSE (OR PROVERSE) YAW, $C_{n_{\delta a}}$

This cross (control) derivative is the change in yawing moment coefficient with change in aileron or spoiler deflection. When ailerons or spoilers are deflected, both induced and profile drag on the wing change. This derivative is due to the difference in drag between upgoing and downgoing wing. For ailerons, $C_{n_{\delta a}}$ is usually negative (adverse) causing the aircraft to yaw in a direction opposite to the desired turn direction. Adverse yaw can sometimes be eliminated by aileron rigging e.g. deflecting ailerons up a different amount than down. For spoilers, $C_{n_{\delta a}}$ is usually positive (complimentary or proverse) causing the aircraft to yaw in the desired turn direction.

Reference 74 gives the approximate transonic variation of $C_{n_{\delta a}}$ as from -0.08 to 0.08. Figure 37 shows typical $C_{n_{\delta a}}$ variations with Mach number. These data show the strong dependence of the value and sign of this derivative on equilibrium lift coefficient or trim angle of attack.

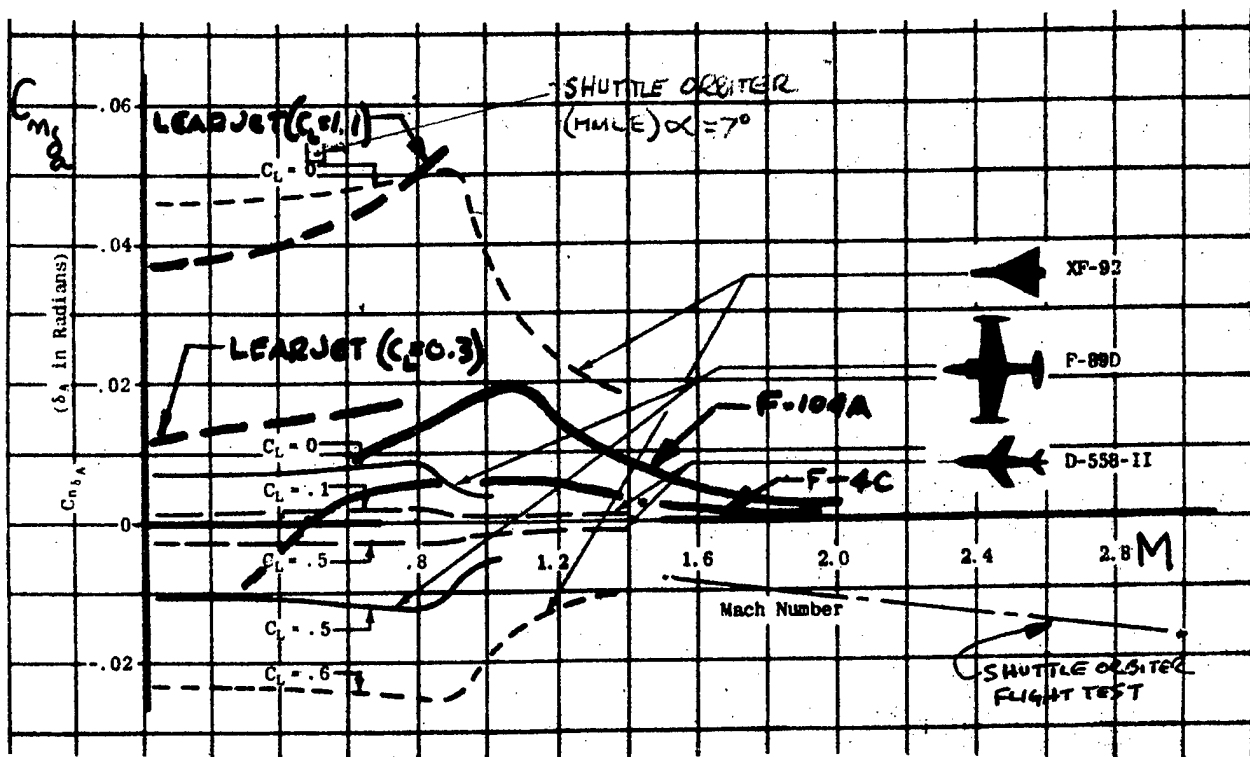
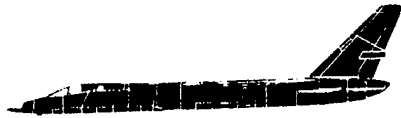


Figure 37: Variation of $C_{n_{\delta_a}}$ with Mach Number

for Several Aircraft. 74,87,88,142,158

ROLL (LATERAL) CONTROL POWER, $C_{l_{\delta a}}$

This control derivative is the change in rolling moment coefficient with change in aileron or spoiler deflection. It is positive by definition.

For lateral-directional dynamics, $C_{l_{\delta a}}$ is the most important control derivative. Roll power, in conjunction with roll damping, C_{l_p} , establishes the maximum rate of roll of an aircraft. Adequate $C_{l_{\delta a}}$ is required for rapid maneuvering at high speed and for counteracting asymmetric gusts at low speeds.⁶⁵

Reference 74 gives the approximate transonic variation of $C_{l_{\delta a}}$ as from zero to 0.4. Figure 38 shows typical $C_{l_{\delta a}}$ variations with Mach number.



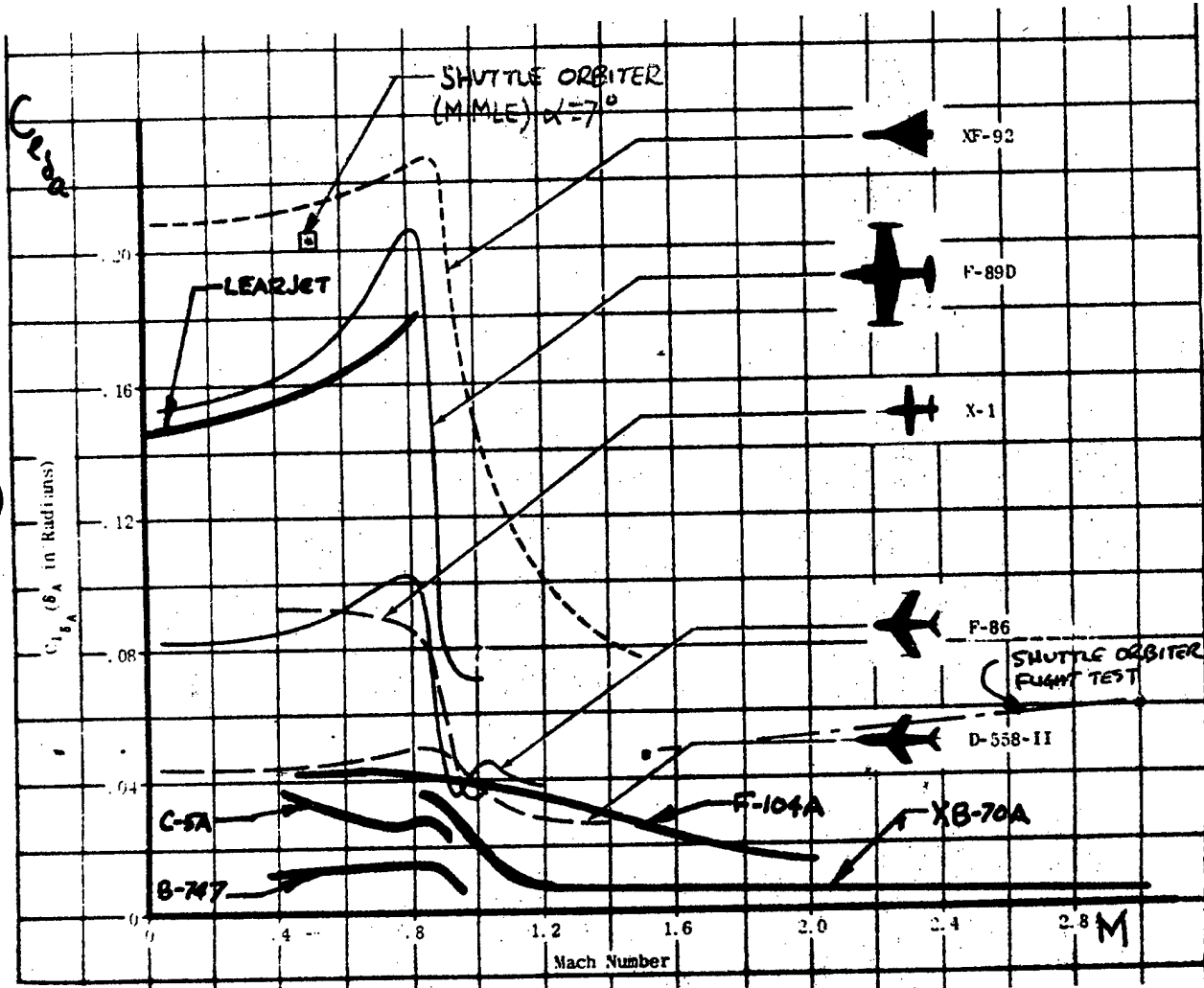
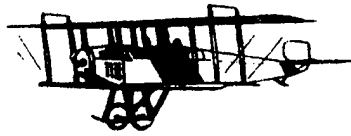


Figure 38: Variation of $C_{l_{\delta_a}}$ with Mach Number

for Several Aircraft. ^{74,87,88,142,158}

CHANGE IN SIDE FORCE COEFFICIENT WITH RUDDER DEFLECTION, $C_{Y_{\delta_r}}$

A positive rudder deflection gives a negative side force; therefore, this control derivative is negative using the School definition of right rudder being positive for tail-to-the-rear aircraft.

For the aircraft alone this derivative is considered to be unimportant in lateral-directional dynamics. It generally has to be considered for autopilot design.⁶⁵ The NT-33A aircraft develops wings-level lateral velocity using the rudder to generate side force.

Reference 74 gives the approximate transonic variation of $C_{Y_{\delta_r}}$ as from zero to -0.5. Figure 39 shows typical $C_{Y_{\delta_r}}$ variations with Mach number.



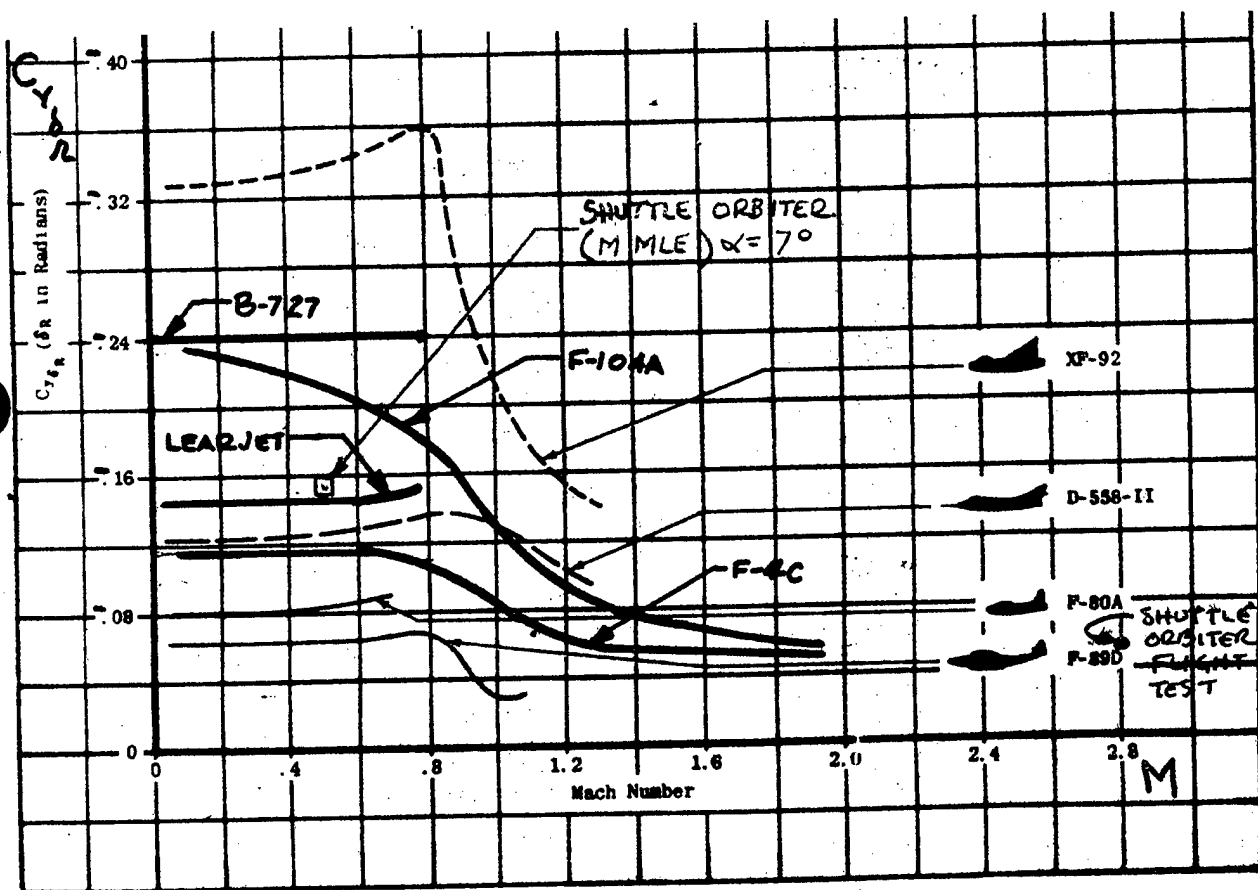
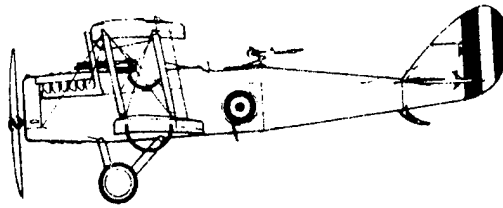


Figure 39: Variation of $C_{Y_{\delta_r}}$ with Mach Number

for Several Aircraft. 74, 87, 88, 142, 158

RUDDER POWER, $C_{n_{\delta_r}}$

This control derivative is the change in yawing moment coefficient with variation in rudder deflection. A positive rudder deflection gives a positive yawing moment; therefore, this derivative is positive using the School's sign convention.

The importance of rudder power in lateral-directional dynamics and flying qualities varies considerably with aircraft type. For fighter aircraft the rudder is usually sized by considering such requirements as counteracting torque (propeller), counteracting adverse yaw in rolls, directional control for crosswind takeoffs and landings, and control during spin recovery.⁶⁵ For multi-engined aircraft the rudder may be sized by asymmetric power considerations.

Reference 74 gives the approximate transonic variation of $C_{n_{\delta_r}}$ as from zero to 0.15. Figure 40 shows typical $C_{n_{\delta_r}}$ variations with Mach number.



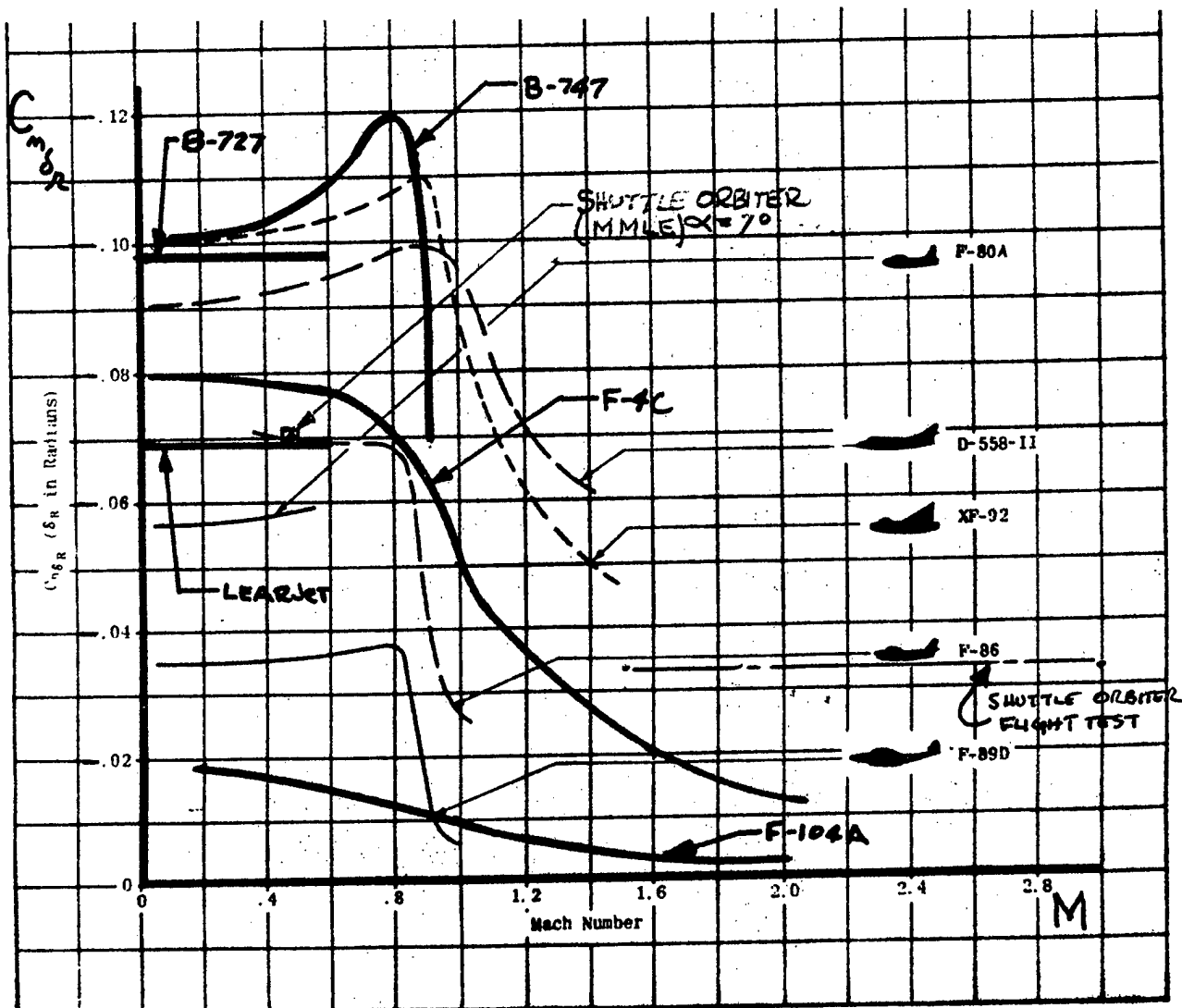


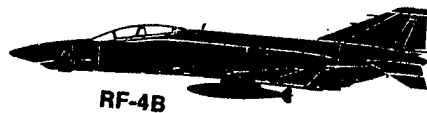
Figure 40: Variation of $C_{n\delta_r}$ with Mach Number
for Several Aircraft. 74,87,88,142,158

ROLL DUE TO RUDDER, $C_{l_{\delta_r}}$

This control derivative is the change in rolling moment coefficient with variation in rudder deflection. A rudder located above the x-axis creates a negative rolling moment for a positive deflection using the School's definition of right rudder being positive for tail-to-the-rear aircraft. $C_{l_{\delta_r}}$ is therefore usually negative in sign. It can be positive, depending on the aircraft configuration and equilibrium lift coefficient or trim angle of attack.

This derivative is considered only minor importance in the lateral-directional dynamics and flying qualities for conventional aircraft. It is sometimes neglected in analysis.⁶⁵

Reference 74 gives the approximate transonic variation of $C_{l_{\delta_r}}$ as from -0.04 to 0.04. Figure 41 shows typical $C_{l_{\delta_r}}$ variations with Mach number.



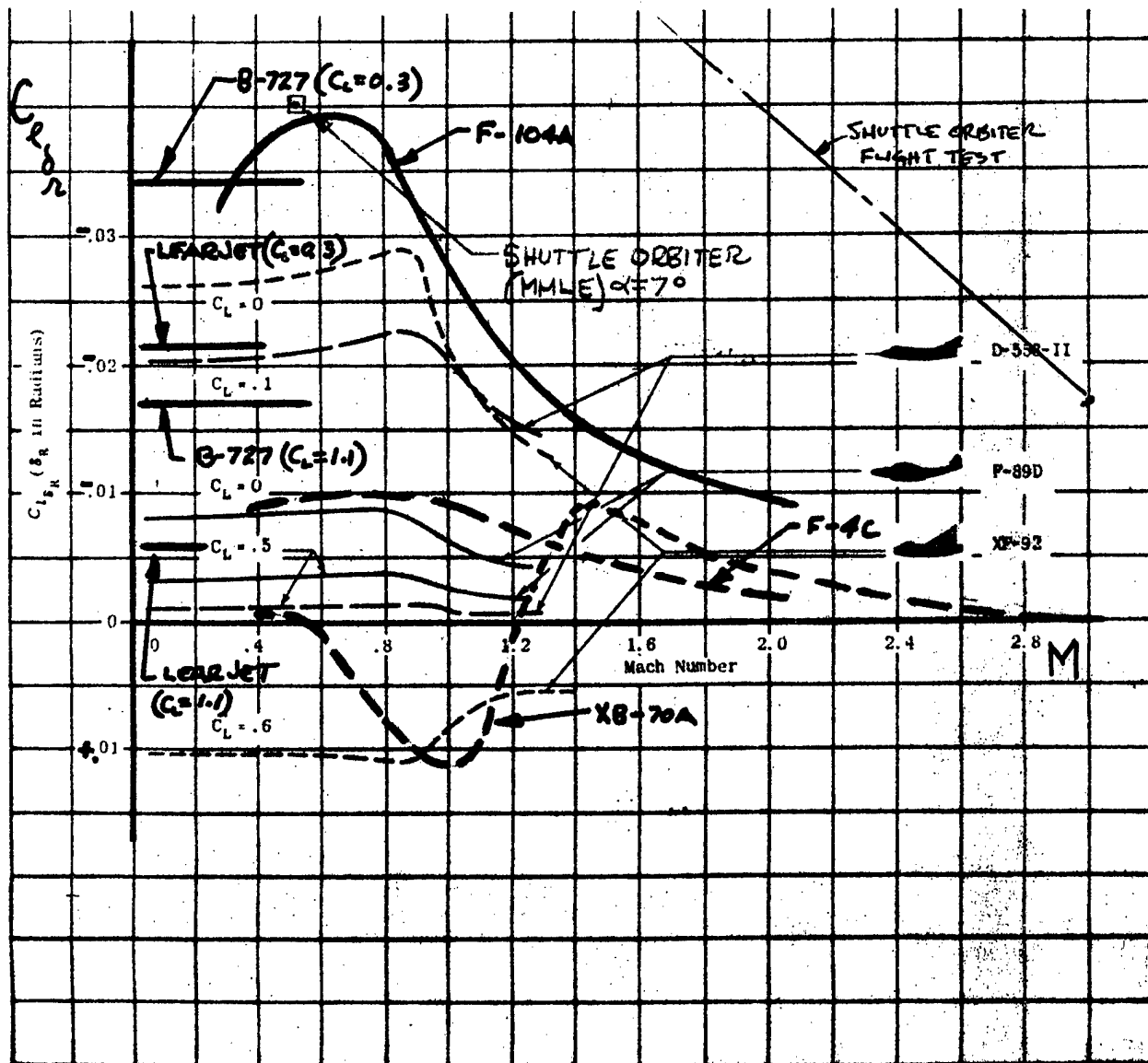


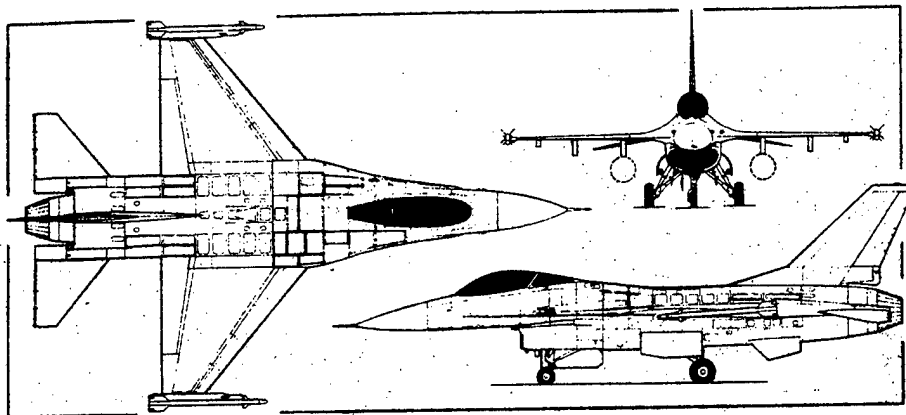
Figure 41: Variation of $C_{l_{\delta_r}}$ with Mach Number

for Several Aircraft. 74, 87, 88, 142, 158

EXAMPLE MMLE DETERMINED DERIVATIVES

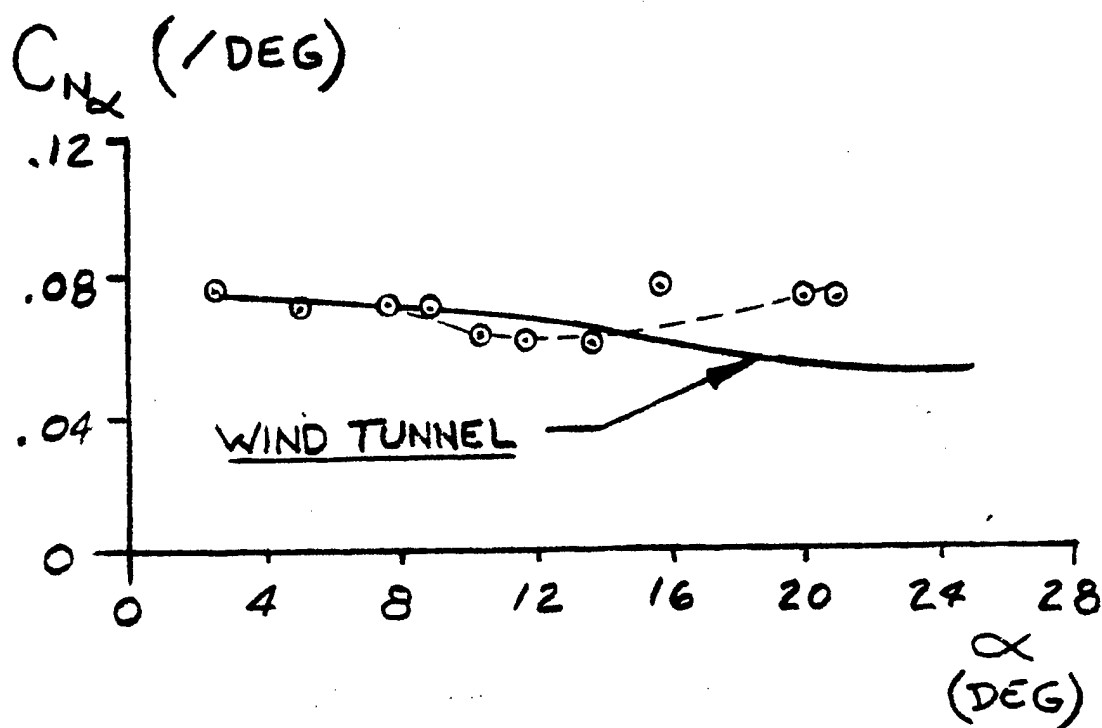
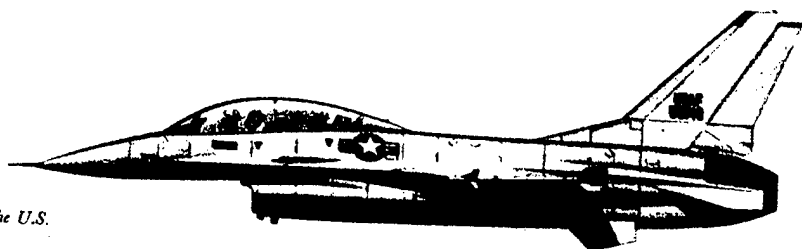
Figures 42 thru 72 present a complete set of YF-16 stability and control derivatives from Reference 92. These derivatives were extracted as functions of angle of attack and Mach number throughout most of the flight test envelope. Test maneuvers consisted of a matrix of pitch, rudder, and aileron doublets accomplished from 2 to 28 degrees angle of attack, and from 0.30 to 1.65 Mach number. Almost all doublets were performed at load factors less than three, where the aircraft could be trimmed for hands-off flight. Stability and control derivatives were extracted from the flight test doublets by using the AFFTC MMLE program.⁹²

The predicted wind tunnel derivative fairings were calculated by AFFTC engineers from rigid wind tunnel data and predicted dynamic pressure effects. The fairings through the flight test data were done at the USAF Test Pilot School. The accuracy and use of these derivatives will be discussed in Sections 5 and 6 of this chapter.



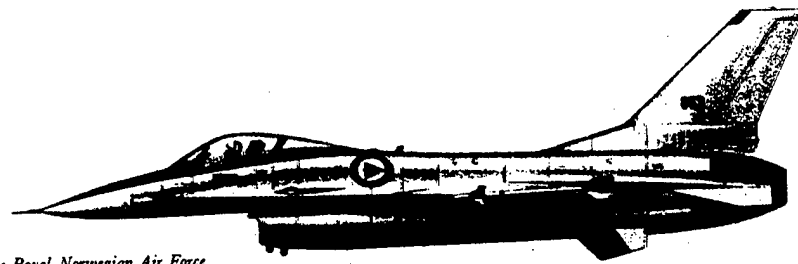
YF-16

F-16B for the U.S.

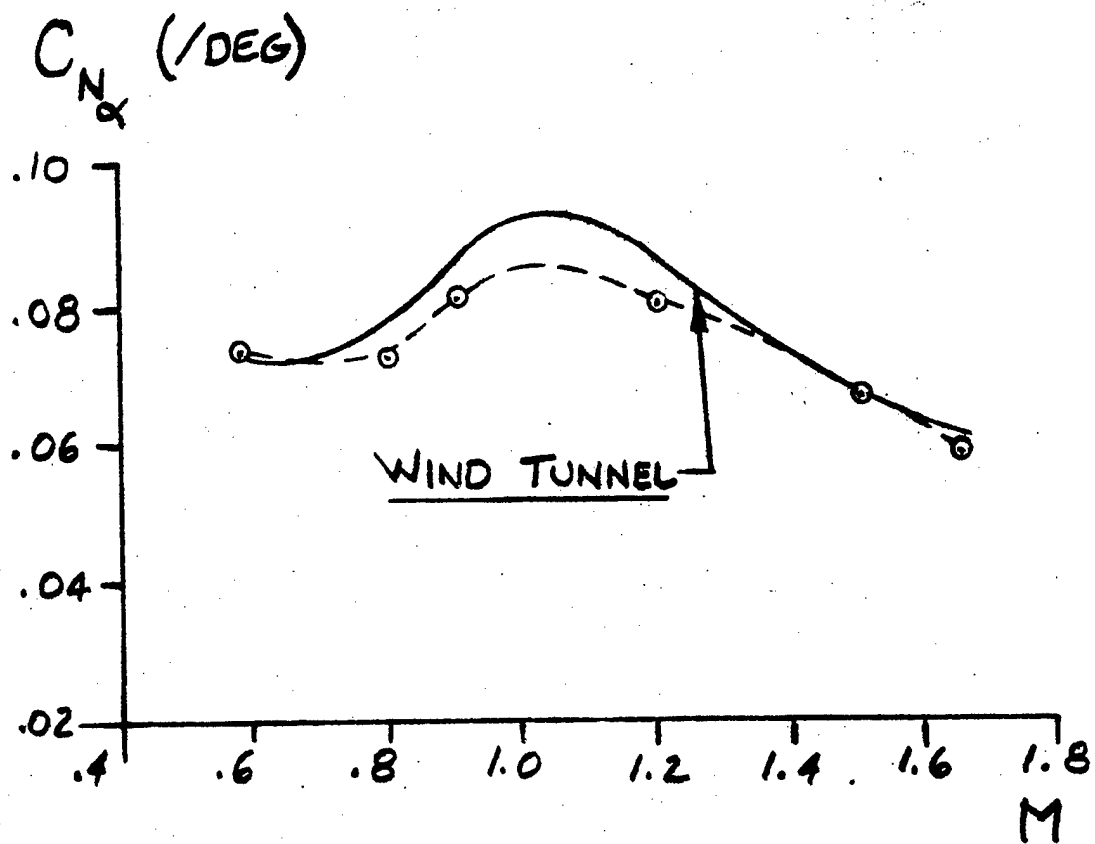


CR cg = 35% MAC M < 0.6 q = 50 - 200 lb/ft²

Figure 42: Flight Test Variation of C_{N_α} with Angle of Attack for the YF-16 Aircraft.⁹²

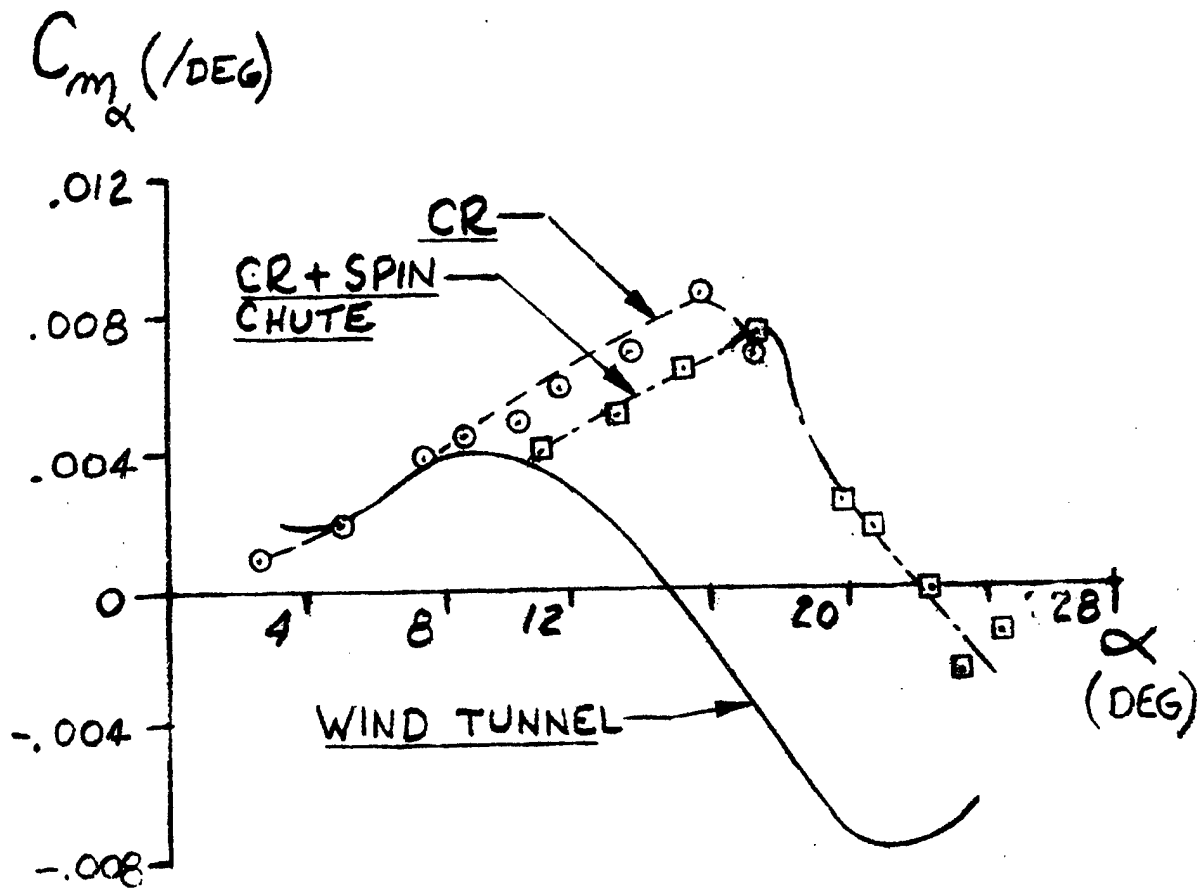


F-16 for the Royal Norwegian Air Force



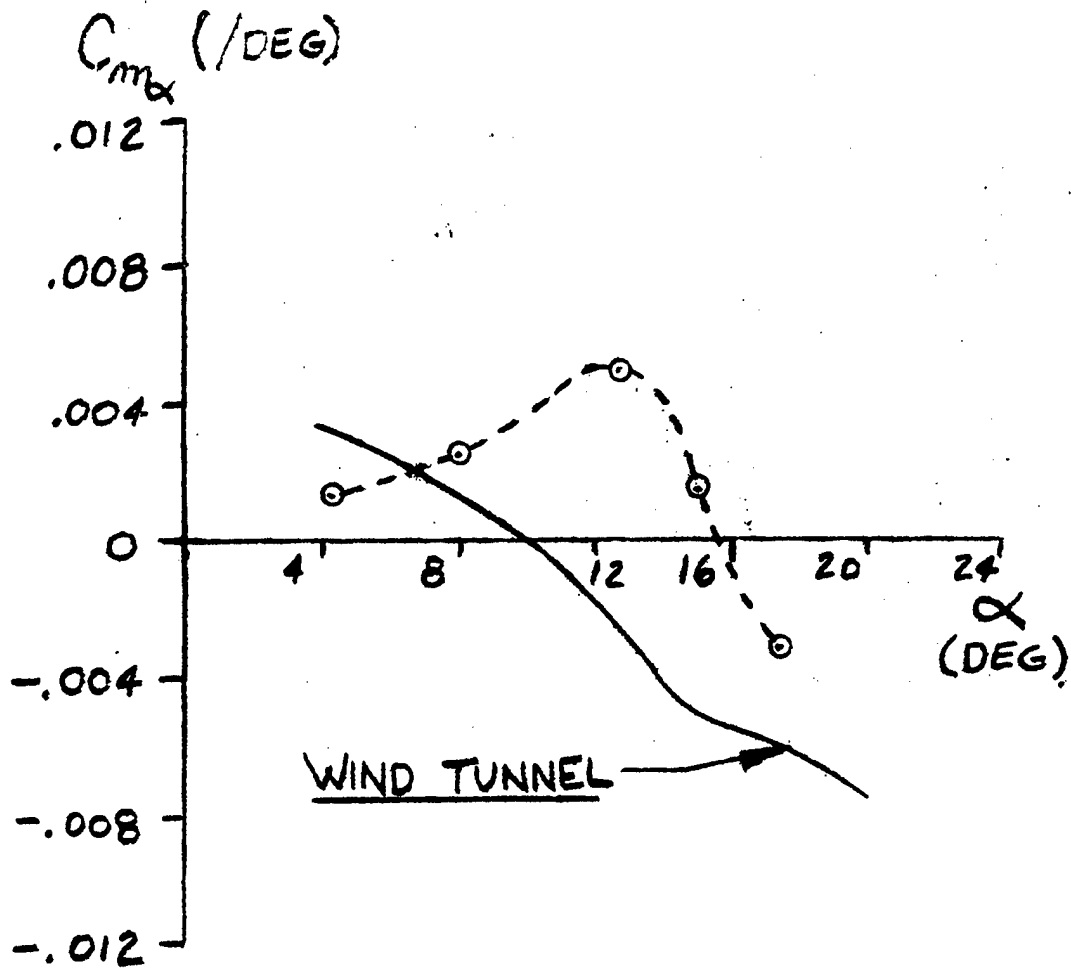
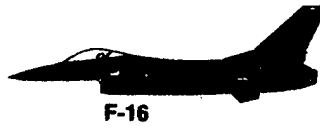
CR $c_g = 35\% \text{ MAC}$ $\alpha = 4^\circ$

Figure 43: Flight Test Variation of $C_{N_{\alpha}}$ with Mach Number for the YF-16 Aircraft.⁹²



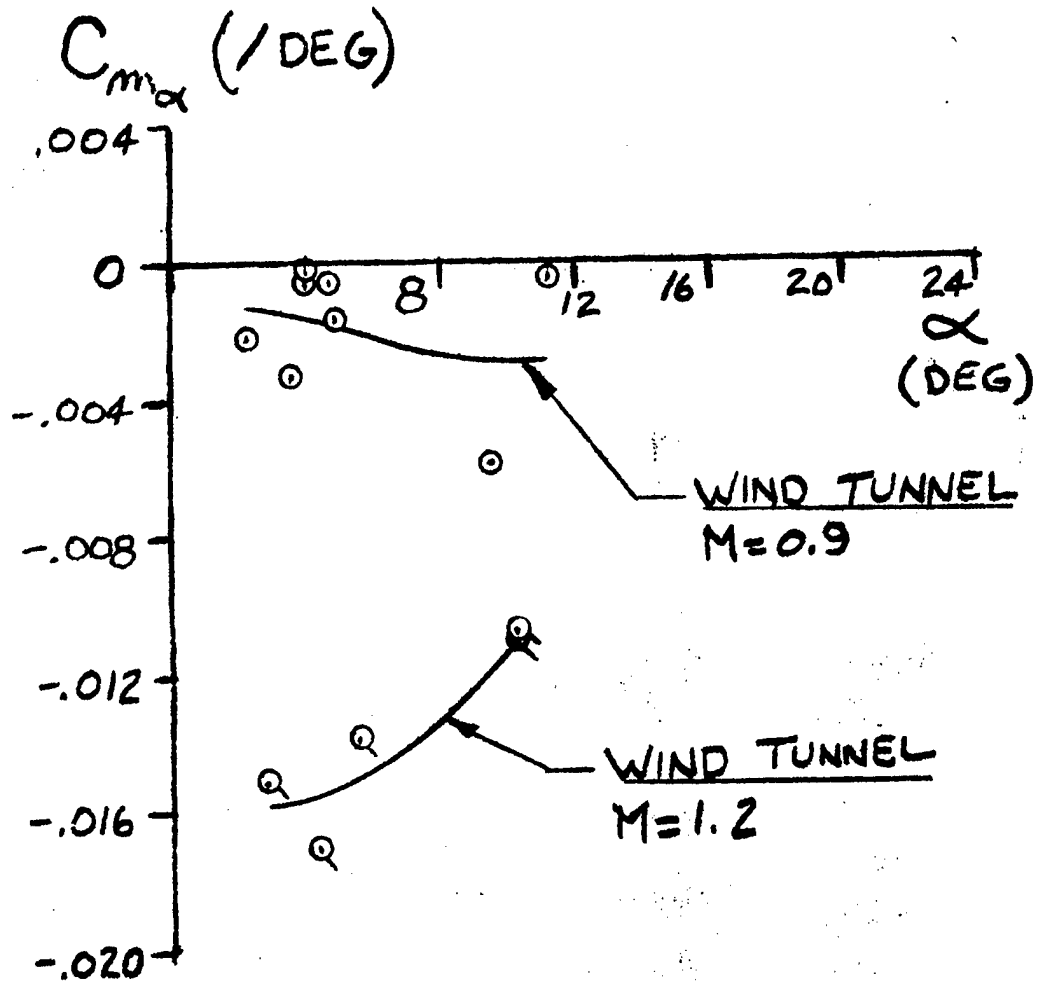
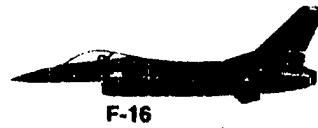
CR cg = 35% MAC M < 0.6 q = 50 - 200 lb/ft²

Figure 44: Flight Test Variation of C_{m_α} with Angle of Attack for the YF-16 Aircraft.⁹²



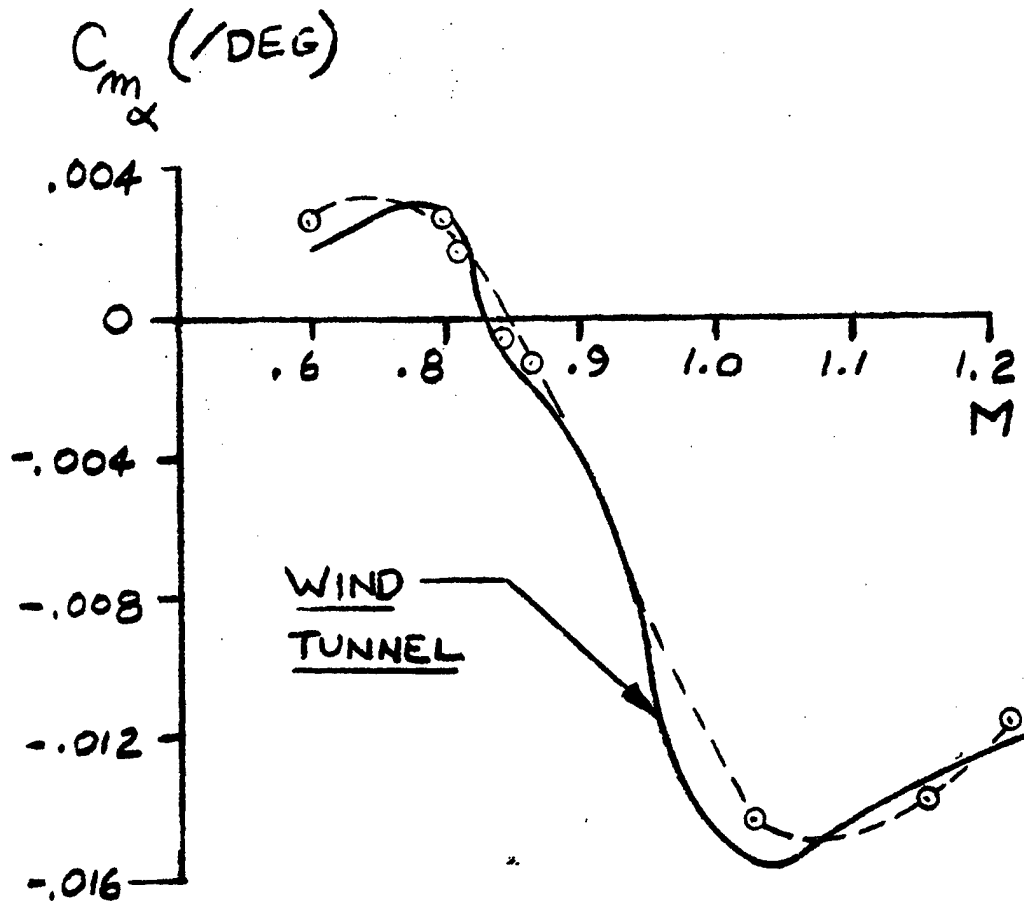
CR $c_g = 35\% \text{ MAC}$ $M = 0.8$ $q = 150 - 250 \text{ lb/ft}^2$

Figure 45: Flight Test Variation of $C_{m\alpha}$ with Angle of Attack for the YF-16 Aircraft.⁹²



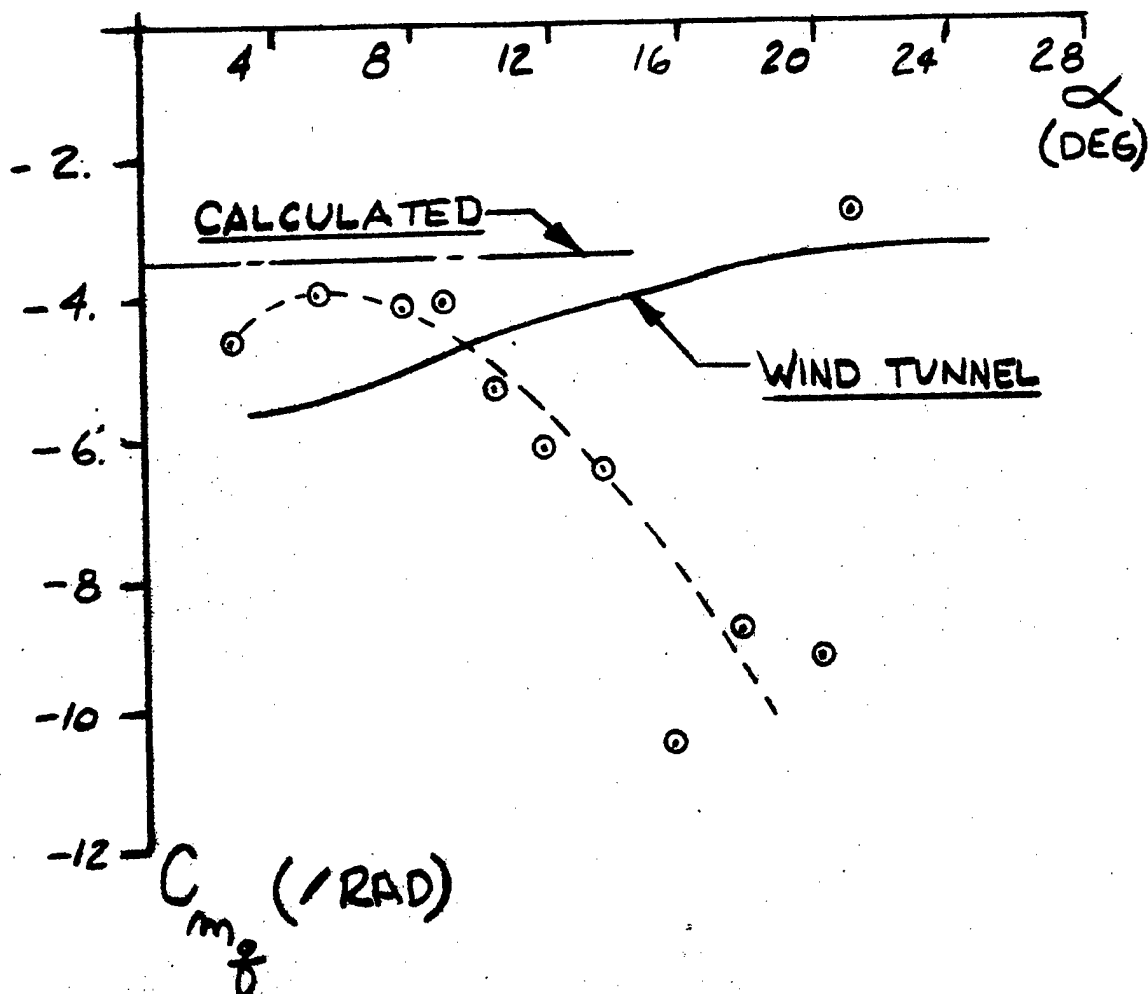
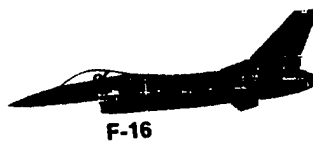
CR cg = 35% MAC M = 0.9, 1.2 q = 350 - 750 lb/ft²

Figure 46: Flight Test Variation of $C_{m\alpha}$ with Angle of Attack for the YF-16 Aircraft.⁹²



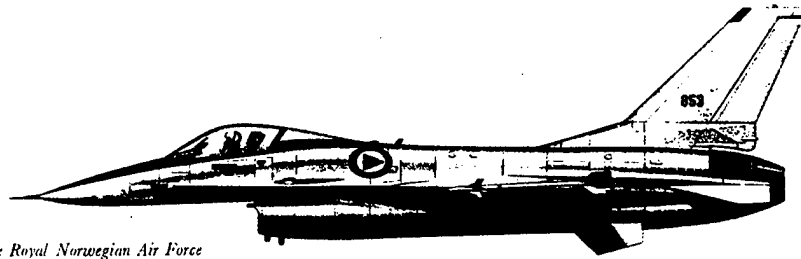
CR cg = 35% MAC $\alpha = 4^\circ$

Figure 47: Flight Test Variation of $C_{m_{\alpha}}$ with Mach Number for the YF-16 Aircraft.⁹²

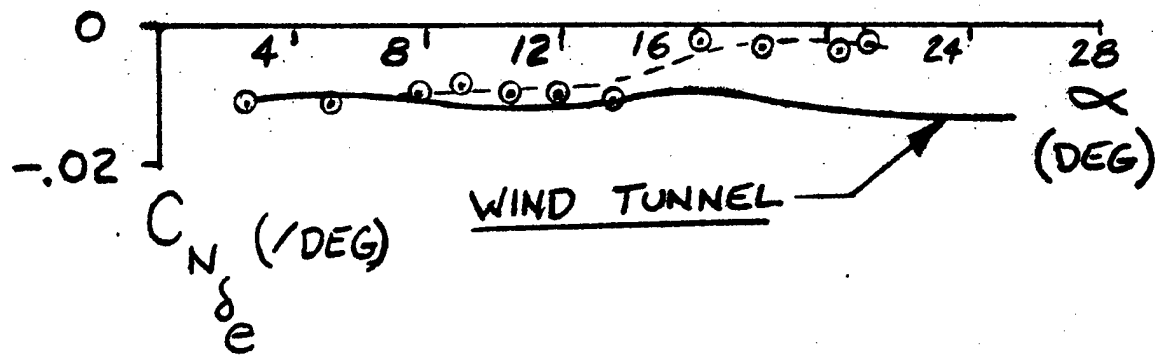


CR cg = 35% MAC $M < 0.6$ $q = 50 - 200 \text{ lb/ft}^2$

Figure 48: Flight Test Variation of C_{mq} with Angle of Attack for the YF-16 Aircraft.⁹²

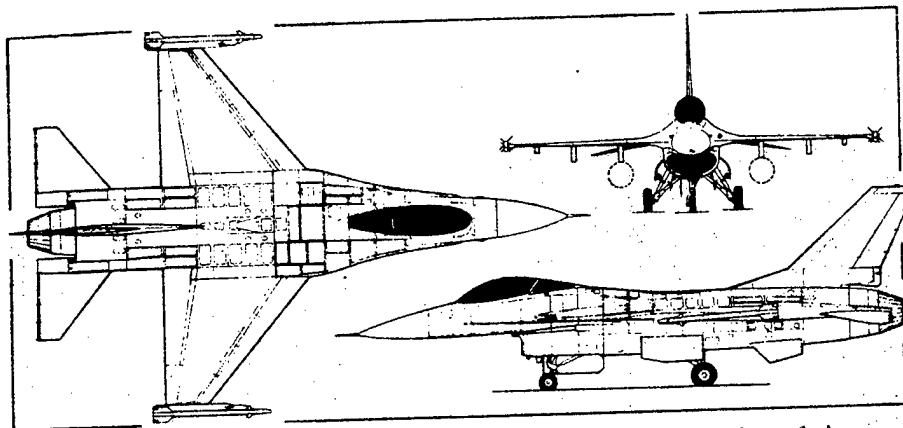


F-16 for the Royal Norwegian Air Force

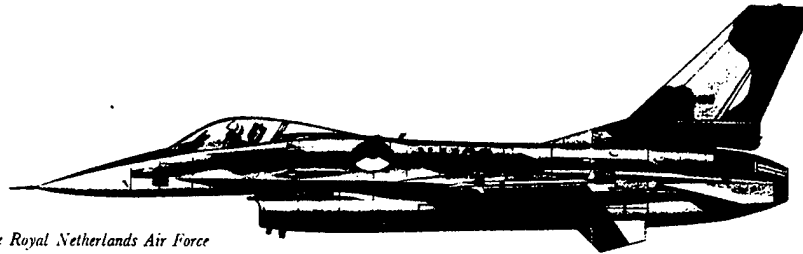


CR cg = 35% MAC $M < 0.6$ $q = 50 - 200 \text{ lb/ft}^2$

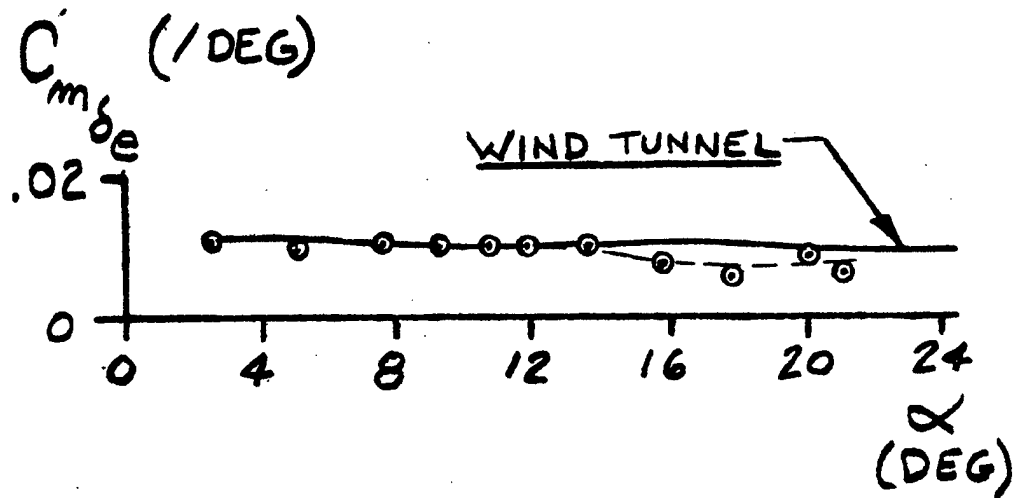
Figure 49: Flight Test Variation of $C_{N\delta_e}$ with Angle of Attack for the YF-16 Aircraft.⁹²



General Dynamics F-16A (Pratt & Whitney F100-PW-100(3) afterburning turbofan engine)

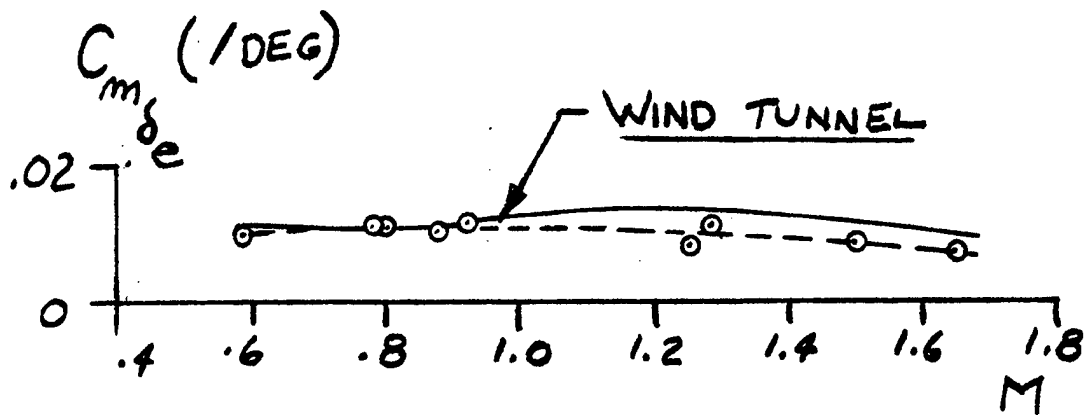
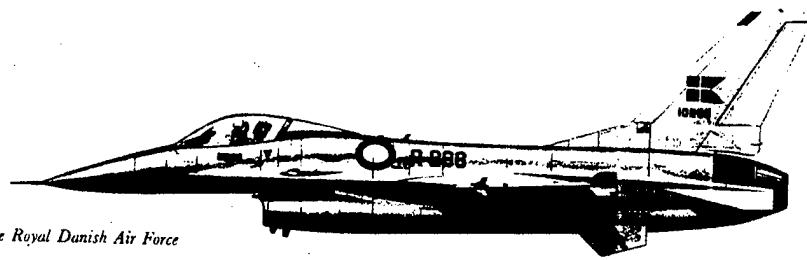


F-16 for the Royal Netherlands Air Force



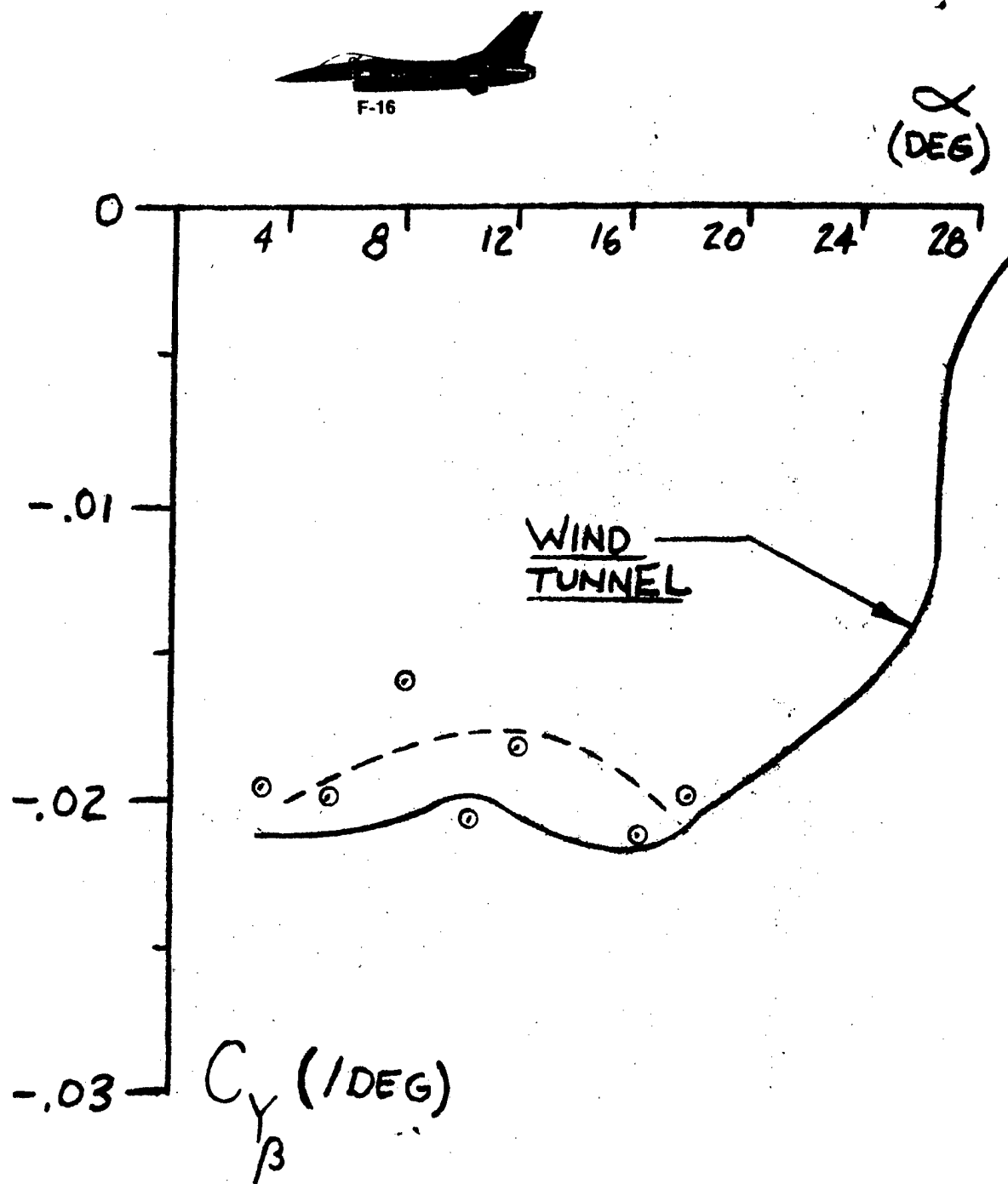
CR $cg = 35\% \text{ MAC}$ $M < 0.6$ $q = 50 - 200 \text{ lb/ft}^2$

Figure 50: Flight Test Variation of $C_{m\delta_e}$ with Angle of Attack for the YF-16 Aircraft.⁹²



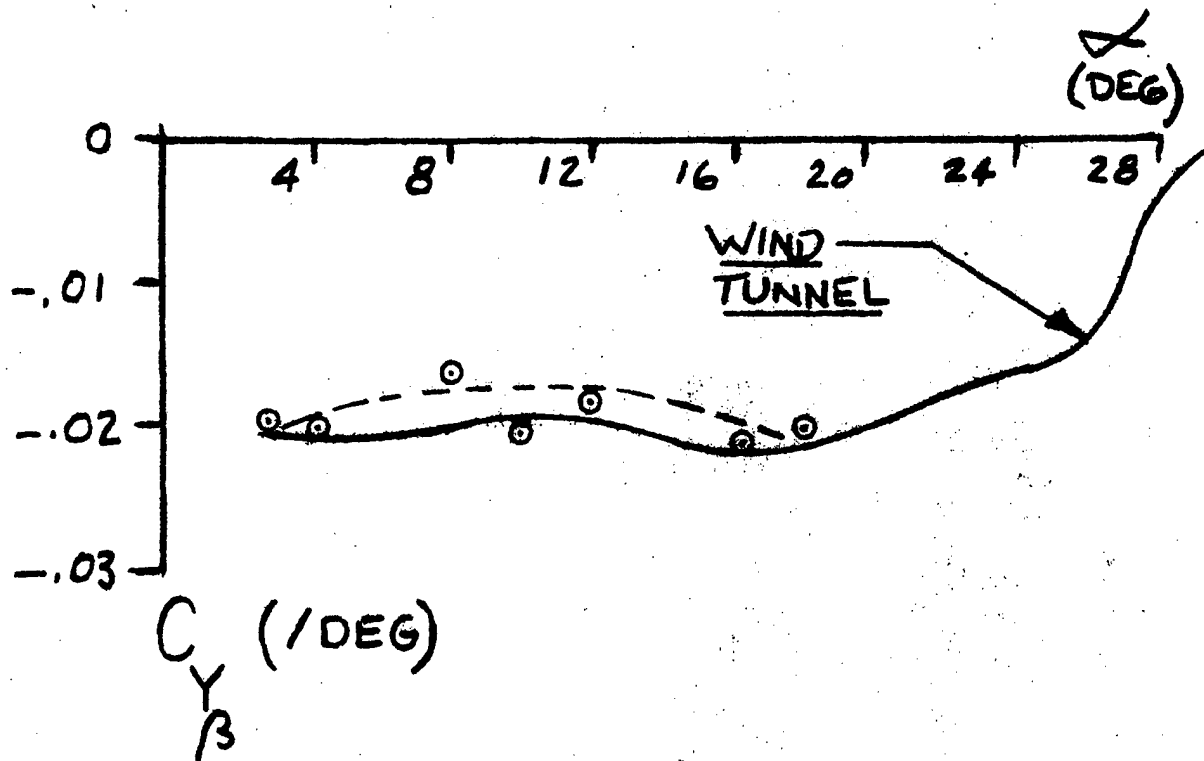
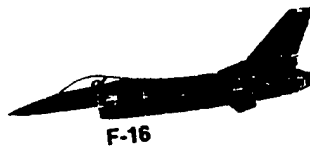
CR cg = 35% MAC $\alpha = 4^\circ$

Figure 51: Flight Test Variation of $C_{m_{\delta_e}}$ with Mach Number for the YF-16 Aircraft.⁹²



CR cg = 35% MAC M < 0.6 q = 50 - 200 lb/ft²

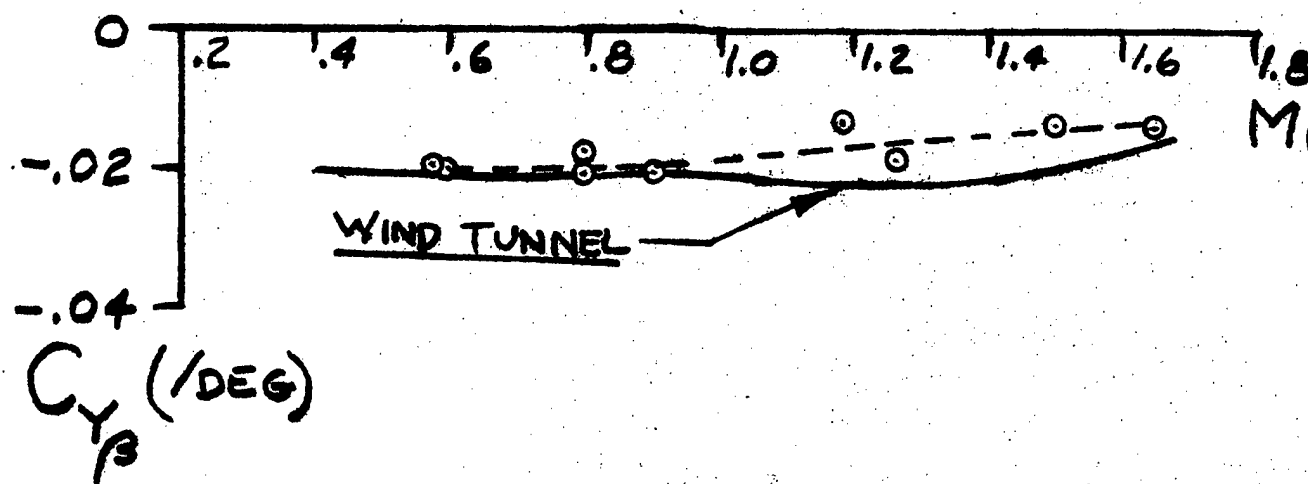
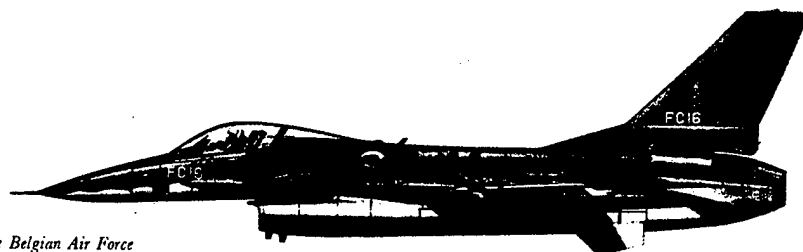
Figure 52: Flight Test Variation of C_{Y_β} with Angle of Attack for the YF-16 Aircraft.⁹²



CR $c_g = 35\% \text{ MAC}$ $M < 0.6$ $q = 50 - 200 \text{ lb/ft}^2$

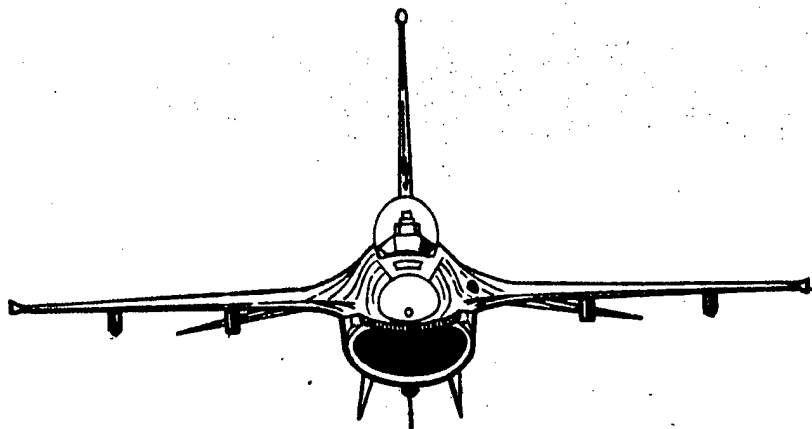
Figure 53: Flight Test Variation of $C_{Y\beta}$ with Angle of Attack for the YF-16 Aircraft.⁹²

F-16 for the Belgian Air Force

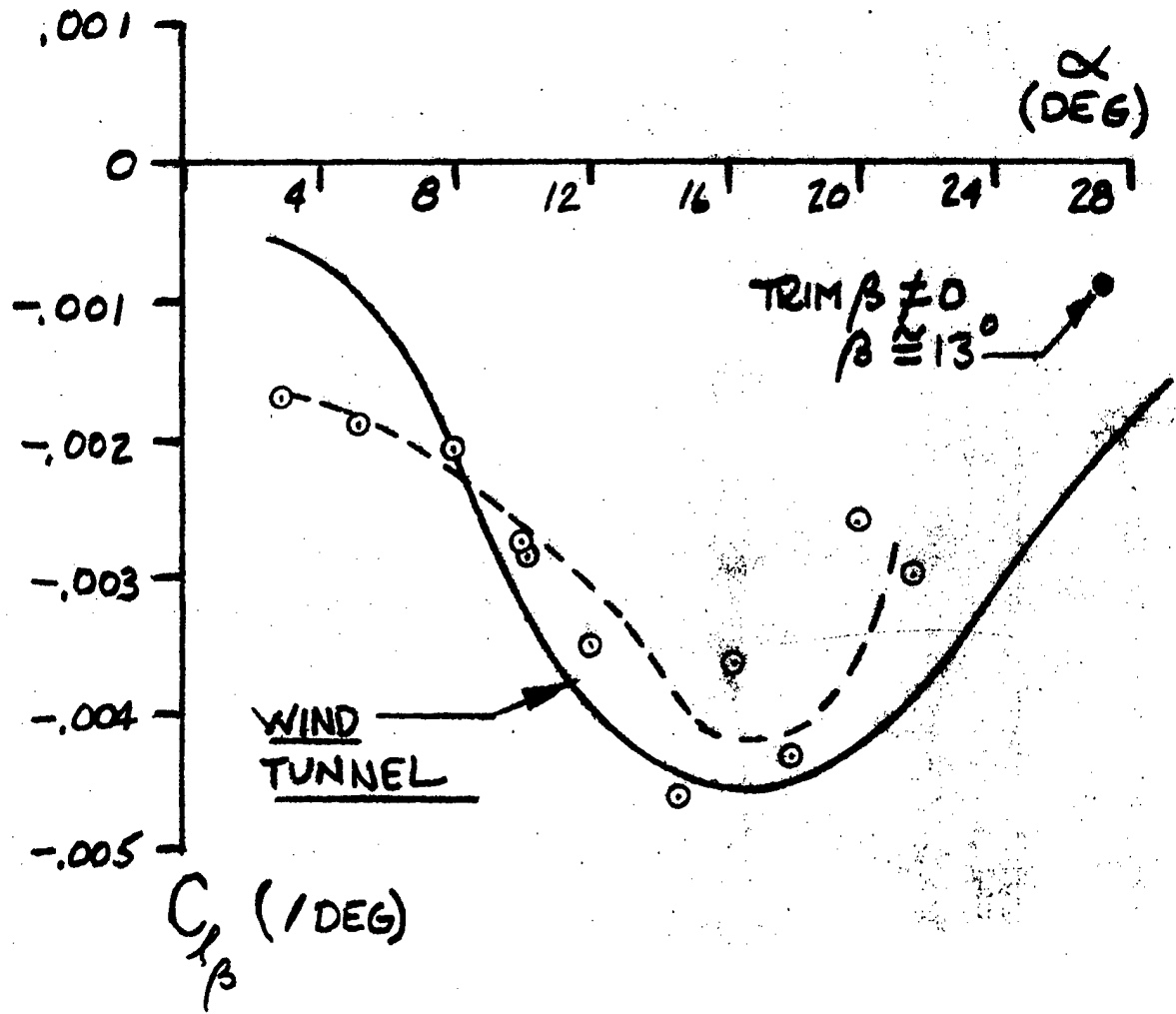
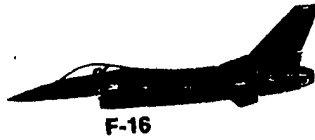


CR $cg = 35\% \text{ MAC}$ $\alpha = 4^\circ$

Figure 54: Flight Test Variation of $C_{Y_{\beta}}$ with Mach Number for the YF-16 Aircraft.⁹²



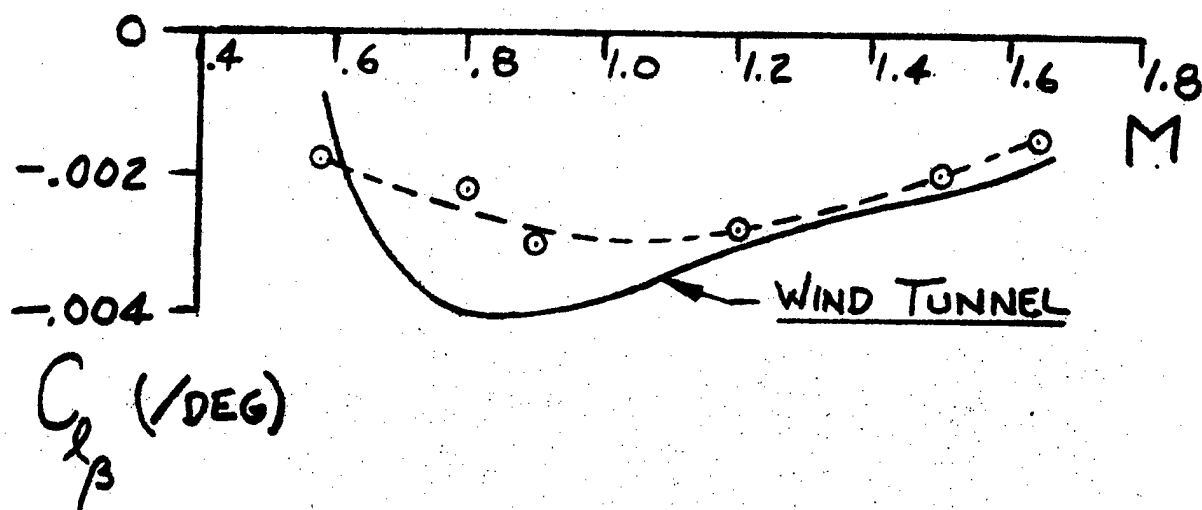
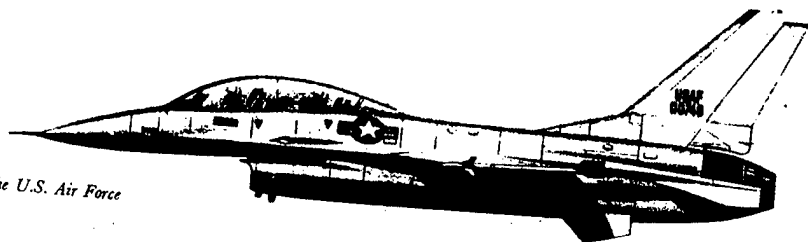
YF-16



CR cg = 35% MAC M < 0.6 q = 50 - 200 lb/ft²

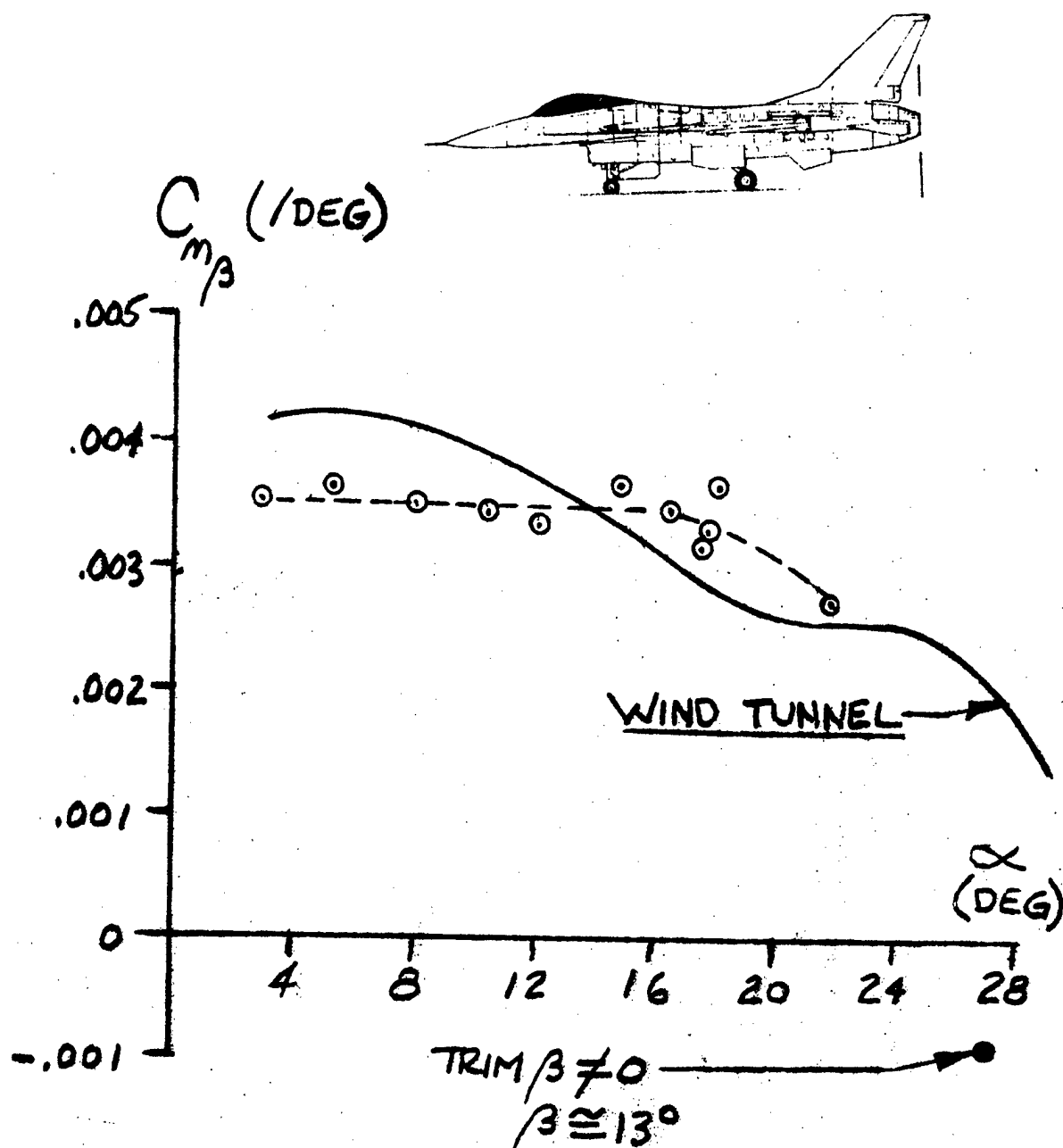
Figure 55: Flight Test Variation of $C_{l_{\beta}}$ with Angle of Attack for the YF-16 Aircraft.⁹²

F-16B for the U.S. Air Force



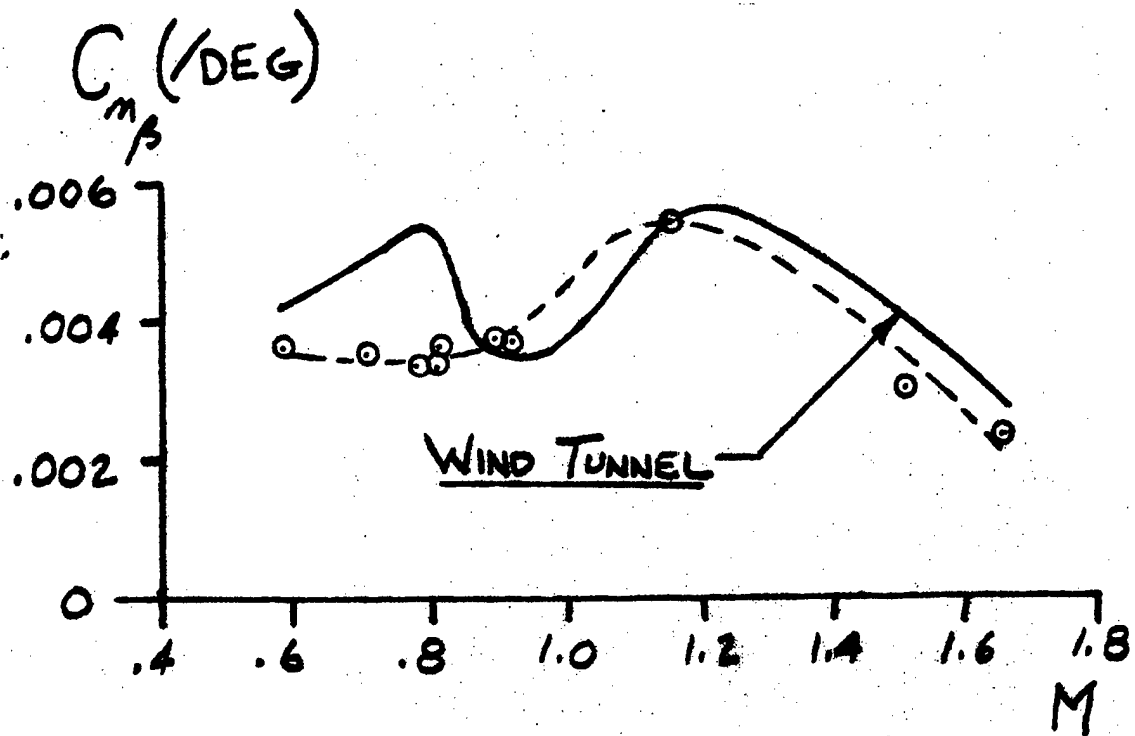
CR cg = 35% MAC $\alpha = 4^\circ$

Figure 56: Flight Test Variation of $C_{l_{\beta}}$ with Mach Number for the YF-16 Aircraft.⁹²



CR cg = 35% MAC M < 0.6 q = 50 - 200 lb/ft²

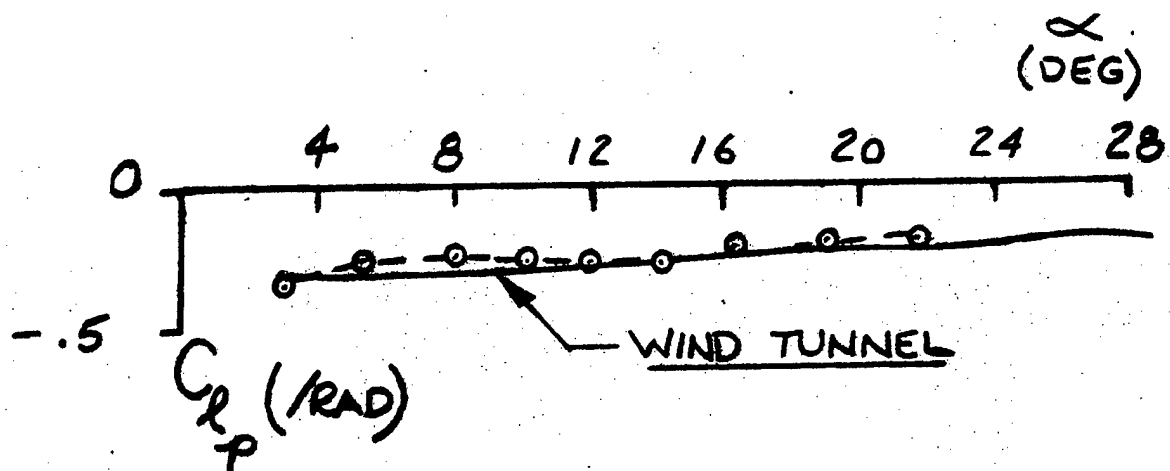
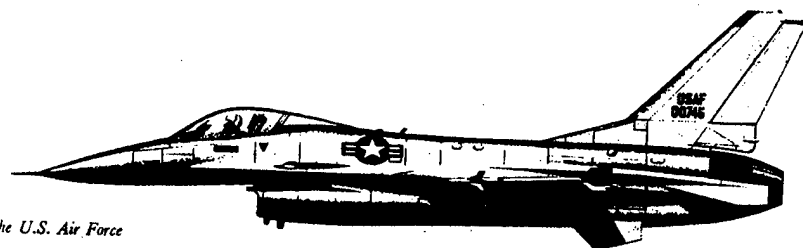
Figure 57: Flight Test Variation of $C_{n\beta}$ with Angle of Attack for the YF-16 Aircraft.⁹²



CR cg = 35% MAC $\alpha = 4^\circ$

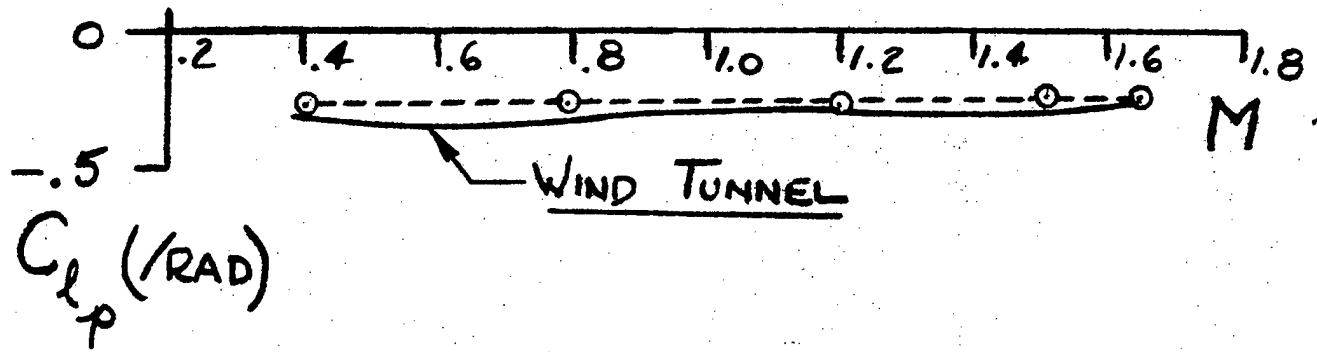
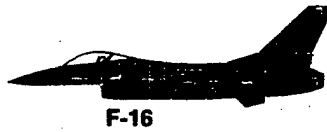
Figure 58: Flight Test Variation of $C_{n\beta}$ with Mach
Number for the YF-16 Aircraft.⁹²

F-16A for the U.S. Air Force



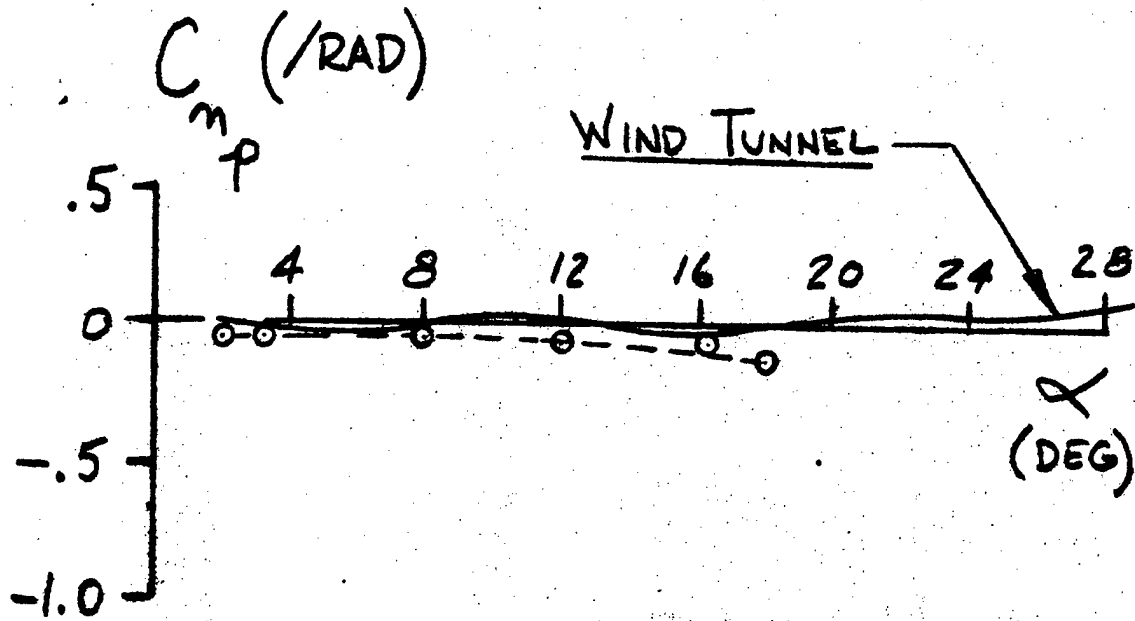
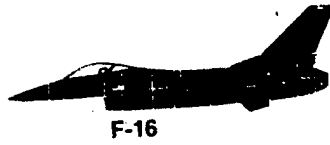
CR $c_g = 35\% \text{ MAC}$ $M < 0.6$ $q = 50 - 200 \text{ lb/ft}^2$

Figure 59: Flight Test Variation of C_{ℓ_p} with Angle of Attack for the YF-16 Aircraft.⁹²



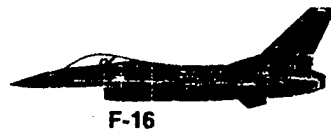
CR cg = 35% MAC $\alpha = 4^\circ$

Figure 60: Flight Test Variation of C_{l_p} with Mach Number for the YF-16 Aircraft.⁹²

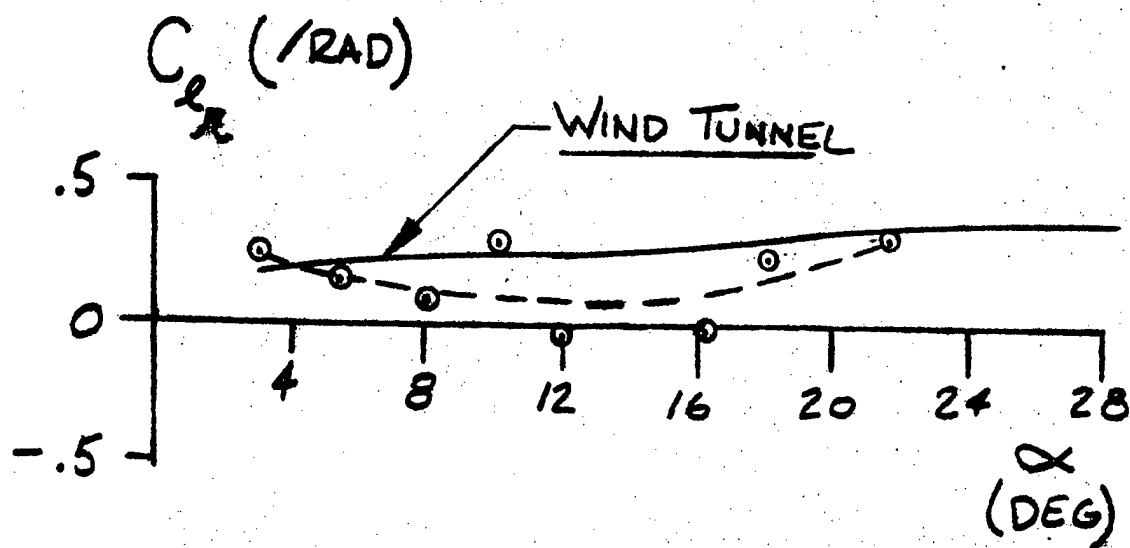


CR $c_g = 35\% \text{ MAC}$ $M < 0.6$ $q = 50 - 200 \text{ lb/ft}^2$

Figure 61: Flight Test Variation of C_{np} with Angle of Attack for the YF-16 Aircraft.⁹²

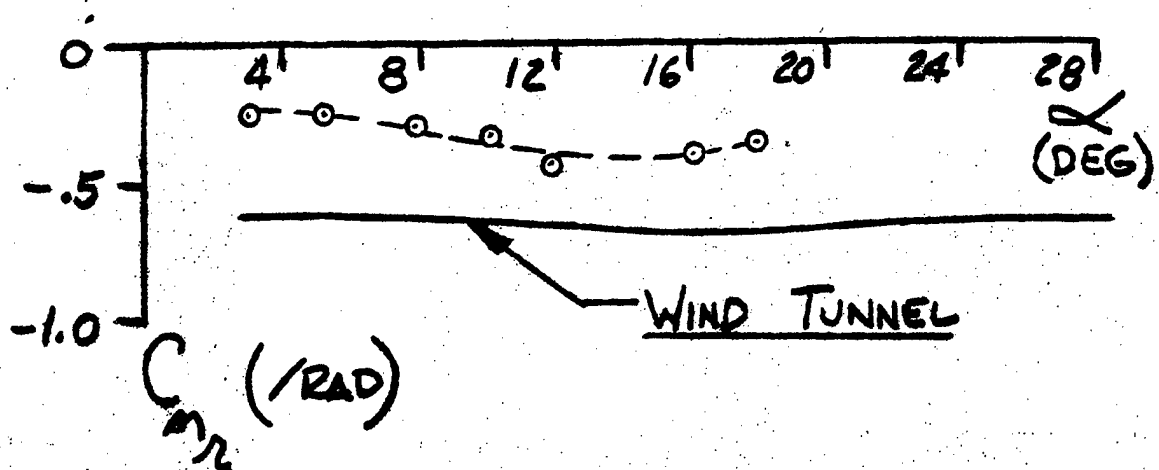
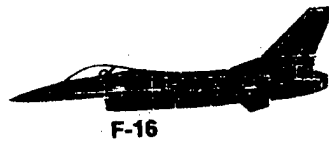


F-16



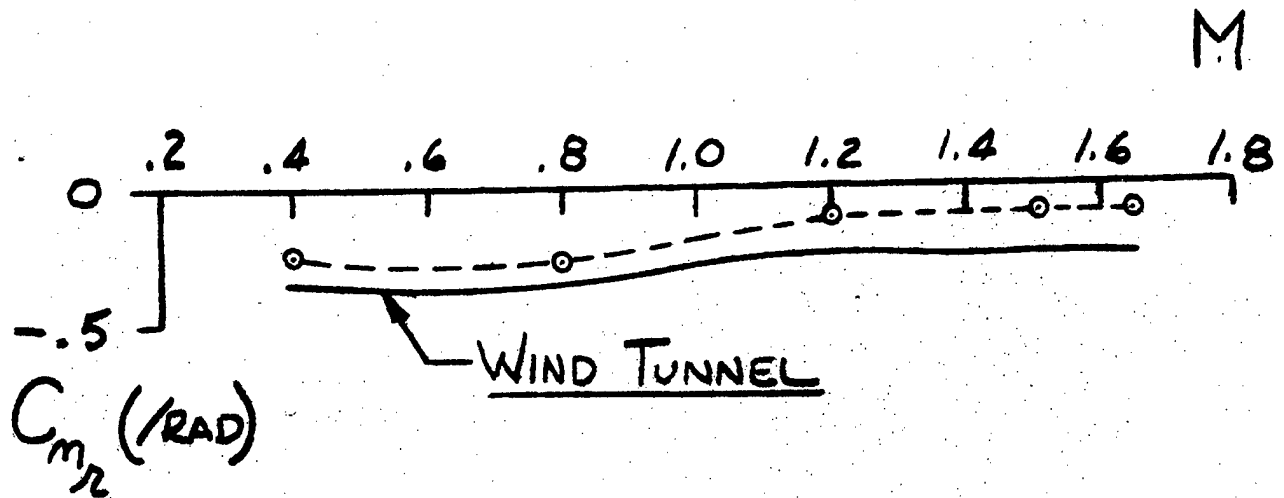
CR cg = 35% MAC M < 0.6 q = 50 - 200 lb/ft²

Figure 62: Flight Test Variation of $C_{l_{\alpha}}$ with Angle of Attack for the YF-16 Aircraft.⁹²



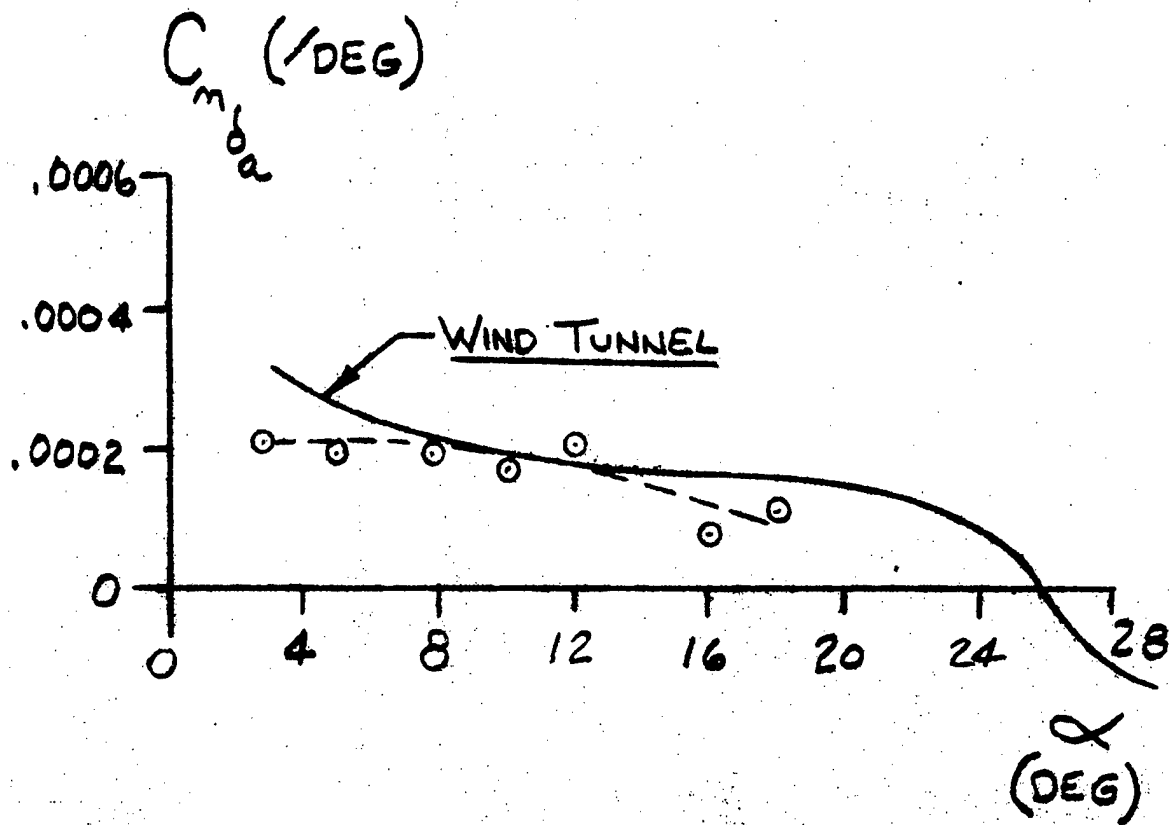
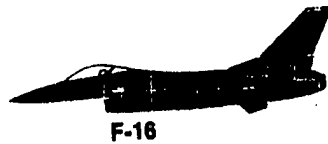
CR $c_g = 35\% \text{ MAC}$ $M < 0.6$ $q = 50 - 200 \text{ lb/ft}^2$

Figure 63: Flight Test Variation of C_{n_r} with Angle of Attack for the YF-16 Aircraft.⁹²



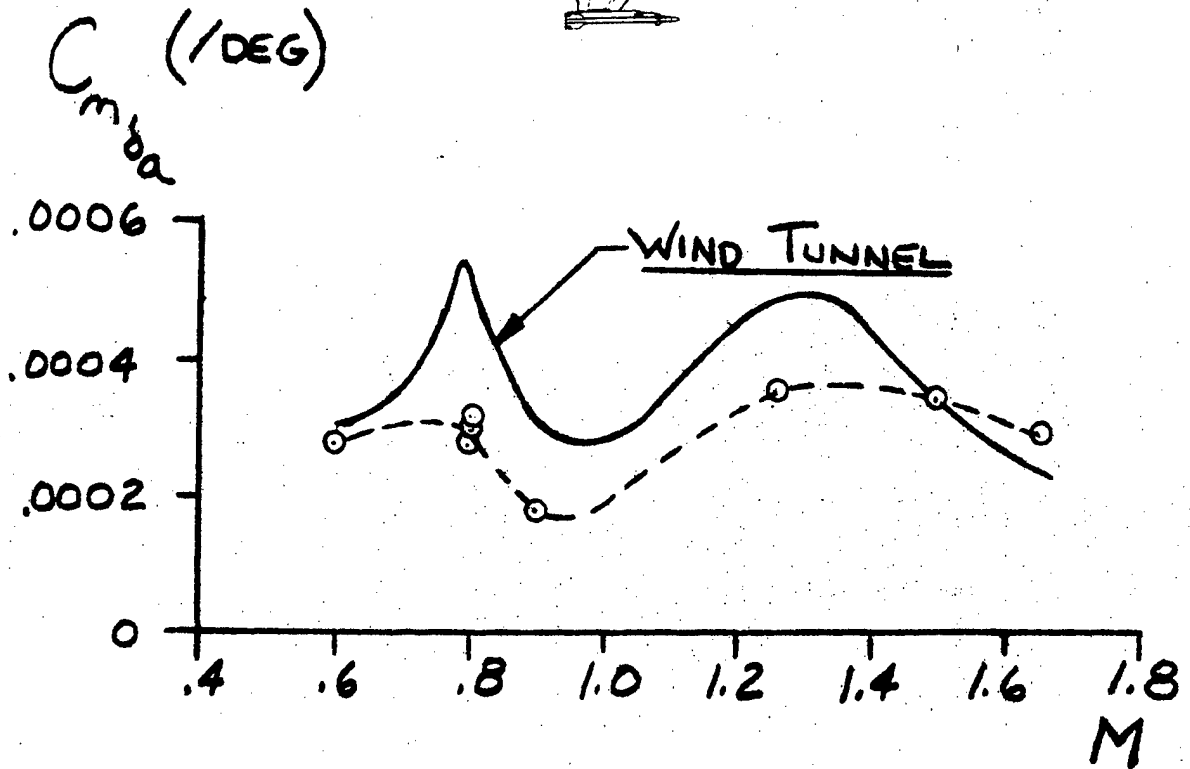
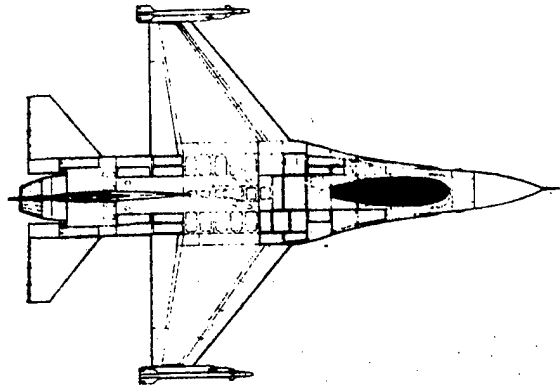
CR cg = 35% MAC $\alpha = 4^\circ$

Figure 64: Flight Test Variation of C_{m_z} with Mach Number for the YF-16 Aircraft.⁹²



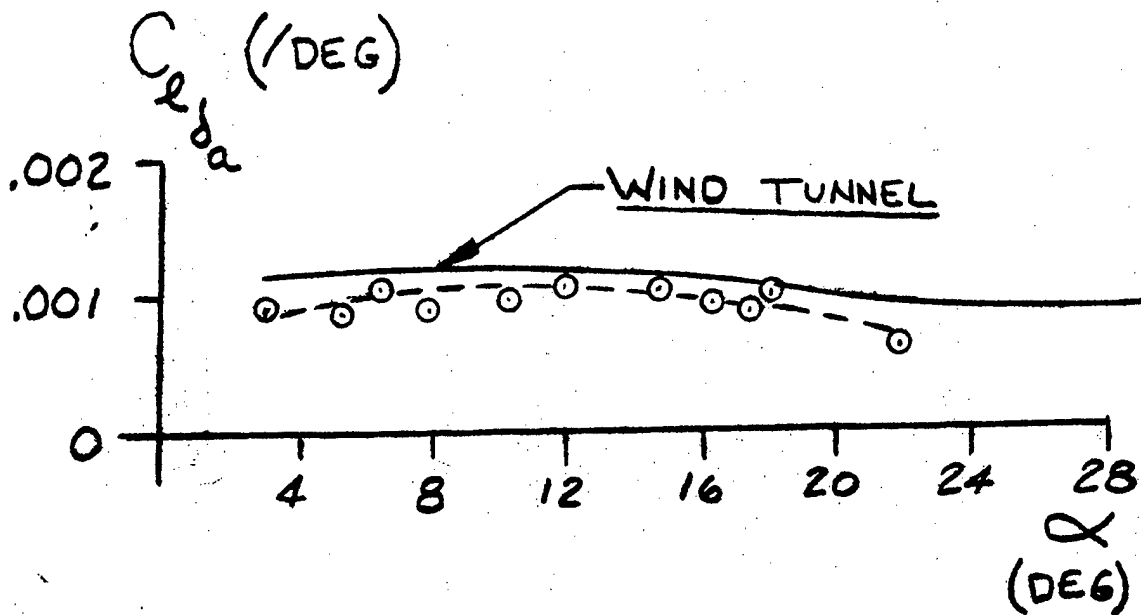
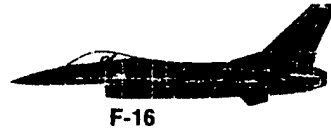
CR $c_g = 35\% \text{ MAC}$ $M < 0.6$ $q = 50 - 200 \text{ lb/ft}^2$

Figure 65: Flight Test Variation of $C_{n\delta a}$ with Angle of Attack for the YF-16 Aircraft.⁹²



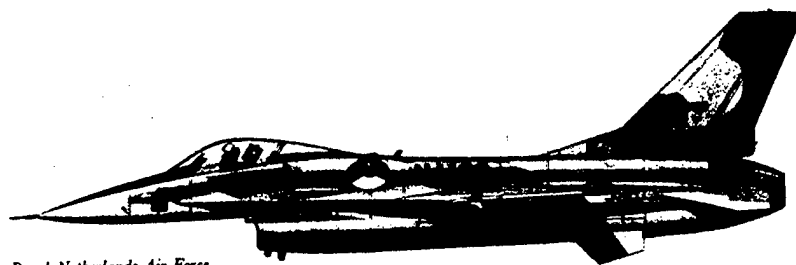
CR cg = 35% MAC $\alpha = 4^\circ$

Figure 66: Flight Test Variation of $C_{n\delta a}$ with Mach
Number for the YF-16 Aircraft.⁹²

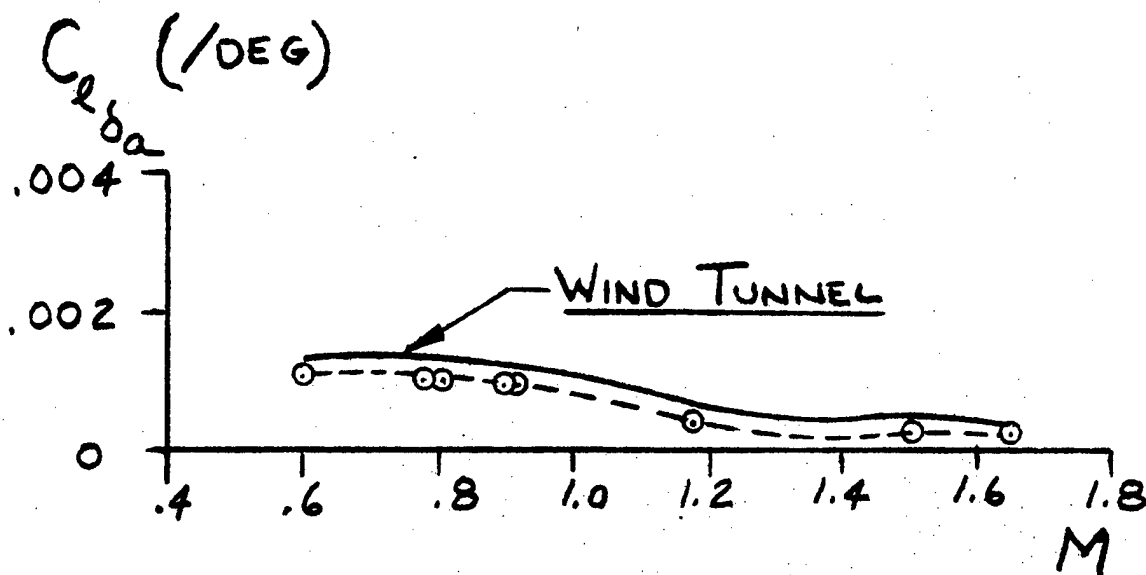


CR cg = 35% MAC M < 0.6 q = 50 - 200 lb/ft²

Figure 67: Flight Test Variation of $C_{l_{\delta a}}$ with Angle of Attack for the YF-16 Aircraft.⁹²

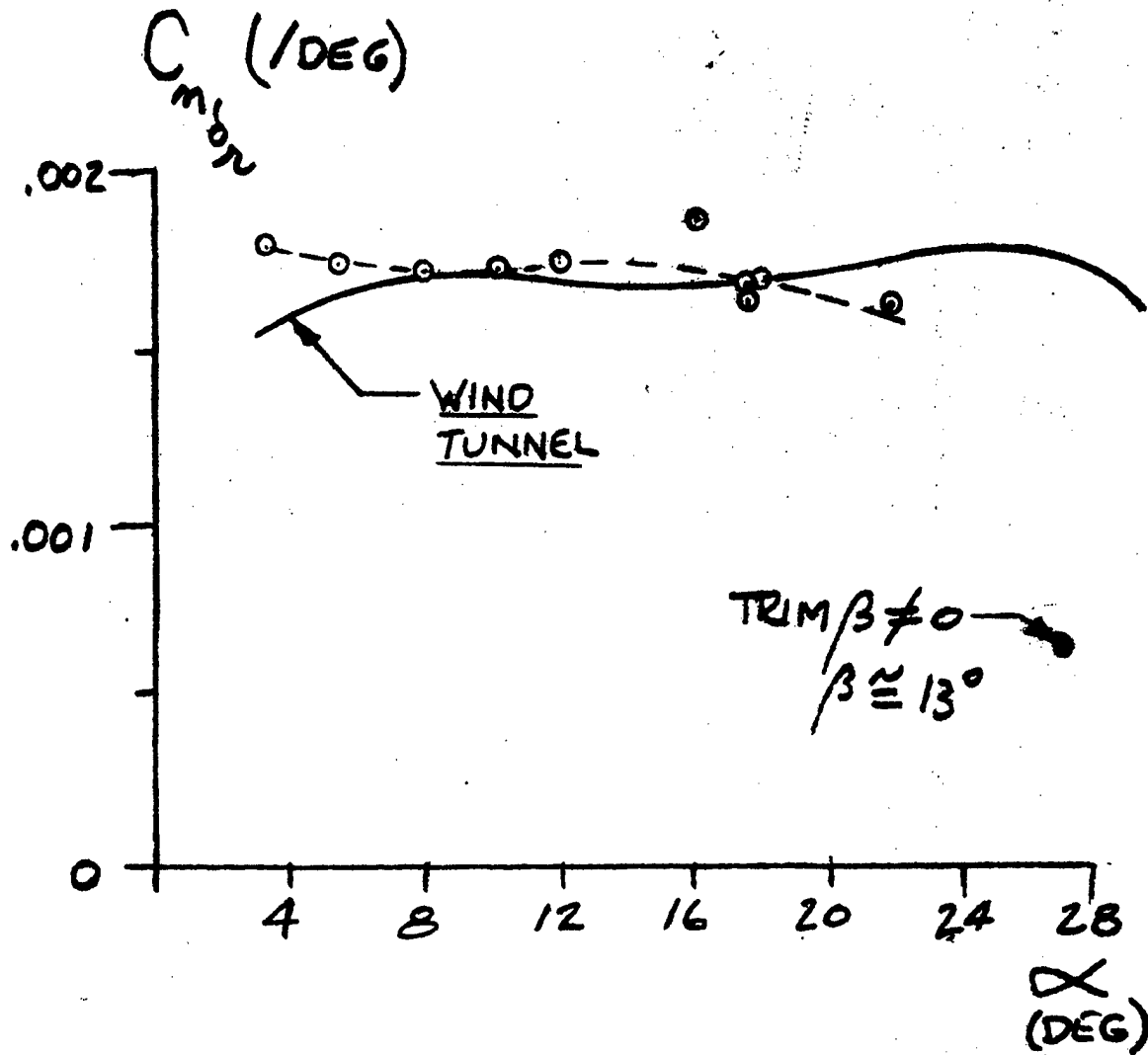
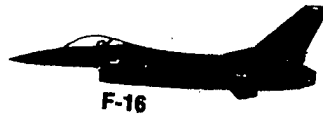


F-16 for the Royal Netherlands Air Force



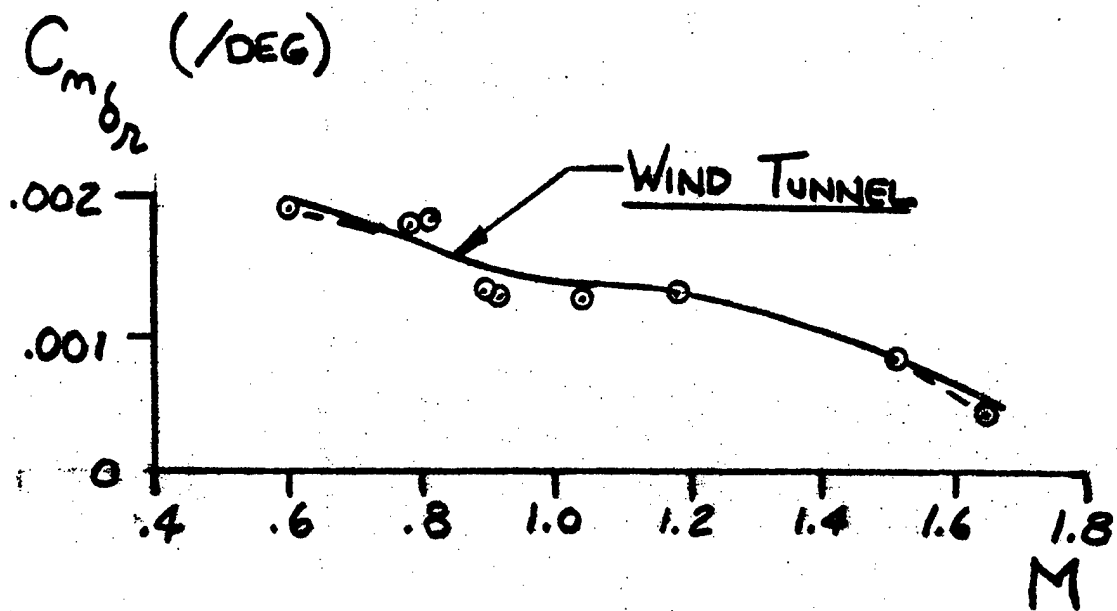
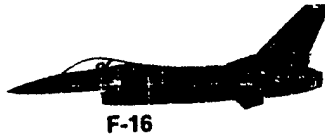
CR cg = 35% MAC $\alpha = 4^\circ$

Figure 68: Flight Test Variation of $C_{l_{\delta a}}$ with Mach Number for the YF-16 Aircraft.⁹²



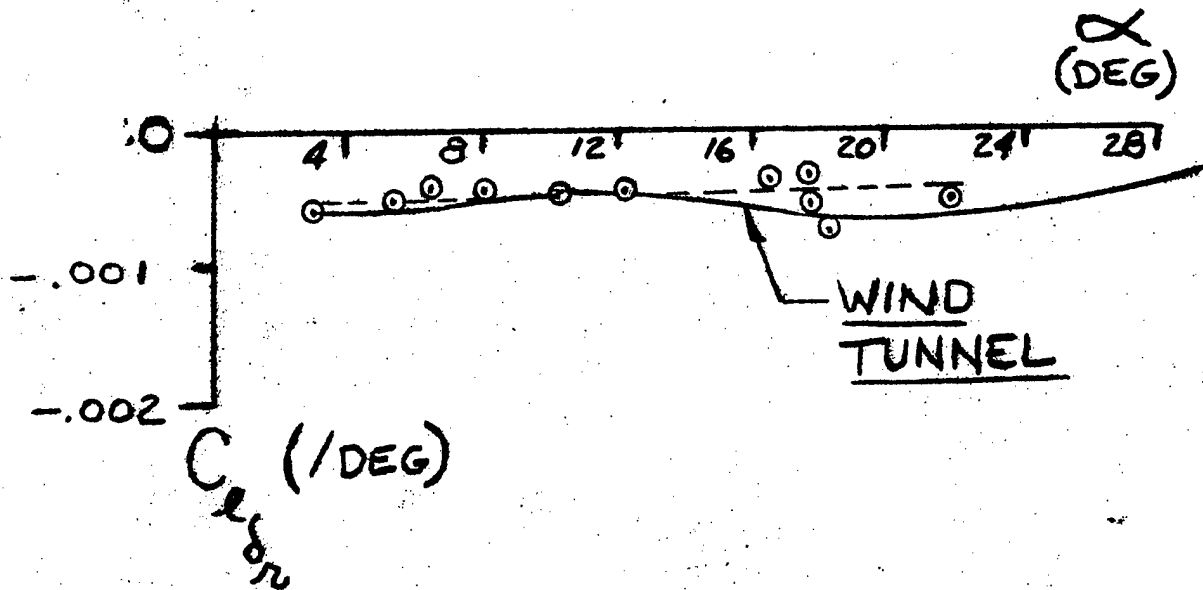
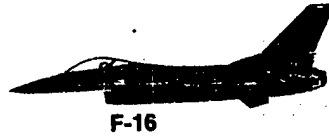
CR $c_g = 35\% \text{ MAC}$ $M < 0.6$ $q = 50 - 200 \text{ lb/ft}^2$

Figure 69: Flight Test Variation of $C_{m_{\delta r}}$ with Angle of Attack for the YF-16 Aircraft.⁹²



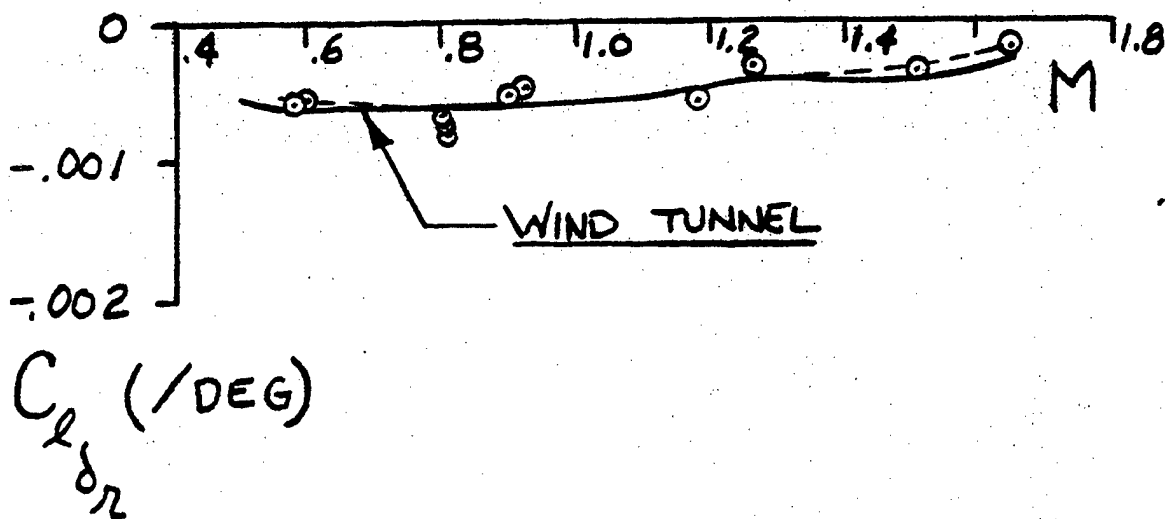
CR cg = 35% MAC $\alpha = 4^\circ$

Figure 70: Flight Test Variation of $C_{n\delta_r}$ with Mach Number for the YF-16 Aircraft.⁹²



CR cg = 35% MAC M < 0.6 q = 50 - 200 lb/ft²

Figure 71: Flight Test Variation of $C_{l_{\delta_r}}$ with Angle of Attack for the YF-16 Aircraft.⁹²



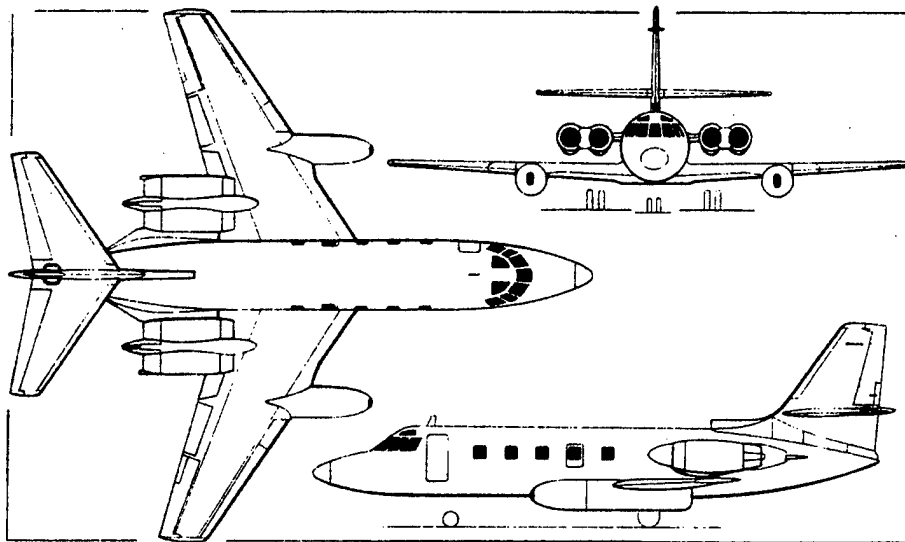
CR cg = 35% MAC $\alpha = 4^\circ$

Figure 72: Flight Test Variation of $C_{l_{\delta_r}}$ with Mach

Number for the YF-16 Aircraft.⁹²

EXAMPLE MMLE DETERMINED PARAMETERS IN TURBULENCE

Figure 72A presents a set of Lockheed Jetstar longitudinal stability and control parameters from Reference 143. These stability parameters were extracted by Tung from NASA Dryden flight test data taken in turbulence. The maneuver time histories and the turbulence level were shown previously on Figures 6A and 6B. The various values for the parameters were computed over different time segments of the four-singlet elevator input time history. The accuracy and use of these parameters will be discussed in Sections 5 and 6 of this chapter.



Lockheed JetStar II executive transport (four Allison TFE 731-3 turboprop engines) (Pilot Press)

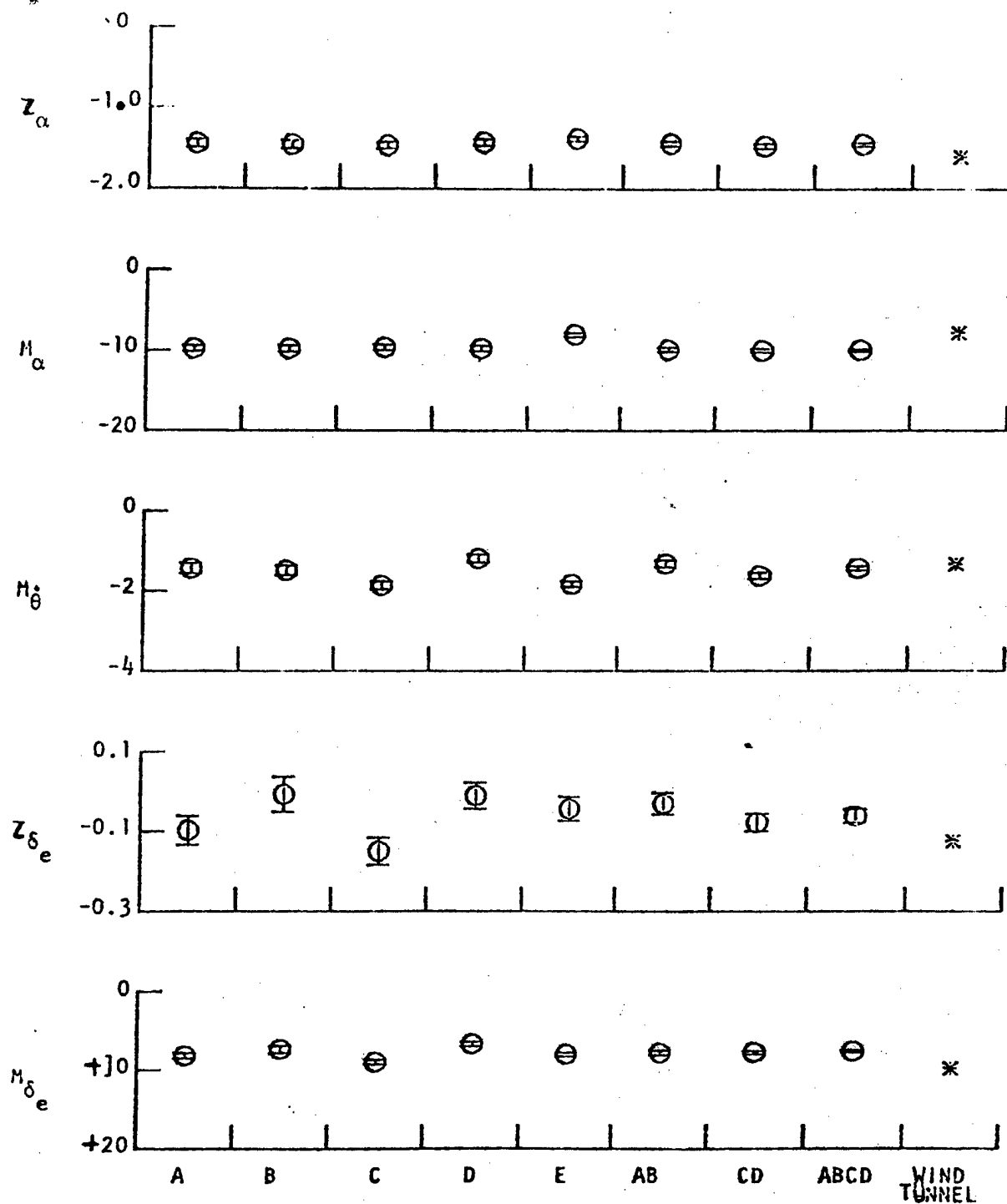
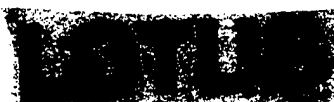
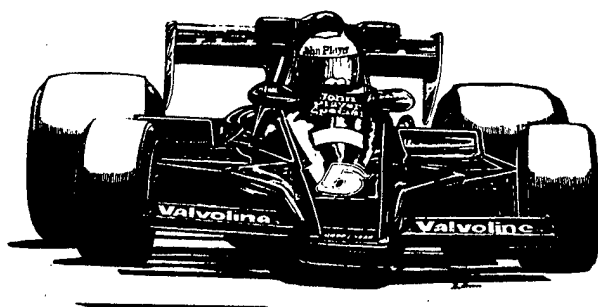
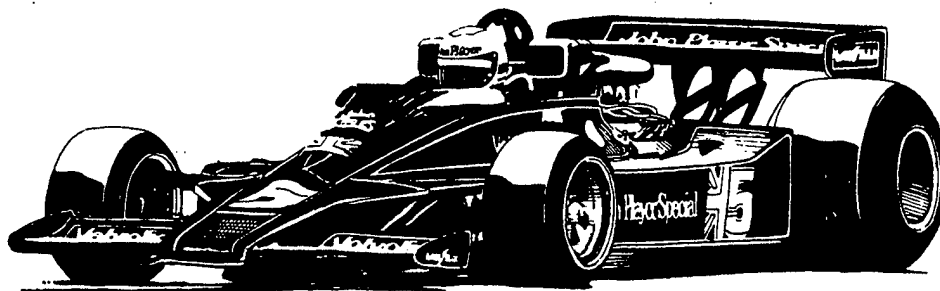
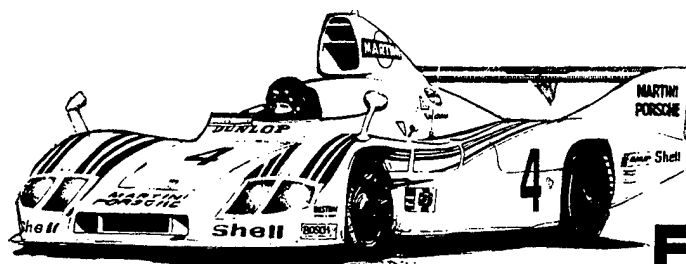


FIGURE 72A: Flight Test Variation of Longitudinal Stability and Control Parameters of a Lockheed Jetstar Extracted from Flight in Turbulence.¹⁴³



John Player Special



PORSCHE

SECTION 5

STABILITY DERIVATIVE ACCURACY

INTRODUCTION

It was pointed out in Section 2 that the term accuracy represents an absolute measure of the error between some estimated derivative and the true derivative value. Since the true value is unknown, accuracy can probably be best evaluated by determining how well estimated stability derivatives used in the equations of motion mathematical model predict random aircraft motion. Very little work has been done to date in this area.

This situation obviously gives problems in trying to assess the accuracy of stability derivatives determined from analysis, wind tunnel tests, or flight tests. The following discussion will concentrate on (1) pointing out the current areas of effort in trying to improve the accuracy of each method of estimating stability derivatives, and (2) discussing some of the more recent efforts made to try to correlate data between methods of estimation.

ANALYTICAL ACCURACY

Stability derivatives cannot all be estimated with the same accuracy. Nor are they equally important. Table 2 and 3 show the degree of accuracy to which Roskam believes the various stability derivatives can be estimated using Datcom analytical methods.^{72,74} Table 2 and 3 also indicate the relative importance of these derivatives in determining the stability and control characteristics of aircraft. For the latter, a numerical rating scale varying from 10 (major importance) to 1 (negligible importance) has been used. These ratings should give some guidance to determine how much effort is warranted in estimating individual stability derivatives.⁷⁴

Much work is being done on developing new and more accurate theoretical approaches. Methods which have very good potential in this regard are

Table 2: Relative Importance and Prediction Accuracy of Longitudinal Stability Derivatives.⁷⁴

Derivative	Relative Importance*	Estimated Prediction Accuracy**
C_{L_α}	10	+5%
C_{m_α}	10	10
C_{D_α}	5	10
$C_{L_\alpha \dot{}}$	4	40
$C_{m_\alpha \dot{}}$	7	40
$C_{D_\alpha \dot{}}$	1	50
C_{L_u}	5	20
C_{m_u}	8	20
C_{D_u}	6	20
C_{L_q}	3	20
C_{m_q}	9	20
C_{D_q}	1	30

* 10 = major, 5 = minor, 0 = negligible

** Using Reference 72 Methods.

Table 3: Relative Importance and Prediction Accuracy of Lateral-Directional Stability Derivatives.⁷⁴

Derivative	Relative Importance*	Estimated Prediction Accuracy**
$C_{Y\beta}$	7	+20%
$C_{\ell\beta}$	10	20
$C_{n\beta}$	10	15
$C_{Y\dot{\beta}}$	2	60
$C_{\ell\dot{\beta}}$	2	60
$C_{n\dot{\beta}}$	4	60
C_{Yp}	4	50
$C_{\ell p}$	10	15
C_{np}	8	90
C_{Yr}	4	30
$C_{\ell r}$	7	40
C_{nr}	9	25

* 10 = major, 5 = minor, 0 = negligible

** Using Reference 72 Methods.

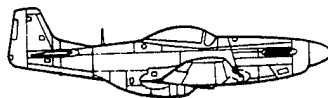
finite-element methods such as those given in Reference 74 by Roskam.^{74,125}

Figures 73 thru 77 are examples of analytical data obtained using finite-element methods. These figures demonstrate the very significant effects of aeroelasticity (dynamic pressure) on longitudinal derivatives.^{74, 126} The data presented are limited to longitudinal derivatives because of the state of the art of influence coefficient aerodynamics; however, the literature shows that basic finite-element analytical methods can be extended to lateral-directional stability derivative determination.^{74,128}

How much accuracy is lost by assuming a rigid aircraft for analysis is a function of where in the operational envelope the aircraft is flying. For example, Figure 73 shows that for the normal transport operation such as immediate climb to high subsonic Mach number, high altitude cruise, the aircraft tends to "fly along" the rigid $C_{L_{\alpha}}$ versus Mach number curve.

Cruising at 35,000 ft at 0.85 Mach number an analytical accuracy of about 15 percent is sacrificed by assuming a rigid aircraft.

Figure 74 does not exhibit a similar trend. At the same cruise conditions of Mach number 0.85 at 35,000 ft, the longitudinal static stability derivative, $C_{m_{\alpha}}$, is computed to be 60 percent too large (more negative) by assuming a rigid aircraft. Obviously, this is a very serious loss of analytical accuracy since it results in the elastic aircraft neutral point being about 12 percent MAC forward of its computed position.



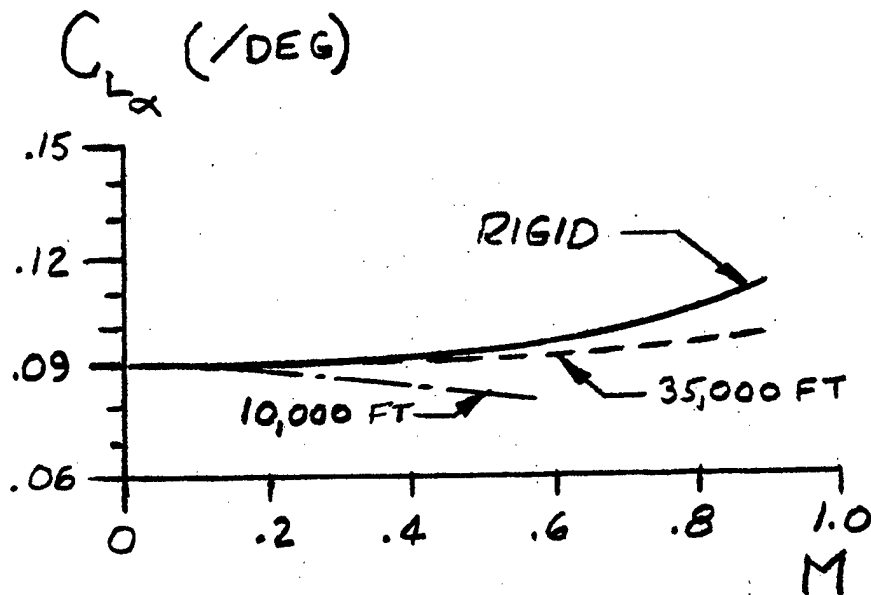


Figure 73: Comparison of Analytical Rigid and Elastic $C_{L\alpha}$ for the Boeing 707-320B.^{74,126}

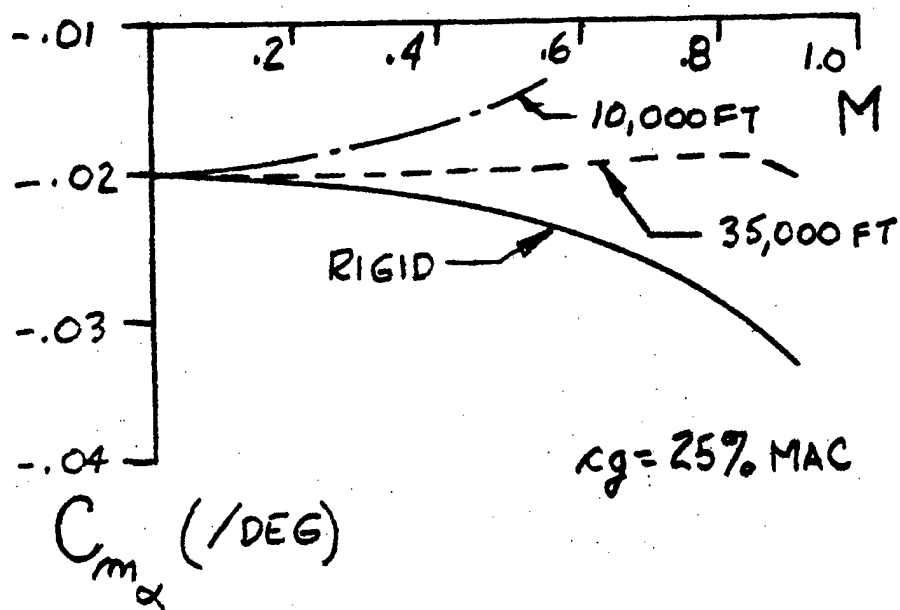


Figure 74: Comparison of Analytical Rigid and Elastic $C_{m\alpha}$ for the Boeing 707-320B.^{74,126}

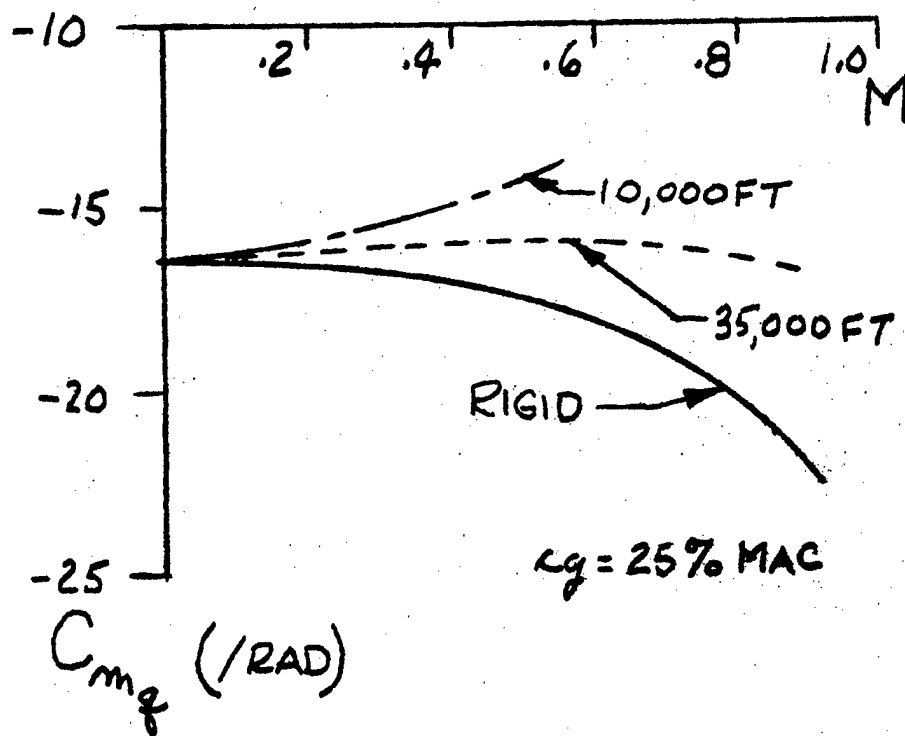


Figure 75: Comparison of Analytical Rigid and Elastic C_{mq} for the Boeing 707-320B.^{74,126}

Figure 75 shows that assuming a rigid aircraft results in computing the pitch damping derivative, C_{mq} , to be 26 percent larger (more negative)

than it is for the elastic aircraft at the same cruise conditions of 0.85 Mach number at 35,000 ft.

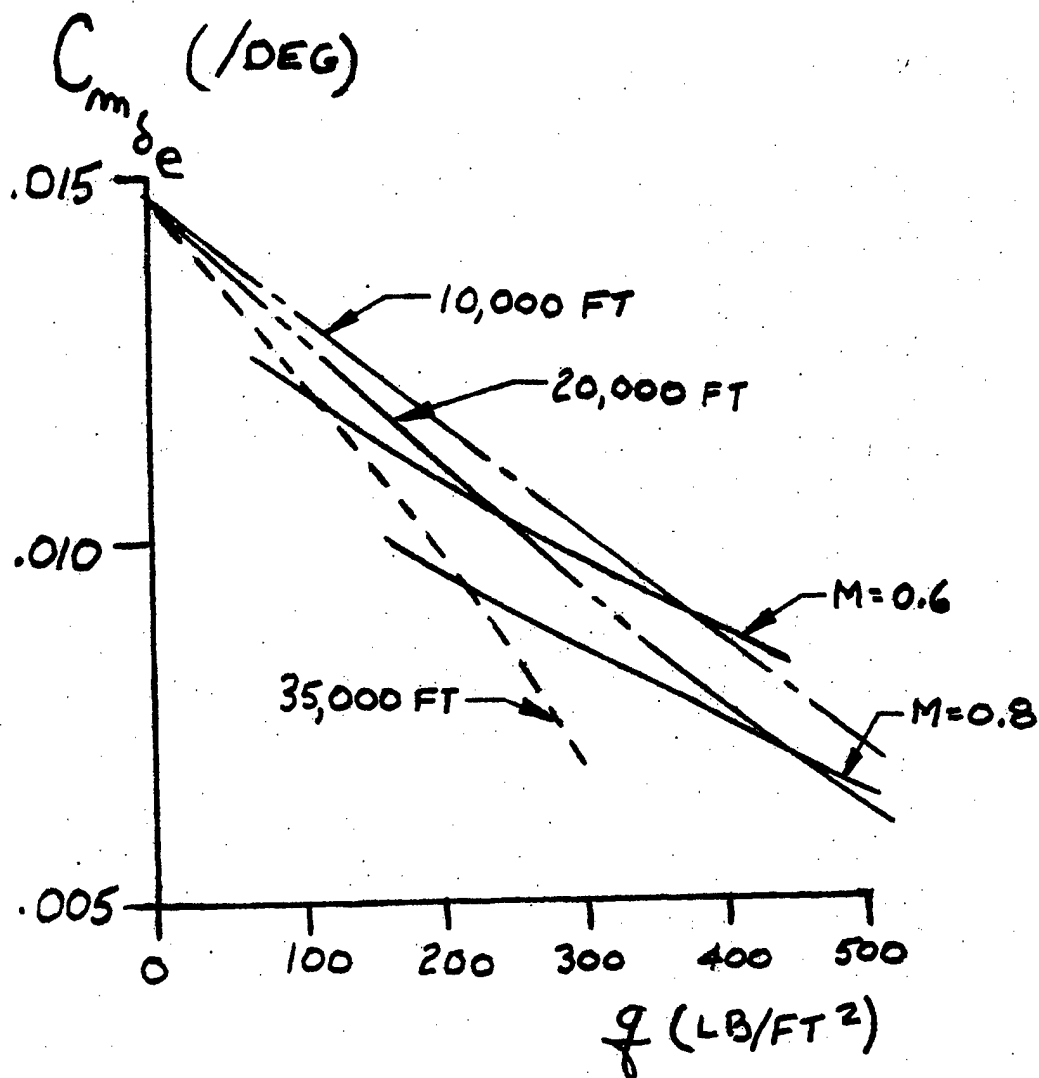


Figure 76: Comparison of Analytical Elastic $C_{m\delta_e}$ for the Boeing 707-320B.^{74,126}

Figure 76 is a plot of longitudinal control power, $C_{m\delta_e}$, versus dynamic pressure with lines of constant Mach number shown. This is another logical way to present computed elastic aircraft stability derivative data since aeroelastic effects are functions of dynamic pressure. In fact, lines of constant dynamic pressure could be shown on Figures 73, 74 and 75.

Figure 76 shows that at a constant dynamic pressure of 250 lb/ft^2 (constant equivalent airspeed, which is nearly constant indicated airspeed of 271 knots), computed elevator power decreases by 23 percent between 10,000 and 25,000 ft.

Figure 77 shows quite clearly that the control power of the Boeing supersonic transport would be estimated about 100 percent too large for a Mach number 2.0 cruise if a rigid aircraft calculation were made.

If nothing else, the preceding five figures and discussion should illustrate that, in general, aeroelastic effects (dynamic pressure) are significant. Maintaining the same external geometry, but changing the structural rigidity or mass distribution of the aircraft also changes the aeroelastic characteristics of the aircraft. This problem of inertial effects is discussed by Roskam in Reference 74.

Obviously, major changes in the longitudinal stability derivatives due to aeroelastic effects cause major changes in the longitudinal modes of motion, the phugoid and short period. Not only do the derivatives change, but the basic equations of motion change since they were derived assuming a rigid aircraft. A complete and rigorous development of the perturbed equations of motion of an elastic aircraft like that found in Reference 127 is beyond the scope of current stability and control textbooks and is certainly beyond the scope of this text and course.⁷⁴

WIND TUNNEL ACCURACY

In general, wind tunnel testing can increase the accuracy of stability derivative prediction considerably.^{65,74} Prior to flight test, wind tunnel estimates remain the primary indicator of how an aircraft will behave.¹⁰⁶

Some of the major sources of error in wind tunnel testing were discussed in Section 3 of this text. A significant point is that small-scale model wind tunnel tests are only analogies of full-scale flight. Therefore, the analytical procedures used to extrapolate wind tunnel test results to full-scale flight conditions and the accuracy of small-scale model tests are

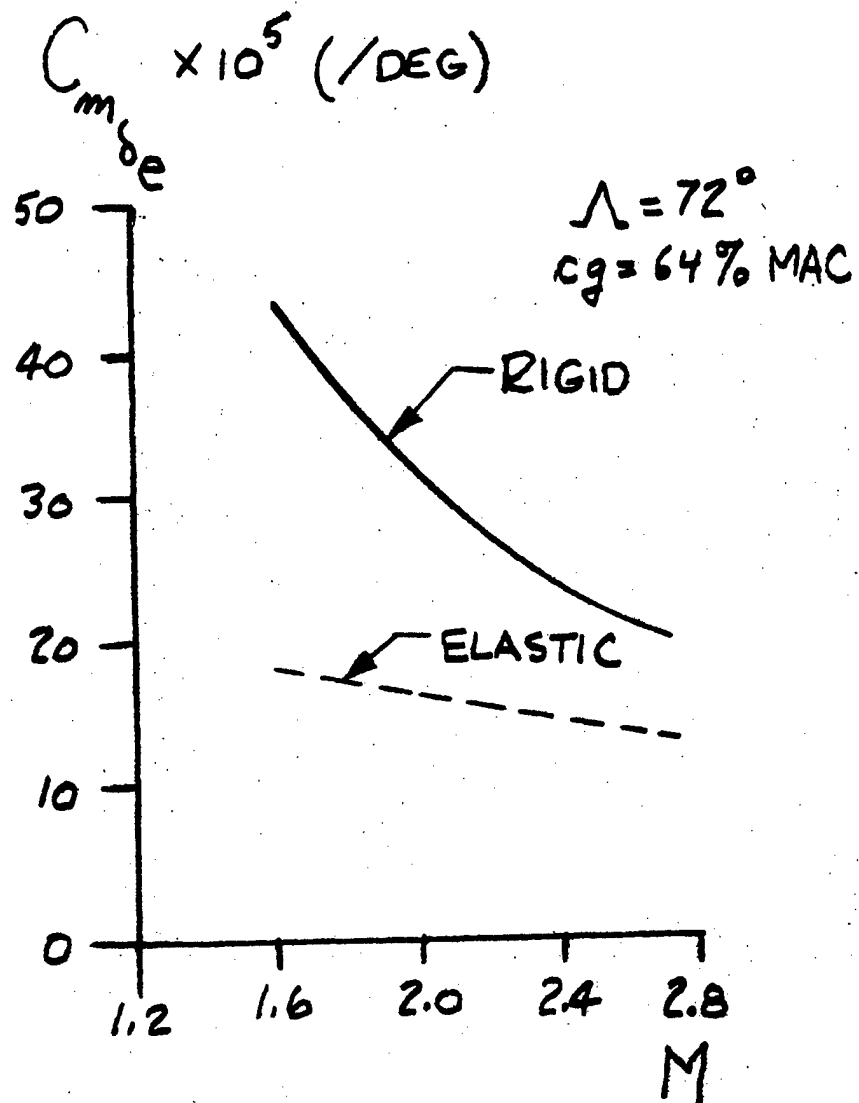


Figure 77: Comparison of Analytical Rigid and Elastic $C_{m\delta e}$ for the

Boeing 2707.^{74,126}

interrelated. Because the wind tunnel test is not a precise duplication of flight, it is unrealistic to attempt to correlate small-scale model test results directly with full-scale flight test derived results. The analytical techniques used for the interpolation, adjustment, and extrapolation of small-scale wind tunnel test results are as much a part of the prediction of full-scale flight characteristics as the actual determination of the wind tunnel test data.¹²² This case is not overstated. There are many examples in the literature of wind tunnel corrections being the same order of magnitude as the data, i.e., the wind tunnel data needs to be doubled (or halved) to predict full-scale aircraft characteristics.

The force and moment coefficients on a rigid small-scale model tested in a wind tunnel will be the same as those on a rigid aircraft in flight if they are both measured at the same angle of attack, Reynolds number and Mach number. Reynolds number is usually used for presentation of wind tunnel data because the small-scale relatively stiff models show first order drag variations with Reynolds number. Flight test results, however, come from testing full-scale vehicles which are flexible or elastic and show first order effects in dynamic pressure.¹³⁰ This problem will be discussed further in assessing the accuracy of flight test stability derivative determination.

A problem worthy of further discussion now is the use of solid models having lower percentage structural deflections under load than does the aircraft. Just as it was for analysis, aeroelastic effects are important in wind tunnel testing.

The obvious solution is to use "elastically similar" models in wind tunnel testing. Designing and building elastic wind tunnel models and using elastic test data is expensive and complicated. In theory, data obtained from testing an "elastically similar" small-scale model in a wind tunnel will give the same force and moment coefficients as those on the actual aircraft in flight if these coefficients are measured at the same angle of attack, Reynolds number, Mach number, and dynamic pressure.

The way in which a wind tunnel model is scaled depends largely on the test objectives. Generally, the objective is to establish aerodynamic

similarity in some flight regime between the wind tunnel model and the aircraft it represents. In the case of relatively rigid aircraft this is done by building a rigid, geometrically scaled model and testing it at full-scale Mach numbers, but generally at some Reynolds number less than full-scale.⁷⁴ Reynolds number corrections to the data are usually required. In this case, the test dynamic pressures are important only because they establish the test Reynolds number.⁷⁴

To simulate the static aerodynamic force and moment characteristics of elastic aircraft on scale models, it is only necessary to simulate static load-deflection relationships on the model. It is not necessary to simulate structural dynamic response of the aircraft.⁷⁴

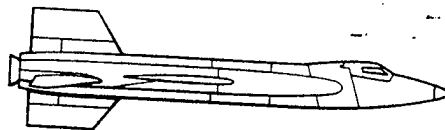
Usually flutter wind tunnel models cannot be used for the type of testing implied here. The reason is that these models are scaled for both mass and stiffness which makes them rather flimsy and precludes testing at full-scale dynamic pressures and Mach numbers.⁷⁴

One objective of wind-tunnel testing of elastic models at full-scale dynamic pressures is to measure and observe geometric shape changes as a function of dynamic pressure and Mach number. In the case of aircraft which exhibit large shape changes, it is important to know accurately the shape in which the aircraft has to be built in its assembly jigs so that it can deflect into its proper optimum shape at some design cruise weight, dynamic pressure, and Mach number.⁷⁴

The second objective for testing a flexible wind tunnel model is to determine aeroelastic effects on the performance and stability and control characteristics of the aircraft, e.g., determine elastic stability derivatives. Because of the 1-g wind tunnel environment, the flexible model will not simulate the aircraft exactly; however, it can be used to measure changes in control power or effectiveness due to the intercoupling of aerodynamic and structural phenomena. Accounting for elastic effects on the aircraft and wind tunnel model multiplies the problems involved with using wind tunnel data to predict full-scale aircraft characteristics. Roskam gives a step-by-step procedure in using elastic wind tunnel data in Reference 74. In addition,

he has summarized the differences between a flexible aircraft and a flexible wind tunnel model as shown in Table 4:

Table 4: Differences Between Aircraft and Wind Tunnel Models. ⁷⁴	
Aircraft	Model
1. Load factor (n) varies with angle of attack.	Tested at constant load factor (n=1) when angle of attack is varied.
2. Completely flexible: wing, tail and body are flexible.	Usually has only partial flexibility: as an example the body, inboard wing and tails may be rigid while the outboard wing and tail panels may be flexible.
3. Weight distribution varies for different flight conditions.	Weight distribution is constant and is not similar to any aircraft weight distribution.
4. Experiences various changes in flexibility because of environmental changes (aero-dynamic heating).	Experiences changes in flexibility caused by wind-tunnel temperatures.



A third objective in determining an aircraft's flexible characteristics by elastic wind tunnel model tests is to substantiate theoretical predictions and analyses.⁷⁴ This objective is directly related to increasing the accuracy of both wind tunnel and analytical methods for estimating stability derivatives.

The interaction of aeroelastic and Reynolds number effects was of concern during the TACT supercritical wing evaluation program. It was thought that some effects on aircraft which were normally attributed to Reynolds number were actually due to flexibility. Therefore, separate identification of these effects was desired. This was accomplished by using elastic wing wind tunnel models. Three flexible wing wind tunnel models were built for this research program. They were 1/24, 1/15, and 1/12-scale models.¹³¹ A major conclusion of the TACT wind tunnel testing was that adequate engineering tools exist for properly estimating transonic aerodynamics.¹³² The use of flexible model technology in the TACT program was considered a step forward in estimating full-scale aircraft aerodynamic characteristics.¹³³

FLIGHT TEST ACCURACY

Stability derivative determination by flight test is generally thought of as being more accurate than determination by either analysis or wind tunnel tests.⁶⁵ Classical steady-state testing and transient response techniques are currently used to extract stability derivatives.

Classical Steady-State Testing

Some stability derivatives can be accurately determined by classical steady-state testing. As an example, methods for extracting longitudinal derivatives were shown in detail in Section 4 of this text.

Lift curve slope, C_{L_α} , can be determined directly for any trim condition. The accuracy of this determination is limited only by the accuracy to which aircraft weight, angle of attack, airspeed (or Mach number), and pressure altitude can be measured.

The derivative C_{D_α} is nonlinear; however, it also can be determined for any trim lift coefficient if values of inflight net thrust can be determined. The accuracy of this derivative estimation is limited by the accuracy to which net thrust, angle of attack, airspeed (or Mach number), and pressure altitude can be measured.

Elevator power, $C_{m_{\delta_e}}$, and the longitudinal static stability derivative, C_{m_α} , can be determined indirectly by measuring elevator deflection. Accuracy of this determination is dependent upon the linearity of the curve of equilibrium lift coefficient versus elevator deflection as well as upon the accuracy to which aircraft weight, airspeed (or Mach number), pressure altitude, aircraft center of gravity, and elevator deflection can be determined.

Lateral-directional derivatives must all be determined indirectly if classical steady-state testing is employed. This is certainly less accurate than the technique just described for determining some of the longitudinal derivatives from steady-state testing. Assessing the accuracy of steady-state lateral-directional derivative determination is a good student homework exercise.

Transient Response Techniques

There are many transient response techniques which can be used to extract stability derivatives if the aircraft free-response is oscillatory. Some of these were discussed in Section 1. If short period damped frequency and damping ratio can be determined easily, then C_{m_α} can be estimated.

Weathercock stability, C_{n_β} , can also be determined if the Dutch roll is oscillatory, but not as accurately because of the coupling in roll and yaw during lateral-directional oscillations. Even general comments on the accuracy of transient response techniques other than MMLT for highly damped aircraft response, i.e., analog matching, or Fourier transform would be speculative. Information available in the literature concerning accuracy of these techniques involves correlation with wind tunnel tests and analysis.⁹⁷

MMLE Transient Response Technique

Increased accuracy is one of the major reasons the AFFTC gives for using MMLE stability derivative extraction techniques.⁶⁰ In an absolute sense, this improved accuracy cannot be shown. One indirect technique described by Maunder has been used to try to validate MMLE derived derivatives. This technique involves a comparison of inflight measured aircraft frequency response, i.e., measured estimates of the aircraft transfer function using SIFT techniques, with the Laplace transformation of the equations of motion, where the Laplace transforms are computed using MMLE extracted stability derivatives. The result is a direct comparison between SIFT determined and MMLE computed aircraft transfer functions in the frequency domain. With respect to the dominant mathematical model parameters, the results of this comparison technique showed the method to be sensitive enough to verify the MMLE derived mathematical model.¹⁰⁶

Statistical error analysis is another technique which can be used to give credibility to claims of MMLE program accuracy. In the computational scheme employed in the MMLE program, there exists the capability (under certain conditions and restrictions) to calculate the statistical variance of the estimated parameter value with respect to the "best estimate" value. Techniques for correcting this variance and confidence level calculated by MMLE have been prepared by Balakrishnan, but have not been used to date in a production aircraft test program.^{106,134} These corrections are based on instrumentation sample rate and measured frequency bandwidth of the noise and their use will probably become common practice.¹⁰⁶ Confidence levels of one standard deviation calculated by the MMLE program have been used as measures of relative accuracy or goodness and will be discussed later along with data correlation. It is hoped that use of the MMLE program for derivative extraction at the USAF Test Pilot School will establish a statistically significant data base which can provide additional evidence of repeatability.

In general, when using parameter estimation techniques, error analysis is extremely important. In the case of the MMLE program, Monte Carlo simulations of the entire process have been made for the purpose of error analysis. This type of simulation has shown that the use of accurate constants in the MMLE derivative extraction program such as aircraft mass,

moment of inertia, and center of gravity location is essential. For example, to have less than a ten percent error in the extracted value of $C_{L_{\delta_e}}$ for the F-4, the aircraft center of gravity must be known to five inches.¹³⁵ As another example, an error in center of gravity location of five inches in a Learjet derivative extraction program caused a thirty percent error in $C_{m_{\alpha}}$.¹³⁶

Aeroelastic and Reynolds Number Effects

A consideration of aeroelastic effects is essential for assessing the accuracy of stability derivatives extracted from flight test data. The test aircraft is obviously elastic. The AFFTC recommends that flight test determined derivatives be presented as a function of dynamic pressure to maintain the linear relationship which usually exists.⁶⁰ Flexibility effects can be assessed from flight test by comparing derivatives obtained at the same angle of attack and Mach number, but at different dynamic pressures. This concept ignores the fact that matching angle of attack, Mach number, and dynamic pressure by varying altitude results in comparing derivatives at different Reynolds numbers. Under these conditions, assuming that coefficient of viscosity is proportional to the square root of the temperature, an astute student can show that:

$$R_{e1}/R_{e2} = T_2/T_1$$

for any two test conditions.

Ignoring Reynolds number differences of this magnitude may not be important for most flight test data points, but it might be for derivatives determined at high angle of attack trim conditions. Current flight test practice is to ignore temperature (Reynolds number) variations.¹³⁰

DATA CORRELATION

Now that factors which effect the accuracy of the various methods for determining stability derivatives have been discussed, typical results of

comparing derivatives determined by analysis, wind tunnel test, and flight test will be presented.

AFFTC MMLE Experience

Figures 78 thru 81 show data which were obtained using the MMLE computer program at the AFFTC. Each data point plotted versus angle of attack represents an independent test condition. The vertical lines presented on these plots represents one standard deviation confidence levels as computed by the MMLE program.

These data exhibited significant repeatability when they were obtained at similar test conditions; however, as expected, some derivatives show more scatter than others. Data are so closely grouped on some plots that it is difficult to distinguish one point from another, e.g.,

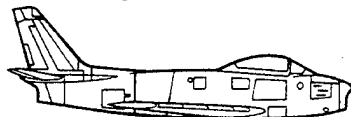
C_{l_β} , C_{n_β} , and C_{Y_β} on Figure 78. However, sideforce due to rudder, $C_{Y_{\delta_r}}$,

and aileron, $C_{Y_{\delta_a}}$, in particular on Figures 79 and 80 show considerable

scatter.

Flight test derivatives determined by MMLE techniques and shown on Figures 78 thru 81 also agree reasonably well with the wind tunnel data shown. Except for some sideforce derivatives, flight test and wind tunnel determined derivatives generally agree within 25 percent. This is not the case in all flight test programs. Some significant disagreements will be discussed in Section 6; however, data presented here are typical of the results obtained on many other flight test programs at the AFFTC. In general, the AFFTC has shown data with significant repeatability which lends confidence that the technique yields at least consistent results.¹⁰⁶

THEOREM XIX: Given perfect data and a perfect model, unique results can be obtained.¹¹⁸



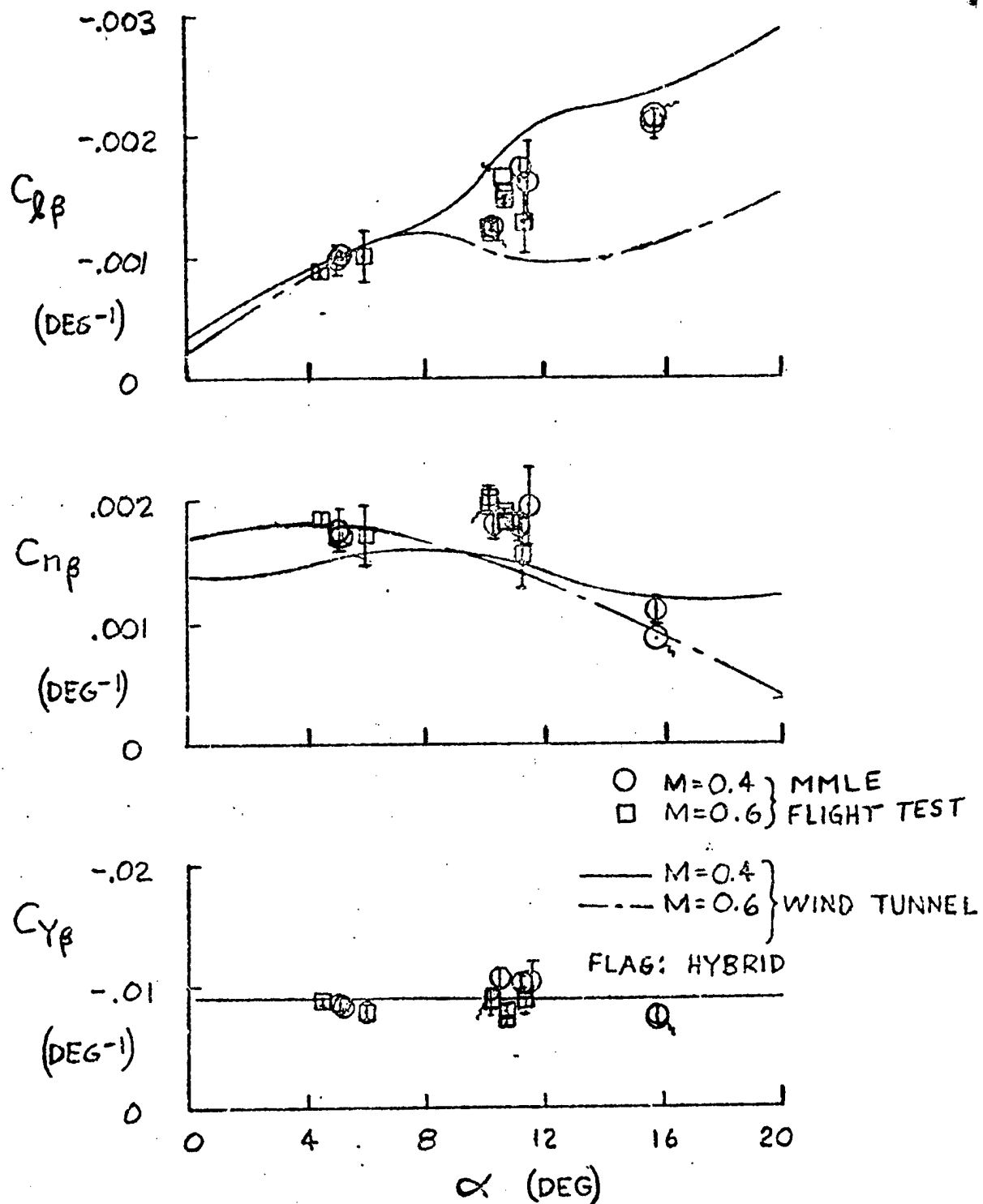


Figure 78: Typical AFFTC MMLE Lateral-Directional Stability Derivative Data.¹⁰⁶

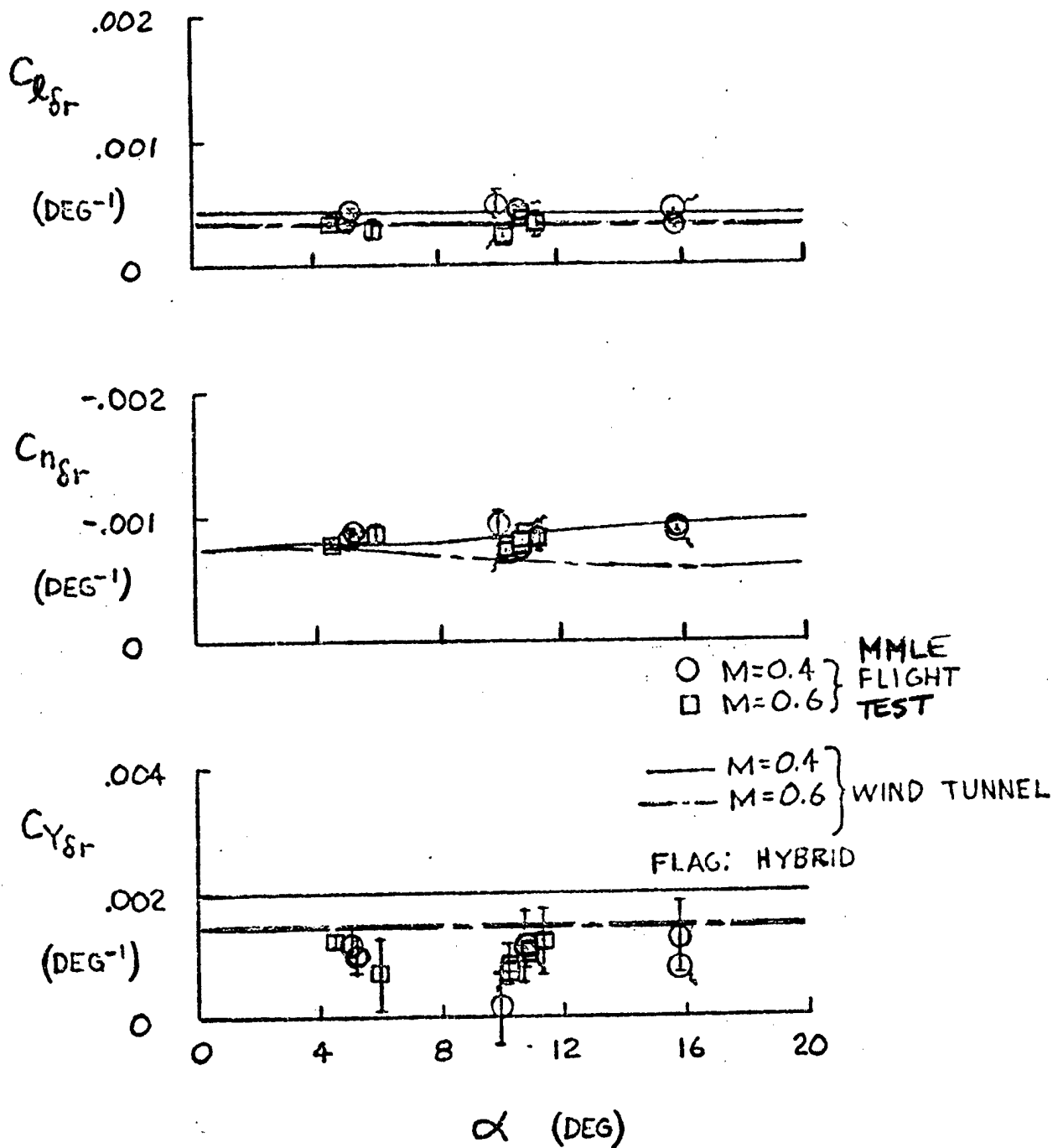


Figure 79: Typical AFFTC MMLE Lateral-Directional Stability Derivative Data.¹⁰⁶

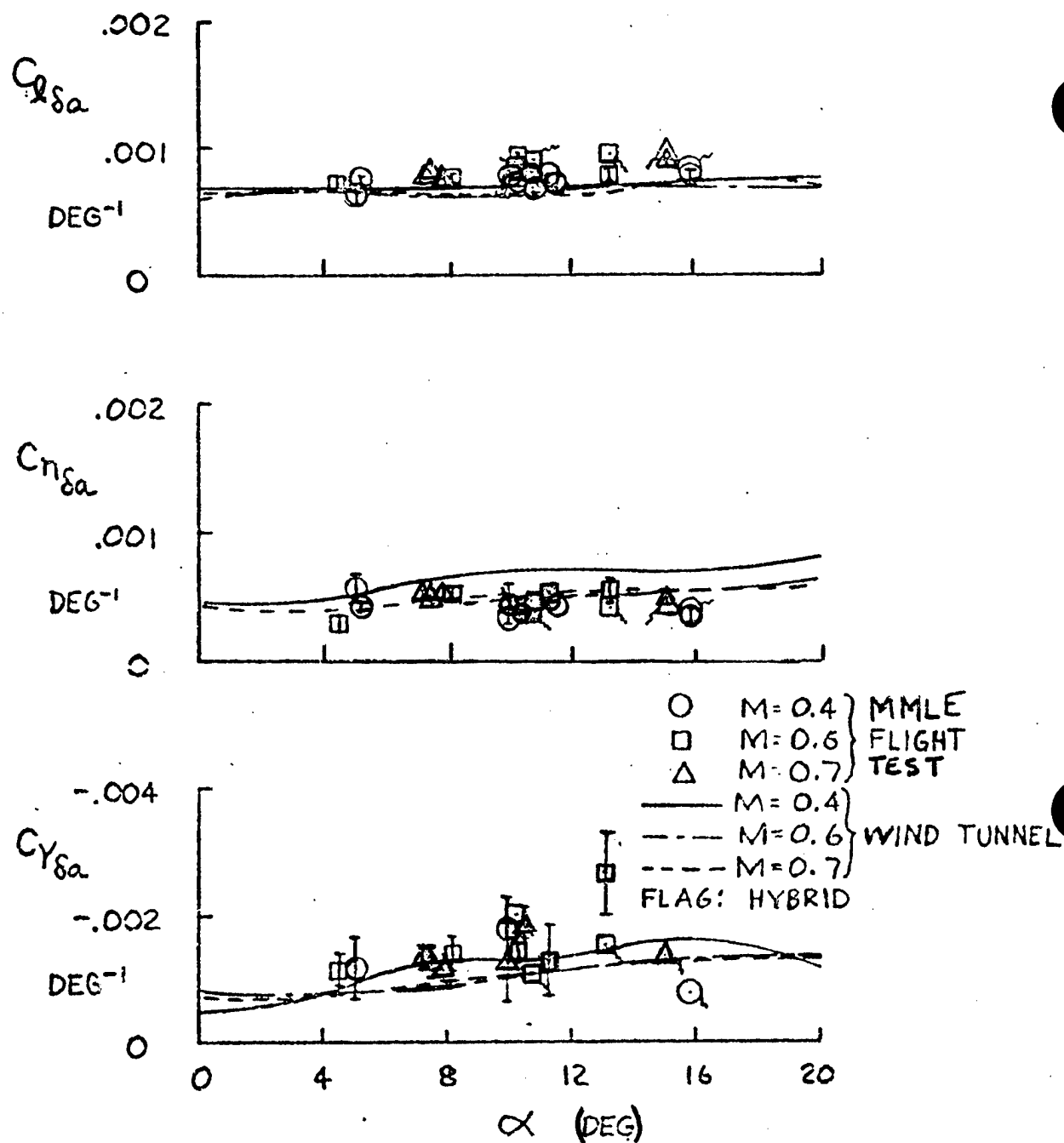


Figure 80: Typical AFFTC MMLE Lateral-Directional Stability Derivative Data.¹⁰⁶

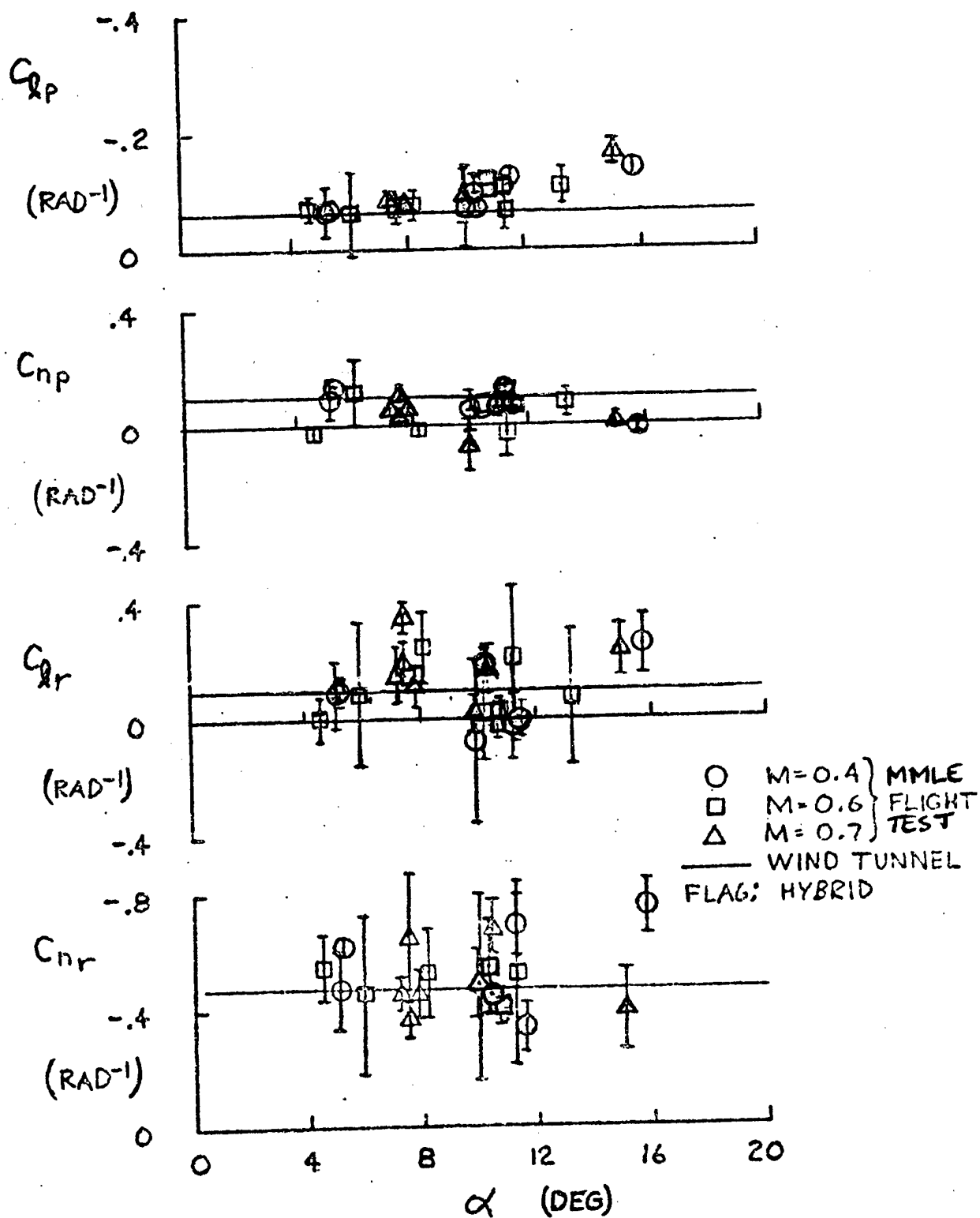


Figure 81: Typical AFFTC MMLE Lateral-Directional Stability Derivative Data.¹⁰⁶

Figures 82 and 83 are typical examples of the correlation between classical steady-state sideslip and MMLE stability derivative extraction techniques. The data symbols plotted on Figure 82 were measurements taken directly from steady-heading sideslip maneuvers, while the faired lines depict data obtained by calculation from MMLE determined derivatives. Figure 83 shows similar data taken over a wide range of Mach numbers. This agreement is graphic evidence that the MMLE stability derivative extraction technique yields nearly identical results as does the classical steady-state, steady-heading sideslip maneuver.¹⁰⁶

A complete set of YF-16 stability derivatives extracted using MMLE techniques was presented in Section 4. Many derivatives agreed extremely well with the wind tunnel data presented. For the derivatives C_{m_α} , C_{Y_β} , C_{ℓ_p} , $C_{n_{\delta_r}}$, and $C_{\ell_{\delta_r}}$ as shown on Figures 47, 53, 59, 70, 71 and 72, the wind tunnel results could just as well be lines faired through the MMLE flight test data. However, there was a significant difference for at least one major derivative, C_{m_α} , as it varied with angle of attack. Figure 44 shows that the wind tunnel estimate for zero static margin $\left(C_{m_\alpha} = 0 \right)$ occurred at about 14.5 degrees angle of attack. The MMLE flight test data shows that zero static margin occurred at about 22.5 degrees angle of attack. The AFFTC believes the wind tunnel data to be in error.¹⁰⁶ Some of these YF-16 stability derivatives will be discussed further in Section 6 and used as examples to illustrate the use of parameter analysis methods.

USAF Test Pilot School students should be very aware of the fact that "apparent accuracy" can be greatly influenced by data presentation methods. See Figures 52 and 53 where the same data and data fairings are presented with different vertical scales.

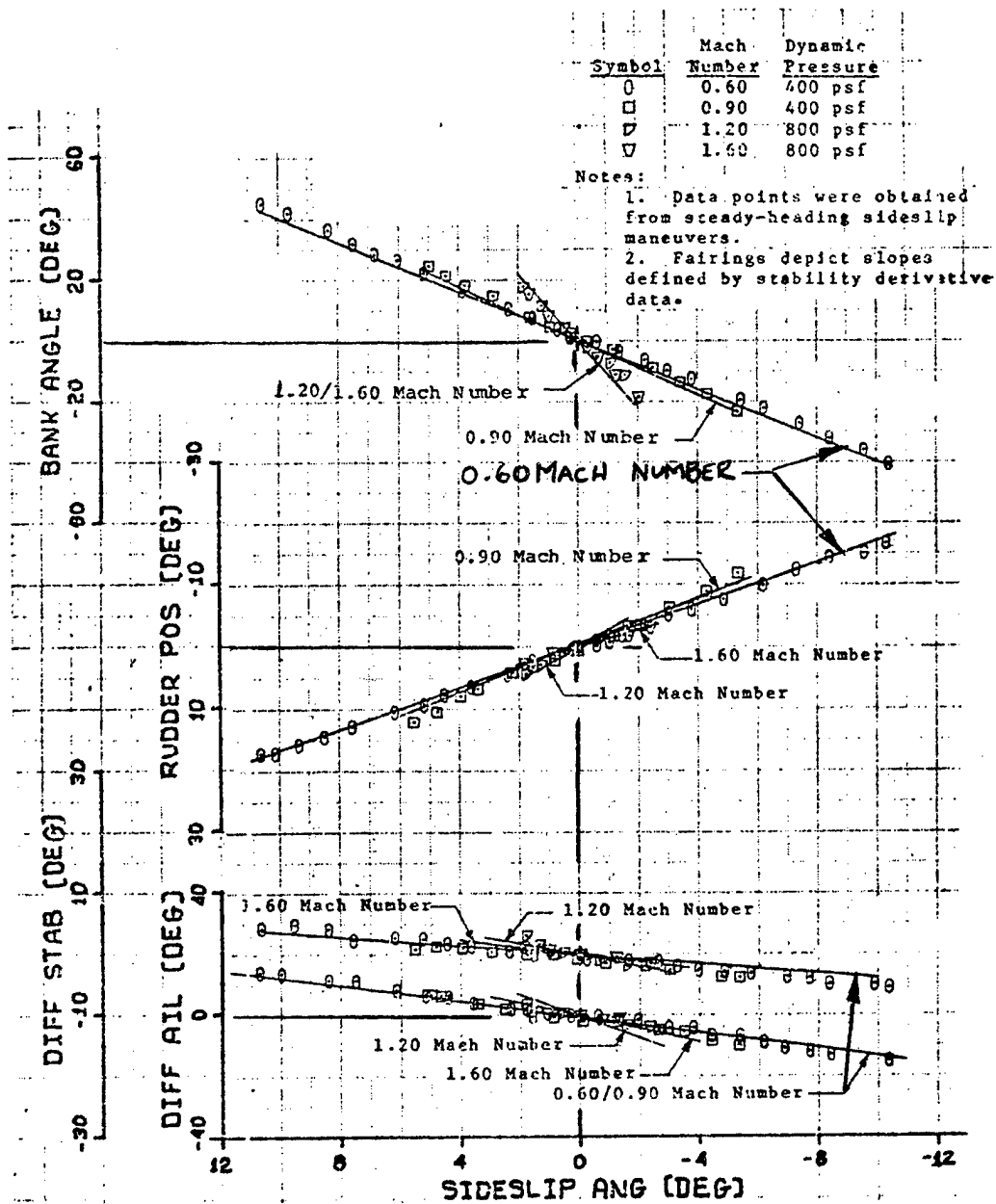


Figure 82: Typical AFFTC Lateral-Directional Data.¹⁰⁶

NOTE: SOLID SYMBOLS CALCULATED
FROM MMLE DERIVATIVES

OPEN SYMBOLS FROM
STEADY HEADING SIDESLIPS

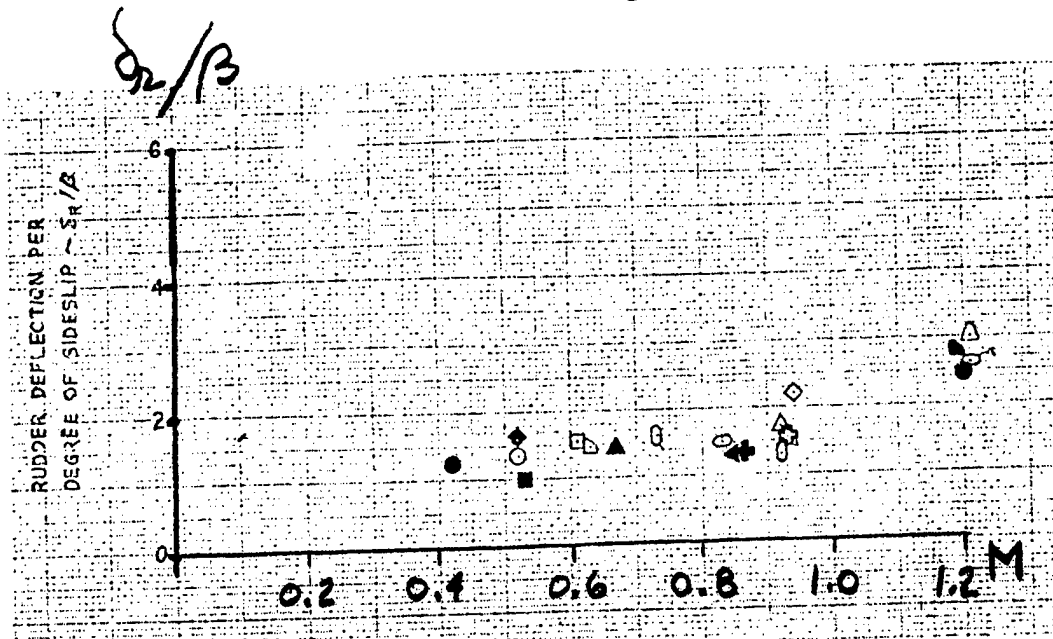
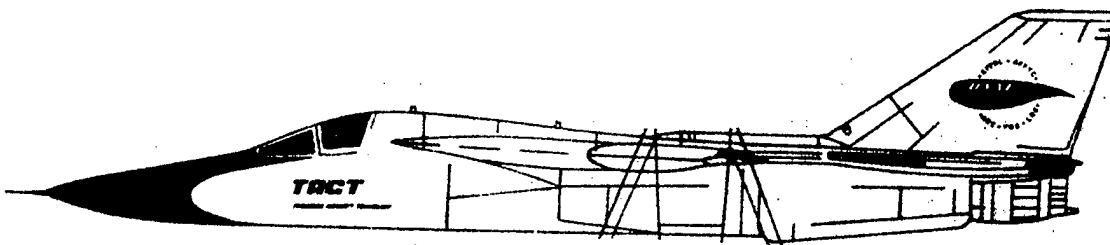


Figure 83: Typical AFFTC Lateral-Directional Data Summary.¹⁰⁶



TACT AIRCRAFT
(MODIFIED F-111A)

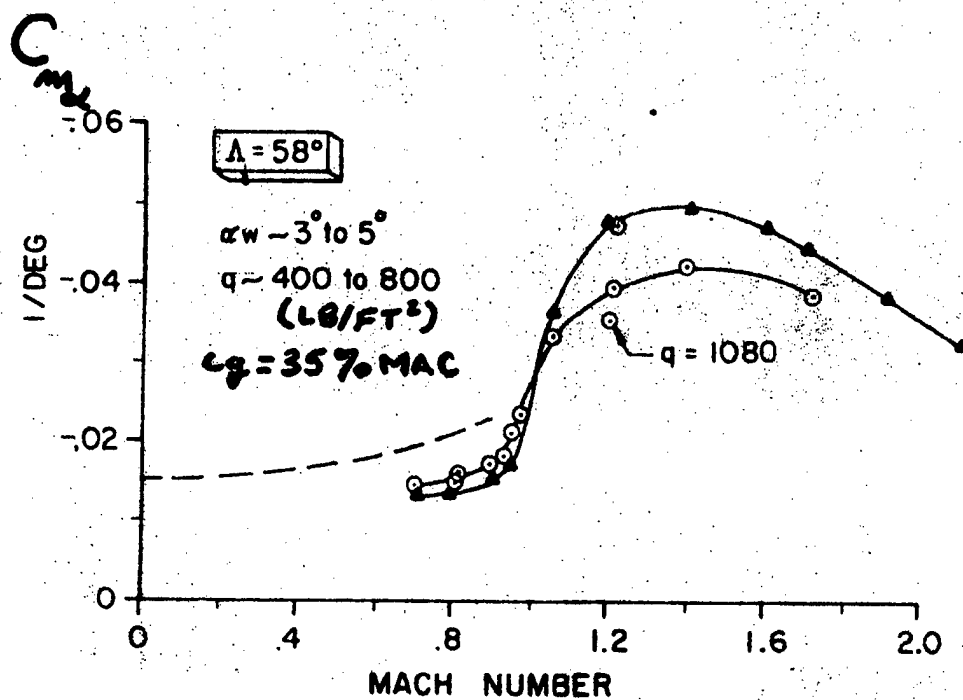
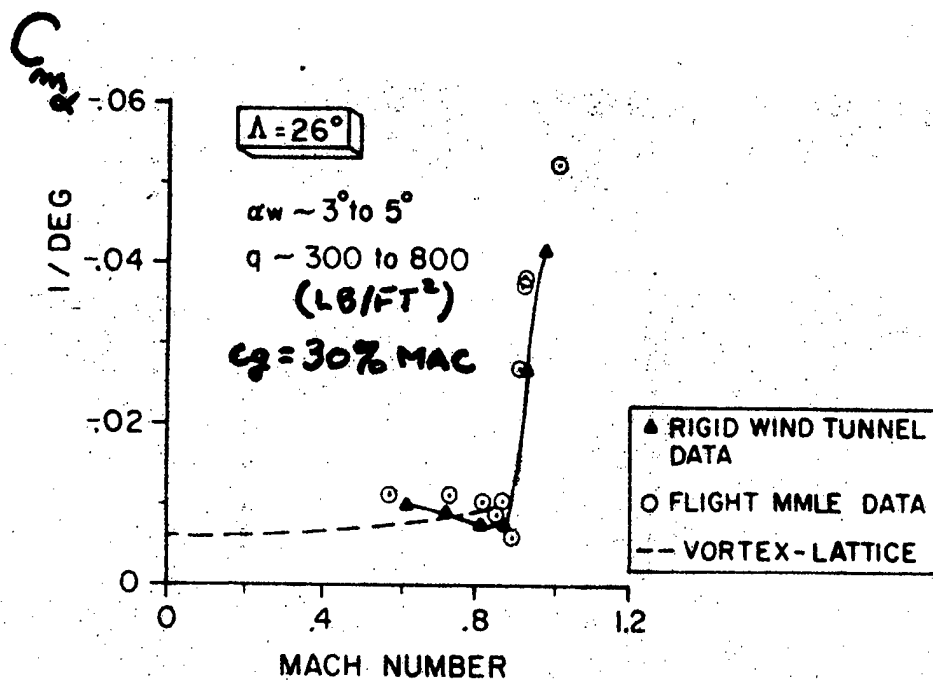
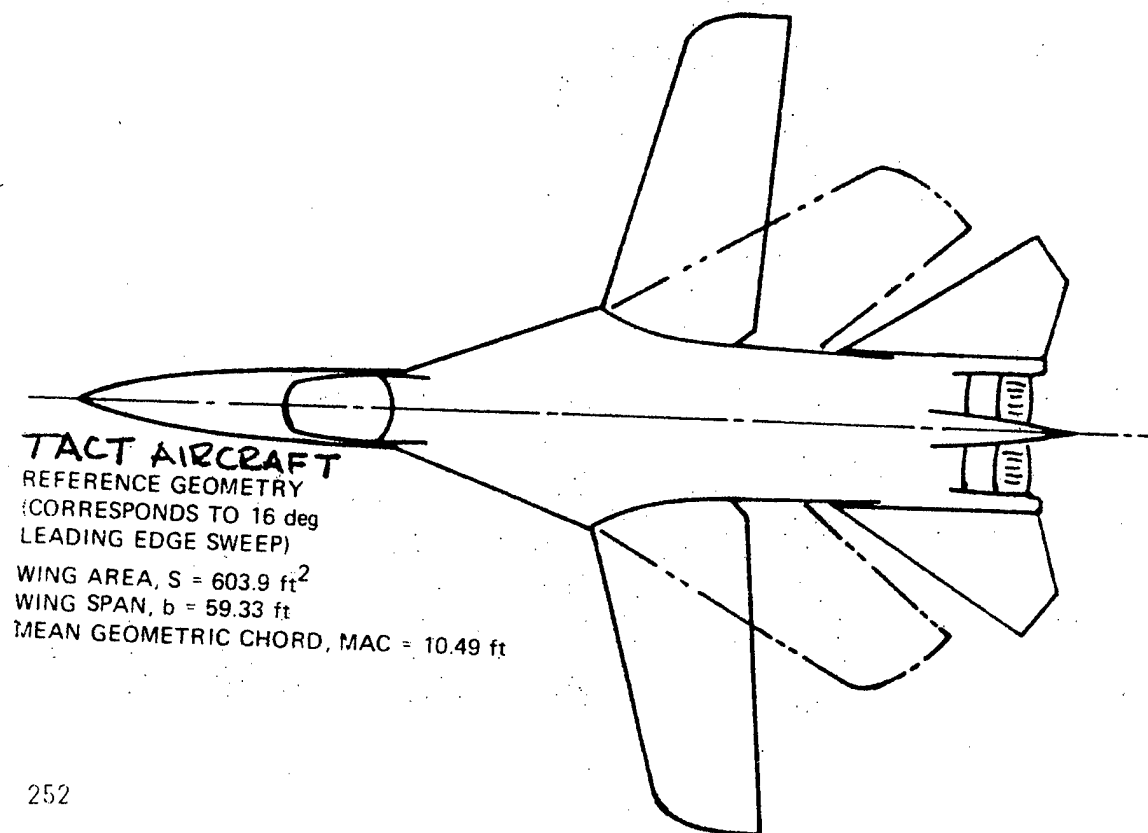


Figure 85: Variation of Longitudinal Stability with Mach Number for the TACT Aircraft.¹²⁹

however, supersonically the flight C_{N_α} extracted using the MMLE program is approximately 30 percent below the rigid wind tunnel data. Since estimated aeroelastic effects account for approximately a 10 percent loss, this difference is considered excessive. Analysis of classical maneuvering flight data shows that the longitudinal dynamic doublets did not provide sufficient information for the MMLE program to separate C_{N_α} and $C_{N_{\delta_e}}$, particularly at the conditions where the aircraft is very stable, and that a high weighting should be applied to the a priori value of $C_{N_{\delta_e}}$ to improve the accuracy of the MMLE extracted C_{N_α} .¹²⁹

The corresponding pitch damping derivatives ($C_{m_q} + C_{m_\alpha}$) and elevator power, $C_{m_{\delta_e}}$, are shown in Figure 86 as functions of Mach number.

These data show considerable scatter; however, these comparisons do indicate that wing sweep has a minor effect on these derivatives.



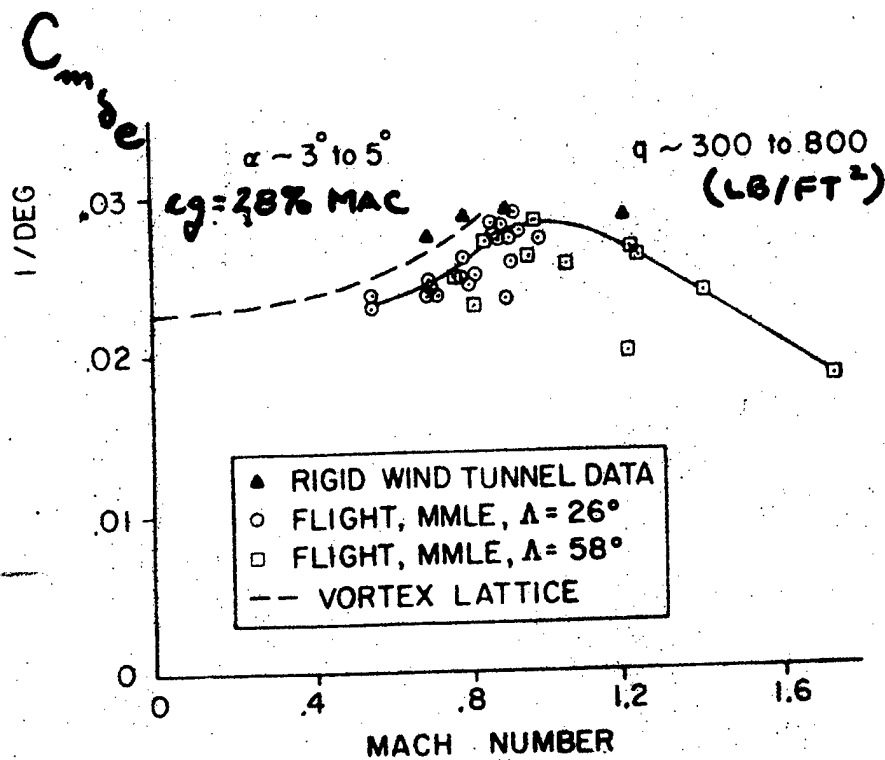
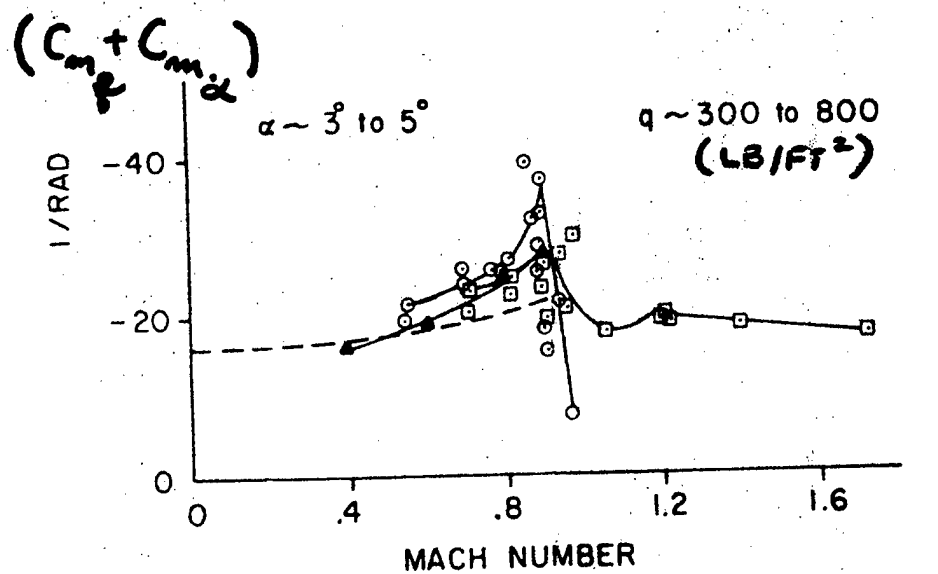
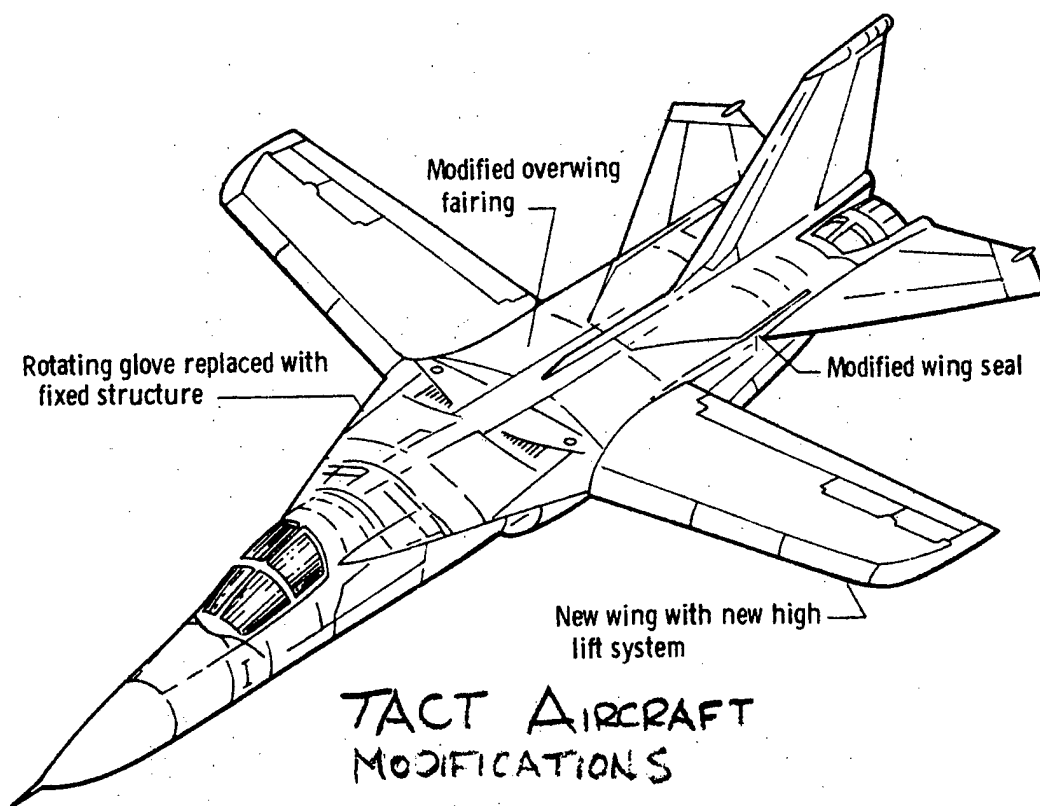


Figure 86: Pitch Damping and Elevator Power Versus Mach Number for the TACT Aircraft.¹²⁹

The variation of C_{N_α} , C_{m_α} , and $(C_{m_q} + C_{m_\alpha})$ with angle of attack is shown in Figure 87 for 26 degree wing sweep at 0.90 Mach number and dynamic pressure of 800 lb/ft². These data are compared to rigid wind tunnel data and indicate the nonlinear nature of these derivatives with angle of attack and point out the need for duplication of angle of attack to obtain a valid correlation between data sets.¹²⁹



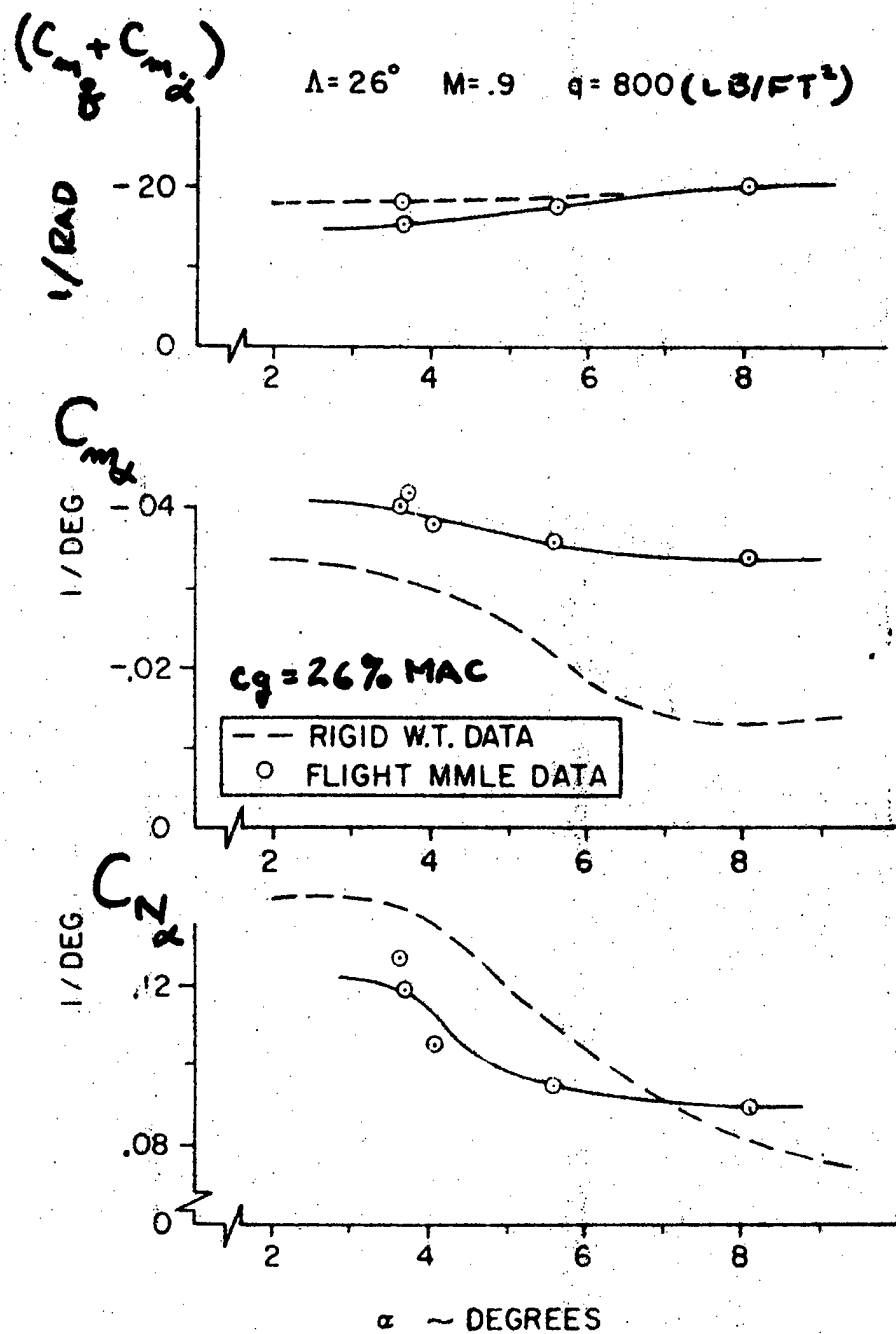
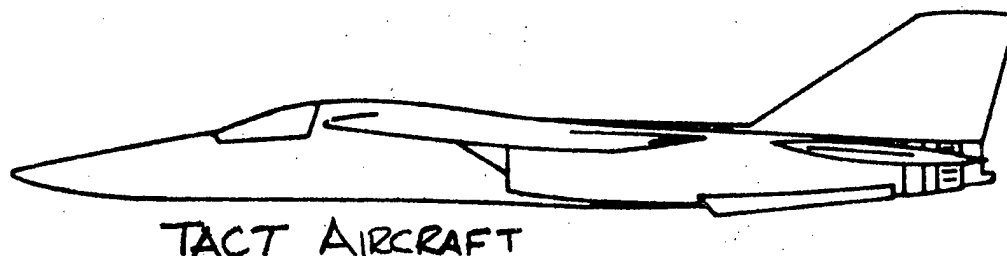


Figure 87: Variation of Longitudinal Derivatives with Angle of Attack for the TACT Aircraft.¹²⁹

The variation of elevator power with dynamic pressure is shown on Figure 88. The rigid wind tunnel data as corrected for flexibility using FLEXSTAB estimates does represent an average of the flight data. This parameter usually is easily identified and should have comparatively little scatter. However, these data do show more scatter than desired, which is probably due to the relatively high stability of these flight conditions.¹²⁹

Reference 129 also presents the variations of the TACT aircraft longitudinal derivatives ($C_{m_q} + C_{m_{\dot{\alpha}}}$), $C_{N_{\alpha}}$, and $C_{m_{\alpha}}$ with dynamic pressure, and $C_{m_{\delta_e}}$ with angle of attack for various wing sweep angles. The presentation in Reference 129 offers a very complete comparison of longitudinal stability derivatives determined from flight test using the MMLE program with wind tunnel and analytical estimates.



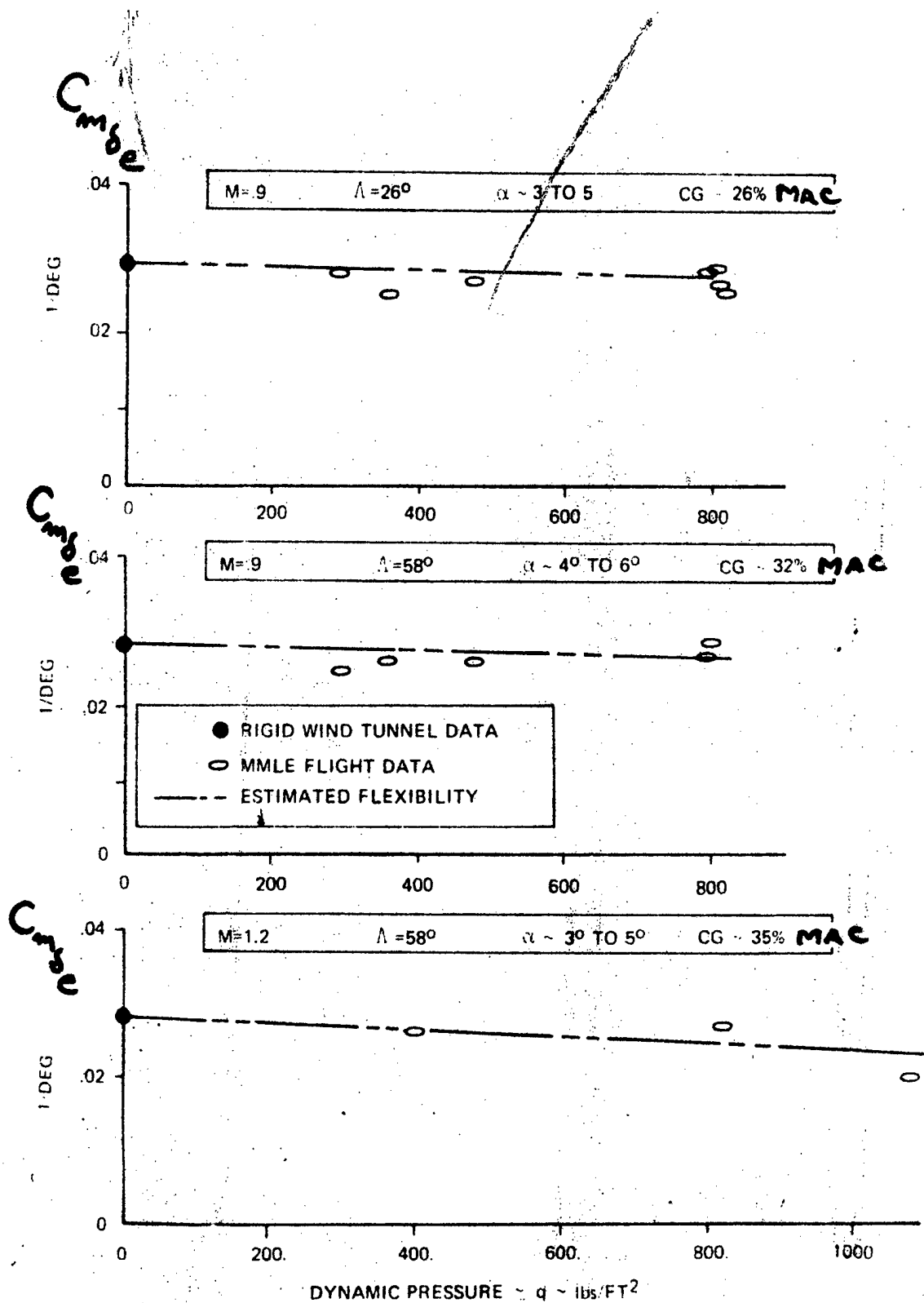
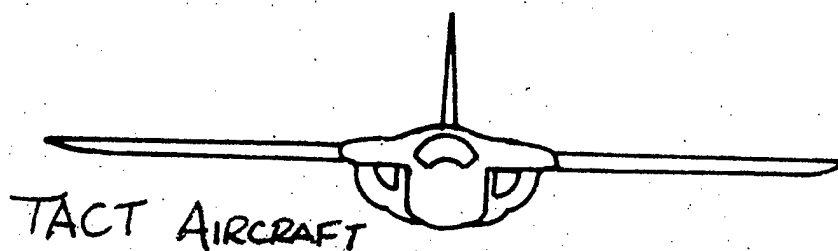


Figure 88: Variation of Elevator Control Power with Dynamic Pressure for the TACT Aircraft.¹²⁹

A limited amount of lateral-directional data are presented here to give an indication of the type and quality of data obtained from the TACT flight test program, and how it correlates with wind tunnel data and aeroelastic corrections.¹²⁹

The lateral-directional derivatives extracted from flight test data using the MMLE program are presented on Figures 89, 90, and 91 for a Mach number of 0.9 at wing sweeps of 26 and 58 degrees as functions of angle of attack. The sideslip derivatives, C_{n_β} and C_{ℓ_β} , presented in Figure 89 show considerable scatter, but definite variations with angle of attack are indicated. The roll rate derivatives, C_{ℓ_p} and C_{n_p} , shown in Figure 90 have more scatter than the sideslip derivatives; however, distinct angle of attack variations can still be defined for both wing sweeps. The yaw rate derivatives, C_{n_r} and C_{ℓ_r} , presented in Figure 91 have a large amount of scatter and only general angle of attack variations can be determined.



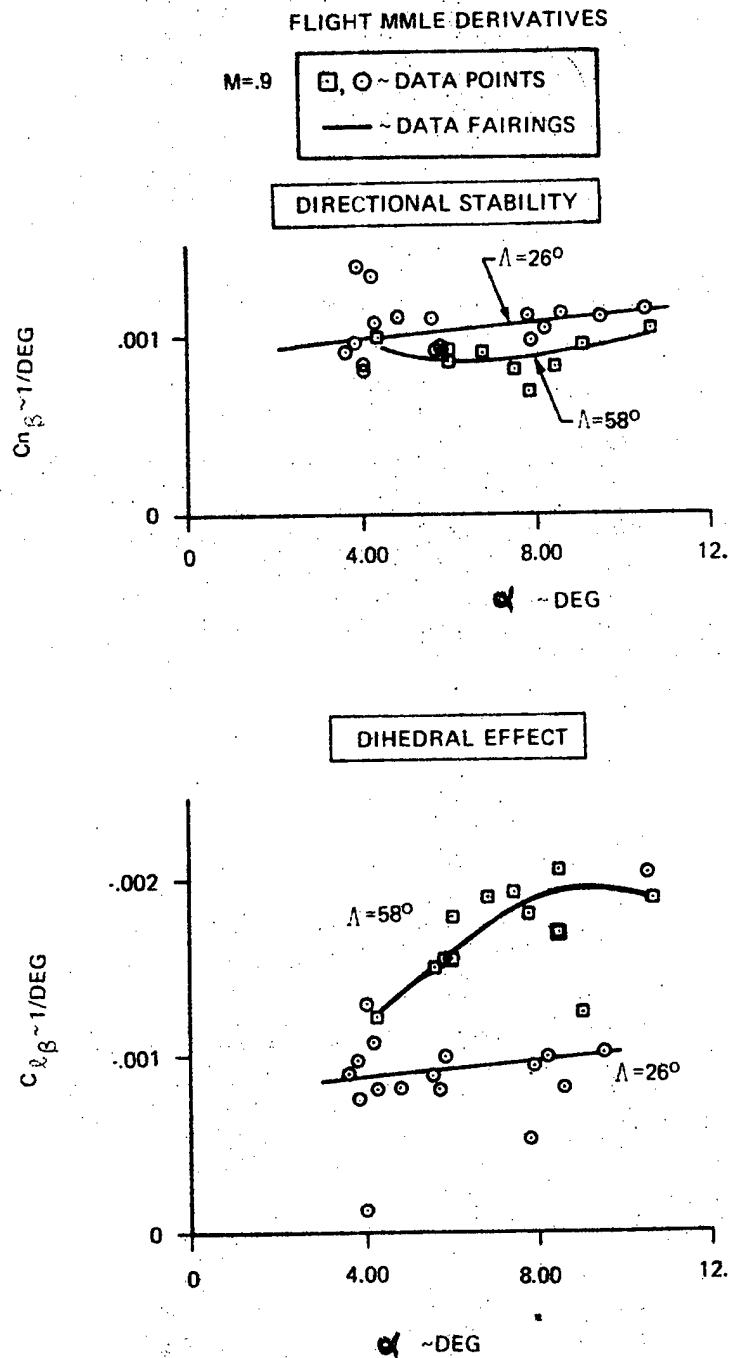


Figure 89: Variation of Sideslip Derivatives with Angle of Attack for the TACT Aircraft.¹²⁹

M=9 FLIGHT MMLE DERIVATIVES

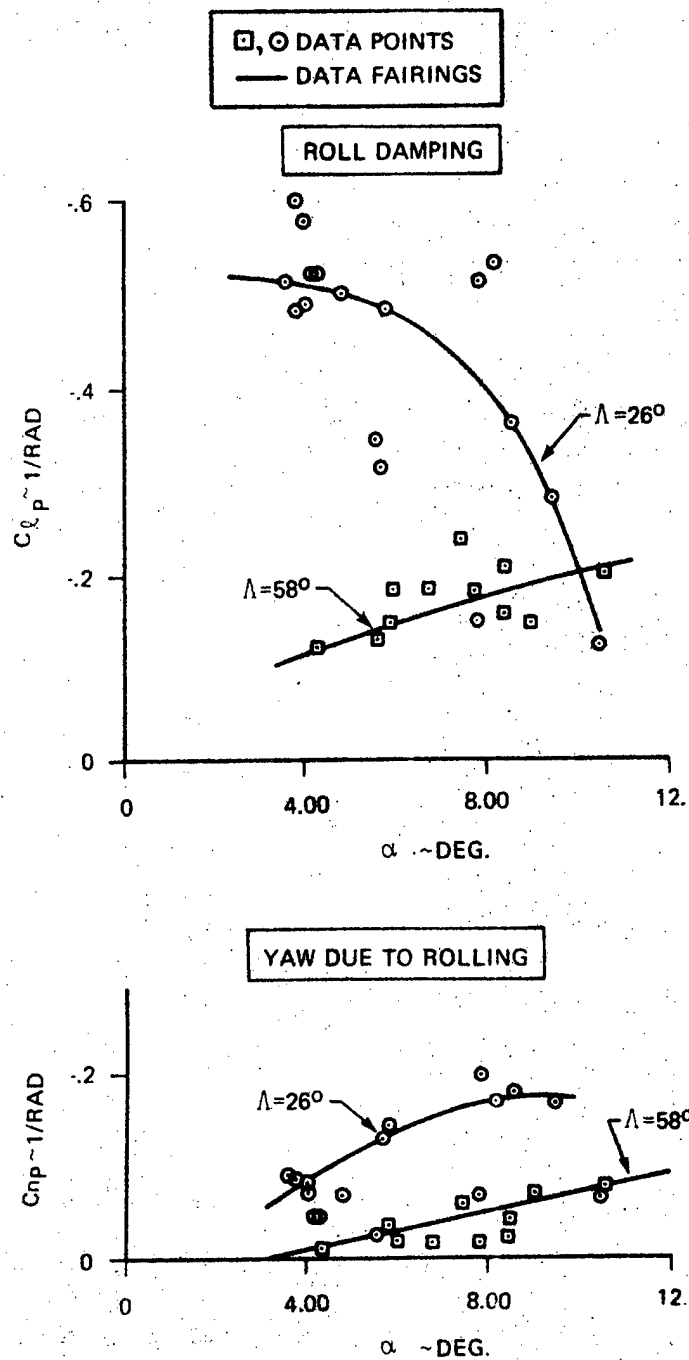


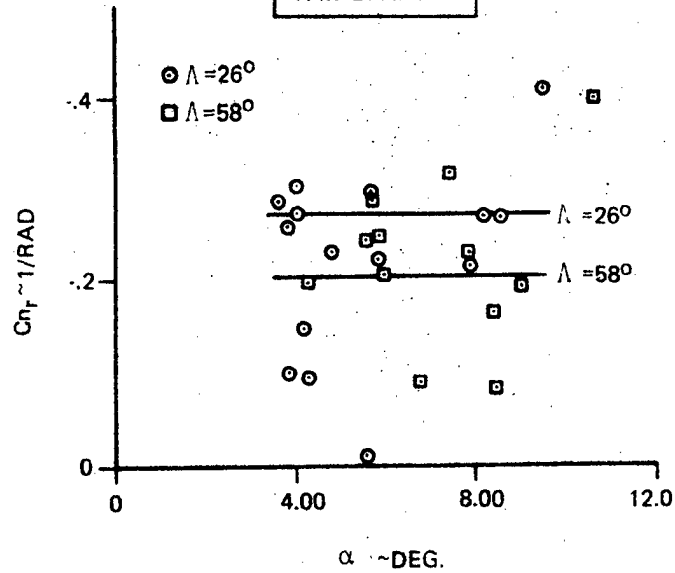
Figure 90: Variation of Roll Rate Derivatives with Angle of Attack for the TACT Aircraft.¹²⁹

M=9

FLIGHT MMLE DERIVATIVES

□, ○ DATA POINTS
— DATA FAIRINGS

YAW DAMPING



ROLL DUE TO YAW RATE

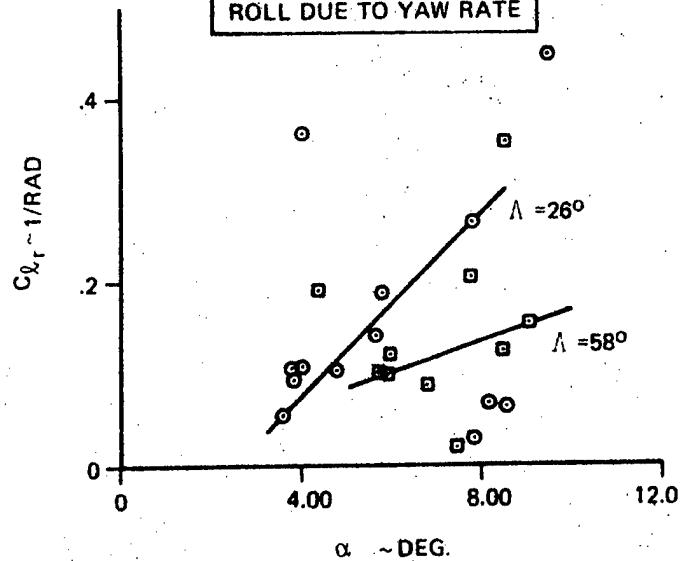
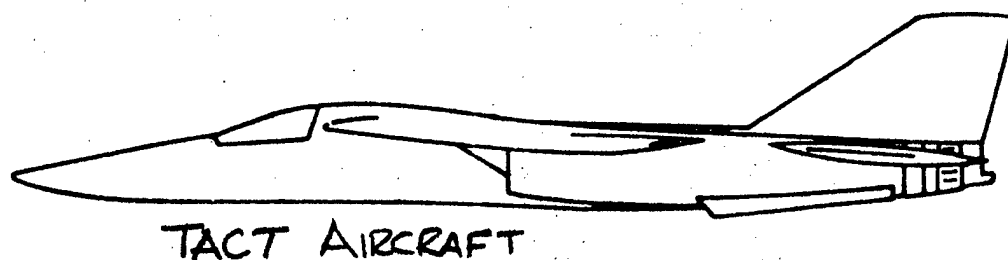


Figure 91: Variation of Yaw Rate Derivatives with Angle of Attack
for the TACT Aircraft. 129

Figures 92, 93, and 94 present TACT aircraft lateral-directional derivatives as functions of dynamic pressure for the Mach number 0.9 and 26 degree wing sweep condition. Also shown for comparison with the flight test MLE program determined derivatives are rigid wind tunnel values or estimated values and the flexible variation with dynamic pressure as predicted by FLEXSTAB analysis.¹²⁹

The sideslip derivatives presented in Figure 92 show that flight test determined directional stability is lower than wind tunnel values, as faired, and has a greater loss with increasing dynamic pressure. Equal weighting for the 500 lb/ft² dynamic pressure point on the C_{n_β} plot would have matched flight test and wind tunnel directional stability trends with dynamic pressure variation. The flight test data also shows that dihedral effect increases with increasing dynamic pressures (C_{l_β} becomes more negative) and that a similar variation is predicted by FLEXSTAB analysis. The wind tunnel value shown here is considerably higher than the flight test values and was obtained from a 1/12-scale model tested in the NASA Ames 11-foot wind tunnel.¹²⁹



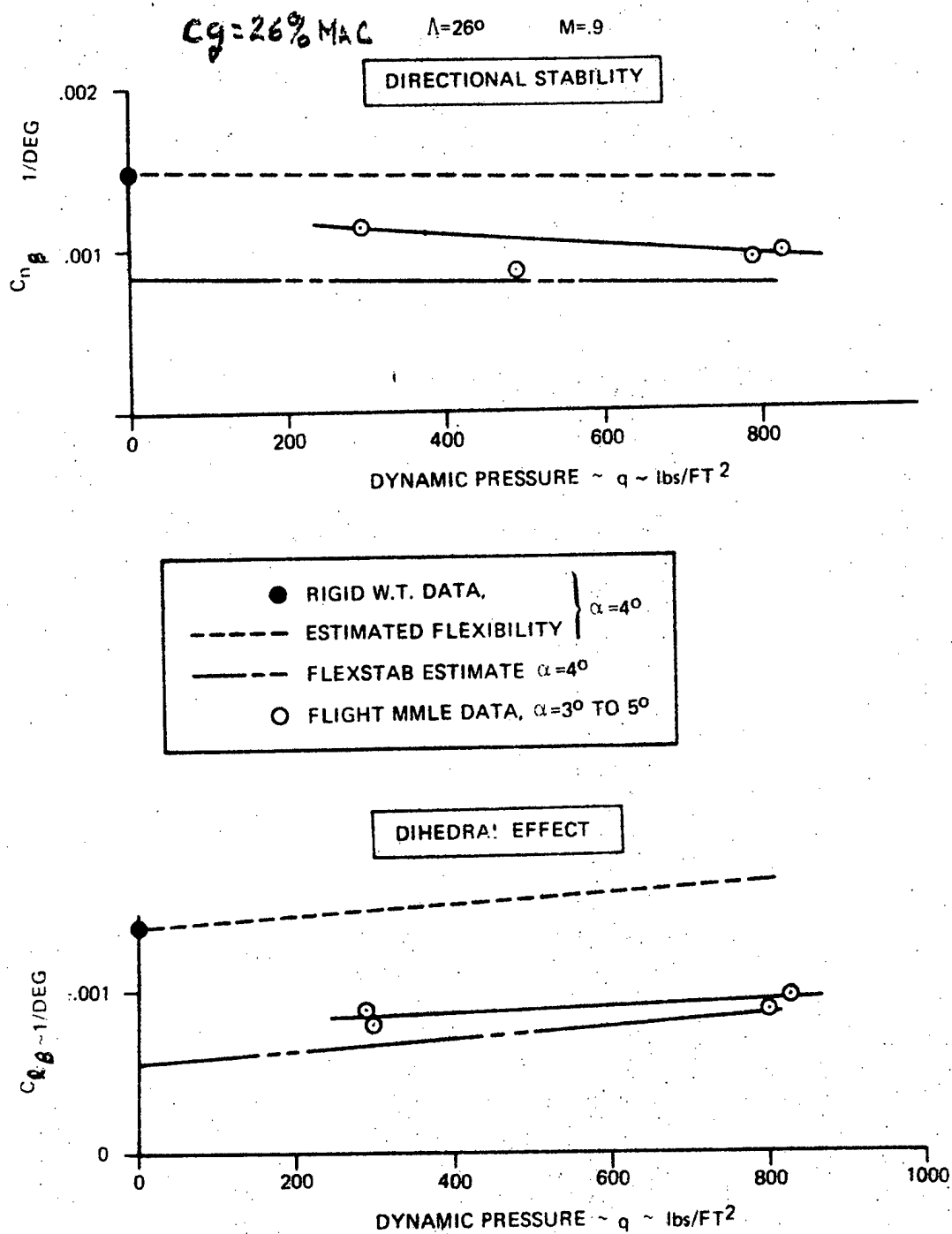
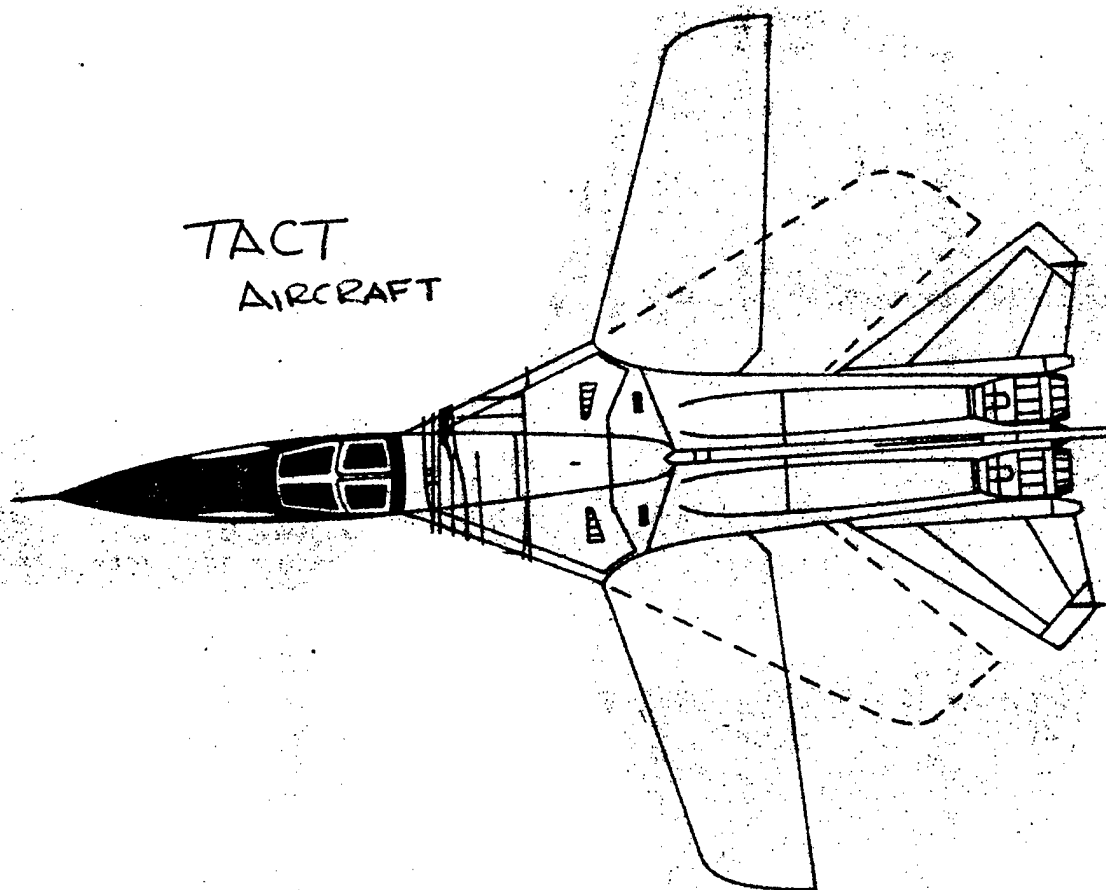


Figure 92: Variation of Sideslip Derivatives with Dynamic Pressure for the TACT Aircraft.¹²⁹

The TACT aircraft roll rate derivatives are presented in Figure 93 and the flight test data show an increase in the magnitude of C_{n_p} with increasing dynamic pressure. The FLEXSTAB analysis predicted a lower value of C_{n_p} and no appreciable change with dynamic pressure. The roll damping, C_{l_p} , as faired from flight test shows a slight decrease with increasing dynamic pressure. However, FLEXSTAB analysis predicted an increase in C_{l_p} with increasing dynamic pressure. The estimated rigid value of C_{l_p} is approximately 20 percent lower than the flight test value.¹²⁹



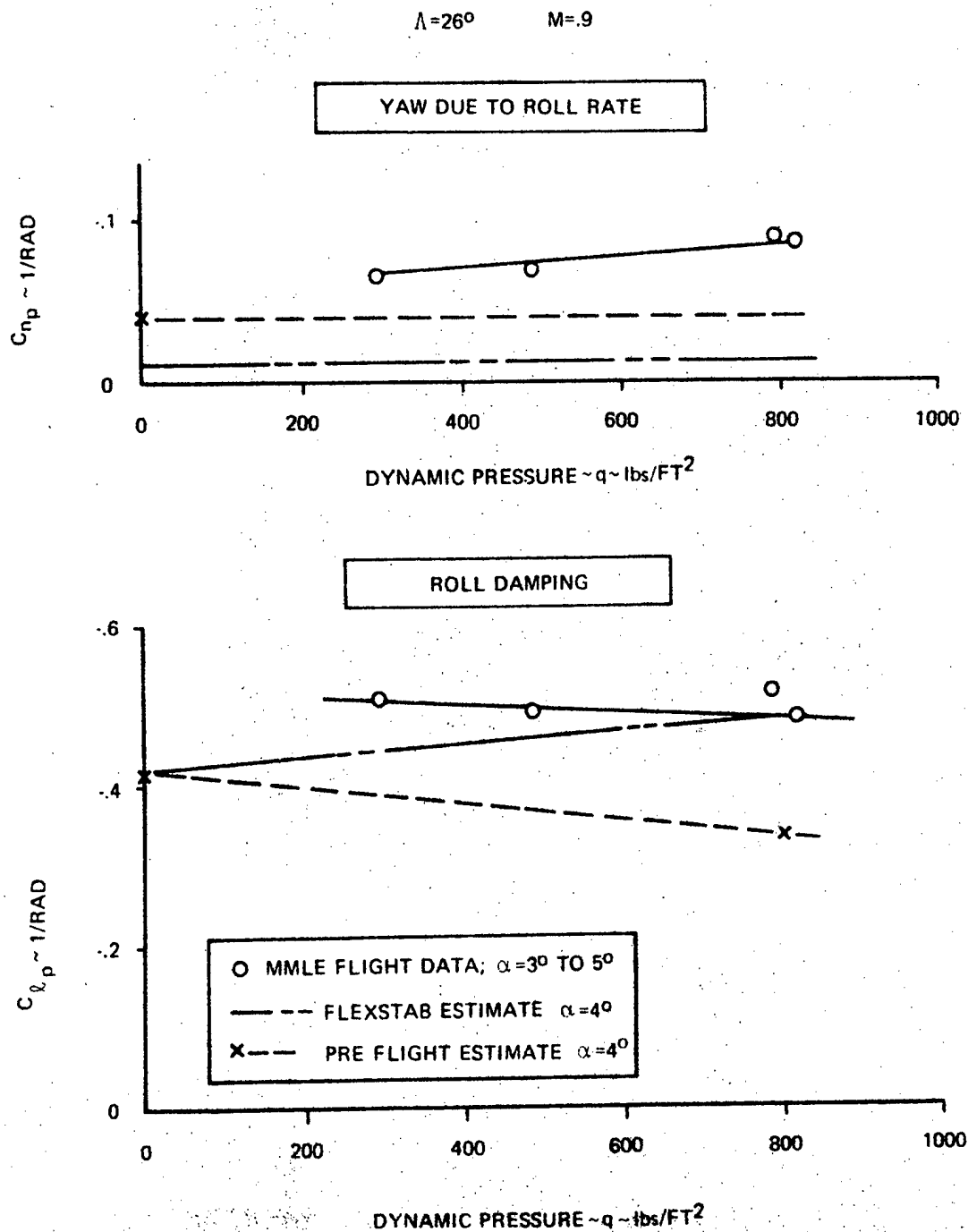
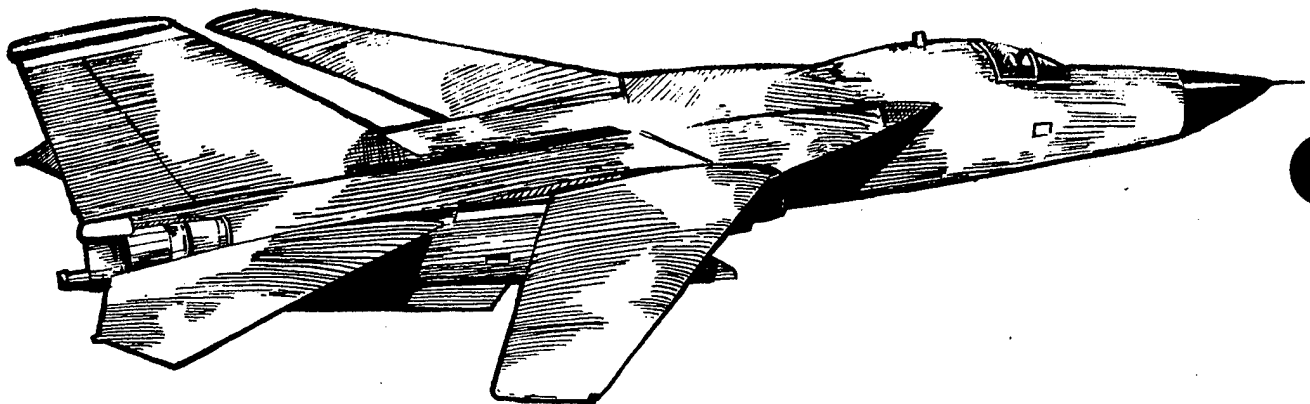


Figure 93: Variation of Roll Rate Derivatives with Dynamic Pressure for the TACT Aircraft.¹²⁹

The TACT aircraft yaw rate derivatives are presented in Figure 94 and the flight test data faired as shown indicates no effect with dynamic pressure. The FLEXSTAB analysis shows a very small decrease in C_{n_r} and a substantial decrease in C_{ℓ_r} with increasing dynamic pressure. Reference 129 attributes this decrease to the decrease in lift coefficient at a constant angle of attack resulting from the increase in wing twist with increasing dynamic pressure. If all flight test data points had been given the same weight in fairing the C_{ℓ_r} curve in Figure 94, this effect would have also been shown in the flight test data.



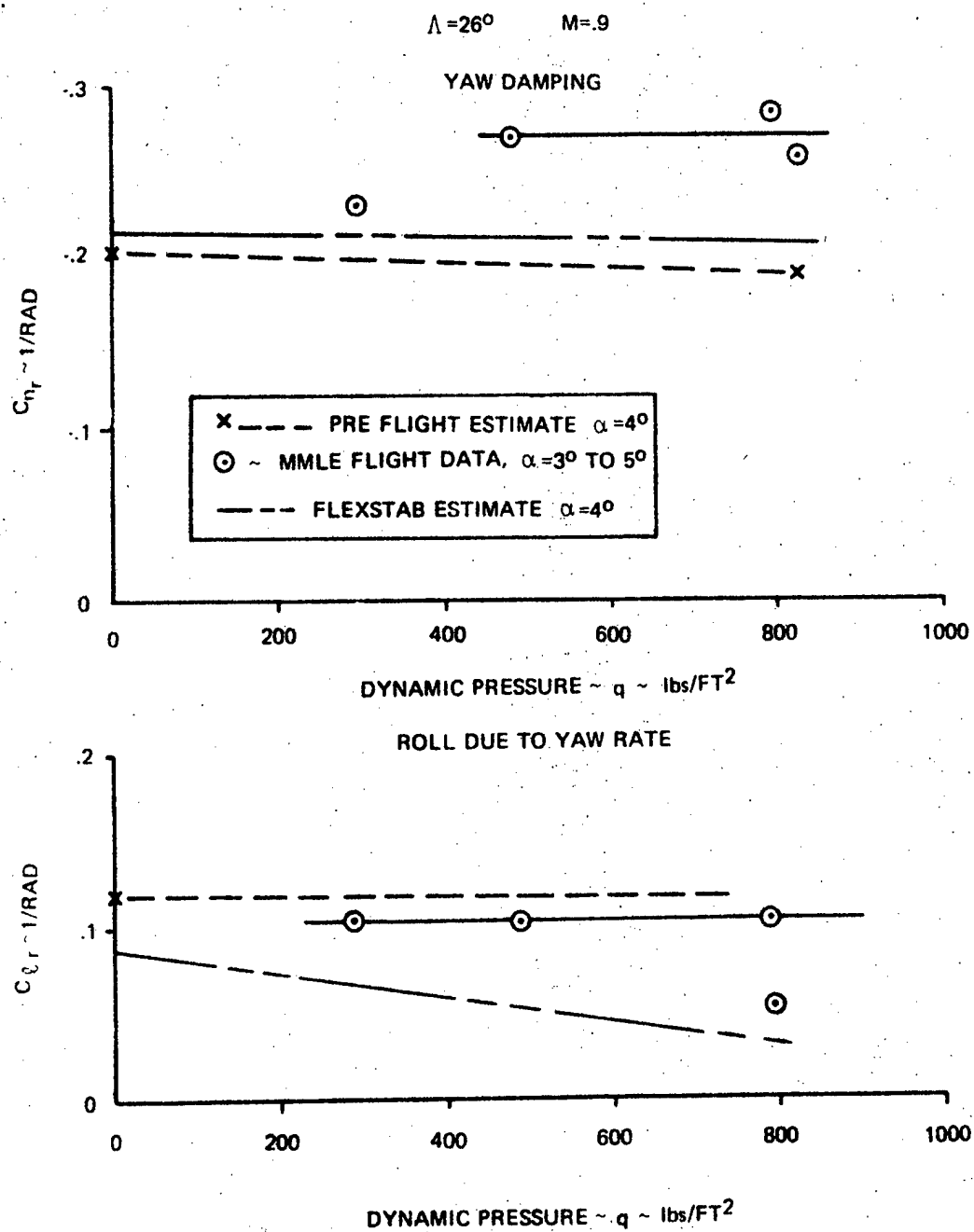


Figure 94: Variation of Yaw Rate Derivatives with Dynamic Pressure
for the TACT Aircraft.¹²⁹

Dynamic Mode Comparison. The TACT aircraft short period damping ratio at some test points decreased to a level that allowed accurate measurements of Period, P , and time to one-half amplitude, $T_{1/2}$, from the aircraft response time histories. These measurements are compared in Table 5 to the P and $T_{1/2}$ values calculated by a digital program that used the MMLE flight derivatives as input data. Significant differences can be seen between the measured and calculated values for some of the listed conditions.¹²⁹ The percentage differences between calculated and measured values of P and $T_{1/2}$ are also shown in Table 5. As expected, the values of P show better correlation. Percentage differences may not be the best way to compare these data. Statistical analysis of the significance of these data is a good student homework exercise. Assuming second order aircraft response, the ability to predict damping ratios and periods of aircraft modes of motion using MMLE determined derivatives would be a valid indicator of derivative accuracy.

Flying Qualities. The AFFDL also determined TACT aircraft dynamic parameters, like longitudinal short period and lateral-directional Dutch roll damping ratio, ζ , and natural frequency, ω_n , in a flying qualities analysis by Yeager.¹²¹ These parameters calculated from MMLE flight test determined derivatives were compared with the same dynamic parameters directly measured from flight test data. These flight test derived dynamics were also compared to Digital Datcom estimates, and Digital Datcom estimates modified by wind tunnel test results.^{119,121}

The AFFDL used a technique similar to the one used by the USAF Test Pilot School in calculating the percentage differences shown in Table 5 to define dynamic parameter error. Both short period and Dutch roll damping ratios and natural frequencies were analyzed by the AFFDL. The differences between values of ζ and ω_n calculated from MMLE determined derivatives and values directly measured from response time histories were determined using the following relation:

TABLE 5: COMPARISON OF LONGITUDINAL SHORT PERIOD DYNAMICS
FOR THE TACT AIRCRAFT.¹²⁹

CASE NUMBER	FLIGHT CONDITIONS				MMLE FLIGHT DERIVATIVES			CALCULATED DYNAMICS		MEASURED DYNAMICS		% DIFFERENCE*	
	Λ	M	\bar{q}	α TRIM	$Cm_{\dot{\alpha}}$	$Cmq + Cm_{\dot{\alpha}}$	$CN_{\dot{\alpha}}$						
53/51	26	.9	291	4.7	-.0284	-32.36	.113	P ~ SEC 2.17	$T_{1/2}$ ~ SEC .82	P ~ SEC 2.15	$T_{1/2}$ ~ SEC .87	P + 0.9	$T_{1/2}$ - 5.7
51/52			293	5.5	-.029	-36.8	.105	2.31	.91	2.34	1.0	- 0.9	- 9.0
53/57			479	5.8	-.0292	-29.74	.095	1.716	.637	1.63	.72	+ 5.5	-11.1
57/53			820	5.6	-.0375	-18.	.095	1.222	.58	1.15	.65	+ 6.1	-10.8
53/56			478	4.0	-.0368	-25.5	.138	1.536	.595	1.54	.7	0	-14.3
57/51			808	3.6	-.0422	-15.2	.119	1.166	.567	1.17	.57	0	0
59/53			804	3.6	-.0432	-18.3	.127	1.132	.486	1.15	.55	- 1.7	-10.9
56/56	58	1.23	406	4.8	-.0483	-19.2	.057	1.422	1.451	1.45	1.45	- 2.1	0
57/55		1.21	823	3.3	-.0356	-19.97	.0576	1.147	.684	1.17	.69	- 1.7	- 1.4
59/54		1.20	1085	3.6	-.0377	-19.5	.0577	1.038	.637	1.05	.69	- 1.0	- 7.2
44/58		.90	300	6.8	-.018	-36.6	.061	2.71	1.13	2.8	1.2	- 3.2	- 5.8
26/56		.91	360	6.0	-.0217	-30.5	.0677	2.29	.89	2.55	.89	-10.2	0
53/55		.90	480	5.1	-.0200	-29.4	.060	2.186	.786	2.15	.95	+ 1.9	-16.8
55/51		.91	798	5.5	-.0200	-29.1	.057	1.74	.55	1.95	.6	-10.8	- 8.3
59/52		.90	803	4.3	-.0198	-26.35	.056	1.71	.568	1.9	.73	-10.0	-21.9
35		.90	808	4.0	NOT PROCESSED					1.9	.68	-	-

$$* \left[\frac{P_{Cal.} - P_{Mea.}}{P_{Mea.}} \right] \times 100, \text{ and } \left[\frac{[T_{1/2}]_{Cal.} - [T_{1/2}]_{Mea.}}{[T_{1/2}]_{Mea.}} \right] \times 100, \text{ calculated at the USAF Test Pilot School.}$$

$$\text{Error Ratio} = \frac{(\omega_n \text{ or } \zeta)_{\text{Mea.}} - (\omega_n \text{ or } \zeta)_{\text{Cal.}}}{(\omega_n \text{ or } \zeta)_{\text{Mea.}}}$$

If this error ratio is multiplied by 100, the result is the percentage disagreement between aircraft dynamic parameters obtained from the two different sources. Mean values of this error ratio and the standard deviations about those means were then determined for individual Mach numbers at the selected wing sweep. Data from all altitudes and angles of attack were combined at each Mach number and wing sweep to obtain a reasonably large sample size (number of test points flown). In addition, means and standard deviations of all error ratios available for each wing sweep and the error ratios for all available data at all wing sweeps were calculated.¹²¹

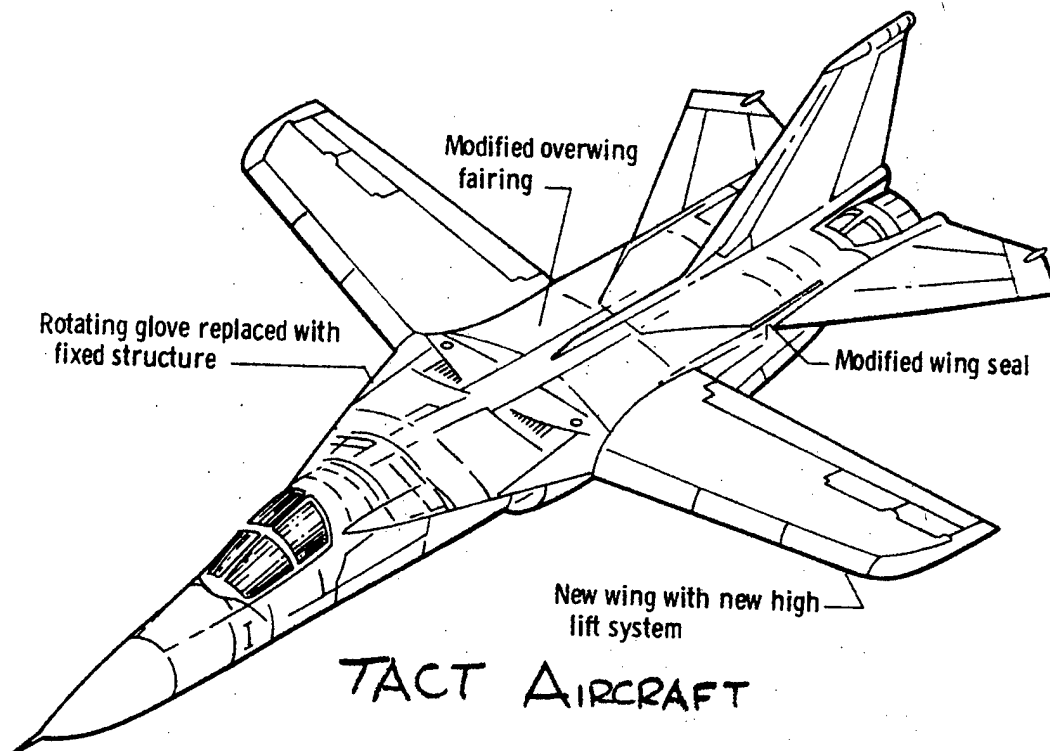
Overall, less than six percent average error was exhibited between values obtained by the two methods: This indicated that mean values of aircraft dynamic parameters obtained from either method had a high degree of interchangeability.¹²¹

The standard deviation of the error ratio about the mean should be very low to allow a direct interchange of individual values derived through the two different methods. The standard deviation of the natural frequencies was quite low (0.05), but the standard deviation of damping ratios was higher than desirable (0.22 - 0.28). USAF Test Pilot School students should not be surprised to learn that the AFFDL believes that a large part of this discrepancy was due to the difficulty of accurately measuring the damping ratio from time histories of well damped responses. Generally, the short period and Dutch roll damping ratios and natural frequencies obtained by calculation from MMLL flight test determined derivatives were considered interchangeable with the measured values.¹²¹

The AFFDL also compared TACT aircraft values of short period and Dutch roll damping ratio and natural frequency determined by calculation from MMLL determined stability derivatives with the same parameters obtained from wind tunnel tests and the Digital Datcom program.¹¹⁹ Aeroelastic effects were not accounted for in determining stability derivative values. The reason given was that flexibility corrections are not usually available during early design stages. These data were also compared against the

flying quality requirements of MIL-F-8785B (ASG).^{3,121}

As an example, the TACT aircraft longitudinal short period damping ratio and natural frequency as a function of angle of attack for a Mach number of 0.7, 26 degrees of wing sweep, at 22,500 feet is shown in Figure 95. Comparison of damping ratios with MIL-F-8785B (ASG) criteria is also indicated on this figure. Figure 96 shows natural frequency as a function of acceleration sensitivity, n/α , for the same Mach number of 0.7 and 26 degrees wing sweep, but at three different altitudes compared to MIL-F-8785B (ASG) requirements. These data show that natural frequency was better predicted at high altitudes than low altitudes. This indicates that natural frequency was being under predicted at high dynamic pressures and was influenced by aeroelastic effects. Compliance with MIL-F-8785B (ASG) was better at low altitudes than at high altitudes. Level 2 requirements were met or exceeded except for one point at an angle of attack of 8.2 degrees.^{3,121}



$\Lambda = 26^\circ$ MACH NUMBER = 0.7 ALTITUDE = 22,500 FEET

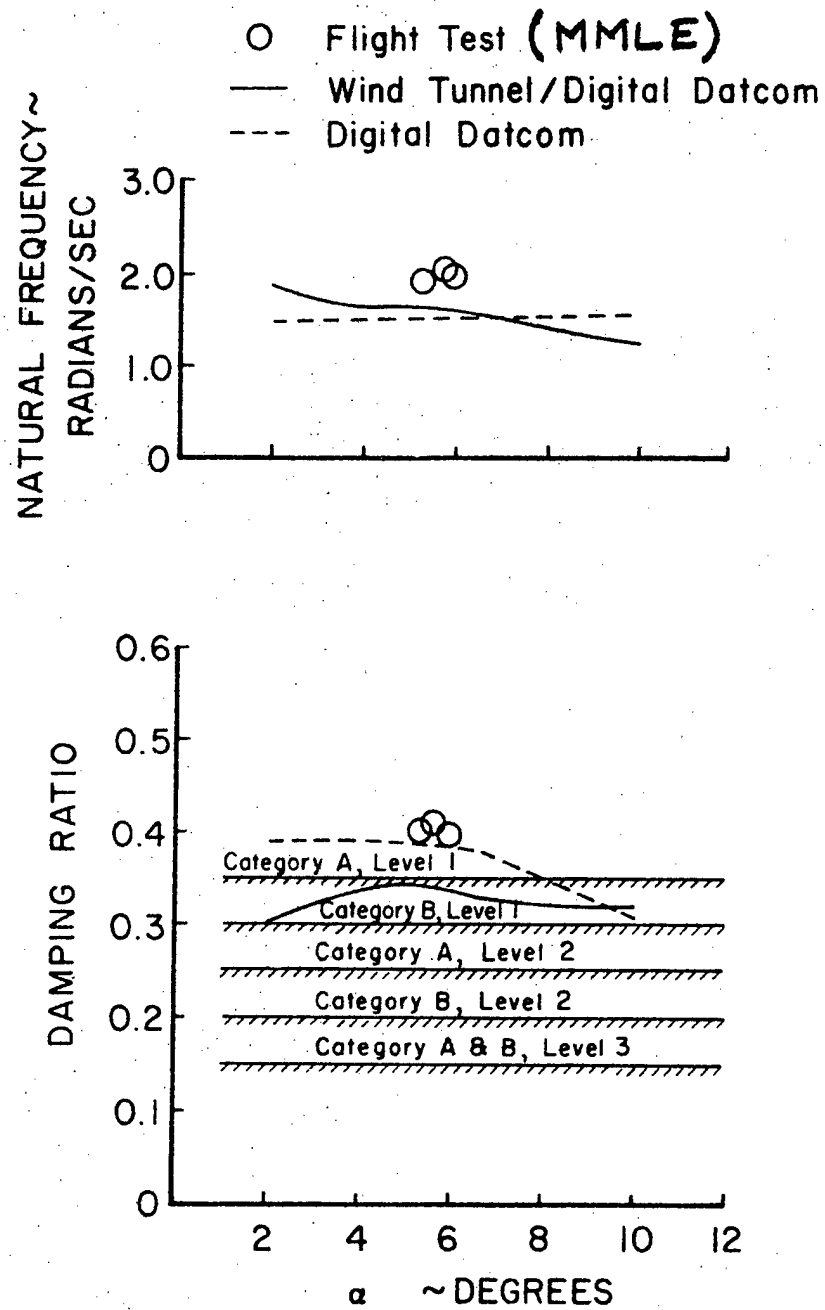


Figure 95: Variation of the Longitudinal Short Period Mode with Angle of Attack for the TACT Aircraft.¹²¹

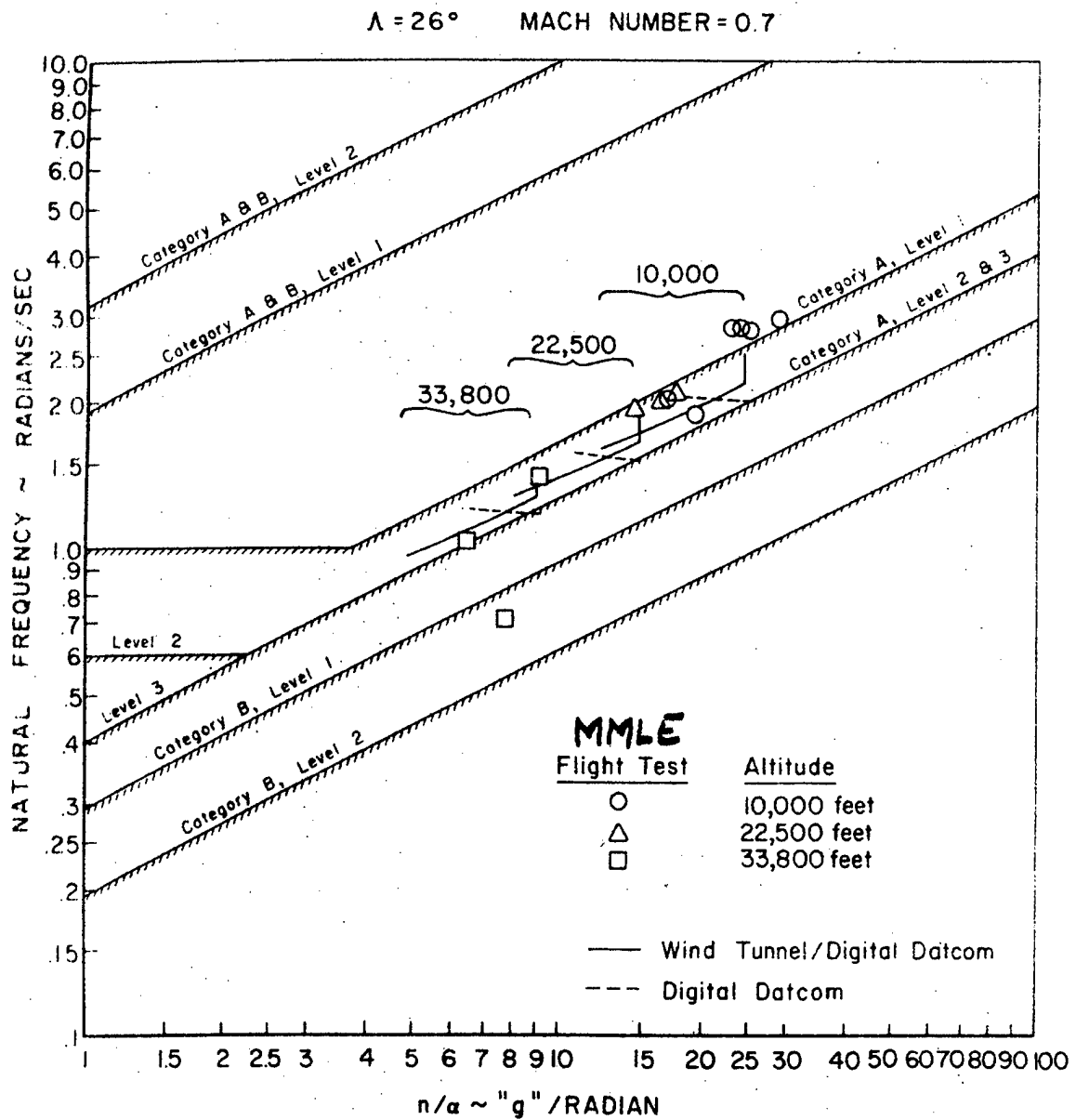


Figure 96: Variation of the Longitudinal Short Period Mode with Acceleration Sensitivity for the TACT Aircraft.¹²¹

The AFFDL also statistically compared TACT aircraft short period ζ and ω_n obtained from Digital Datcom and Digital Datcom modified by wind tunnel tests with the same parameters calculated from MMLE flight test determined derivatives. An error ratio similar to the one previously discussed was also determined for these data. The small (0.06) Digital Datcom natural frequency error ratio was improved to 0.03 with the use of wind tunnel data. This meant that natural frequency could be well predicted in either the preliminary or developmental design phases. Unfortunately, the standard deviations were rather large (0.22) for Digital Datcom predictions and improved only to 0.18 with the use of wind tunnel data. This indicated that individual predicted natural frequency values must be considered with reservation. The short period damping ratio appeared to be considerably under predicted by either set of aerodynamic data. The Digital Datcom damping ratio error of about 0.24 was not improved with the use of wind tunnel data. In addition, the standard deviation was marginal (0.22) for Digital Datcom predictions and improved only to 0.18 with the use of wind tunnel data.

In an attempt to obtain better results, the same data were investigated for one-g conditions at a constant dynamic pressure instead of constant Mach number. As an example, longitudinal short period damping ratio and natural frequency at a dynamic pressure of 500 lb/ft² is presented in Figure 97 for 26 degrees wing sweep.

A statistical analysis of longitudinal short period mode characteristics at constant dynamic pressure showed that error ratio standard deviations were very small which indicated good predictability of individual values; however, there was considerable variation in the error ratio means (as much as 0.40 in one case), indicating that some correction factor needs to be applied. Unfortunately, it is not obvious how to determine this factor for each wing sweep angle and dynamic pressure. Another variable constant has been discovered! It would normally be suspected that the correction factor would be a function of dynamic pressure due to the previously mentioned unapplied flexibility (aeroelastic) corrections. Yeager concluded that this was not borne out by the variation of values of the error ratio means.¹²¹

$\Lambda = 26^\circ$

1 "g"

$q = 500$ PSF

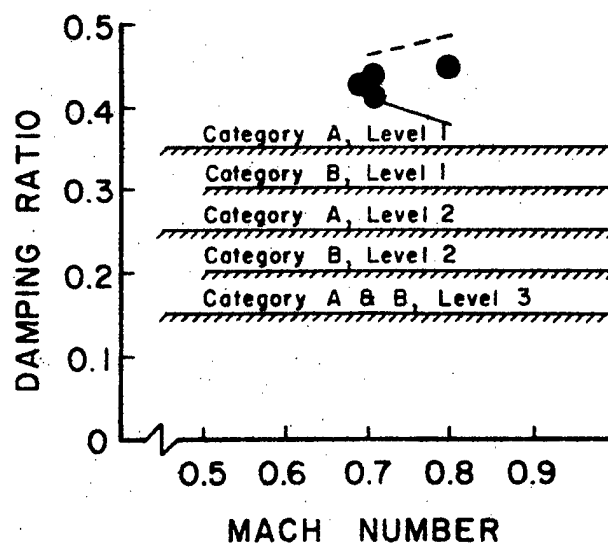
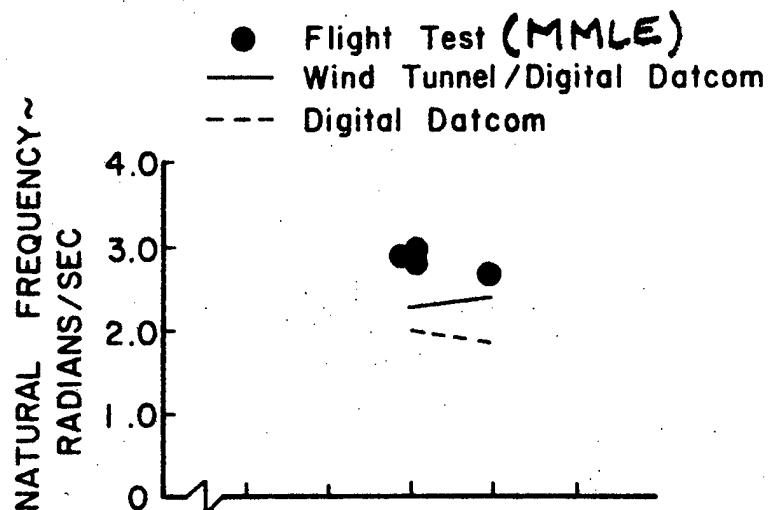
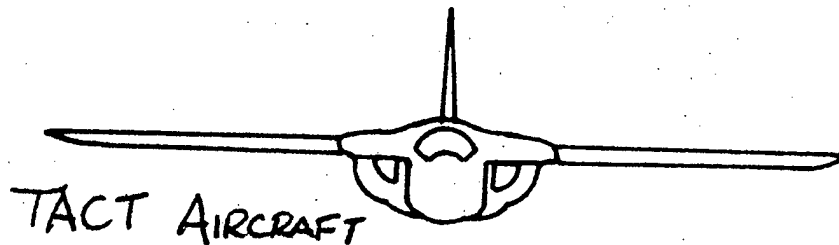


Figure 97: Variation of the Longitudinal Short Period Mode with Mach Number for the TACT Aircraft.¹²¹

The TACT aircraft lateral-directional Dutch roll mode was analysed by the AFFDL in the same manner as the longitudinal short period mode. Example predicted and exhibited natural frequencies and damping ratios are presented in Figure 98 for the 26 degree wing sweep configuration at a Mach number of 0.7 at 10,000 ft. Figure 99 shows typical predicted and flight test damping ratios and natural frequencies compared to MIL-F-8785B (ASG) requirements. Compliance with the flying qualities specification is depicted directly on this figure. However, MIL-F-8785B (ASG) also specifies requirements as a function of the phi to beta ratio, ϕ/β . If the phi to beta ratio is unacceptable, the predicted value is indicated by a heavy line. Some of the Digital Datcom predictions at low altitude (not shown) failed to satisfy the Category B Level 1 ϕ/β criteria. All points at all wing sweeps satisfied Level 2 ϕ/β requirements.¹²¹



$\Lambda = 26^\circ$

MACH NUMBER = 0.7

ALTITUDE = 10,000 FEET

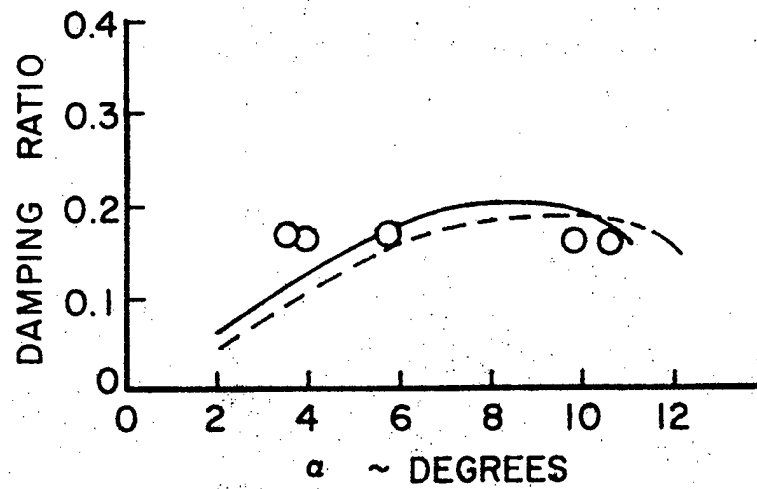
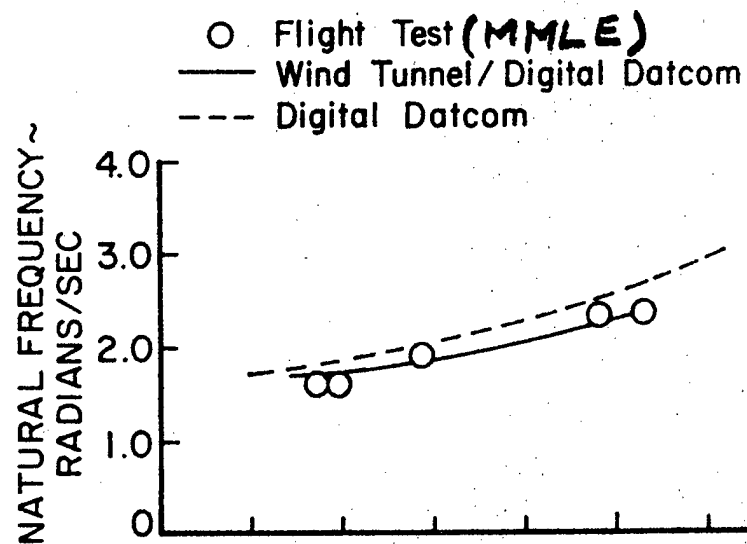


Figure 98: Variation of the Lateral-Directional Dutch Roll Mode with Angle of Attack for the TACT Aircraft.¹²¹

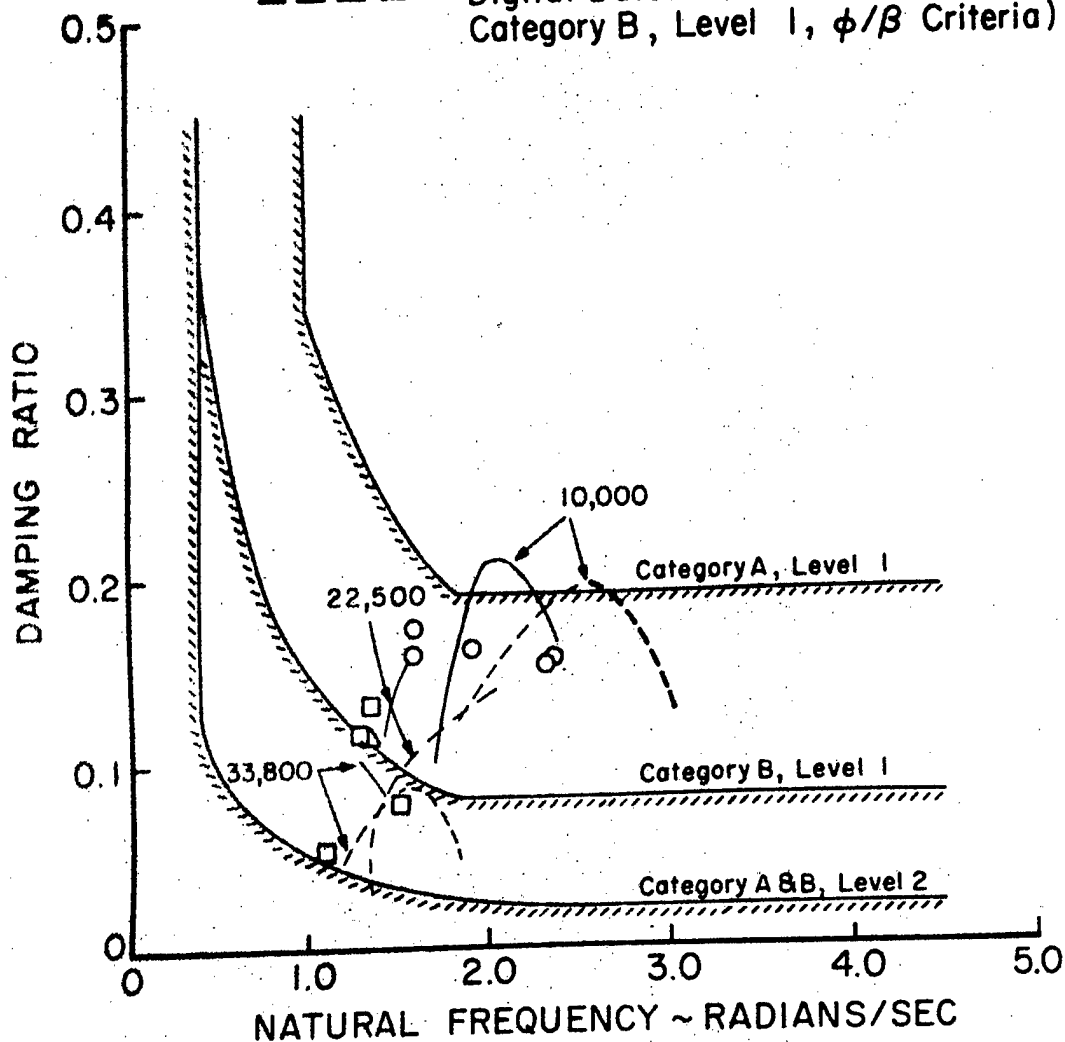
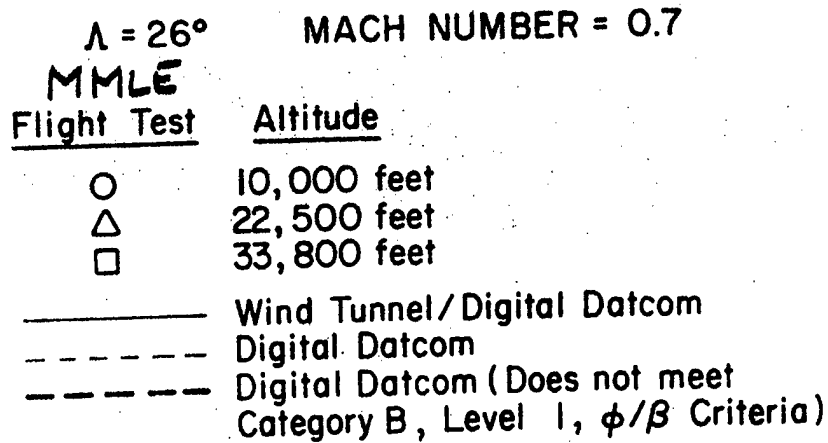
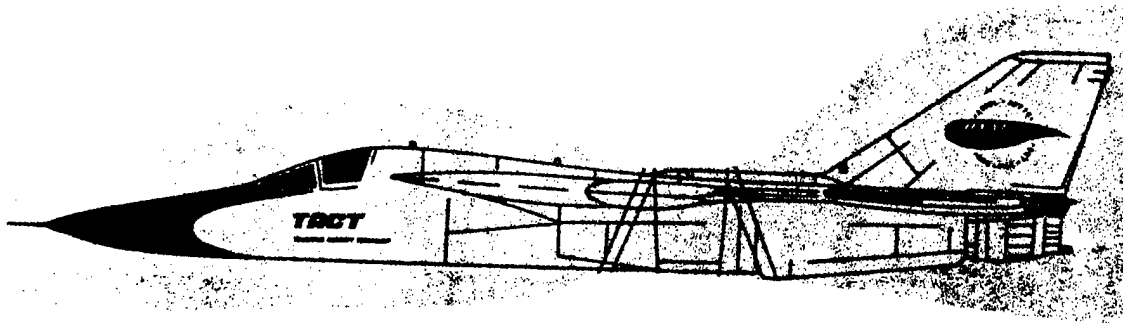


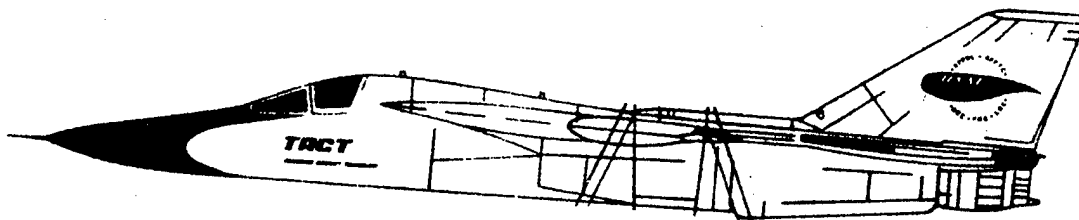
Figure 99: Variation of the Lateral-Directional Dutch Roll Damping Ratio with Natural Frequency for the TACT Aircraft.¹²¹

The AFFDL accomplished a statistical analysis for the lateral-directional mode by the same methods as the longitudinal mode analysis for all altitudes, wing sweeps, and angles of attack. The error ratio means indicated that some damping ratios were considerably under predicted. The standard deviations of the error ratios were also undesirably high for some wing sweeps. Natural frequency was predicted very well. Again, as in the longitudinal case, modifying Digital Datcom data with wind tunnel results indicated an improvement in flying qualities prediction over using only Digital Datcom data.¹²¹

On the average, modified Digital Datcom Dutch roll damping ratio estimates were within 17 percent of MLE calculated ratios. Similarly, natural frequency results agreed within seven percent. However, the standard deviation of damping ratio error was high (0.29).¹²¹



Example TACT aircraft lateral-directional Dutch roll damping ratios and natural frequencies for constant dynamic pressure are shown in Figure 100. A statistical analysis for constant dynamic pressure, as in the longitudinal case, showed that error ratio standard deviations were acceptably low for both damping ratio (0.04) and natural frequency (0.01). However, the error ratio means, again as in the longitudinal case, exhibited considerable variation which was not readily explained. Damping ratio error ratio mean was 0.37 and natural frequency error ratio mean was 0.13. It was also observed that the error ratio means in the constant dynamic pressure analysis generally exceeded those in the constant Mach number analysis. The determined error ratio means showed that damping ratio was considerably less well predicted than natural frequency.¹²¹



$\Lambda = 58^\circ$

1 "g"

$q = 300$ PSF

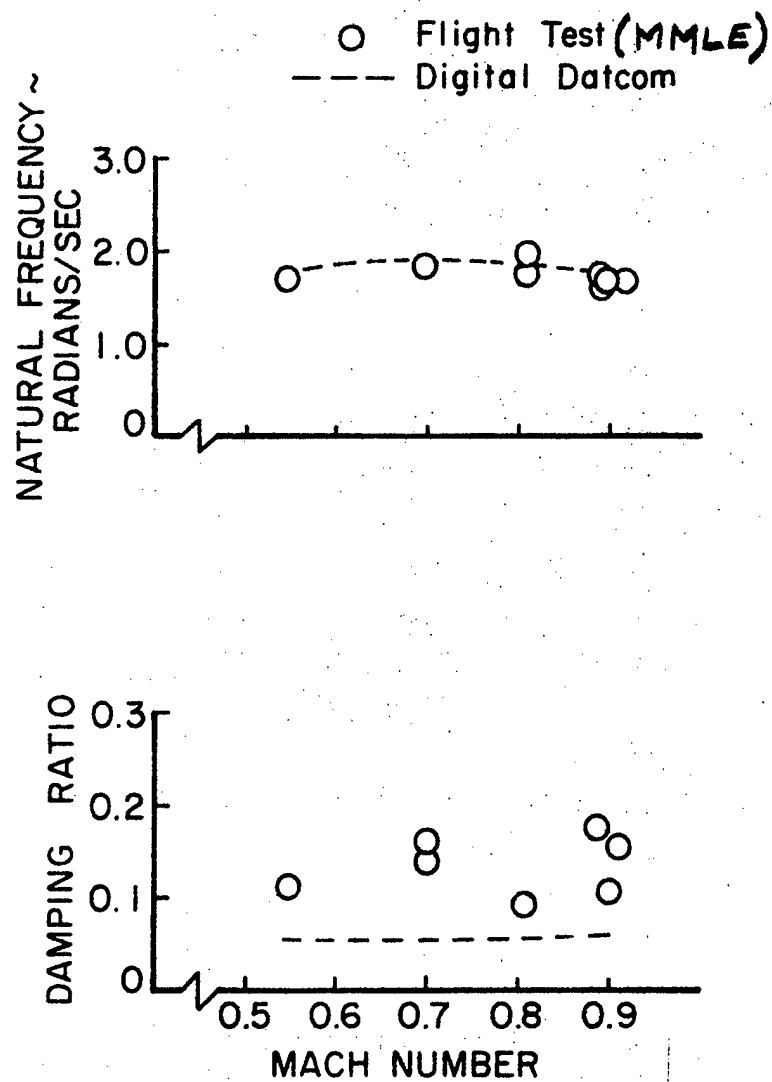


Figure 100: Variation of the Lateral-Directional Dutch Roll Mode with Mach Number for the TACT Aircraft.¹²¹

SUMMARY

Although various referenced opinions have been presented, an overall assessment of the adequacy of the stability derivative accuracies discussed in this section will be left to the student. In general, data presented in this section confirm that flight test is the most accurate of the current methods of determining stability derivatives, and that theoretical or empirical estimates can be improved by the use of wind tunnel results. Some derivatives can be determined more accurately than others. Fortunately, the most important derivatives can be determined most accurately.

Analytical estimates which neglect aeroelastic effects can be seriously in error. Wind tunnel tests which use flexible models can account for aeroelastic effects and improve the accuracy of stability derivative determination. Aeroelastic effects can be isolated in flight test by presenting extracted derivatives as functions of dynamic pressure.

Some stability derivatives, in particular static longitudinal derivatives, can be accurately determined by classical steady-state flight testing. Other derivatives, such as C_{m_α} , can be determined easily and accurately from aircraft transient response if it is oscillatory.

The accuracy of flight test stability derivative extraction using MMLE techniques has been documented by both the AFFTC and NASA. The AFFTC has found that on current flight test programs, MMLE determined derivatives are within 25 percent of wind tunnel determined values.

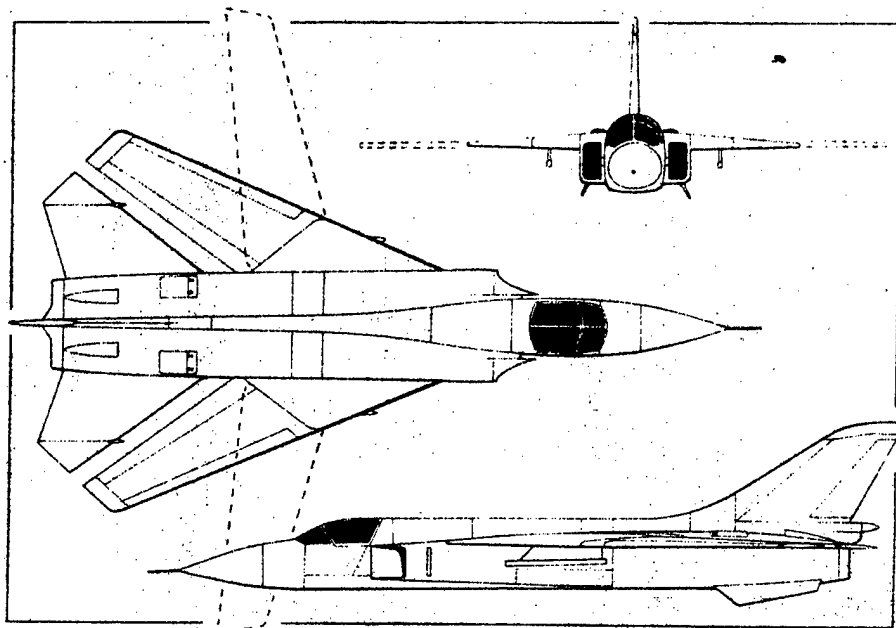
The TACT aircraft flight test program demonstrated that longitudinal derivatives can be more accurately determined than lateral-directional derivatives. Both NASA and the AFFDL compared longitudinal short period and lateral-directional Dutch roll dynamic parameters calculated using MMLE determined derivatives with values measured from aircraft response time histories. A NASA analysis showed that the MMLE calculated period of the short period mode differed from measured values by ten percent or less.

Similarly, MMLE calculated time to one-half amplitude differed from measured values by an average error of about eight percent.

The AFFDL determined that MMLE calculated damping ratios and natural frequencies for both the short period and Dutch roll modes agreed with measured values within six percent. However, the standard deviation of the damping ratio error was high, about 25 percent.

It was also found in the TACT program that Digital Datcom derivative estimates could be improved by modifying predictions with wind tunnel results. The AFFDL compared longitudinal short period and lateral-directional Dutch roll damping ratios and natural frequencies calculated using MMLE determined derivatives with wind tunnel modified Digital Datcom estimates. Analysis showed that the MMLE calculated short period natural frequencies differed from the modified Digital Datcom estimates by an average of only three percent; however, the standard deviation of this error was 18 percent. The modified Digital Datcom short period damping ratio estimates differed from MMLE calculated results by 24 percent, and the standard deviation of these errors was 18 percent. Similarly, MMLE calculated Dutch roll natural frequencies differed from the modified Digital Datcom estimates by an average of seven percent. MMLE Calculated Dutch roll damping ratio differed from estimates by 17 percent with an error standard deviation of 29 percent.

Derivative accuracy certainly effects the utility of using stability derivatives for engineering analysis. Results of dynamic parameter analysis using stability derivatives are very sensitive to variations in the values of the various derivatives used. This sensitivity, and how it relates to accuracy will be examined in Section 6.



SECTION 6

PARAMETER ANALYSIS

INTRODUCTION

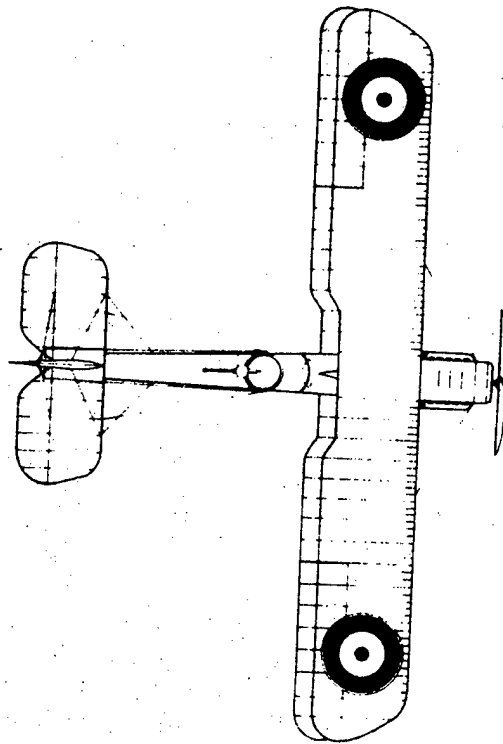
Parameter analysis is putting results obtained thru the use of parameter estimation techniques to good use. This includes using stability derivatives in the analysis of aircraft flying qualities. The most obvious application is the construction of an engineering or operational simulator which "flies" exactly like the real aircraft. This requires "very good" aircraft and control system mathematical models and "accurate" stability derivatives. The terms "very good" and "accurate" remain undefined even after the discussion in Section 5.

Parameter estimation techniques which are used to extract stability derivatives from flight test data provide an independent test whose results can be correlated with classical and SIFT flight test results. The AFFTC has found that the independence of test techniques allows the development of a more optimum test plan which uses both the new and classical test methods. Significant reductions have been made in the amount of flight test time necessary to define flying quality characteristics.¹⁰⁶

Stability derivatives have been extracted using MMLE techniques during most of the recent prototype and production aircraft flight test programs at the AFFTC. During one of these programs, records were maintained of the dedicated flight test time devoted to classical stability and control maneuvers and those flight hours devoted to parameter estimation using MMLE techniques. An analysis, based on hindsight, showed that flying qualities flight test time could have been reduced nearly 75 percent by the proper application of MMLE techniques; however, this total time did not include the evaluation of all flying quality parameters. The evaluation of longitudinal characteristics such as the variation of elevator control force and deflection with velocity and certain roll performance parameters must be done using

classical flight test techniques. However, the longitudinal short period frequency and damping ratios of aircraft with active control systems can only be quantified using MMLE techniques.¹⁰⁶

The AFFTC has had significant success with the method of parameter identification, and many evaluations recently accomplished would have been impossible without its use.¹⁰⁶ Current examples of the application of parameter analysis techniques will be given in later revisions of this chapter if there is an increase in the scope of the Dynamic Parameter Analysis course presently taught at the USAF Test Pilot School.



SECTION 7

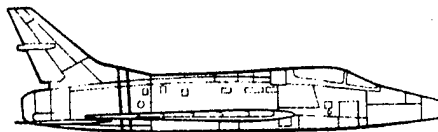
OTHER USES OF SYSTEMS IDENTIFICATION

This section will include application of systems identification and parameter estimation techniques to flight test problems other than the extraction of stability and control derivatives, e.g., aircraft performance and associated weapons system analysis.

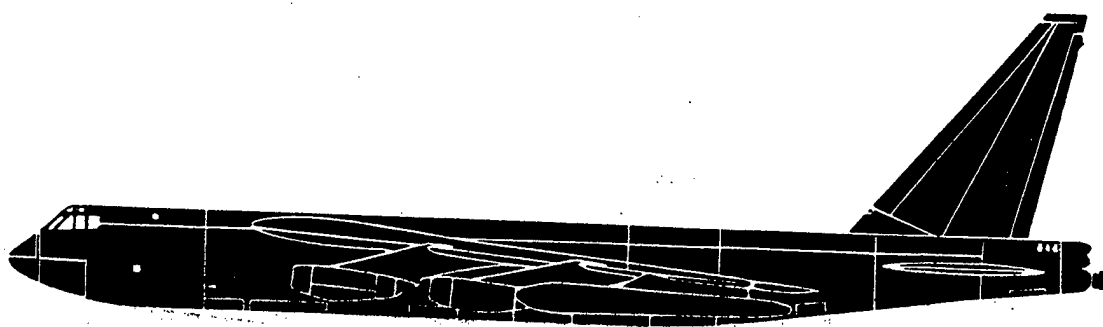
SECTION 8

THE MMLE PROGRAM

This section will discuss in detail the use of MMLE techniques at the USAF Test Pilot School for the extraction of stability derivatives. It will be included in this text at some future date when the School develops an in-house derivative extraction capability. Until that time Reference 60, Nagy's report will serve as the "cookbook" for use of the AFFTC MMLE program.



REFERENCES



REFERENCES

1. Jacobs, A. M., Will She Fly?, in Popular Mechanics Magazine, Vol. 51, No. 3, March 1929, p. 378-385.
2. Anon., Flying Quality Tests and Data Reduction, in Engineer's Handbook for Aircraft Performance and Flying Qualities Flight Testing, Ch. IV, Flight Test Engineering Division, 6510th Test Wing, Edwards AFB, CA, 93523, 1 May 1971, p. IV-A-1.
3. Anon., Military Specification, Flying Qualities of Piloted Aircraft, MIL-F-8785B (ASG), 7 Aug 69, Amendment 2, 16 Sep 74.
4. Bryan, G. H., Stability in Aviation, MacMillan, London, 1911, p. 192.
5. Baristow, L., Jones, B. M., et al., Investigation into the Stability of an Aeroplane, with an Examination into the Condition Necessary in Order That the Symmetric and Asymmetric Oscillations Can Be Considered Independently, R and M No. 77, 1913, Great Britain Aeronautical Research Committee Annual Report 1912-1913, p. 135-171.
6. Perkins, C. D., Development of Airplane Stability and Control Technology, AIAA Journal of Aircraft, Vol. 7, No. 4, Apr 1970, p. 290-301.
7. Hunsaker, J. C., Dynamical Stability of Aeroplanes, Smithsonian Miscellaneous Collection, Vol. 6, No. 5, June 1916, Smithsonian Institution, Wash D.C., p. 78.
8. Warner, E. P., and Norton, F. H., Preliminary Report on Free Flight Tests, NASA Report No. 70, 1919.

9. Norton, F. H., and Brown, W. G., Controllability and Maneuverability of Airplanes, NACA Report No. 153, 1922.
10. Norton, F. H., A Study of Longitudinal Dynamic Stability in Flight, NACA Report No. 170, 1923.
11. Soule', H. A., and Wheatley, J. B., A Comparison Between the Theoretical and Measured Longitudinal Stability Characteristics of an Airplane, NACA Report No. 442, 1933.
12. Rediess, H. A., An Overview of Parameter Estimation Techniques and Applications in Aircraft Flight Testing, NASA TN D-7647, Apr 74.
13. Gilruth, R. R., Requirements for Satisfactory Flying Qualities of Airplanes, NACA TR No. 755, 1943.
14. Perkins, C. D., and Walkowicz, A. C., Stability and Control Flight Test Methods, AAF Technical Report No. 5242, Army Air Forces Air Technical Services Command, Dayton, Ohio, 14 Jul 45.
15. Anon., Stability and Control Requirements for Airplanes, Army Air Forces Specification C-1815, 1943, and R-1815A 1945.
16. Anon., Flying Qualities Flight Test Handbook, Theory and Flight Test Techniques, AFFTC-TTH-79-1, Air Force Flight Test Center, Edwards AFB, CA, 93523, 1 Aug 79.
17. Soule', H. A., Preliminary Investigation of the Flying Qualities of Airplanes, NACA Report No. 700, 1940.
18. Phillips, W. H., Appreciation and Prediction of Flying Qualities, NACA Report No. 927, 1949.

19. Milliken, W. F. Jr., Progress in Dynamic Stability and Control Research, Journal of the Aeronautical Sciences, Vol. 14, No. 9, Sep 1947, p. 493-519.
20. Anon., Flying Qualities of Piloted Airplanes, Navy BuAer Specification SR-119B, and USAF Specification C-1815B, 1 Jun 48.
21. Seamans, R. C., et al., The Pulse Method for the Determination of Aircraft Dynamic Performance, Journal of the Aeronautical Sciences, Vol. 17, No. 1, Jan 1950, p. 22-38.
22. Greenberg, H., A Survey of Methods for Determining Stability Parameters of an Airplane From Dynamic Flight Measurements, NACA TN 2340, 1951.
23. Donegan, J. J., et al., Determination of Lateral-Stability Derivatives and Transfer-Function Coefficients From Frequency Response Data for Lateral Motions, NACA Report No. 1225, 1955.
24. Shinbrot, M., On the Analysis of Linear and Nonlinear Dynamical Systems from Transient-Response Data, NACA TN 3288, 1954.
25. Angle, E. E., and Holleman, E. C., Determination of Longitudinal Stability of the Bell X-1 Airplane From Transient Responses at Mach Numbers up to 1.12 at Lift Coefficients of 0.3 and 0.6, NACA RM L 50106a, 1950.
26. Zaleski, C. D., Capt., USAF, et al., An Analysis Technique and Computer Program for Extracting the Primary Lateral-Directional Stability Derivatives From Flight Test Data, Flight Research Division Office Memo AV-65-13, AFFTC, Edwards AFB, CA, 93523, Nov 65.

27. Doetsch, K. H., The Time Vector Method for Stability Investigations, Report Aero 2495, Royal Aircraft Establishment, Aug 1953.
28. Wolowicz, C. H., Time-Vector Determined Lateral Derivatives of a Swept-Wing Fighter-Type Airplane With Three Different Vertical Tails At Mach Numbers Between 0.70 and 1.48, NACA RM H 56C20, 1956.
29. McMaster, D. C., Comparison of Methods For Determining (Damping Ratio) and (Natural Frequency) From Flight Test Data, FTC-TIM-68-1002, AFFTC, Edwards AFB, CA 93523, Jan 68.
30. Trimmer, J. D., Response of Physical Systems, John Wiley and Sons, Inc., New York, NY, 1950.
31. Dolbin, B. H., Jr., Study of Some Hand-Computing Techniques to Determine the Approximate Short Period, Mode from Airplane Responses, Cornell Aeronautical Laboratory, Inc., Buffalo, NY, 1967.
32. Yancy, R. B., et al., Aerodynamic-Derivative Characteristics of the X-15 Research Airplane as Determined From Flight Tests for Mach Numbers from 0.6 to 3.4, NASA TN D-1060, 1962.
33. Triplett, W. C., and Smith, G. A., Longitudinal Frequency-Response Characteristics of a 35° Swept-Wing Airplane as Determined From Flight Measurements, Including a Method for the Evaluation of Transfer Functions, NASA RM A51G27, 1951.
34. Rampy, J. M., and Berry, D. T., Determination of Stability Derivatives From Flight Test Data by Means of High Speed Repetitive Operation Analog Matching, FTC-TDR-64-8, AFFTC, Edwards AFB, CA 93523, May 1964.

35. Wolowicz, C. H., Considerations in the Determination of Stability and Control Derivatives and Dynamic Characteristics From Flight Data, AGARD Report 549 - Part 1, 1966.
36. Chalk, C. R., et al., Background Information and User Guide for MIL-F-8785B (ASG), "Military Specification - Flying Qualities of Piloted Airplanes," AFFDL-TR-69-72, Wright-Patterson AFB, OH, August 1969.
37. Anon., Military Specification, Flying Qualities of Piloted V/STOL Aircraft, MIL-F-83300, 31 Dec 70.
38. Chalk, C. R., et al., Background Information and User Guide for MIL-F-83300, "Military Specification - Flying Qualities of Piloted V/STOL Aircraft," AFFDL-TR-70-88, March 1971.
39. Westbrook, C. B., The Status and Future of Flying Quality Requirements, AFFDL-FDCC-TM-65-29, Air Force Flight Dynamics Laboratory, Research and Technology Division, Wright-Patterson AFB, OH, June 1965.
40. Shinbrot, M., A Least Squares Curve Fitting Method With Applications to the Calculation of Stability Coefficients From Transient-Response Data, NACA TN 2341, 1951.
41. Larson, D. B., Identification of Parameters by the Method of Quasi-Linearization, CAL Report No. 164, Cornell Aero. Lab., Inc., May 14, 1968.
42. Taylor, L. W., Jr., and Iliff, K. W., A Modified Newton-Raphson Method for Determining Stability Derivatives From Flight Data, from Computing Methods in Optimization Problems - 2, Zadeh, et al., eds., Academic Press, 1969, p. 353-364.

43. Iliff, K. W., and Taylor, L. W., Jr., Determination of Stability Derivatives From Flight Data Using a Newton-Raphson Minimization Technique, NASA TN D-6579, 1972.
44. Balakrishnan, A. V., ed., Communication Theory, McGraw-Hill Book Co., c.1968.
45. _____, Techniques of System Identification, Facoltà di Ingegneria, Università di Roma, Corso di Specializzazione in Ingegneria dei Controlli Automatici, SISTEMA (Via Umberto Biancamano 23, Roma), Sept 1968.
46. _____, and Peterka, V., Identification in Automatic Control Systems, Survey Paper 9, presented at Fourth Congress of the International Federation of Automatic Control, Warsaw, Poland, June 16-21, 1969.
47. Mehra, R. K., Maximum Likelihood Identification of Aircraft Parameters, Preprints of Technical Papers presented at 1970 Joint Automatic Control Conference of the American Automatic Control Council, Georgia Institute of Technology, Atlanta, Ga., June 22-26, 1970, p. 442-444.
48. Denery, D. G., Identification of System Parameters From Input-Output Data With Application to Air Vehicles, NASA TN D-6468, 1971.
49. Balakrishnan, A. V., Identification and Adaptive Control: An Application to Flight Control Systems, J. Optimization Theory and Applications, Vol. 9, No. 3, Mar. 1972, p. 187-213.
50. Mehra, R. K., Identification of Stochastic Linear Dynamic Systems Using Kalman Filter Representation, AIAA J., Vol. 9, No. 1, Jan. 1971, p. 28-31.

51. Chen, R. T., et al., Development of Advanced Techniques for the Identification of V/STOL Aircraft Stability and Control Parameters. CAL Rep No. BM 2820-F-1, Cornell Aero. Lab., Inc., Aug. 1971.
52. Sage, A. P., and Melsa, J. L., System Identification, Academic Press, N.Y., 1971.
53. Moritsugu, R. S., Detailed Procedure for Obtaining Longitudinal Derivatives From Flight Test Data by Analog Matching, Flight Research Branch Office Memo, AFFTC, Edwards AFB, CA 93523, Aug 1967.
54. Hoey, R. G., Choosing Test Conditions For Stability Derivative Maneuvers, Flight Test Technology Branch Office Memo, AFFTC, Edwards AFB, CA 93523, Apr 1973.
55. Klung, H. A., Capt, USAF, Frequency Response Method of Determining Aircraft Longitudinal Short-Period Stability and Control System Characteristics in Flight, FTC-TR-66-24, AFFTC, Edwards AFB, CA 93523, Aug 1966.
56. Maine, R. E., and Iliff, K. W., A User's Guide for Three Fortran Computer Programs to Determine Aircraft Stability and Control Derivatives from Flight Data, NASA TN D-7831, NASA Flight Research Center, Edwards, CA 93523, April 1975.
57. Iliff, K. W., and Maine, R. E., Practical Aspects of Using a Maximum Likelihood Estimation Method to Extract Stability and Control Derivatives from Flight Data, NASA TN D-8209, NASA Dryden Flight Research Center, Edwards CA 93523, April 1976.
58. _____, Further Observations on Maximum Likelihood Estimates of Stability and Control Characteristics Obtained From Flight Data, AIAA

Paper 77-1133, AIAA Atmospheric Flight Mechanics Conference, Hollywood, FL, Aug 8-10, 1977.

59. Maine, R. E., Maximum Likelihood Estimation of Aerodynamic Derivatives for an Oblique Wing Aircraft From Flight Data, AIAA Paper 77-1135, AIAA Atmospheric Flight Mechanics Conference, Hollywood, FL Aug 8-10, 1977.
60. Nagy, C. J., A New Method for Test and Analysis of Dynamic Stability and Control, AFFTC-TD-75-4, AFFTC, Edwards AFB, CA 93523, May 1976.
61. Åström, K.-J., and Eykoff, P.,: System Identification - a survey, Identification and Process Parameter Estimation, Part 1, Preprints of the 2nd Prague IFAC Symposium, Czechoslovakia, 15-20, June 1970.
62. Aoki, M.,: Introduction to Optimization Techniques, The MacMillan Co., N.Y., 1971.
63. Mehra, Raman K.,: Optimal Inputs for Linear System Identification, Preprints of Technical Papers presented at 1972 Joint Automatic Control Conference of the American Automatic Control Council, Stanford Univ., Stanford, Calif., Aug. 16-18, 1972, p. 811-820.
64. Anon., Stability and Control Theory, Stability and Control, AFFTC-TIH-77-1, Vol. I, Air Force Flight Test Center, Edwards AFB, CA 93523.
65. Anon., Dynamics of the Airframe, BU AER Report AE-61-4II, Bureau of Aeronautics, Navy Dept., Sep 1952.
66. Thelander, J. A., Aircraft Motion Analysis, FDL-TDR-64-70, Air Force Flight Dynamics Laboratory, Wright-Patterson AFB, OH, March 1965.

67. Iliff, K. W., Maximum Likelihood Estimates of Lift and Drag Characteristics Obtained from Dynamic Aircraft Maneuvers, Proceedings of the AIAA 3rd Atmospheric Flight Mechanics Conference, 1976, p. 137-150.
68. Jones, R. L., Maj., USAF, Introduction to VSTOL Technology, Lecture notes used at the USAF Aerospace Research Pilot School, Edwards AFB, CA 93523, Dec 1970.
69. Seckel, E., Stability and Control of Airplanes and Helicopters, Academic Press, New York, NY, 10003, 1964.
70. Powell, M. J., A Survey of Numerical Methods for Unconstrained Optimization, Studies in Optimization 1, Society for Industrial and Applied Math, c. 1970, p. 43-61.
71. Anon., Instrumentation Handbook, USAF Test Pilot School, Feb 78.
72. Hoak, D. E., and Finck, R. D., USAF Stability and Control Datcom, Flight Control Division, Air Force Flight Dynamics Laboratory, Wright-Patterson AFB, OH, Oct 1960, Revised Apr 1976.
73. Woodcock, R. J., Estimation of Flying Qualities of Piloted Airplanes, AFFDL-TR-65-218, Air Force Flight Dynamics Laboratory, Wright-Patterson AFB, OH, Apr 1966.
74. Roskam, J., Flight Dynamics of Rigid and Elastic Airplanes, Roskam Aviation and Engineering Corporation, Lawrence, Kansas, 1972.
75. MacLachlan, R., and Letko, W., Correlation of Two Experimental Methods of Determining the Rolling Characteristics of Unswept Wings, NACA Technical Note TN 1309, Langley Memorial Aeronautical Laboratory, Langley Field, Va., May 1947.

76. Bird, J. D., et.al., Effect of Fuselage and Tail Surfaces on Low-Speed Yawing Characteristics of a Swept-Wing Model as Determined in Curved-Flow Test Section of Langley Stability Tunnel, NACA Technical Note TN-2483, Langley Memorial Aeronautical Laboratory, Langley Field, Va., Oct 1951.
77. Kuethe, A. M., and Chow, C. Y., Foundations of Aerodynamics: Bases of Aerodynamic Design, 3rd Ed., John Wiley & Sons, New York, N.Y., 1976.
78. Goodman, A. and Feigenbaum, D., Preliminary Investigation at Low Speeds of Swept Wings in Yawing Flow, NACA Research Memorandum, RM L7109, Langley Memorial Aeronautical Laboratory, Langley Field, Va., Feb 1948.
79. Shortal, J. A., and Osterhout, C. J., Preliminary Stability and Control Tests in the NACA Free-Flight Tunnel and Correlation with Full-Scale Flight Tests, NACA Technical Note, TN 810, Langley Memorial Aeronautical Laboratory, Langley Field, Va., Jun 41.
80. Wilson, D. B., and Winters, C. P., F-15A Approach-to-Stall/Stall/Post-Stall Evaluation, AFFTC-TR-75-32, Air Force Flight Test Center, Edwards AFB, CA, 93523, Jan 76.
81. Iliff, K. W., et.al., Subsonic Stability and Control Derivatives for an Unpowered Remotely Piloted 3/8-Scale F-15 Airplane Model Obtained From Flight Test, NASA TN D-8136, 1976.
82. Anon., The Shape of Fighters to Come, Flight International, Vol 113, No. 3602, IPC Business Press, 1 Apr 78, p. 910.

83. Kogler, R. H., The Application of Fourier Transforms to the Determination of Aircraft Dynamic Performance From Flight Test Data Obtained Using Pulse Inputs, FTC-TIM-71-1004, AFFTC, Edwards AFB, CA 93523, Jun 71.
84. Millikan, W. F., Jr., Dynamic Stability and Control Research, Cornell Aero, Lab., Inc., Report No. Cal.-39, Cornell Res. Foundation, Buffalo, NY, 1951.
85. Anon., Aerodynamic Theory, Performance, FTC-TIH-70-1001, Vol. I, Air Force Flight Test Center, Edwards AFB, CA 93523, Jan 73.
86. Etkin, B., Dynamics of Atmospheric Flight, John Wiley & Sons, Inc., New York, NY.
87. Heffley, R. K., and Jewell, W. F., Aircraft Handling Qualities Data, STI Tech. Rpt. 1004-1, Systems Technology Inc., Hawthorne, CA, May 1972.
88. Anon., Dynamics of the Airframe Addendum, PU AER Rpt, AE-61-4-11, Bureau of Aeronautics, Navy Dept., Sep 52.
89. Anon., Proposals for Revising MIL-F-8785B, "Flying Qualities of Piloted Aircraft," AFFDL-FGC-Working Paper, Vol. II, Air Force Flight Dynamics Laboratory, Flight Control Division, Control Criteria Branch, Wright-Patterson AFB OH, Aug 17, corrected Feb 78.
90. Rolfe, R., and Dawydoff, A., Airplanes of the World 1490-1962, Simon and Schuster, New York, NY, 1962.
91. Funderburk, T., The Fighters, Grosset and Dunlap, New York, NY, 1965.

92. Eggers, J. A., and Bryant, W. F., Flying Qualities Evaluation of the YF-16 Prototype Lightweight Fighter, AFFTC-TR-75-15, Air Force Flight Test Center, Edwards AFB CA 93523, Jul 75. DISTRIBUTION LIMITED.
93. Perkins, C. D., and Hage, R. E., Airplane Performance Stability and Control, John Wiley & Sons, Inc., New York, NY, 1949.
94. Kolk, R. W., Modern Flight Dynamics, Prentice-Hall, Inc., Englewood Cliffs, NJ, 1961.
95. Blakelock, J. H., Col., USAF, Automatic Control of Aircraft and Missiles, John Wiley & Sons, Inc., New York, NY, 1965.
96. Mollenberg, E. F., and Seif, G. W., Flight Test Determination of Aircraft Stability and Control Derivatives from Frequency Response Data, Rep, No. ADR 07-01a-61.0, 5 Sep 61, Grumman Aircraft Engineering Corp., Bethpage, NY.
97. Lyster, H. N. C., A Critical Review of Techniques for the Flight Determination of Aircraft Dynamic Stability and Response Characteristics with Illustrative Examples from Measurements on a Subsonic Jet Fighter, Aero. Rep. LR-336, National Research Council of Canada, Ottawa, Canada, Mar 62.
98. Laurie-Lean, D. E., Frequency Response of an Aircraft as Determined from Transient Flight Tests Using the Fourier Transformation Method of Analysis, CoA Note Aero. No. 175, The College of Aeronautics Cranfield, Great Britian, May 67.
99. Gaines, T. G., and Hoffman, S., Summary of Transformation Equations and Equations of Motion Used in Free-Flight and Wind-Tunnel Data Reduction and Analysis, NASA SP-3070, NASA Langley Research Center, Hampton, VA, 1972.

100. Bennett, R. M., et. al., Wind-Tunnel Technique for Determining Stability Derivatives from Cable Mounted Models, AIAA Journal of Aircraft, Vol. 15, No. 5, May 1978, p. 304-310.
101. Stengel, R. F., and Berry, P. W., Stability and Control of Maneuvering High-Performance Aircraft, AIAA Journal of Aircraft, Vol. 14, No. 8, Aug 1977, p. 787-794.
102. Anon., Test Facilities Handbook, Vol 4, 10th Ed., Arnold Engineering Development Center, Arnold AF Station, TN, May 74.
103. Twisdale, T. R., and Ashurst, T. A., JR., System Identification from Tracking (SIFT), A New Technique for Handling Qualities Test and Evaluation (Initial Report), AFFTC-TR-77-27, Air Force Flight Test Center, Edwards AFB CA 93523, Nov 77.
104. Chanute, O., Progress in Flying Machines, 1st Ed., 1884, republished by Lorenz and Herwig, Long Beach, CA, 1976.
105. Ritchie, M. L., The Research and Development Methods of Wilbur and Orville Wright, AIAA Astronautics & Aeronautics, Vol. 16, No. 7, Jul/Aug, 1978, p. 56-67.
106. Maunder, D. P., 1st Lt, AFFTC Parameter Identification Experience, Paper presented at Society of Flight Test Engineers National Symposium, Arlington, TX, Oct 78.
107. Kirsten, P. W., and Ash, L. G., A Comparison and Evaluation of Two Methods of Extracting Stability Derivatives from Flight Test Data, AFFTC-TD-73-5, Air Force Flight Test Center, Edwards AFB, CA, 93523, May 74.

108. Anon. Request for Proposal: Lightweight Fighter Prototype Aircraft, F33657-72-R-0235, Aeronautical Systems Division, Wright-Patterson AFB, OH, 6 Jan 72, CONFIDENTIAL.
109. Anon. Proposed Lightweight Fighter Prototype, FZP-1401, General Dynamics Convair Aerospace Division, Fort Worth, Texas, 18 Feb 72, CONFIDENTIAL.
110. Baldwin, W., Symposium on Transonic Aircraft Technology (TACT), AFFDL TR-78-100, Air Force Flight Dynamics Laboratory (AFFDL/FXS), Wright-Patterson AFB, OH 45433, Aug 78. DISTRIBUTION LIMITED.
111. Twisdale, T. R., and Franklin, D. L., Capt., USAF, Tracking Test Techniques for Handling Qualities Evaluation, AFFTC-TD-75-1, Air Force Flight Test Center, Edwards AFB, CA 93523, Aug 75.
112. Glover, K., and Williams, J. C., Parameter Identifiability of Linear Dynamical Systems, in Parameter Estimation Techniques and Applications in Aircraft Flight Testing, NASA TN D-7647, Apr 74, p. 281-289.
113. Taylor, L. W. Jr., A New Criterion for Modeling Systems, in Parameter Estimation Techniques and Applications in Aircraft Flight Testing, NASA TN D-7647, Apr 74, p. 291-314.
114. Jones, J. G., Modeling of Systems with a High Level of Internal Fluctuation, in Methods for Aircraft State and Parameter Identification, AGARD-CP-172, Advisory Group for Aerospace Research and Development, North Atlantic Treaty Organization, 7 rue Ancelle, 92200 Neuilly sur Seine, France, May 75, paper No. 1.
115. Eckholdt, D. C., Capt., and Wells, W. R., A Survey of Parameter Estimation Efforts and Future Plans, in Parameter Estimation Techniques and Applications in Aircraft Flight Testing, NASA TN D-7647, Apr 74, p. 19-38.

116. Taylor, L. W. Jr., Application of a New Criterion for Modeling Systems, in Methods for Aircraft State and Parameter Identification, AGARD-CP-172, Advisory Group for Aeronautical Research and Development, North Atlantic Treaty Organization, 7 rue Ancelle, 92200 Neuilly sur Seine, France, May 75, Paper No. 4.
117. Balakrishnan, A. V., Some After-Dinner Reflections on System Identification, in Parameter Estimation Techniques and Applications in Aircraft Flight Testing, NASA TN D-7647, Apr 74, p. 381-385.
118. Suit, W. T. and Williams, J. L., Extraction of Derivatives from Flight Data for Several Aircraft, Using the LRC Interactive Computer System, in Parameter Estimation Techniques and Applications in Aircraft Flight Testing, NASA TN D-7647, Apr 74, p. 49-76.
119. Williams, J. E., and Vukelich, S. R., The USAF Stability and Control Digital Datcom, AFFDL-TR-26-45, Air Force Flight Dynamics Laboratory, Wright-Patterson AFB, OH, Nov 76.
120. Griffin, J. M., Digital Computer Solution of Aircraft Longitudinal and Lateral-Directional Dynamics Characteristics, SMC TR-66-52. Aeronautical Systems Division, Wright-Patterson AFB, OH, Dec 67.
121. Yeager, R. B., A Comparison of F-111 TACT Estimated and Measured Flying Qualities, in Symposium on Transonic Aircraft Technology (TACT), AFFDL-TR-78-100, Flight Controls Group, Air Force Flight Dynamics Laboratory, Wright-Patterson AFB, OH, 45433, Aug 78, p. 428-469, DISTRIBUTION LIMITED.
122. Dougherty, J. C., Techniques and Procedures Used for Wind-Tunnel Tests in Support of the TACT Correlation Program, in Symposium on Transonic Aircraft Technology (TACT), AFFDL-TR-78-100, Flight Controls Group, Air Force Flight Dynamics Laboratory, Wright-Patterson AFB, OH, 45433, Aug 78, p. 66-96. DISTRIBUTION LIMITED.

123. Bryant, W. H., and Hodge, W. F., A Monte Carlo Analysis of the Effects of Instrumentation Errors on Aircraft Parameter Identification, in Methods for Aircraft State and Parameter Identification, AGARD-CP-172, Advisory Group for Aeronautical Research and Development, North Atlantic Treaty Organization, 7 rue Ancelle, 92200 Neuilly sur Seine, France, May 75, Paper No. 5.
124. Anon., Additional Control Surfaces Studied, Aviation Week & Space Technology, Vol. 109, No. 11, McGraw-Hill, Inc., New York, NY 10020, Sep 11, 78, p. 113.
125. Rodden, W. P., and Giesing, J. P., Application of Oscillating Aerodynamic Theory for Estimation of Dynamic Stability Derivatives, AIAA Journal of Aircraft, Vol. 7, No. 3, May-Jun 1970.
126. Anon., An Analysis of Methods for Predicting the Stability Characteristics of an Elastic Airplane, Appendix B--Methods for Determining Stability Derivatives, Boeing Document D6-20659-3, NASA Contractor Report CR-73275, Nov. 68.
127. ———, Appendix A--Equations of Motion and Stability Criteria, Boeing Document D6-20659-2, NASA Contractor Report CR-73274, Nov 68.
128. ———, Summary Report, Boeing Document D6-20659-1, NASA Contractor Report CR-73277, Nov 68.
129. Lash, S. F., and Sim, A. G., F-111/TACT Stability and Control Characteristics: Flight, Tunnel, and Analytical, in Symposium on Aircraft Technology (TACT), AFFDL TR-78-100, Air Force Flight Dynamics Laboratory (AFFDL/FXS), Wright-Patterson AFB, OH. 45433, Aug 78, p. 382-426, DISTRIBUTION LIMITED.
130. Rawlings, K., et. al., Transonic Aircraft Technology Flight Test Lift and Drag Data Methods and Results, in Symposium on Aircraft Technology (TACT), AFFDL TR-78-100, Air Force Flight Dynamics Laboratory (AFFDL/FXS), Wright-Patterson AFB, OH. 45433, Aug 78, p. 133-135, DISTRIBUTION LIMITED.

131. Frost, R. C., TACT Supercritical Wing Development, in Symposium on Aircraft Technology (TACT), AFFDL TR-78-100, Air Force Flight Dynamics Laboratory (AFFDL/FXS), Wright-Patterson AFB, OH. 45433, Aug 78, p. 12-62, DISTRIBUTION LIMITED.
132. Baldwin, W. and Burnett, D., Flight Demonstration of the TACT Supercritical Wing and Correlation with Wind Tunnel Results, in Symposium on Aircraft Technology (TACT), AFFDL TR-78-100, Air Force Flight Dynamics Laboratory (AFFDL/FXS), Wright-Patterson AFB, OH. 45433, Aug 78, p. 135-184, DISTRIBUTION LIMITED.
133. Poth, G. E., The Impact of Wind Tunnel Testing Techniques on Longitudinal Aerodynamic Parameters, in Symposium on Aircraft Technology (TACT), AFFDL TR-78-100, Air Force Flight Dynamics Laboratory (AFFDL/FXS), Wright-Patterson AFB, OH. 45433, Aug 78, p. 185-224, DISTRIBUTION LIMITED.
134. Balakrishnan, A. V., and Maine, R. E., Improvements in Aircraft Extraction Programs, NASA CR-145090, Apr 76.
135. Stepner, D. E., A Unified Approach to Aircraft Parameter Identification, in Parameter Estimation Techniques and Applications in Aircraft Flight Testing, NASA TN D-7647, Apr 74, p. 243-260.
136. Wingrove, R. C., Estimation of Longitudinal Aerodynamic Coefficients and Comparison with Wind-Tunnel Values, in Parameter Estimation Techniques and Applications in Aircraft Flight Testing, NASA TN D-7647, Apr 74, p. 125-147.
137. Luckring, J. M., Some Recent Applications of the Suction Analogy to Asymmetric Flow Situations, in Vortex-Lattice Utilization, NASA SP-405, 1976, p. 219-236.
138. Bills, G. R., et. al., A Method for Predicting the Stability Characteristics of an Elastic Airplane, Vol. II, FLEXSTAB 3.01.00, User's Manual, AFFDL TR-77-55, Air Force Flight Dynamics Laboratory, Wright-Patterson AFB, OH 45433.

139. McElroy, C. E., and Sharp, P. S., Stall/Near Stall Investigation of the F-4E Aircraft, AFFTC-FTC-SD-70-20, Air Force Flight Test Center, Edwards AFB, CA 93523, Oct 70, DISTRIBUTION LIMITED.
140. Hall, E. W., Jr., and Gupta, N. K., System Identification for Nonlinear Aerodynamic Flight Regimes, AIAA Journal of Spacecraft, Vol. 14, No. 2, Feb 77, p. 73-80.
141. Daniel, D. C., Schoelerman, D. B., Atmospheric Flight Mechanics: Highlight 1978, AIAA Astronautics & Aeronautics, Vol. 16, No. 12, Dec 78, p. 40-42.
142. Hoey, R. G., et. al., AFFTC Evaluation of the Space Shuttle Orbiter and Carrier Aircraft--NASA Approach and Landing Test, AFFTC-TR-28-14, Air Force Flight Test Center, Edwards AFB, CA 93523, May 78, DISTRIBUTION LIMITED.
143. Balakrishnan, A. V., Systems Identification Theory Course Notes, Optimisation Software Inc., 1100 Glendon Ave, Los Angeles, CA 90024, Jan 79.
144. _____, and Peterka, V., Identification in Automatic Control Systems, Automatica, Vol. 5, Pergamon Press, Great Britain, 1969, pp. 817-829.
145. _____, Lectures given in a course titled Theory and Techniques of Parameter Identification, at Edwards AFB, CA, Feb 79.
146. Wells, W. R., and Queijo, M. J., Simplified Unsteady Aerodynamic Concepts with Application to Parameter Estimation, AIAA. Journal of Aircraft, Vol. 16, No. 2, Jan 79, p. 90-94.
147. Williams, J. L., and Suit, W. T., Extraction from Flight Data of Lateral Aerodynamic Coefficients for F-8 Aircraft with Supercritical Wing, NASA TN D-7749, Nov 74.
148. Wells, W. R. and Ramachandran, S., Multiple Control Input Design for Identification of Light Aircraft, IEEE Transactions on Automatic Control, Vol. AC-22, Dec 77, p. 985-987.
149. Black, G. T., et. al., Summary and Concluding Remarks, in Proceedings of AFFDL Flying Quality Symposium Held at Wright State University 12-15 September 1978, AFFDL-TR-78-171, Air Force Flight Dynamics Laboratory (AFFDL/FGC), Wright-Patterson AFB, OH 45433, Dec 78, p. 613-621.
150. Twisdale, T. R., SIFT Pilot-in-the Loop Handling Qualities Test and Analysis Techniques, in Proceedings of AFFDL Flying Quality Symposium Held at Wright State University 12-15 September 1978, AFFDL-TR-78-171, Air Force Flight Dynamics Laboratory (AFFDL/FGC), Wright-Patterson AFB, OH 45433, Dec 78, p. 414-435.

151. Anon., Military Specification, Flying Qualities of Piloted Airplanes, MIL-F-8785C, 5 Nov 80, ASD/ENESS, Wright-Patterson AFB, OH 45433.
152. Smith, R. H. and Geddes, N. D., Handling Quality Requirements for Advanced Aircraft Design: Longitudinal Mode, AFFDL-TR-78-154, Wright-Patterson AFB, Ohio 45433, Aug 79.
153. Smith, R. H., A Theory for Handling Qualities with Applications to MIL-F-8785B, AFFDL-TR-75-119, Wright-Patterson AFB, Ohio 45433.
154. Hess, R. A., A Pilot Modeling Technique for Handling Qualities Research, Paper No. 80-1624, presented at a workshop on pilot-induced oscillations held at the NASA Dryden Flight Research Center, Nov 18-19, 1980.
155. Westbrook, C. B., McRuer, D. T., Handling Qualities and Pilot Dynamics, Aerospace Engineering, May 59, p. 26-32.
156. Ashkenas, I. L., and McRuer, D. T., A Theory of Handling Qualities Derived from Pilot-Vehicle Systems Considerations. Aerospace Engineering, Feb 62, p. 60-102
157. Arniotis, E., Capt., et. al., YA-7D DIGITAC II Limited Lateral Control Law Optimization Using a Hot Line Gunsight and Lead Computing Optical Sight, Class 80A Letter Report, USAF Test Pilot School, Edwards AFB, CA 93523, Dec 80, DISTRIBUTION LIMITED.
158. Anon., Evaluation of the Space Shuttle Orbiter First Orbital Flight Descent Phase, AFFTC-TR-81-21, Office of Advanced Manned Vehicles, Air Force Flight Test Center, Edwards AFB, CA 93523, 12-14 Apr 81, DISTRIBUTION LIMITED.
159. Pape, J. K., and Garland, M. P., F-16A/B Flying Qualities Full Scale Test and Evaluation, AFFTC-TR-79-10, Air Force Flight Test Center, Edwards AFB, CA 93523, Sep 79, DISTRIBUTION LIMITED.

160. Hoh, R.H., et.al., Preliminary copy of Proposed MIL Standard
(and Handbook) - Handling Qualities of Piloted Airplanes,
AFWAL-TR-82, Systems Technology, Inc., 13766 S. Hawthorne Blvd.,
Hawthorne, CA 90250, Dec 81.

NORTHROP F-5G

